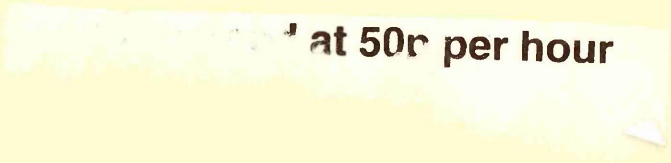



ProQuest LLC.
789 East Eisenhower Parkway
P.O. Box 1346
Ann Arbor, MI 48106 – 1346

# CONVENTIONAL AND MODULAR DESIGN

# OF DOMESTIC HEAT PUMPS

**Jack Ward**

**A thesis submitted in partial fulfilment of the requirements of Sheffield Hallam University for the degree of Doctor of Philosophy.**

**March 1999**

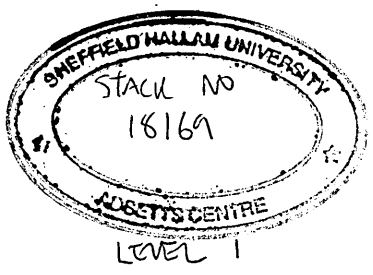
SHEFFIELD HALLAM UNIVERSITY
STACK NO
18169
LOSETT'S CENTRE
LEVEL 1

# Declaration

I declare that no part of this work has been submitted towards any other academic award.

Jack Ward.
August 1998.

# Acknowledgements

It is with sincere gratitude that I thank the Director of Studies Dr M.J. Denman and Professor A.T. Howarth for all the support freely given. Also for the assistance given by Mr C. Hague when constructing the test rigs and Mr R. Wilkinson and Mr B Palmer for making available the necessary items of instrumentation and control equipment and for the guidance in their application to the test rigs..

It gives me the greatest of pleasure that I acknowledge the friendly way I have been treated by the staff of Sheffield Hallam University and in particular by the staff of the School of Engineering with whom the research described in this thesis was undertaken.

To Mrs Audrey Ward, my wife, I give to her my thanks for all the support given and patience shown when she was left on her own for long periods. Without my wife's support, it would not have been completed. The assistance given by Mr Neil Radford was greatly appreciated when he so kindly did the typing and computerised sketches into figures shown in the thesis.

# ABSTRACT

This thesis is concerned with an experimental and theoretical investigation of domestic heat pumps. The development of heat pumps in the 1970's did not meet the original expectations and this thesis examines the reasons why. The items considered included cycling and unsteady conditions created whilst matching the heat pump's output to meet a space heating load. A detailed study was made of the hermetically sealed refrigerant compressor, the heat exchangers, and the refrigerant pressure and temperature control systems. In addition to the conventional heat pump a study was made of the advantages gained from modular designed heat pumps.

The application of heat pumps to U.K. dwellings and climatic conditions was studied together with the suitability of thermostatic control. Initial studies were made of the operation of a demonstration unit. This showed how intermittent operation would reduce a heat pump performance and was followed by the development of a computer model which simulated the complete refrigerant circulation system. This allowed a study to be made of a heat pump performance at part load conditions. A computer model of the complete refrigerant cycle was developed which aided in the design and construction of a heat pump which used refrigerant R12. This was followed by the construction of a second test rig using R134(a). The completed R134(a) test rig was installed in an environmental chamber which could simulate outdoor weather conditions. Results from the test rigs indicated that the performance was greatly affected by on/off cycling an item that was further investigated.

# CONTENTS

Contents Continued.

Contents Continued

# CHAPTER 1 - INTRODUCTION

## 1.1 BACKGROUND INFORMATION

### 1.1.1 Energy resources in the United Kingdom

The research for this thesis has been conducted over a number of years, starting in 1982. Over this period there have been dramatic changes in usage of energy and perceived future use of energy.

The benefits from abundant supplies and the low cost of fuels were enjoyed in the United Kingdom for a great number of years, but the energy crises of the 1970s brought this to an end. The crisis concerning Middle Eastern oil supplies was followed shortly afterwards by a second in the UK, when the extent of the untapped resources of North Sea Gas were questioned. Both of these events caused fuel costs to rise, making economy in the use of energy a necessity. Since that time there have been wide fluctuations in the cost of crude oil along with increasing concern regarding future energy supplies.

Until the early 1970s, the United Kingdom relied heavily for energy supplies on solid fossil fuels. In 1974, 11.74% of electricity generated by the major power producers was from Nuclear Reactors [1]. By 1993 this had risen to almost 30%. In 1989 the power produced from gas was negligible, and by 1993 this had risen to over 9%. Energy used for electrical power generation for the years 1989 and 1993 was calculated from the Government Statistical Service publication "Energy Trends, September 1994" [2].

The supply of known resources was therefore limited and for the most part exhaustible. Plans to meet future energy demands needed to be made, not only because the supply of fossil fuels will eventually be exhausted, but also because research has shown that waste gases from the combustion of fossil fuels is causing serious damage to the Earth's environment [3].[1]

[1] The consequences of limited energy supplies to meet global demands in the long term future are unknown. Currently, this is the subject of scientific debate and publications as shown in references [4] to [7].

### 1.1.2 Impact of Atmospheric Pollution on the Earth's Environment

In the 1980s, at a time in the UK when it was becoming accepted as an unpleasant necessity that the price of fuel made it essential to economise in, the use of energy and problems of even greater concern and of global magnitude were realised. Observations made by researchers produced a clear indication that the Earth's stratosphere was being seriously damaged. This layer is vital to human, animal and plant existence. The cause is believed to be the discharge of large volumes of noxious gases into the atmosphere from combustion and other chemical processes after referred to as greenhouse gases [8].

### 1.1.3 Predicted Long Term Effects of Atmospheric Pollution

Due to the world-wide magnitude of the problem of atmospheric pollution, the time scale and final outcome is unknown, but it has been the subject of a wide range of predictions. It is now being accepted by western governments, that if the discharge of pollutants into the atmosphere continues at its present rate, there is a high likelihood that it will cause alarming changes to the world's interglacial and seasonal weather patterns. Increased atmospheric pollution could upset the regular seasonal change in the world's temperatures that are linked to the tilt and orientation of the Earth as it orbits around the sun. A report of the processes and modelling of the possible changes to the Earth's oceans and climate is provided by the Intergovernmental Panel on Climatic Change [9], [10] and [11].

It is concluded that if the current trends do not change, and the release of the Atmospheric Greenhouse Gases continues to increase at their present rate, there is a distinct possibility that irrevocable damage could occur to the Earth's environment.

### 1.1.4 Atmospheric Pollution - The Role of the Heat Pump

Ideally, the Domestic Heat Pump that increases the temperature of a low grade heat source to provide useful heat energy, does not cause atmospheric pollution. The accidental spillage of refrigerant, however, chiefly due to malfunction and inadequate maintenance of the heat pump,

can have this effect. The use of heat pumps would abolish the $CO_2$ emissions that are associated with the domestic combustion of fossil fuels. Fundamentally, all refrigerants irrespective of type, are thoroughly safe so long as they are captive [12].

Electrical energy that is generated from fossil fuels and used to drive the heat pump is not environmentally friendly, but alternative energy sources are being developed.

### 1.1.5 Protecting the Earth's Environment

The following is an extract from the publication Guidelines on Environmental Issues [13], by The Engineering Council, September 1994, under the heading of "International code of environmental ethics for engineers":

> *"Through the ages, the engineering profession has made a major contribution to the health and well being of mankind by developing the potential of an Earth rich in natural resources. However, there is a new, pressing challenge, created by the adverse effects of depletion of planetary resources, environmental pollution, rapid population growth and damage to the fragile ecosystems through which life on Earth can survive."*

Publication of these guidelines gave detailed statements to members of the Engineering Council that for the future, they must foster an environmental awareness and strive to accomplish the objectives of their work with the lowest possible consumption of natural resources and energy. Within this context it is necessary to consider the proposed use of heat pumps for domestic space heating.

### 1.1.6 Electrical Power Generation

Due to the useful lifespan of certain nuclear power stations in the UK coming to an end, it is necessary for decisions to made concerning their replacement. Both the Institution of Mechanical Engineers and the Institution of Electrical Engineers have made representations to the British

Government asking that new nuclear power stations be built [14]. Nuclear power provides a means of generating electrical energy without discharging environmentally harmful carbon monoxide and carbon dioxide into the atmosphere. This is, however, replaced by the problem of nuclear waste.

In its efforts not to increase atmospheric pollution, the UK government has announced its objective of retaining the 1990 level of carbon dioxide emissions up to the year 2000. Part of the strategy, made in 1995, to achieving this goal was to raise the target capacity from 4000 MW to 5000 MW of electricity generating capacity to be from combined heat and power generating plants [15].

## 1.2 APPLICATION OF DOMESTIC HEAT PUMPS IN THE UK

### 1.2.1 Principle of operation

Heat naturally flows unaided from a hot body to a cooler one. The heat pump makes it possible for energy at a low grade (low temperature) to be transferred to a body at a higher one. Basic concepts of the heat pump are not new, having been outlined by Lord Kelvin back in 1852 [16]. It was mainly due to lack of available technology that little development took place for nearly a century .

There are a number of possible sources of low grade heat supply that may be used for domestic heat pumps. Energy can be obtained from any of the following: soil, lake, river or well water, wind turbines and solar power. An advantage of this when used in conjunction with a plenum heat source is that heat can be recovered from air extracts.

The heat source used for this study is atmospheric air, because it is the most universally available supply of low grade heat. A disadvantage encountered with this heat source is in the availability of thermal energy output, which decreases as the outdoor temperature falls, and is the inverse of the heat demand for space heating. Techniques are examined by which energy can be extracted from atmospheric air and transferred to the hot water circulation system to provide domestic space heating.

The second law of thermodynamics states that it is impossible for heat to flow from a cold substance to a hotter one without the aid of external work [17]. For the purpose of this study, external work is supplied to the heat pump by electrical power.

### 1.2.2 Potential for development

Heat pumps are being used successfully to recover low grade energy in industrial processes. Energy is also being saved by their use in space heating and air conditioning in both commercial and industrial buildings [18]. A number of domestic space heating systems were installed between the late 1970s and the mid 1980s, but they proved unsuccessful for a variety of reasons [19]. The principle reason for their loss of popularity was that the installation and maintenance costs could not be justified at that time by the cost savings of fuel.

## 1.3 HEAT PUMP THEORY

The heat pump being studied operated on the vapour compression cycle. The ideal standard of performance for this is the reversed Carnot cycle. There are many references to the basic theory and application of the vapour compression cycle, some of which were studied in the course of this research [20].

For the utilisation of low grade heat by vapour compression and expansion, there are a number of thermodynamic cycles that are applicable. The cycle used mainly for this research was devised by Sadi Carnot [21]. This cycle consists of four reversible processes, two isothermal and two adiabatic. It has the highest possible efficiency of any cycle, but in normal practice this ideal standard is not obtained. The Carnot Cycle was originally developed for heat engines, but for a heat pump, the reversed cycle is used, see Figures 1 and 2.

In addition to the Carnot Cycle, reference is made to the vapour compression cycle, which provides results of lower efficiency, but closer to normal practice.

### 1.3.1 The Heat Pump Thermodynamic Cycle

The reversed Carnot Cycle takes energy from a low grade heat source and with an input of mechanical energy, supplies heat to the heat sink. The direction of heat flow in the heat pump is shown in Figure 2.

The heat engine cycle is shown on the temperature-entropy diagram. It is a closed cycle, but is normally considered to start at point 'a' as shown in Figure 3. It comprises of an increase of entropy followed by an adiabatic reduction of temperature, then a reduction of entropy followed by an increase of temperature to complete the cycle.

The ideal Reversed Carnot Cycle of the heat pump is normally considered to start at point '1' with processes similar to the heat engine, but in the reverse direction of rotation, as shown in Figure 4.

The variation of output capacity from continuous operation of a heat pump plotted against changing atmospheric temperatures is shown in Figure 5. Also shown is the variation of space heating load for the same temperature range. The design point, alternatively referred to as the balance point, is shown to be the atmospheric temperature when the heat pump output and the space heating load are equal. Off-design point conditions are any other atmospheric temperatures within the operating range of the heat pump.

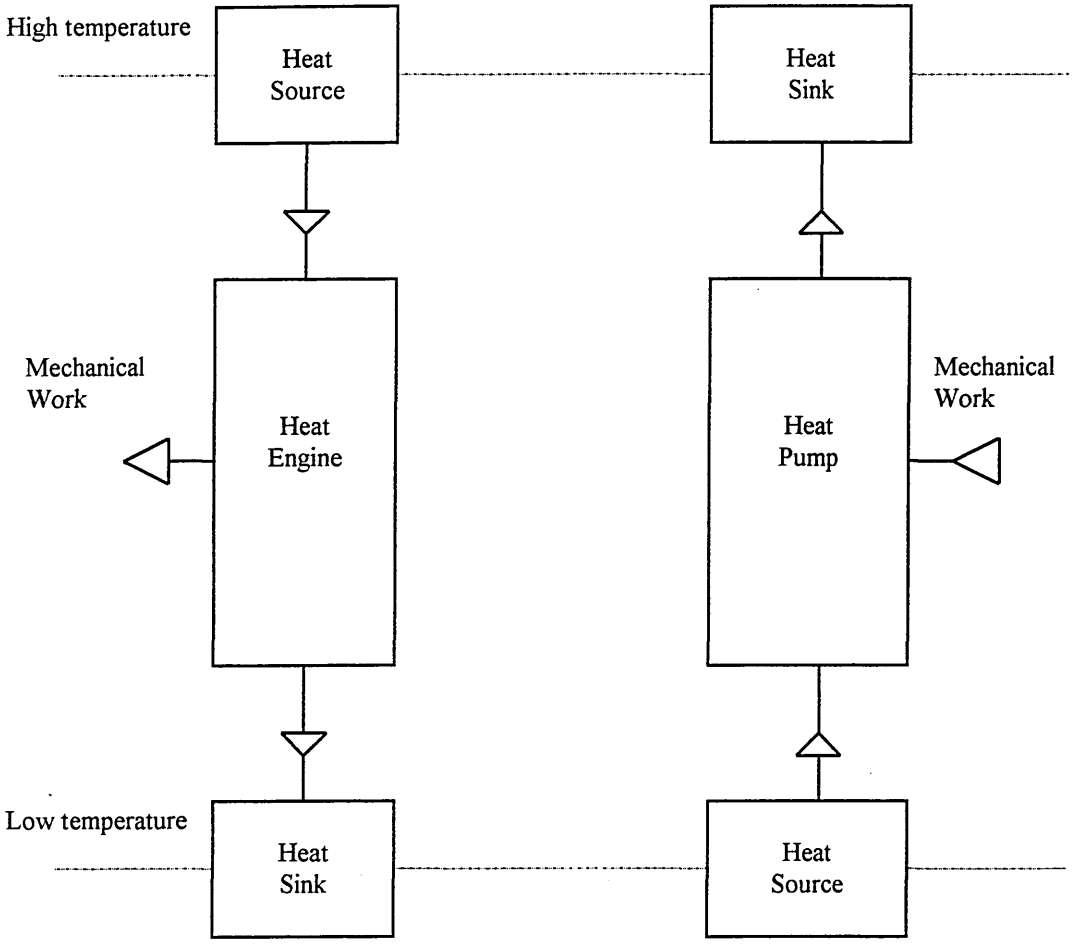


FIGURE 1
HEAT ENGINE OPERATION




FIGURE 2
HEAT PUMP OPERATION

SCHEMATIC REPRESENTATION OF THE HEAT FLOW IN THE HEAT ENGINE AND HEAT PUMP

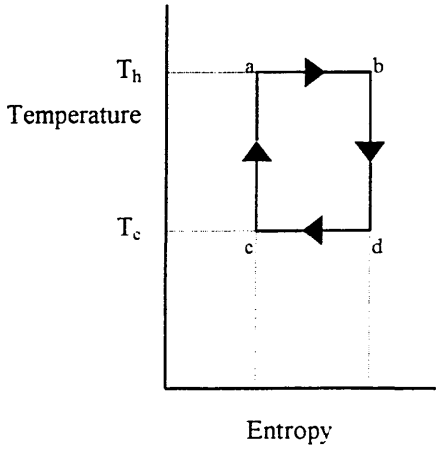


FIGURE 3
CARNOT CYCLE
(HEAT ENGINE)

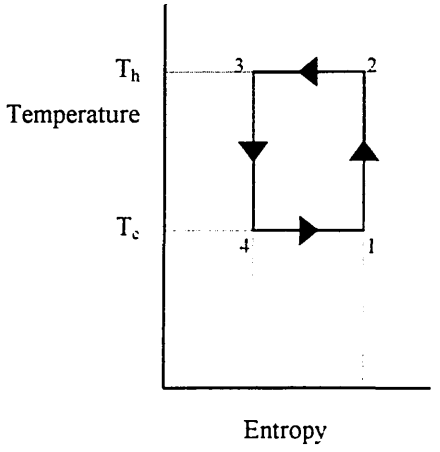


FIGURE 4
REVERSED CARNOT CYCLE
(HEAT PUMP)

TEMPERATURE - ENTROPY DIAGRAMS OF CARNOT CYCLE AND REVERSED CYCLE

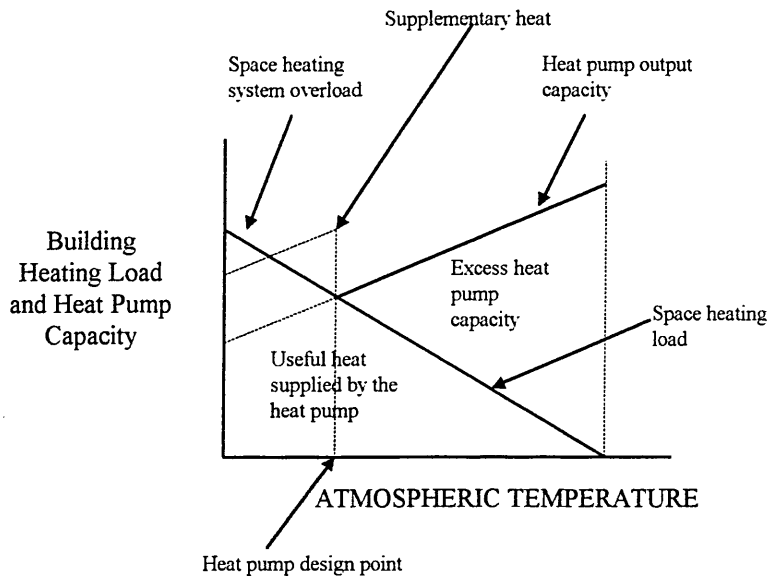


FIGURE 5

SCHEMATIC ARRANGEMENT OF HEAT PUMP AND SPACE HEATING LOAD

### 1.3.2 Performance of Refrigeration Plant

Thermal performance of a heat pump is higher than that for an equivalent refrigerator operating with the same heat source and sink temperature. In the heat pump cycle, the input energy from the compression process is available as useful heat for domestic space heating. The operation of a refrigerator calls for heat generated in the vapour compression to be dissipated from the condenser, this not serving any useful purpose.

As a result of this, the ratio of thermal energy input to thermal energy output of a heat pump, known as the Coefficient of Performance (or COP), is always greater than one and performance of the heat pump is represented by the following equation: $COP_H = COP_C + 1$

where $COP_H$ = Heat Pump Coefficient of Performance

$COP_C$ = Refrigerator Coefficient of Performance

### 1.3.3 Heat Pump Coefficient of Performance

The ideal COP that gives the highest expectation of thermal performance is based on the reversed Carnot cycle.

Carnot COP: Energy Input = $(T_h - T_c) \times (S_1 - S_4)$

Energy output = $T_h (S_2 - S_3)$

but $(S_2 - S_4)$ = $(S_2 - S_3)$, from Figure 4

Carnot COP = $$\frac{T_h(S_2 - S_3)}{(T_h - T_c) \times (S_2 - S_3)} = \frac{T_h}{T_h - T_c}$$

where: $T_h$ = Condensing Temperature (abs.)

$T_c$ = Evaporating Temperature (abs.)

$S_1 - S_4$ = Entropy input to the cycle

$S_2 - S_3$ = Entropy output from the cycle

### 1.3.4 Vapour Compression COP

The second method of calculation is the vapour compression cycle which is a step nearer to a practical heat pump and, therefore, produces a lower value of COP. This method takes into consideration the sensible and latent enthalpies of the refrigerants as shown in Figure 6:

Figure 6

Vapour Compression thermodynamic cycle

$$COP = \frac{h_h - h_{liq}}{h_h - h_c}$$

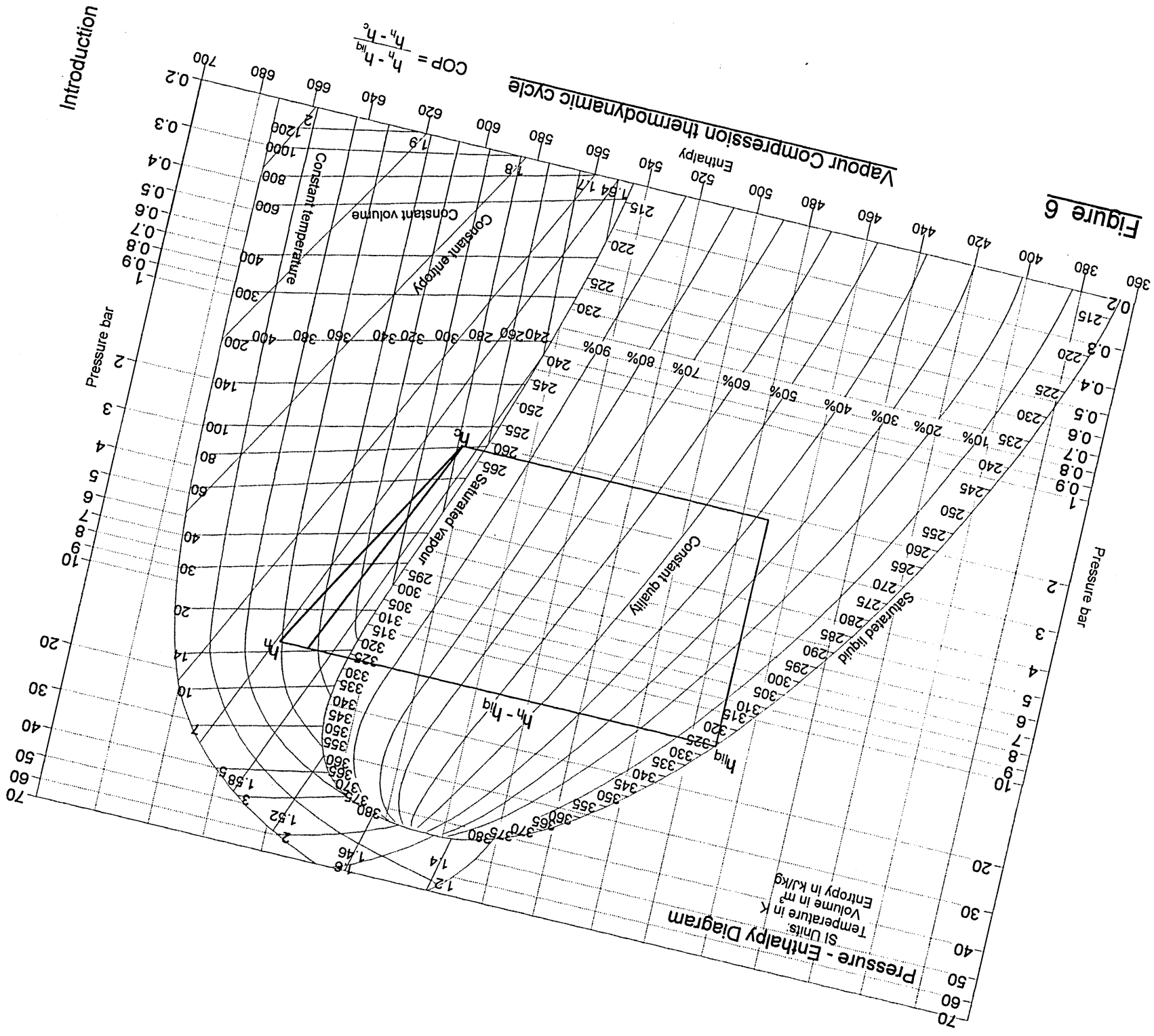

Vapour Compression: = $\frac{h_h - h_{liq}}{h_h - h_c}$

where the enthalpy values are:

$h_c$ = Vapour entering the compressor

$h_h$ = Vapour leaving the compressor

$h_{liq}$ = Liquid leaving the condenser

Comparison was made between the heat pump ideal performance of the reversed Carnot cycle and the vapour compression cycle, see Figure 7. Calculations for the vapour compression cycle are made using Refrigerant 12.

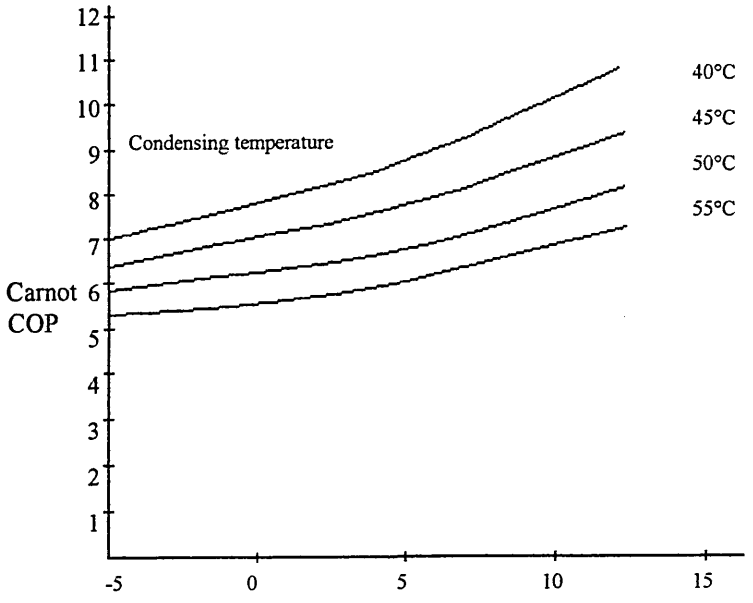


REVERSED CARNOT IDEAL STANDARD CYCLE

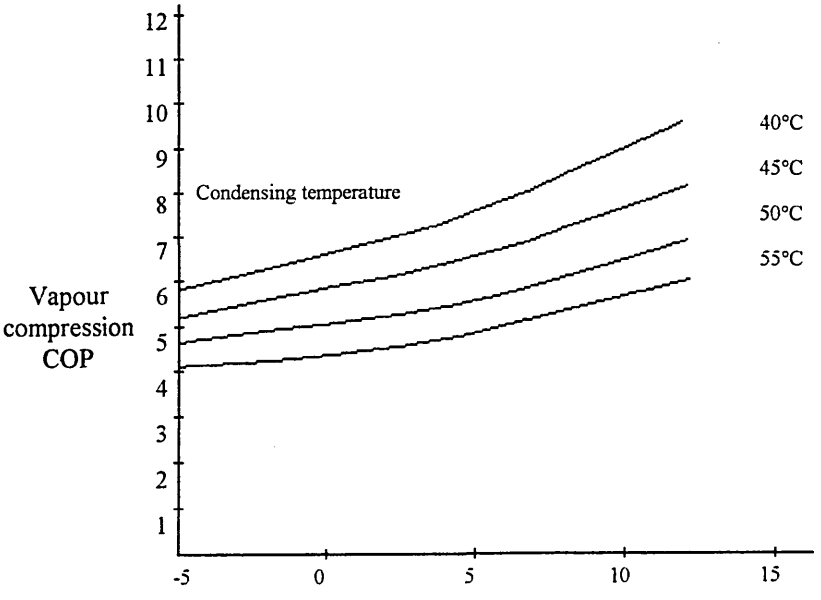


REVERSED VAPOUR COMPRESSION STANDARD CYCLE (REFRIGERANT R12)

FIGURE 7

THEORETICAL STANDARD PERFORMANCE CURVES.

## 1.4 SCOPE OF THE PROJECT

A study was made of heat pump operation and the thermodynamic performance of the basic units within the cycle that produce the compression, the expansion, the condensation and the evaporation of the refrigerant. The initial objective of the study was to investigate steady state design conditions, but it was later found that a study of both steady and unsteady conditions was needed. This was necessary due to the magnitude of the heat pump on/off cycling losses caused by the capacity control whilst matching heat pump output to the space heating load.

Research into the application of domestic heat pumps was directed principally towards the optimisation of thermal output and thermal efficiency. This included the matching of thermal output to the space heating load. Seasonal temperature and humidity levels pertinent to the UK climate were also considered in conjunction with the possible benefits of a number of modular heat pump units operating in parallel. Individual units would be switched on and off to represent the varying seasonal space loads.

A theoretical study was made of the volumetric and isentropic efficiencies and how these were affected by varying degrees of superheat at the compressor suction. Research was made into the performance of the condenser and evaporator.

Application of the heat pump introduces the possibility of air conditioning and cooling in the summer months but it is a possible development for the future not included in this study. A report of field trials, [19], stated that the supply of domestic hot water may be best obtained, other than by using the heat pump designed for domestic space heating. It claims that large cost savings can be made by installation of an immersion heater to operate with night rate, low cost electricity. Study of the supply of domestic hot water from a heat pump designed for domestic space heating was not included.

This project has been undertaken over a long period of time, which is shown by changes in technology that have occurred. The computing power, available at the outset, has increased considerably from the calculators, magnetic tape and the BBC computer, to the more recently used VIG SX-20 HD40VC computer with 2MB of RAM. Similarly, at the start of the project, the refrigerant used was R12, which has now been superseded by R134(a).

# CHAPTER 2 - OPERATION OF A HEAT PUMP DEMONSTRATION UNIT

## 2.1 BACKGROUND INFORMATION

### 2.1.1 Demonstration heat pump and mathematical model

In order to gain experience of the operation of heat pumps, a series of tests were carried out at Brighton Polytechnic, using the P. A. Hilton Demonstration Heat Pump, Figure 8. The refrigerant used was R12, because at that time the extent of the forthcoming changes of refrigerant discussed in chapter one were not known. Comprehensive reports of field trials that were made available by an industrial body, and studied in conjunction with the above research [22]. These studies provided a clear demonstration of the characteristics, principles and laws governing heat pump operation and the practical application of these. They also highlighted the need to investigate the problems of cycling with heat pump systems.

In conjunction with the above, Chapter 3 details the mathematical model of the complete refrigeration cycle, this being an exercise to show the four main units of the heat pump and the thermal interaction between them on an annual basis. The mathematical model was computerised in four sections to run in series on a BBC computer as there was insufficient random access memory to programme the computer in only one section.

### 2.1.2 Reports on Field Trials

Detailed reports [22] were made available by private arrangements. These related to trials on 36 domestic dwellings of varying size, age and design. All heat pumps operated on the vapour compression cycle, but installations varied in design, using heat pumps supplied by a number of manufacturers. When used in conjunction with the laboratory testing, these reports were a valuable aid and were instrumental in providing a foundation for the development of this research project.

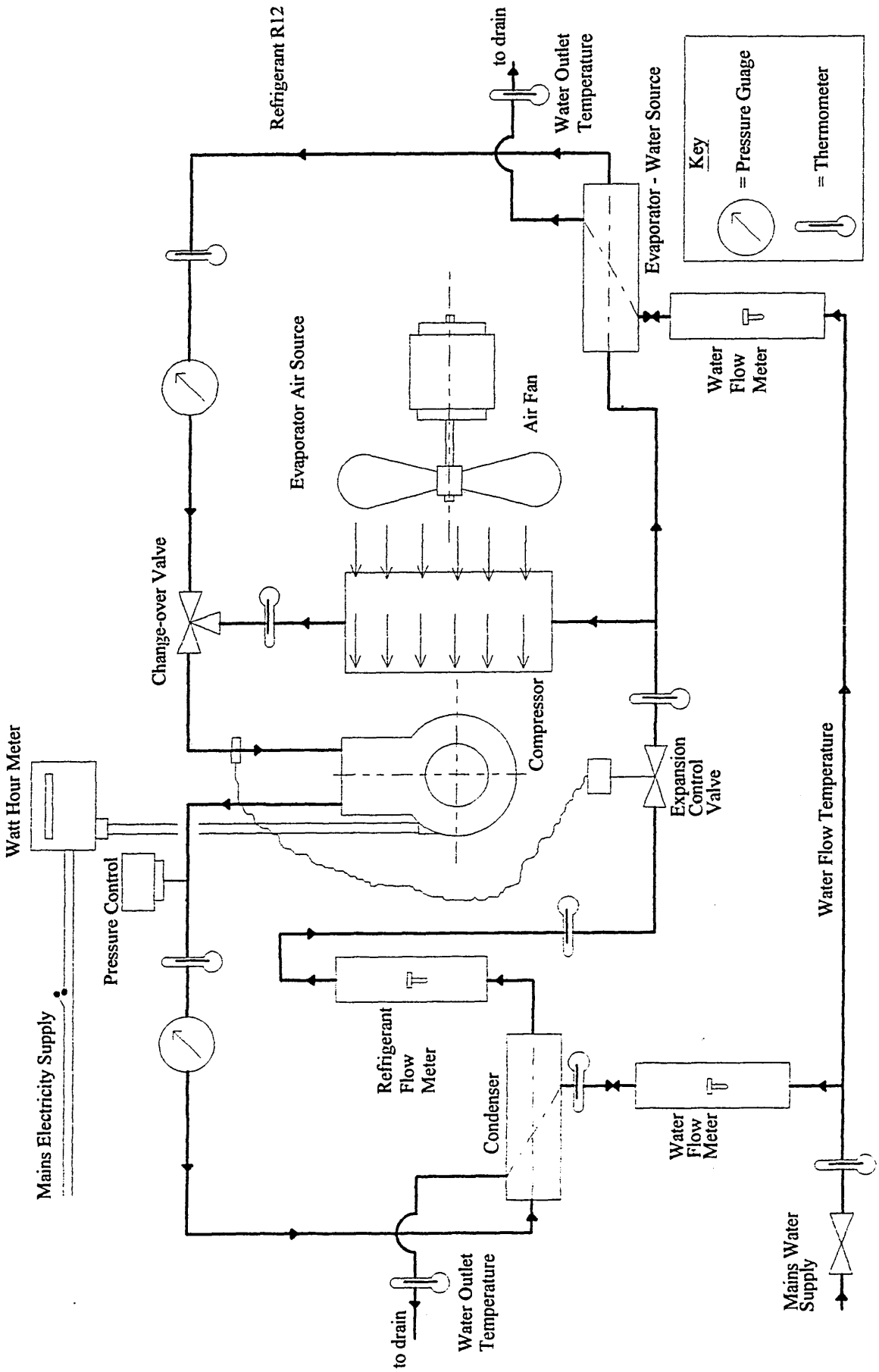


Figure 8
Schematic diagram - Hilton Air and Water Heat Pump

### 2.1.3 Description of Laboratory Test Equipment

The Hilton Air and Water Heat Pump was not a commercially available unit, but was designed for laboratory demonstration purposes. The heat output capacity could be varied between 1.25kW and 2kW by adjusting water flow rates, using needle valves. It was fully instrumented to measure power consumption, water and refrigerant mass flow, as well as pressures and temperatures within the refrigerant cycle. There was a change-over system allowing the heat source to be either room air or towns water. This latter was used to provide the heat sink. Figure 8 is a schematic diagram of the heat pump and instrumentation.

## 2.2 STEADY STATE HEAT PUMP TRIALS

Observations made of heat pump performance during one of the trial runs is shown in Table 1. The derived results from the calculations are given in table 2. In this test run, energy was extracted from room air by the evaporator and transferred to the water flow through the condenser.

The compressor volumetric efficiency was obtained from calculation of the refrigerant mass flow. Calculations of isentropic efficiency were based on enthalpy change within the refrigerant cycle. During the trial, observations were made of changing heat pump performance caused by gradually reducing the water mass flow through the condenser. The trial was started with a flow rate of 18.8g/s and reduced as the trial proceeded. When the flow rate was reduced below 10g/s the trial was stopped, because of refrigerant pressure fluctuations

The test demonstrated the importance of condenser performance on heat pump thermal efficiency and thermal output. Reduction of water mass flow caused the refrigerant pressure difference to rise and therefore energy input to the compressor to increase. COP and thermal output were notably reduced due to the reduction of water flow through the condenser and the subsequent reduction in the water temperature.

LABORATORY HEAT PUMP TRIALS

BRIGHTON POLYTECHNIC

AIR WATER OPERATIONS

QUASI-STEADY STATE CONDITIONS

TABLE 1 OBSERVATIONS

| Time - Minutes from Start-Up: | | | | 15 | 30 | 45 | 60 | 75 | 90 | 105 | 120 | 135 |
|---|---|---|---|---|---|---|---|---|---|---|---|---|
| Refrigerant R12 | Compressor Suction Pressure | $p_1$ | bar.g | 2.2 | 2.2 | 2.3 | 2.4 | 2.4 | 2.5 | 2.6 | 2.6 | 2.5 |
| | Condenser Pressure | $p_2$ | bar.g | 10 | 10.2 | 10.4 | 10.5 | 12 | 14 | 16 | 20 | 14 |
| | Compressor Suction Temperature | $t_1$ | °C | 10 | 8 | 9.5 | 9.8 | 9.5 | 6.5 | 11 | 12 | 11 |
| | Compressor Delivery Temperature | $t_2$ | °C | 89 | 90 | 91.5 | 94 | 96 | 105 | 107 | 113 | 107 |
| | Condenser Outlet Temperature | $t_3$ | °C | 30 | 30.8 | 33.5 | 35 | 38.5 | 43 | 49.5 | 57.5 | 44.8 |
| | Evaporator Inlet Temperature | $t_4$ | °C | 5 | 4.5 | 5 | 5.4 | 5.4 | 5.5 | 7 | 7.6 | 7 |
| Air Source | Inlet Temperature | $t_a$ | °C | 12.6 | 12.8 | 12.8 | 12.8 | 13 | 13.8 | 14.8 | 15.6 | 14.8 |
| | Outlet temperature | $t_{10}$ | °C | 11 | 11 | 11.2 | 11.2 | 11.2 | 11.8 | 13.2 | 12.8 | 12.4 |
| Condenser Water | Water Flow | $m_c$ | g/s | 18.8 | 18.1 | 16 | 14 | 12 | 10 | 8 | 6 | 10 |
| | Inlet Temperature | $t_8$ | °C | 13.8 | 14 | 14.2 | 14.7 | 15 | 15.4 | 15.5 | 16.4 | 16.2 |
| | Outlet Temperature | $t_9$ | °C | 33.5 | 33 | 35.8 | 39.2 | 42.5 | 48 | 55.2 | 65 | 49.5 |

TABLE 2 DERIVED RESULTS

| Time - Minutes from Start-Up: | | 15 | 30 | 45 | 60 | 75 | 90 | 105 | 120 | 135 |
|---|---|---|---|---|---|---|---|---|---|---|
| Pressure Ratio | $p_2/p_1$ | 4.55 | 4.64 | 4.52 | 4.38 | 5 | 5.6 | 6.15 | 7.69 | 5.6 |
| Volumetric Efficiency | % | 84 | 83 | 84 | 85 | 82 | 79 | 77 | 70 | 79 |
| Isentropic Efficiency | % | 54 | 55 | 52 | 54 | 60 | 72 | 73 | 74 | 47 |
| Input | W | 443 | 441 | 457 | 470 | 489 | 516 | 554 | 608 | 524 |
| Output | kW | 1.55 | 1.44 | 1.45 | 1.44 | 1.38 | 1.37 | 1.33 | 1.22 | 1.40 |
| Heating $COP_H$ | - | 3.49 | 3.26 | 3.17 | 3.06 | 2.82 | 2.65 | 2.40 | 2.00 | 2.67 |
| Carnot COP | - | 6.1 | 6 | 6.1 | 6.2 | 5.7 | 5.4 | 5 | 5 | 5.4 |
| Carnot Efficiency | % | 57 | 54 | 52 | 49 | 49 | 49 | 48 | 40 | 49 |

2.2.1 Determination of Volumetric Efficiency of the Compressor

Theoretical volumetric efficiency is defined as the ratio of the actual volume induced per cycle by the compressor to swept volume. The operator's manual for the demonstration heat pump for these tests [23], provides an equation for calculation of the compressor volumetric efficiency:

$$\text{Vol Effy} = \frac{SuctionVolume}{CompressorSweptVolume} = 1-\left(\frac{V_c}{V_s}\right)\left[\left(\frac{p_2}{p_1}\right)^{\frac{1}{n}}-1\right]$$

where:

| | | |
|---|---|---|
| Vol Effy | = | volumetric efficiency |
| $V_c$ | = | clearance volume |
| $V_s$ | = | swept volume |
| $p_2$ | = | compressor delivery pressure |
| $p_1$ | = | compressor suction pressure |
| n | = | index of expansion |

For small compressors $V_c/V_s$ may be taken to be 0.05 and 'n' may be taken to be 1.05 [23].

2.2.2 Determination of Isentropic Efficiency

Evaluation of isentropic efficiency is obtained from the ratio of isentropic input to indicated thermal input. Physical and thermodynamic properties used in the calculations were obtained from the Handbook of Thermodynamic Tables and Charts [24].

$$IsenEffy = \frac{h_{2s}-h_1}{h_2-h_1}$$

| | | |
|---|---|---|
| where: Isen Effy= | | Isentropic efficiency |
| $h_1$ | = | Enthalpy compressor suction |
| $h_{2s}$ | = | Enthalpy isentropic delivery |
| $h_2$ | = | Enthalpy indicated delivery |

Adjustments to condenser coolant mass flow rates caused the compressor to produce a wide variation of values of isentropic efficiency between 50% and 95%. The reduction of isentropic efficiency after start up was due to the input to the refrigerant from the motor windings.

2.2.3 Determination of Power Consumed, Thermal Output and the Coefficient of Performance

Data on electrical power consumption was obtained from readings of an integrated electrical energy meter used in conjunction with a timer. The thermal output was calculated from multiplication of water mass flow rate, the specific heat and the temperature rise through the condenser. Coefficient of performance was obtained in a similar way to calculation of thermal efficiency, i.e. by dividing thermal output by power consumed.

Performance curves shown in Figure 9, obtained from laboratory tests, indicate how COP and thermal output increase when the condenser outlet temperature is reduced.

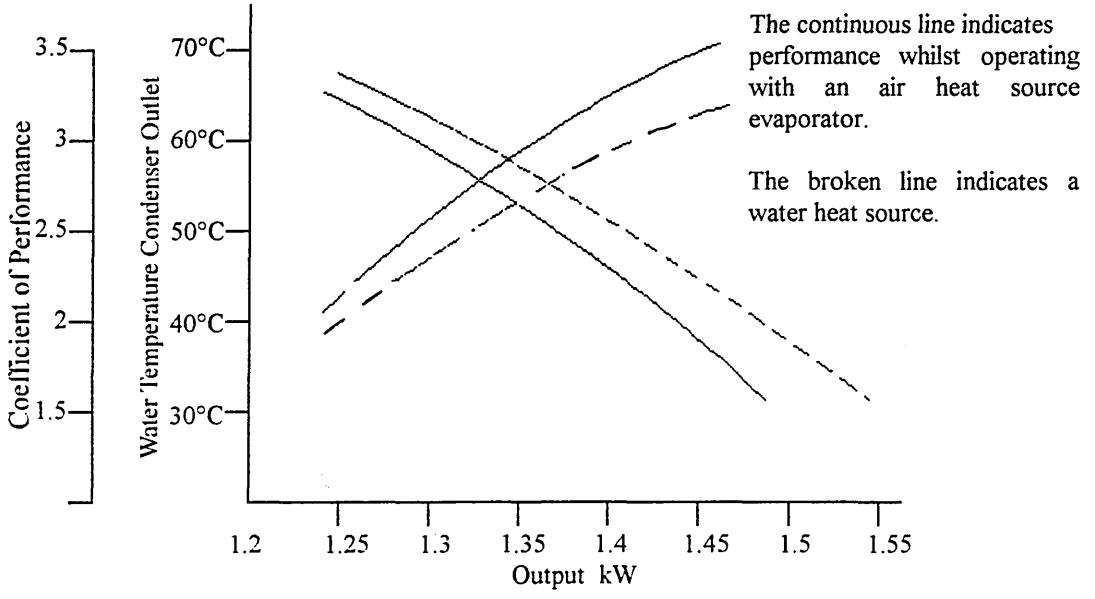


FIGURE 9

Laboratory Tests on the Hilton Heat Pump.

### 2.2.4 Thermal Performance of the Heat Exchangers

The amount of heat transferred in the various stages and changes of state of the refrigerant were studied for both the evaporator and the condenser.

### 2.2.5 Heat Transfer - Evaporator - Refrigerant Side

Heat transfer to the wet refrigerant vapour entering the evaporator is first by evaporation followed by superheating. The refrigerant then passes to the compressor. The amount of superheat is controlled by setting the control valve that regulates the refrigerant entering the evaporator.

### 2.2.6 Atmospheric Air - Heat Pump Heat Source

The air side of an evaporator normally has a finned extended heating surface. Heat is transferred from the air by forced convection and, therefore, higher air velocities increase the turbulence and the heat transfer rate. Condensation of the humidity contained in the atmospheric air increases the heat transfer without reduction of the mean temperature difference, which is an advantage. Ice is formed on the heat exchange surface when the temperature falls below freezing temperature. This reduces the rate of heat transfer, negating the advantage gained. To reduce the possibility of ice bridging the gap between the fins, they should be spaced at least 5mm apart.

### 2.2.7 Heat Transfer - Condenser - Refrigerant Side

There are two main processes of heat transfer from the refrigerant to the hot water circulation space heating system. The first stage of heat transfer utilises the superheat, whilst the second is the refrigerant condensation. Additionally, heat may be obtained by sub-cooling the liquid refrigerant. The amount of heat obtained from liquid sub-cooling is strictly limited, because the main temperature difference between the refrigerant and the water circulation system is quickly reduced, due to temperature drop of the liquid refrigerant.

Observation and further study of this part of the laboratory testing enabled a deeper understanding to be gained of heat and mass transfer, particularly in the change of state and also into the fundamental operation of the vapour compression cycle.

## 2.3 DISCUSSION OF STEADY STATE LABORATORY TESTING

It was found that the thermal interaction between the four basic units of the heat pump (these being the compressor, the condenser, the expansion control and the evaporator), needed to be studied further. For example, a compressor of low isentropic efficiency makes it necessary to have a larger condenser to recover the additional superheat at the compressor outlet.

A domestic heat pump installation is designed, at steady state, to meet specified indoor and outdoor conditions. These, however, occur for only relatively short periods during the year. A true indication of the efficiency of a domestic heat pump can only be obtained from values of Seasonal COP. In practice, Seasonal COP is obtained by taking records for a whole calendar year and then dividing annual energy output of the heat pump by the annual energy consumption. To predict Seasonal COP, both the steady state and unsteady state performances at off-design conditions of the heat pump need to be included in research.

These calculation techniques made allowance for the flexibility that was necessary at this stage of the research. The introduction of off-design point calculations, at a later stage, showed that this procedure was inadequate for future research on this project.

It was whilst carrying out these laboratory tests and giving consideration to off-design point operating conditions that the advantages were realised of a mathematical model, first to analyse the interaction between the four basic processes involved in the Vapour Compression Cycle and secondly to analyse off-design point conditions. Research into the published literature on the subject of mathematical modelling of heat pump performance was undertaken. Following on from this study, the steady state mathematical model of the heat pump was developed and is detailed in Chapter 3.

## 2.4 UNSTEADY STATE HEAT PUMP TRIALS

### 2.4.1 The Cause of Unsteady State Heat Pump Operation

Whilst operating at part space heating load conditions, both the on/off time and the capacity control system can be the cause of unsteady state operating conditions. Time control systems cause unsteady state conditions whilst preheating a dwelling ready for occupation. During the preheat phase, there is a continuous temperature change between the heat distribution system and the contents of the heated space. The heat transfer rate of the radiators is, at first at a maximum, but reducing as the room temperature increases.

Energy is saved by preheating the heated space in the shortest possible time. During preheat, therefore, the full capacity from the heat pump is required. When atmospheric temperature is higher than the design temperature of the heat pump there is an increase in the capacity of the heat pump. Unless the heat emitters within the heated space are of sufficient capacity for the emission of the increased capacity of the heat pump, the full output capacity cannot be used. Under these conditions there are two causes of energy loss:

(i) the heat pump operates intermittently and at an unsteady state and,

(ii) the space heating preheat time is extended unnecessarily.

The capacity control system matches thermal output of the heat pump to the space heating load. Design of the space heating system and time control are discussed in Chapter 4. On/off capacity control of domestic heat pumps is the system most frequently used in practice and is the control system studied in connection with this project. When atmospheric temperature is above the design point, the space heating load is reduced, but the continuous output of the heat pump increases. To reduce output, the heat pump is operated intermittently under the control of a thermostat.

If the thermal output of the heat distribution system is equal in capacity to that of the heat pump at design conditions, then at part load conditions when the COP is higher, the full heat pump capacity cannot be emitted from the heat distribution system. The heat pump will, therefore, operate intermittently, due to the heat pump water temperature control. In these conditions heat up time

could be reduced and running costs reduced by increasing the heating surface of the heat distribution system.

### 2.4.2 Condenser Water Temperatures - Intermittent Operation

It was not possible in the Brighton Polytechnic Laboratory to arrange for the demonstration heat pump to control room temperature, therefore the effects on the heat pump were simulated manually. To observe the effects of cyclic operation in the laboratory testing, a thermograph was connected in order to record water outlet temperatures from the condenser. The heat pump was intermittently operated by switching on and off manually, varying the length of idle and operational periods.

From the tests, it was observed that the time taken to restore the condenser working temperature after switching on was approximately two minutes. It was also observed that 60% of the working temperature difference was lost in the first 30 seconds after switching off. Within two minutes of shut off the condenser water inlet and outlet temperatures were the same.

A typical section taken from the thermograph charts indicating the temperature change through one complete cycle is shown in Figure 10. This thermograph shows that from the moment the heat pump was switched off, the water temperature was reduced. Within a few seconds of the water temperature falling, the useful heat flow to the heated space is quickly reduced to zero. The heat pump was unable to sustain the operating temperature after shut off. On start up, therefore, the heat pump used electrical energy for a comparatively long period of time before operating conditions were fully restored.

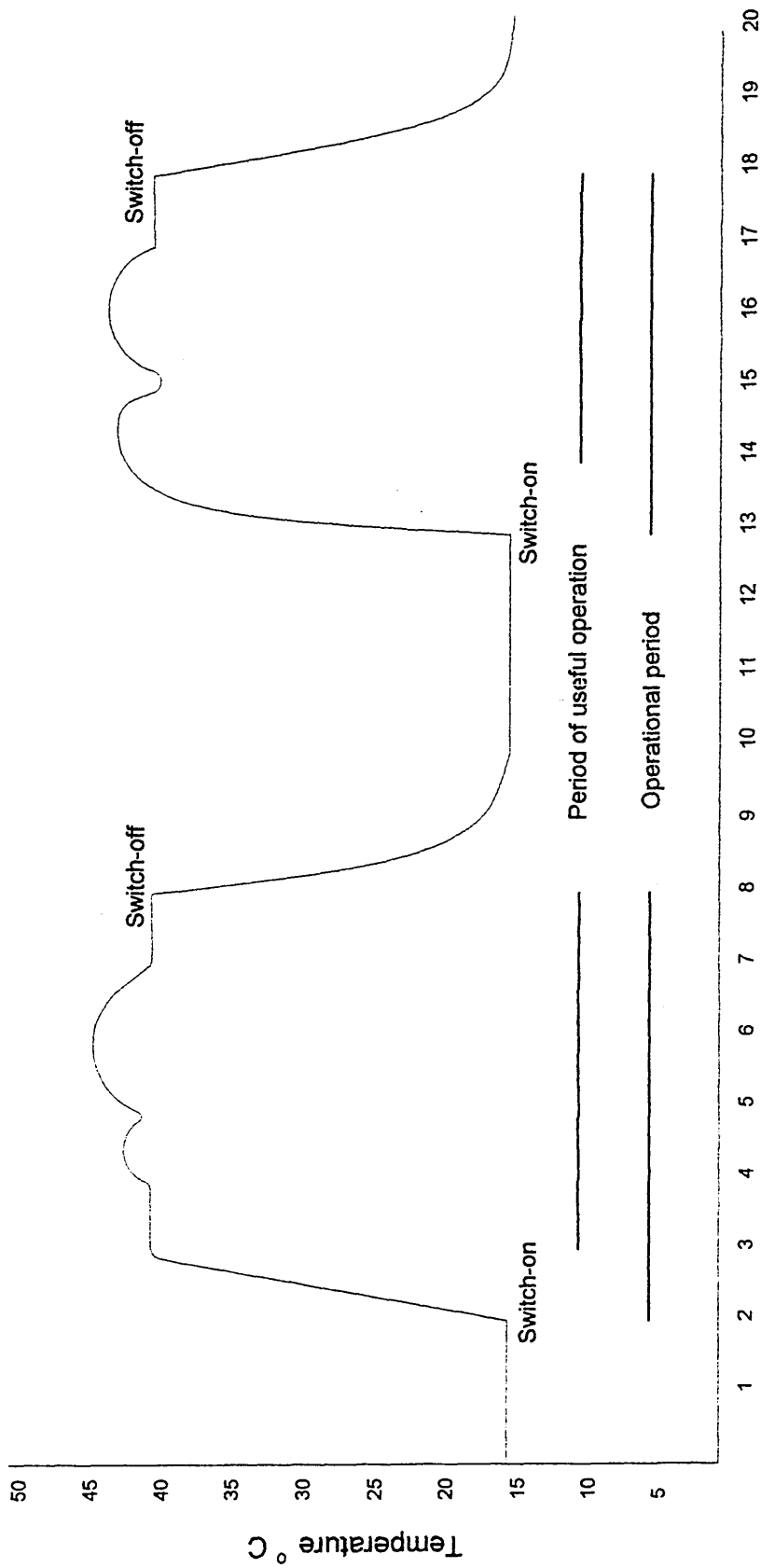


Figure 10

Intermittent Heat Pump Operation
Condenser Water Outlet Temperatures

These laboratory tests gave an indication that thermal losses could be caused by heat pump cycling. The next stage of investigation is the study of temperature and pressure changes caused by on/off cycling.

### 2.4.3 Variation of Condenser Pressures - Intermittent Operation

Investigation into the transitory conditions whilst on/off cycling was made by manually reading the refrigerant pressures of the condenser and evaporator in the periods just after shut off and start up. Sensitive equipment capable of recording change of condenser pressures as they occurred was not available. Bourdon pressure gauges were used to take visual readings at 15 second intervals.

Figure 11 shows the observations made in eight tests of condenser and evaporator pressures immediately after switching off the heat pump. In the first 45 seconds, the pressure difference is reduced to between 30% and 40% of the working pressure. The reduction of condenser pressure occurred simultaneously to a rise in evaporator pressure. The pressure difference after one minute continued to reduce, but at a much slower rate of change.

A similar series of nine pressure variation tests following starting up, provided results reproduced in graphical form in Figure 12. These showed that it took between 45 and 60 seconds to build up the condenser working pressures from starting up the heat pump.

### 2.4.4 Power Consumed During the Starting Up Period

Tests were made of the power used by the compressor during the starting up period. These did not reveal any differing rate of consumption to that of the normal operation. With this information, estimates of percentage energy loss during the starting up period were taken to be directly related to the heat pump operating time.

FIGURE 11 Condenser and Evaporator Pressure Variations During the First Two Minutes After Compressor Shut-Off

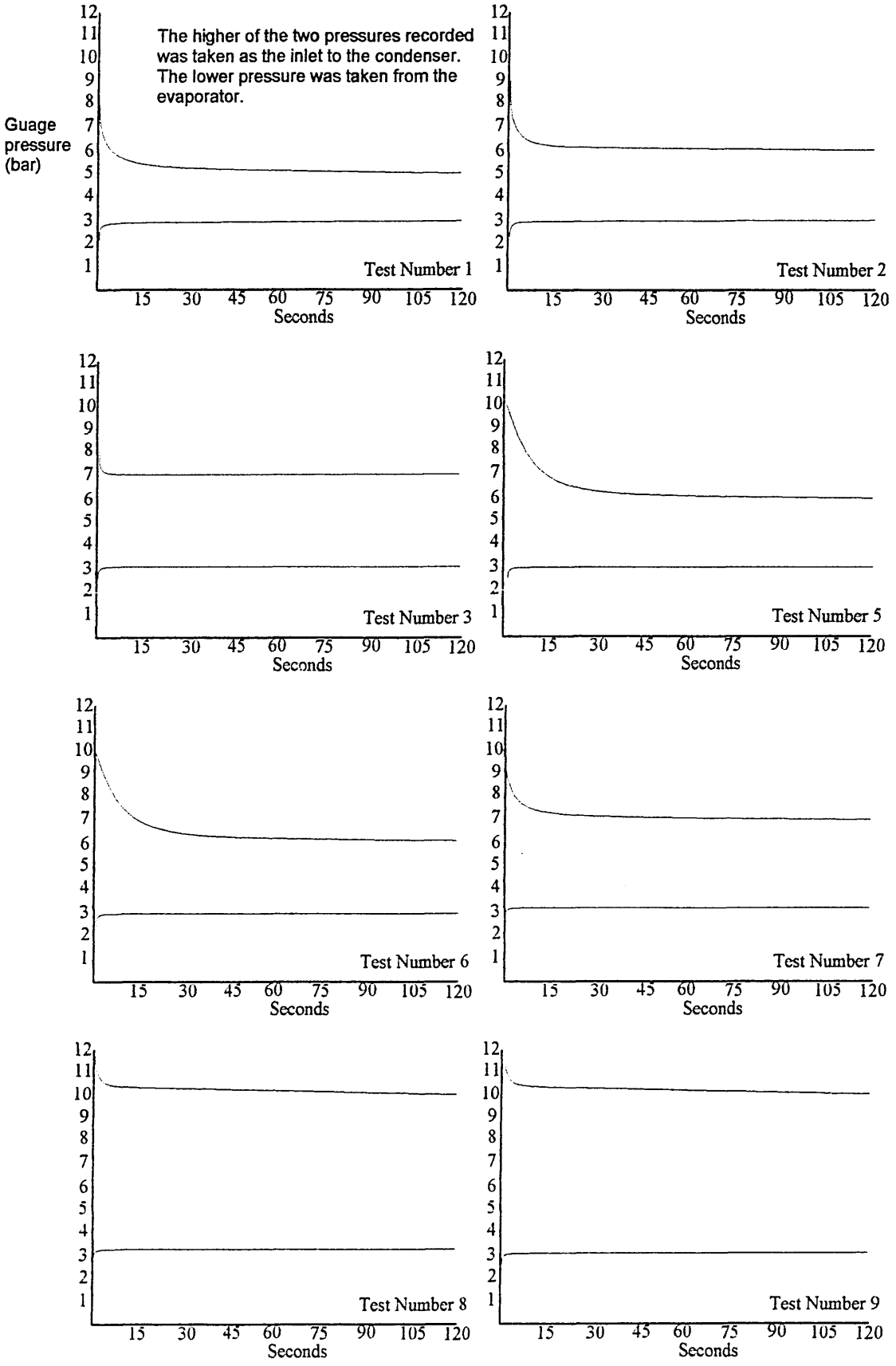

FIGURE 12 Condenser and Evaporator Pressure Variations During the First Two Minutes After Compressor Start-Up

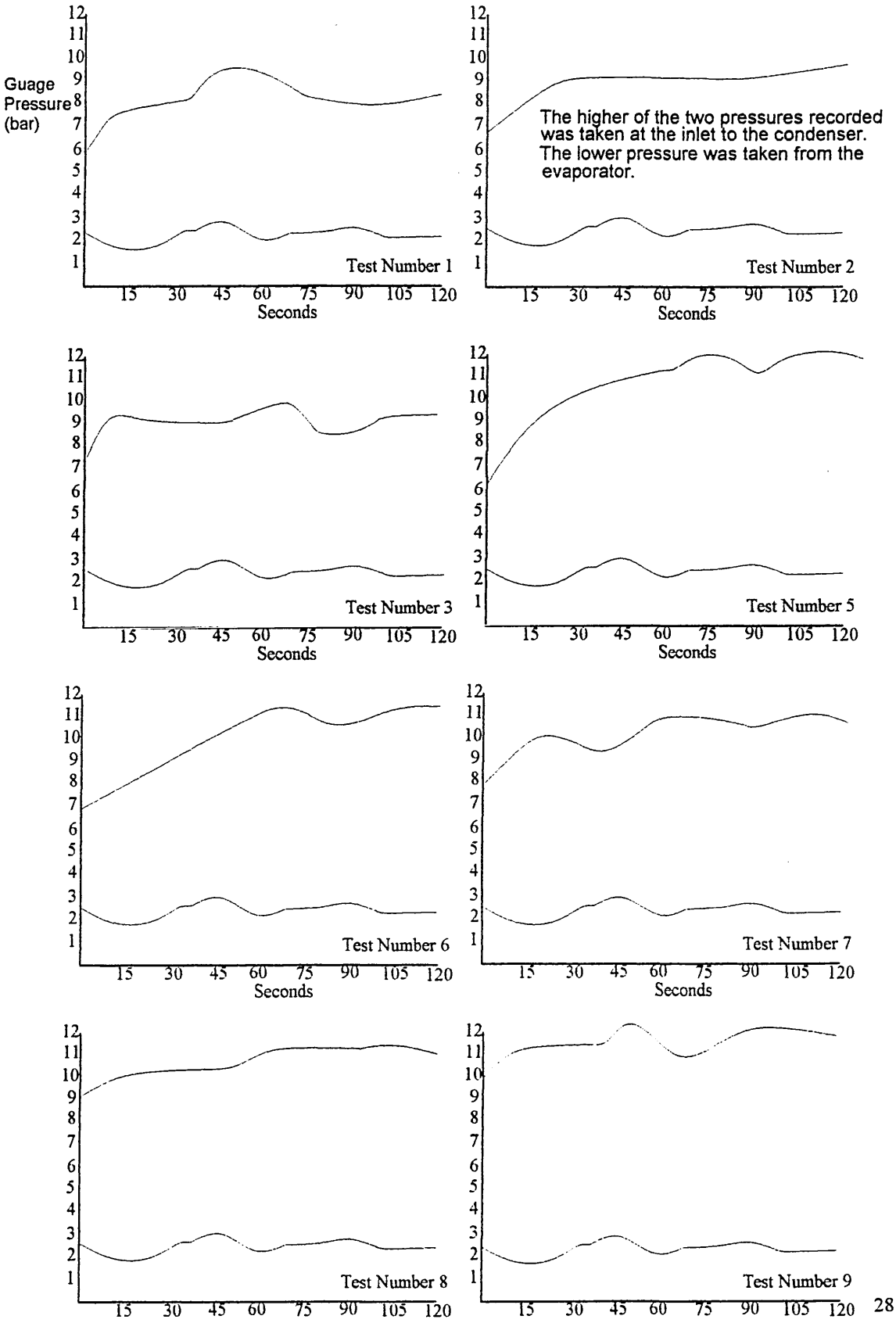

### 2.4.5 Condenser Water Temperatures During Tests

The above tests were made using town's water entering the condenser at approximately 15°C. The outlet water was put to drain. In practice the water flows in a closed circuit where the inlet temperature to the condenser would be in the order of 40°C to 45°C. The temperature rise and fall throughout the system is about 5°C.

## 2.5 DISCUSSION OF UNSTEADY STATE LABORATORY TESTING

A study of the transitory states when starting up and shutting off of the heat pump were made. Due to the relatively short time taken for the heat pump working temperature and pressure differences to decay after shutting off, the laboratory tests showed that a significant amount of energy was required to reinstate working conditions, even after short periods.

It was observed that immediately after shutting off, refrigerant pressure in the evaporator increased at the same time as the condenser pressure was reduced. It is concluded that after shutting off, the temperature drop at the heat pump was due to useful heat being transmitted to the building.

Lowering of the condenser/evaporator pressure differences could be due to either one or both of the following:

(i) the physical leakage of refrigerant to the evaporator, back through the compressor or through the expansion valve or,

(ii) a continuation of the heat transfer process, condensing the refrigerant static vapour in the condenser after shutting off and liquid evaporation in the evaporator.

Calculations on the results from laboratory testing based on the proportion of starting up time against normal operating time, indicated that the power used in the starting up period was 20% of the total power consumed, for the cycling shown in Figure 10.

Site conditions where the condenser operates in a closed water circulation system were not fully represented during these laboratory tests at Brighton Polytechnic. When the on/off cycling of the heat pump was being simulated, the effect of the thermal storage in the water distribution system

could not be accommodated on the demonstration heat pump being used. To truly represent these conditions, a programme of heat pump field trials would be required.

In practice, immediately after the heat pump shut off, the heat contained in the distribution system begins being emitted to the building with a consequential lowering of temperature. After start up however, an amount of heat must be produced by the heat pump and transferred to the heat distribution system before stable operating conditions are again obtained. The heat emission after shut off and heat generated to raise the heat distribution to its normal operating temperature have been assumed to be the same. The energy loss by the intermittent operation of the heat pump is considered to be that required to reinstate the refrigerant working pressure differential following the pressure loss whilst the heat pump was inoperative.

### 2.5.1 Literary Searches of Unsteady State Heat Pump Trials

Reports on the field trials referred to in paragraph 2.1 indicated that there was a considerable variation of cycling rates between domestic heat pump installations. The extremes of the sample taken were from 0.2 to 6 starts an hour. The cycling frequency tended to peak when atmospheric temperature was between 6°C and 8°C.

Results from field trials and laboratory testing of domestic heat pumps at the BP Research Centre, Middlesex [25], provide heat pump performance data at varying ambient air temperatures. Values of COP are given for both continuous and cyclic operation. With ambient temperatures of 15°C, the heat pump operates at part load conditions. The COP is reported to be 1.31, rising to 3.13 with the heat pump at full load. With low ambient air temperatures, the heat pump operates continuously and the COP falls from 2.06 to 1.50 with the reduction of temperature from 4°C to -6°C.

Reports of the field trials made available by private communications [19] and the laboratory testing by as referred to above [25], both confirm the findings of this laboratory research in that heat pump operation whilst on/off cycling, was found to be 80% of that achieved under

continuous operation. Following on from these studies of heat pump cyclic operation, research into how heat pump performance is affected by capacity and time controls are detailed in chapter 4.

## 2.6 HEAT PUMP FIELD TRIAL REPORTS

It is reported [19] that frosting of the evaporator did not produce a problem with atmospheric temperatures above 3°C, but below this temperature, frosting could seriously reduce the thermal output capacity of the heat pump. At -1°C the reduction in heating capacity was 19% with reverse cycle defrost and 25% with a hot gas defrosting system.

Two methods were employed to initiate defrosting. The fixed timer system of control proved to be the more efficient and reliable when compared to demand based systems. In the UK, the number of unnecessary defrost cycles by the fixed timer were found to be insignificant. The reports conclude that thermal losses caused by defrosting requirements have an insignificant effect on Seasonal COP. For systems where the design output temperature is below 3K, allowance needs to be made for loss of heat pump output due to ice formation in the evaporator.

# CHAPTER 3 - STEADY STATE MODELLING SIMULATION

## 3.1 INTRODUCTION

Performance of each of the major units in the heat pump were studied independently and also, in association with the heat pump laboratory experimentation. At this stage, the co-ordination of the performance of the compressor, condenser, refrigerant flow control valve and the evaporator needed to be produced. The long term objective being to study the procedures by which the seasonal thermostatic efficiency could be quickly calculated at the design stage. This would enable a heat pump design to be produced with a known thermal efficiency over the whole range of operating conditions and the seasonal COP before the start of manufacture. This would also be the maximum practically obtainable.

Study of the results obtained from trials using the Hilton heat pump demonstration unit, indicated that a greater understanding was needed of steady state operating conditions. Malfunction or mismatching of design of any one of the individual units forming the heat pump cycle could adversely effect its performance. A steady state model was required, therefore, to study the effect of the operating efficiency of individual units within the cycle. This chapter discusses the development and application of the steady state mathematical model.

## 3.2 PUBLISHED RESEARCH OF HEAT PUMP MODELLING

Research by James, Marshall and Saluja [26] produced a model based on an empirical analysis of experimental work to predict the behaviour of the heat pump in a variety of conditions. A simulation programme, produced by Domanski and McLinden [27], allows the preliminary evaluation of the performance and of the mixtures of refrigerant. Consideration was given to the statement by Ahrens [28], that the choice of the level of detail in modelling/simulation depends on the required accuracy.

Research into previous work on the subject of heat pump mathematical models was instructive. The mathematical model may be created by analysis of laboratory trials or, alternatively, built up from fundamental heat and mass transfer equations. It was found that a model based principally upon laboratory testing and empirical equations had the advantage of being the simpler approach, due to the reduction of the number and complexity of the equations.

## 3.3 PLANNING OF THE STEADY STATE MODEL

It was decided that to use empirical equations based on test results, could only supply satisfactory results over a specified small range of performance. To provide a model to meet the requirements for the flexibility of the research now being undertaken, it was decided that fundamental design equations, as applied to heat engine theory only, would be used. A survey of published literature did not reveal the details of a mathematical model that would satisfy the needs of this project. A decision was made, therefore, to produce a heat pump mathematical model based on the vapour compression cycle, using fundamental heat and mass transfer equations, such as those produced by Butterworth [29] and Hewitt and Taylor [30].

Whilst this research was being undertaken it became clear that refrigerant R12, on which the mathematical model was based, was soon to be abandoned. It was to be replaced by a more environmentally friendly refrigerant, but, at that stage of the research, the details of the replacement refrigerant were not known. The above approach in designing the mathematical model, was, therefore, kept as flexible as possible. Design procedures used in the mathematical model may be used for the calculation of performance with replacement refrigerants. The only change that is required to the model is to alter the thermodynamic properties pertinent to the replacement refrigerants.

Input data to the model includes compressor volumetric and isentropic efficiencies. To produce a steady state mathematical model of heat pump performance, the procedures of modelling and simulation were carried out as described below.

### 3.3.1 Performance Specification

This is a statement of operational requirements to be met by the heat pump. The operational feasibility of this specification was tested by preliminary design and calculation. The performance specification was to become the initial input data of the mathematical model.

### 3.3.2 Heat Pump Design Specification

The performance specification was used as a basis for the design of individual components that operate in a closed cycle and, together, form the heat pump. The heat pump design specification contains details of the operating cycle and the performance and capacities of the compressor, heat exchangers and the refrigerant control valve. Also included are energy inputs and outputs as well as the efficiency of operation. All of these data, in the form of a steady state mathematical model, produces these specifications. The Flow Diagram, Figure 13, shows the processes of calculation involved in producing this steady state mathematical model.

It is common practice for domestic installations to use a hermetically sealed compressor to prevent the leakage of refrigerant, with the benefits of lower noise levels and the high thermal efficiency. Details of the operation of hermetically sealed compressors will be discussed in later chapters.

### 3.3.3 Development of the Steady State Model

The first concept of the mathematical model was to produce, from a performance specification, the operational requirements for each of the individual units of the heat pump, in addition to predicting the actual thermal input, thermal output and operating efficiencies. Using the same fundamental equations, the performance specification (input data) of the model could be changed from the original program. This made it possible to further assess heat pump performance and simulate changes in this of individual units of the heat pump. Assessment of the effects of a change in design of any of the heat pump components can be obtained by using the same fundamental equations now used in the computer program.

## 3.4 STEADY STATE SIMULATION - DESIGN POINT CONDITION

The flow diagram in Figure 13 outlines the procedure followed in the construction of the mathematical model, starting with a study of the input data. In a practical situation, the items listed on the flow chart as input data would need to be studied prior to the start of detailed calculations. These are: space heating system, atmospheric conditions, heat pump design and heat pump control. It can also be seen in the flow chart, Figure 13, that at two stages, whilst the basic design of the heat pump is being formulated, the data and preparatory results from calculations should be reviewed to confirm that the design produces a practical solution and is the best one suited to meet the requirements of the initial specification. For example, it may be found that heat exchanger tube diameters and lengths may not be practical, or that the thermal performance may be enhanced by modification, in which case the design could be modified.

Calculations start at the compressor suction and follow the path of the refrigerant circulation. Being a closed cycle, the thermodynamic conditions of the refrigerant when the cycle is completed, must be identical to the input data adopted at the start of the calculations. For the purpose of the calculations, at each stage in the cycle the thermodynamic conditions being discharged from the unit immediately proceeding the one being measured, is taken to be the input conditions. With the exception of the compressor, no allowance is made for heat loss or gain to the surroundings.

The following is a brief description of the procedures adopted whilst developing the mathematical model shown at Appendix A3.1. The model is divided into five numbered sections, the first four sections referring to the principal units within the heat pump cycle, the fifth summarising items of heat pump performance.

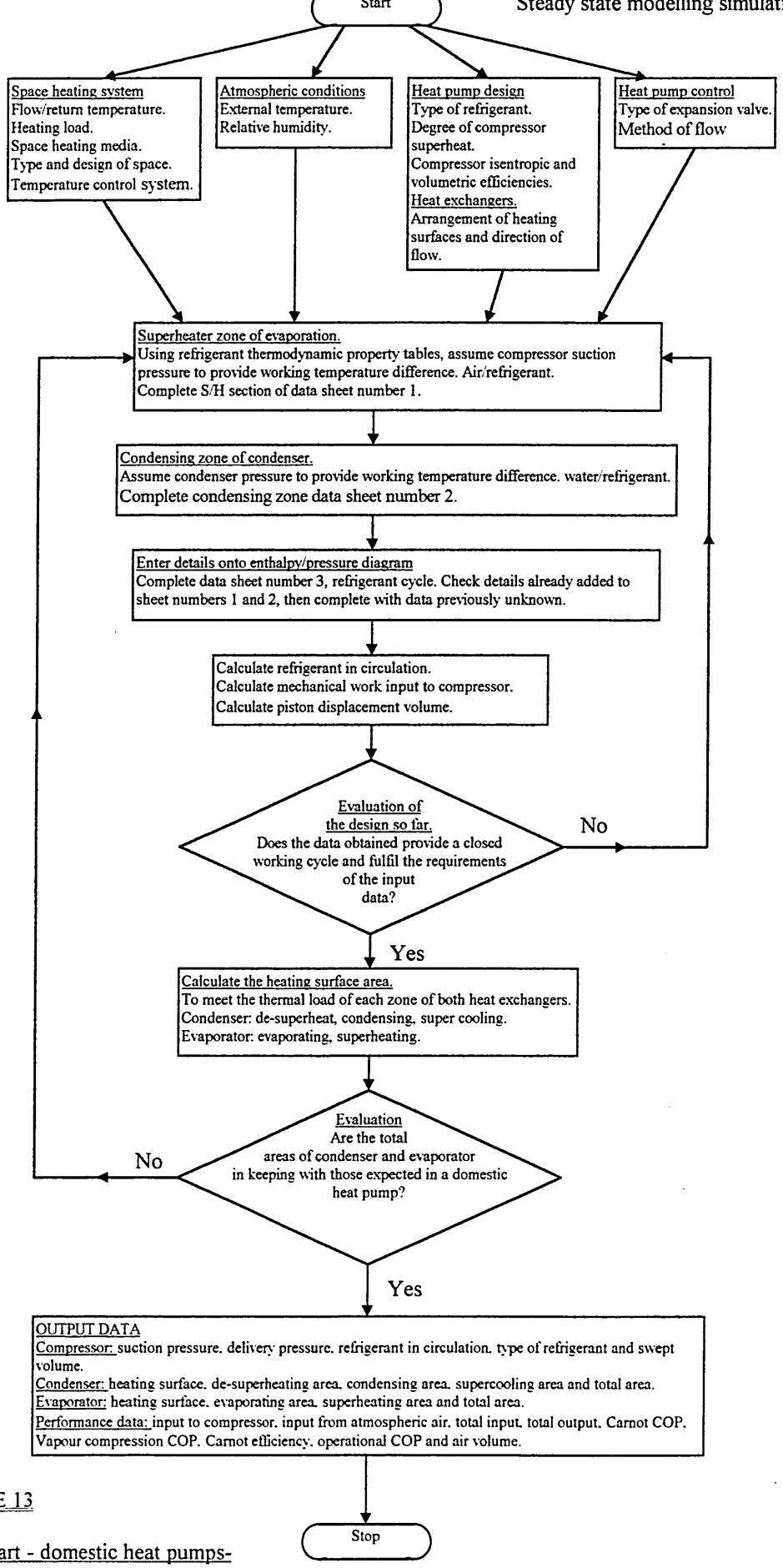


FIGURE 13

Flow chart - domestic heat pumps-mathematical model

### 3.4.1 Section 1 - *Compressor*

As previously stated domestic installations tend to use hermetically sealed compressors. This type of compressor recovers energy emitted from the drive motor windings and transmits it to the refrigerant at the compressor suction. On entering the outer shell and before entry to the compression cylinder, there is a pressure drop and a temperature rise of the refrigerant which effects heat pump performance.

The first step in the performance calculations was to decide on the thermodynamic properties of the refrigerant. Thermodynamic conditions of the refrigerant leaving the compressor and also the temperatures of refrigerant and water passing through the condenser are shown in. Figure 14.

#### 3.4.1.a Isentropic Efficiency

Assuming the compressor to have an isentropic efficiency of 60%, the specific enthalpy of the refrigerant at the compressor delivery was calculated. Isentropic efficiencies of this order are typical of hermetically sealed compressors.

#### 3.4.1.b Mechanical Performance

Compressor specifications required to provide the heat pump performance, were made by assuming the isentropic efficiency which enabled the specific enthalpy of the refrigerant at suction and delivery to be calculated. Volumetric efficiency was calculated from the compression ratio at which the compressor would be needed to operate, as outlined in section 2.2.1.

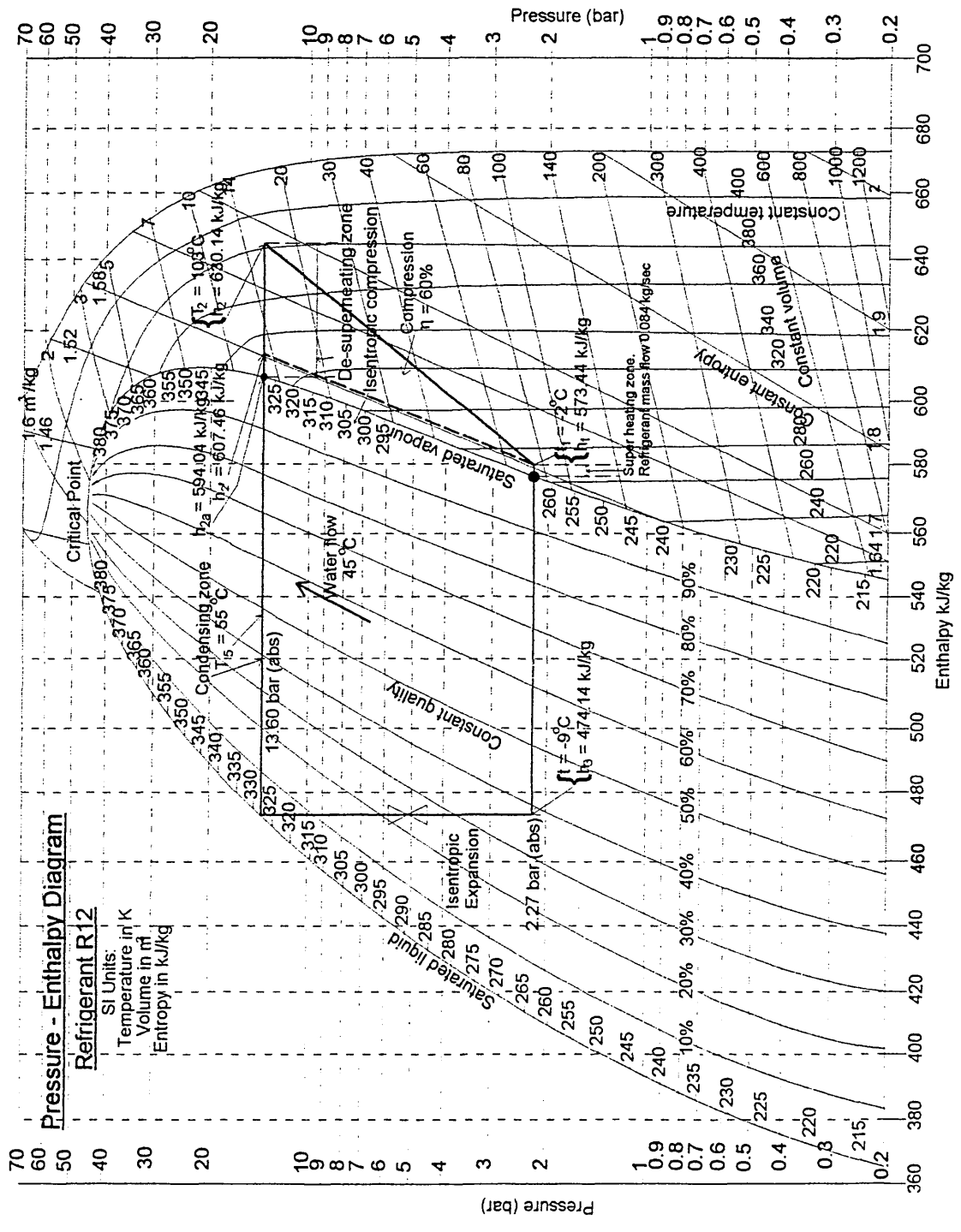


FIGURE 14 Design Conditions - Refrigerant Cycle Data Refrigerant R12.

### 3.4.2 Section 2 - *Condenser*

The condenser consisted of two concentric tubes, the cross section of which is shown in Figure 15. To reduce heat loss to the atmosphere, the refrigerant was positioned so as to flow through the inner tube, as it was at a higher temperature compared to that of the water circulation system. The cooling water is assumed to flow in the annulus between the two tubes, counter current to the refrigerant in the centre tube.

The overall coefficient for the flow of heat from the refrigerant to water was considered in three components. These were the forced convection through the film resistance to heat flow from refrigerant to the tube wall, conduction through the tube wall and the film resistance from the tube wall to the water.

The condenser was designed to be constructed longitudinally as one component, but for the heat transfer it was considered in two functional zones of heat transfer, the de-superheater followed by the condensing zone. Whilst the overall heat transfer coefficient differs between the two zones, the heat transfer film coefficient from the water to the metal tube, is assumed to be the same for both zones.

#### 3.4.2.a De-superheating Zone.

On the refrigerant side in the de-superheater zone, vapour is reduced from the superheated temperature delivered from the compressor, to the saturation temperature at which the condenser is set to operate. The mode of heat transfer in this zone is single-phase forced convection.

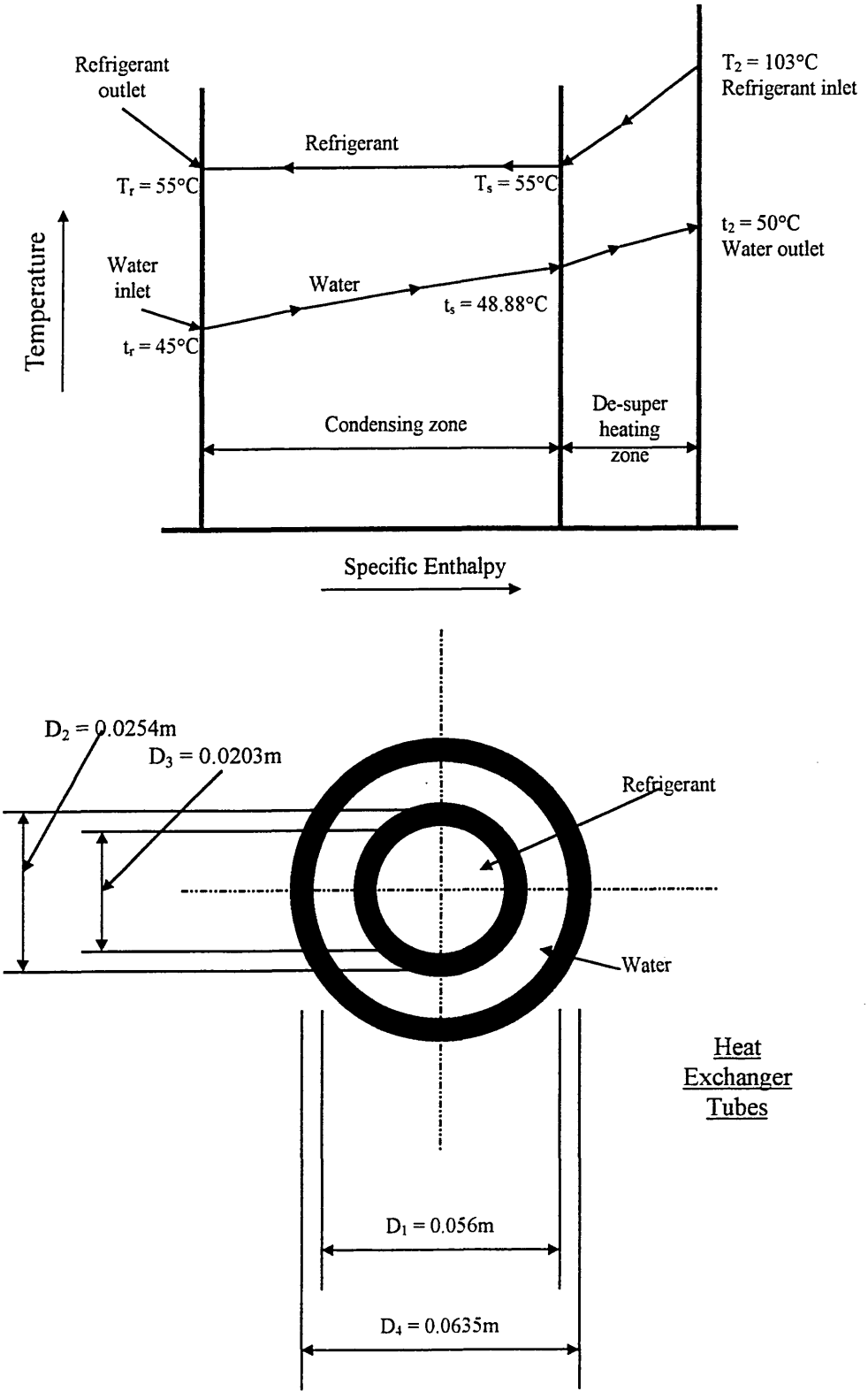


FIGURE 15

Condenser Design

3.4.2.b Condensing Zone.

The condensing zone is two-phase heat transfer, removing latent heat from the refrigerant and converting vapour to a liquid at the same saturated temperature and pressure. To calculate the rate of condensing heat transfer by change of state, forced convective condensation of the refrigerant inside a tube, there are two interdependent unknown values. The condensation rate per metre length of tube had to be found, in order to calculate the rate of heat transfer per square metre of heating surface. To deal with this, a nominal value for the tube length was estimated. Based on this assumed value, the condensation rate per unit length of the tube and the heat transfer area were calculated. Differing values for the estimated and calculated tube length were obtained. The calculated tube length was used to replace the previously estimated value and the calculation repeated until the estimated and calculated values were the same. For the above calculations, the computer was programmed to make a sequence of iterations on a closed loop until the energy transfer and the condensation rate were in agreement accurate to two decimal places. For the purposes of mathematical model at Appendix A3.1, the calculated tube length previously obtained by a sequence of computer calculations was used.

3.4.3 Section 3 - *Control Valve and Thermal Control of the Refrigerant Cycle*

A cross section showing the construction of a refrigerant control valve is shown at Figure 16. This valve modulates the compression ratio and refrigerant flow for the proportional control of the refrigerant superheat at the compressor suction. Increase of the compressor suction temperature above the high limit set at the sensing bulb, causes refrigerant inside the bulb to expand and increase pressure on the flexible diaphragm in the control valve. Raised pressure deflects the diaphragm, opening the valves to increase refrigerant flow. Modulation of refrigerant mass flow through the thermostatic valve, controls the amount of superheat at the compressor suction. Variously sized orifice assemblies are available, the size being selected according to the required refrigerant mass flow.

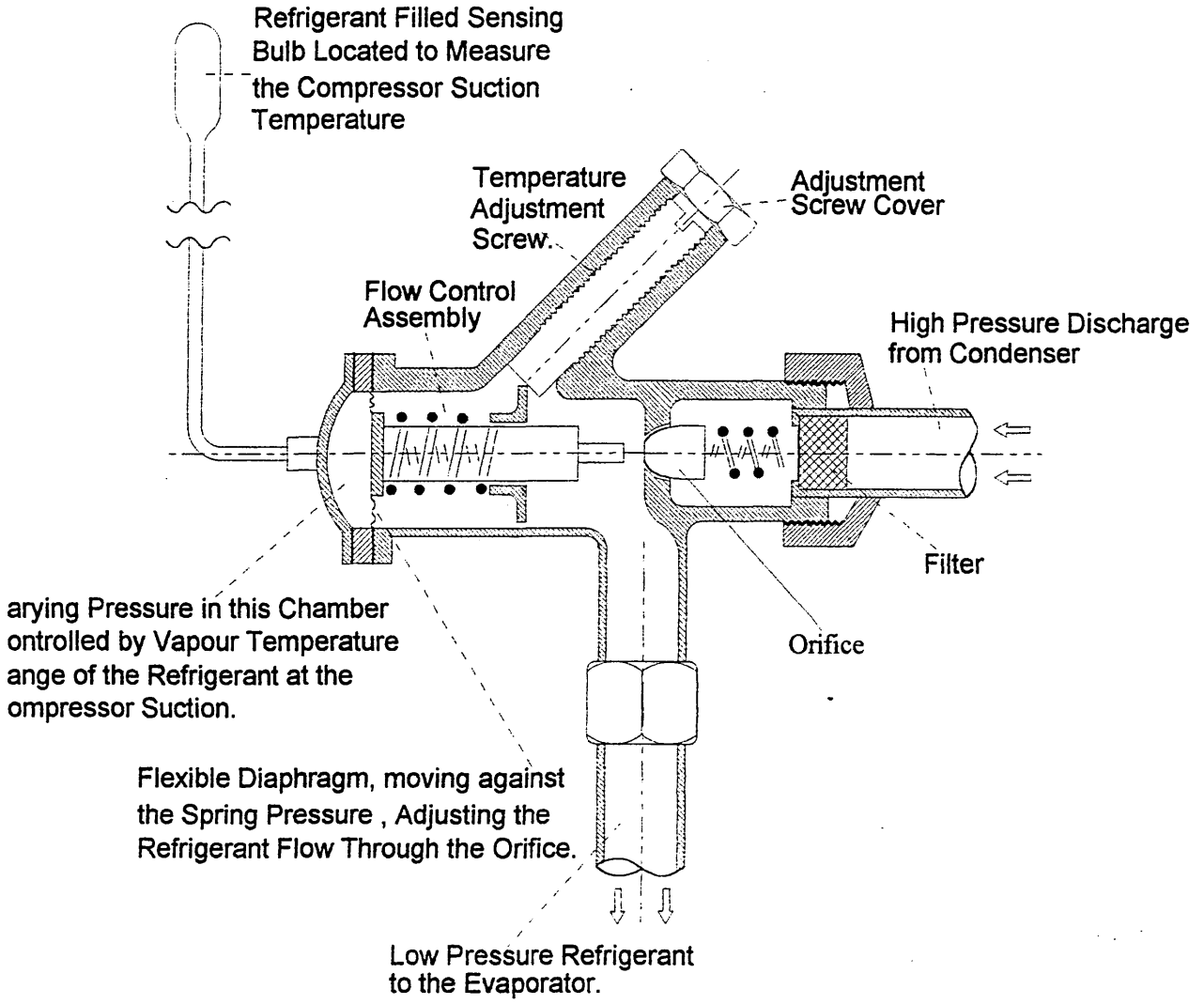


FIGURE 16 Cross Section of Thermostatic Control Valve

The thermostatic control valve was considered to be isenthalpic, because of the negligible change of specific enthalpy of the refrigerant flow through the thermal control valve. Refrigerant discharged from the condenser is normally saturated liquid, but after passing through the expansion valve, low pressure refrigerant entering the evaporator normally consists of both liquid and vapour. The refrigerant vapour discharged from the control valve serves no useful purpose whilst passing through the evaporator.

An increase of thermal output of the heat pump may be obtained by sub-cooling the refrigerant before it is discharged from the condenser. This would reduce the specific enthalpy of the refrigerant flow to the thermostatic control valve and reduce the dryness fraction or quality of the vapour entering the evaporator. Sub-cooling causes a reduction of refrigerant temperature that is limited by the water to refrigerant mean temperature difference for heat transfer.

Whilst deciding the operating temperatures and pressures within the refrigerant cycle for the mathematical model, it was noted that the minimum possible mean temperature difference (M.T.D.), was governed by the refrigerant temperature leaving the evaporator. If the energy gained from condenser sub-cooling could be utilised to superheat the compressor suction, the M.T.D. of the evaporator may be reduced. In addition to energy conservation within the refrigerant cycle, energy would be saved by reducing the pressure rise through the compressor.

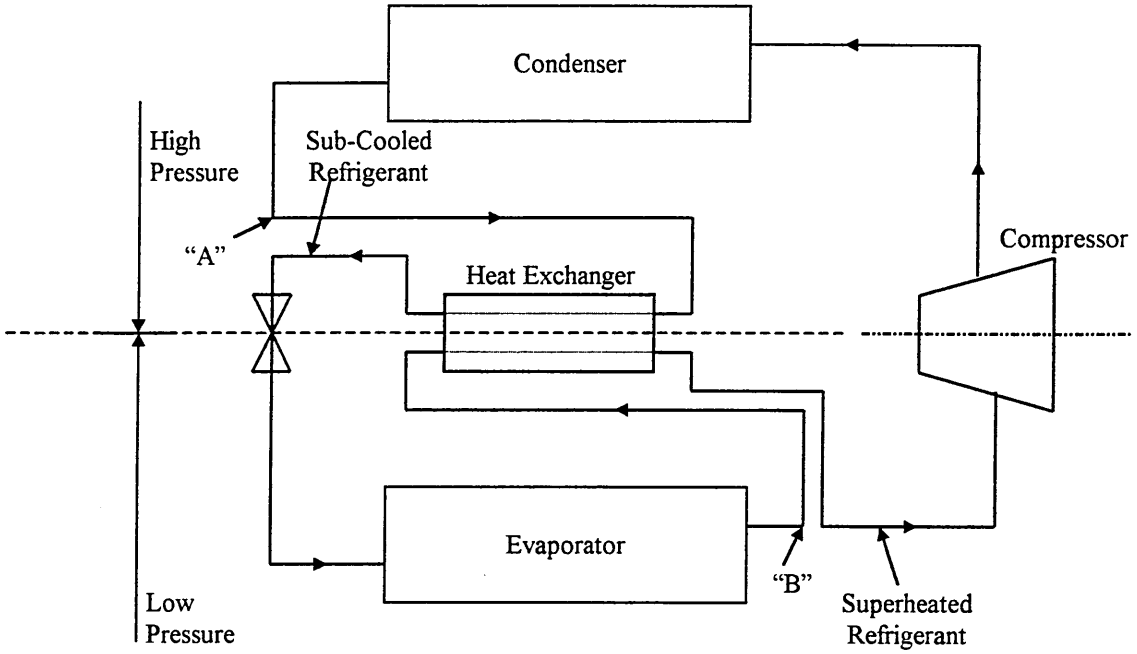


Figure 17

Heat Exchanger to Sub-Cool the High Pressure Refrigerant at Condenser Outlet, Point "A" to Superheat the Low Pressure Refrigerant at Point "B".

3.4.3.a Modifications to the Refrigerant Cycle.

Condenser Output - Sub-Cooling of the Refrigerant.

A change that frequently occurs within the refrigerant cycle is that the refrigerant is subcooled, prior to leaving the condenser. The benefits of a useful heat gain from this source are limited because it normally takes only a small reduction of the refrigerant liquid temperature and therefore only a small amount of heat is recovered, before the temperature difference between refrigerant to water is nullified.

Additional Heat Exchanger.

Another approach, designed to increase thermal output of the heat pump, would be to introduce an additional heat exchanger into the refrigerant circulation system. This would be installed in the refrigerant pipework between the condenser output and input to the control valve. The heat exchanger would be designed to sub-cool the liquid refrigerant leaving the condenser and provide additional superheat to the refrigerant immediately before entering the compressor.

In order to assess the increased thermal output of the heat pump, the operating conditions used for the initial calculations of the mathematical model and subsequently for the computer program, were used. See Appendix A3.1. A final temperature of the superheat was to be selected and therefore it was fixed at 32°C, in agreement with the CECOMAF test conditions. The details are shown in Figure 17 where a heat exchanger would extract heat from the liquid refrigerant at point 'A', to increase the superheat at point 'B'. This change causes an increased specific enthalpy gain of both condenser and evaporator.

The added heat exchanger, as shown in Figure 18, provides a 15% increase the specific enthalpy available to the space heating system, but to a great extent this is negated by a reduction of refrigerant mass flow in circulation, caused by changing conditions at the compressor suction. The actual refrigerant volume flow passing through the compressor remains unchanged but the superheat temperature increase, causes an increased specific volume of the refrigerant at the compressor suction, and therefore a reduction of refrigerant mass flow.

Refrigerant Mass Flow and Resulting Thermal Performance.

Neglecting any small pressure loss in the refrigerant flow through an additional heat exchanger, there should be little or no change to the compressor pressure ratio and therefore,

the suction volume at the compressor suction will not be subject to change. The increased degree of superheat at the compressor suction causes an increase to the specific volume in the refrigerant as shown in Figure 18. Due to the compressor suction volume remaining unchanged and the specific volume being increased, the refrigerant mass flow is reduced [31]. The thermodynamic property data of refrigerant R12 records an increase of specific volume of the refrigerant from $0.0727m^3/kg$ to $0.0828m^3/kg$. This indicates a 12% reduction of refrigerant mass flow and, therefore, a similar reduction in specific thermal output from the heat pump. However, overall the resulting gain in the heat pump output caused by the gain of specific enthalpy and reduction of refrigerant mass flow was estimated to be 3%.

The above calculations were based only on one set of operating conditions from which the above thermal performance was obtained. To be conclusive it would be necessary to examine a whole range of conditions, producing varying degrees of superheat at the compressor suction and therefore varying thermal output of the heat pump. From the above, it is indicated that the additional costs of the heat pump should be examined against the savings made.

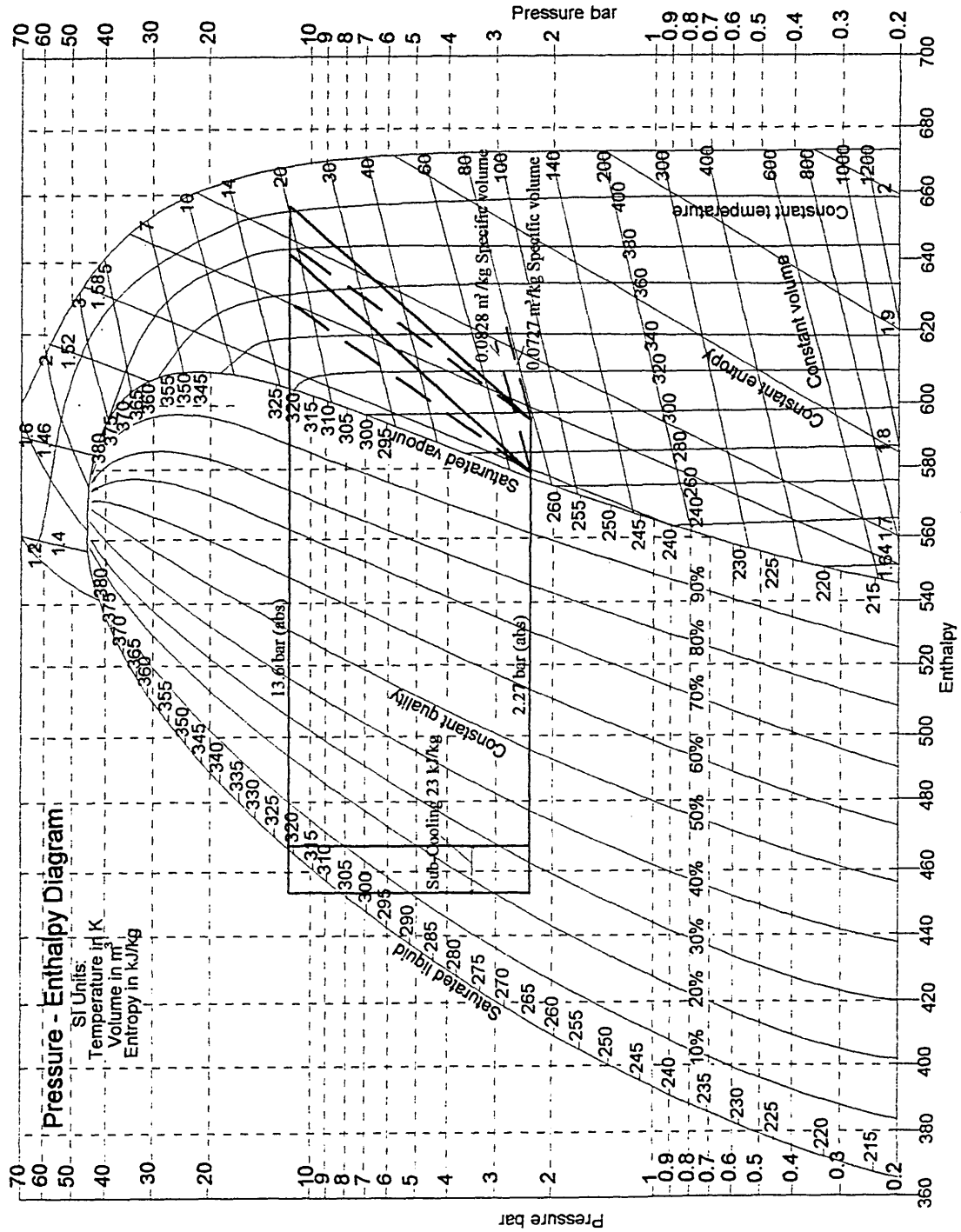


Figure 18

Additional heat Exchanger
Condenser Outlet / Compressor Suction

The Granryd Cycle

From calculations, it is suggested that the performance of the evaporator might be increased by 25% relative to the conventional cycle by use of the Granryd Cycle [32]. The basic Granryd cycle passes the refrigerant through a throttle valve, then into a flash chamber. The vapour then bypasses the evaporator and is returned into the circulation system at the compressor suction. The advantages of this are that the evaporator becomes smaller and more efficient, also it is a cheap and effective method of controlling refrigerant flow to the evaporator.

Based on the Granryd Cycle, the above reference outlines further developments where the energy may be saved. This includes installing a turbine to be driven by the expanding refrigerant, the energy recovered can be utilised to drive the compressor. There are aspects of these developments that cause concern, one being that periodic switching of the compressor to regulate heat pump output to meet the varying space heating loads may place excessive strains upon it.

### 3.4.4 Section 4 - *Evaporator*

Heat Exchanger Design.

For the purpose of design-point calculations, it was assumed that a cross flow evaporator consisted of two zones. The first is the refrigerant evaporation zone, where both sensible and latent heat are transferred from air to refrigerant, which changes phase from liquid to vapour. Following on from this is the refrigerant superheating zone where additional heat raises the temperature of the refrigerant before it enters the compressor. The heat transfer coefficient on the refrigerant side of the heat exchanger is calculated independently for each zone, but for the air side and conduction coefficient through the tube wall, there is assumed to be no change between the two zones.

The reason for dissimilar calculations on the refrigerant side of the heat exchanger between the two zones, is due to the differing mode of heat transfer. In the refrigerant evaporation

zone, the heat transfer is two phased, forced convection boiling and for the superheating zone, single phase, forced convection heat transfer.

Air flow over the heat exchanger tubes is driven by a fan. When compared to most liquids, atmospheric air, because of its low density, has a low heat transfer coefficient. To mitigate this effect fins are fixed to the external surface of the tubes to provide an extended heating surface. The heat transfer is increased over that of the refrigerant backed heating surface. When atmospheric temperatures fall below 5°C, atmospheric moisture contained in the air begins to freeze, depositing ice onto the fin extended heating surface. In severe conditions, bridging may occur causing a complete blockage in the air space between the fins. Restriction of the cross sectional area available for the air flow, caused by ice formation, reduces the thermal performance of the evaporator at times when the maximum space heating output is required. To reduce the probability of bridging, the minimum space between the fins is normally specified to be between 4 and 5 mm. The tube and fin dimensions on the evaporator are shown in Figure 19. The heat transfer coefficient for air side was calculated based on the fin dimensions and their spacing. Allowance was made due to the rate of heat transfer per unit area of the fins being less than that of the refrigerant backed area. Data required to calculate the mean temperature difference between air and refrigerant of both zones of the evaporator are shown in Figure 20.

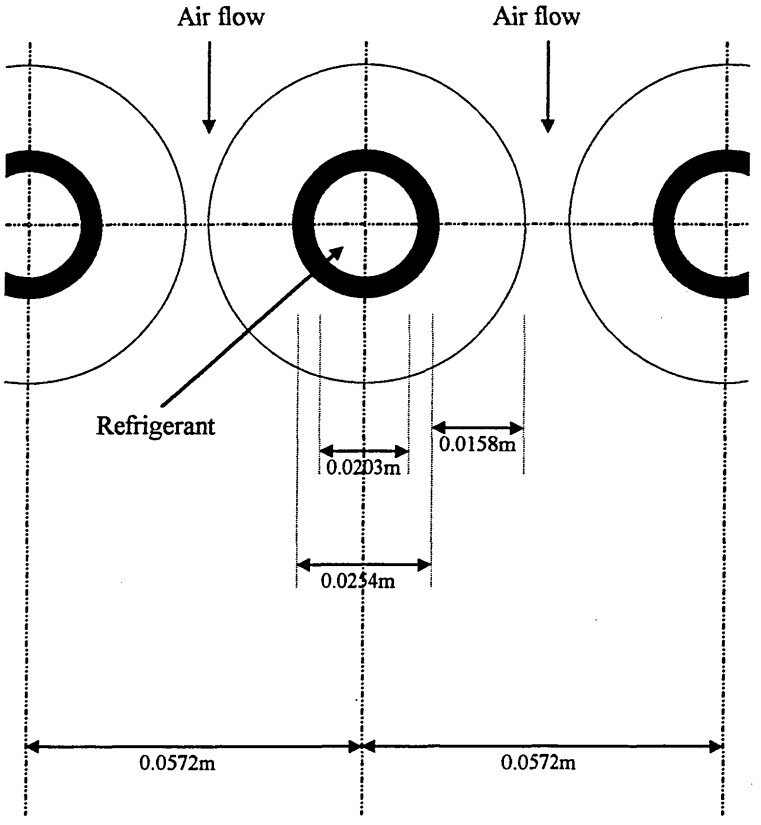


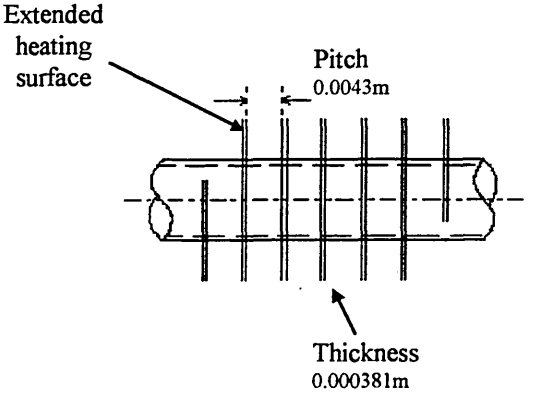


Cross Flow

FIGURE 19

Evaporator Heat Transfer Surface

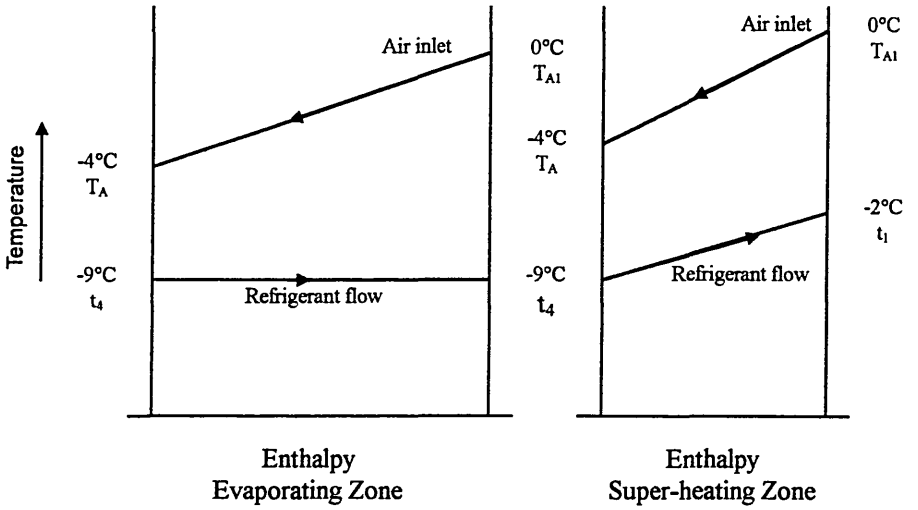


FIGURE 20

Evaporator Design Data

Evaporation Zone.

There are two distinct modes for boiling liquids, known as pool boiling and forced convective boiling. Pool boiling is that which is applied to a liquid within a container which is static until heated. Whilst being heated, agitation within the liquid is caused by the bubbles that are formed on the inner surface of the container breaking away and then moving to the surface of the liquid.

The other method, and the one used in these calculations, is forced convective, where fluid is impelled through a heat exchanger tube. The liquid and vapour temperature entering the evaporator zone are at saturation. There are, therefore, three regions of heat transfer in the change from liquid and vapour to fully vaporised. First within the liquid phase, bubbles are formed and then break away from the tube surface. In the second region there is an annular flow with a liquid film on the tube surface and a core of vapour with suspended liquid globules. Third is the dry wall region with suspended liquid globules that are subsequently evaporated. These processes of forced convective boiling are based on those described by Rogers & Mayhew [33].

The two phase, refrigerant side heat transfer coefficient for forced convection boiling was obtained from the summation of two heat transfer coefficients, namely the nucleate and the convective components. The large number of bubbles forming on the hot surface then

travelled through the liquid constituting the heat transfer by the nucleate component. Forced heat convection is the process by which heat is transferred through a fluid by the forced motion of the fluid through the tube.

Refrigerant Side - Superheating Zone

The single phase flow coefficient for the heat transfer within the superheat zone of the evaporator is designed to protect against liquid carry-over to the compressor. Refrigerant discharged from the evaporation zone, although theoretically refrigerant vapour, may contain liquid globules or mist which would cause damage to the compressor. The compressor is not designed to handle liquid and, therefore, a small degree of superheat is added as a safety factor to evaporate any traces of liquid carried over by the vapour. The heat exchanger is designed for cross flow air and refrigerant temperatures. A cross section of the tube, complete with the extended heating surface, are detailed on Figure 19.

Effect of Oil on Evaporator Performance.

Lubricating oil is necessary for efficient operation of the compressor, but there is an unavoidable pick up and carry-over of oil from the compressor to the refrigerant cycle. If necessary, an oil separator may be fitted to the compressor discharge, but dependent upon the type and quantity of oil in circulation, the oil can either hinder or enhance good performance from the evaporator [34].

Defrost

Following the field trials carried out by the Electricity Council in the U.K., it was reported that defrosting seriously reduced the heat pump space heating capacity during cold weather. At -1°C ambient, the reduction of heating capacity was 19%. At higher temperatures, loss of heating capacity becomes significantly less, being considered marginal at 3°C. The defrosting requirement was found to be insignificant in terms of seasonal COP, [19].

In the practical application of the domestic heat pump to space heating, loss of heat output due to defrosting must be considered according to location and exposure of the site. Climatic conditions tend to be diverse and are, therefore, not included in the model.

### 3.4.5 Summary of calculated results.

Thermal input and output are included as are the cycle efficiencies for the comparison of heat pump thermal performance. The following is an outline of the procedures adopted whilst developing the mathematical model, as shown in Appendix A3.1. The section numbers given below are those used in the model make reference to the individual components of the heat pump.

#### Space heating demand.

There are two operational conditions to be fulfilled by the space heating system. Firstly preheating prior to occupation and secondly in the steady state comfort conditions that are maintained during occupation.

#### Preheating Prior to Occupation.

Whilst preheating the dwelling prior to occupation and at times when the ambient temperature is above that of the design conditions, increased output from the heat pump is available. In these conditions, providing that the heat emitters within the heated space are suitably sized, a reduction in the time taken to preheat may be achieved. This can save energy because the reduction in the time taken for preheat reduces the time that heat energy is being lost by air leakage from the heated space and through the building fabric.

Another consideration is to optimising start time control systems by scanning atmospheric and room temperatures with the object of delaying start-up of the preheat period to the latest cogent time. Heat pump sizing has an effect on this issue, because if it is increased, it could

reduce the warm-up period. This increases the economy of the system, particularly if the dwelling is intermittently occupied throughout the day.

## 3.5 SEASONAL PERFORMANCE - PART LOAD & OVER LOAD CONDITIONS

The mathematical model previously discussed, details heat pump performance at design load conditions. When compared with the deviancy of the space heating load throughout the heating season, this is shown to be applicable infrequently over the course of a year. The object, therefore, when designing a heat pump, should be to review the whole range of operating conditions and the frequency at which they occur. Design of the heat pump could then be directed to obtaining maximum seasonal COP and minimum annual energy consumption.

### 3.5.1 Heat pump Performance at Part Load Conditions.

Changing conditions within the heat pump cycle, due to changes in ambient temperature are shown in Figure 21.

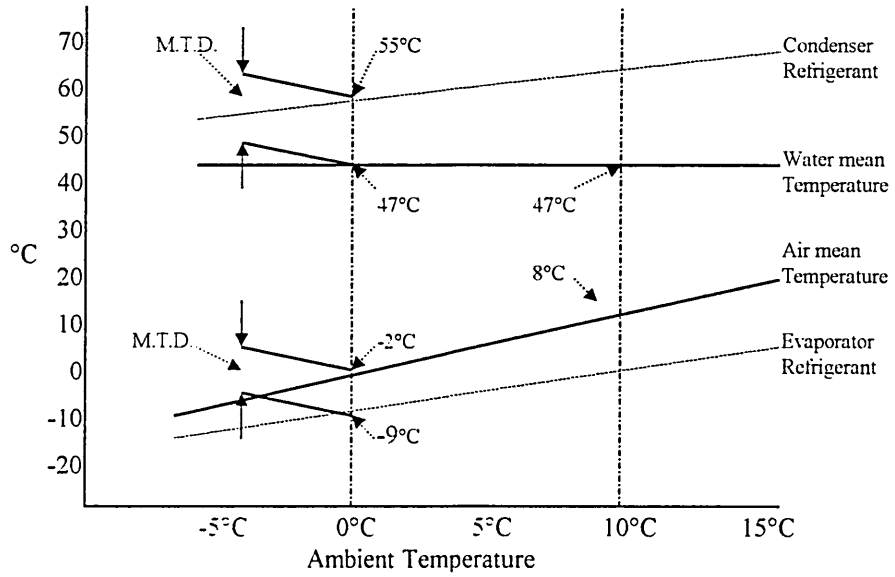


FIGURE 21

Steady State - Part Load Conditions

To procure the unknown condensing and evaporating temperatures at part load conditions.

Figure 21 shows the thermodynamic conditions, taking an example of an atmospheric temperature of 10°C.

Design point conditions at the air inlet are shown to be 0°C. The temperature drop of the air through the evaporator is known to be 4K and, therefore, the mean temperature is shown to be -2°C. At the design point, water flow temperature from the heated space enters the condenser at 45°C and leaves the condensing zone at 49°C, the mean being 47°C. Operating details at the design conditions are shown on the pressure enthalpy diagram, Figure 22. The set control at 5K superheat at the compressor suction and the mean condenser water temperature are unchanged when atmospheric temperature increases, but the operating mean temperature difference in the heat exchangers of both condenser and evaporator increases. Under this change of operating conditions the thermal output of the heat pump is enhanced.

In practice a range of operating conditions, both above and below the design point, would be calculated to accomplish a representation of the seasonal conditions. Seasonal change of air temperature entering the evaporator is shown, but the water temperature, being thermostatically controlled, is assumed not to change due to the seasonal ambient changes.

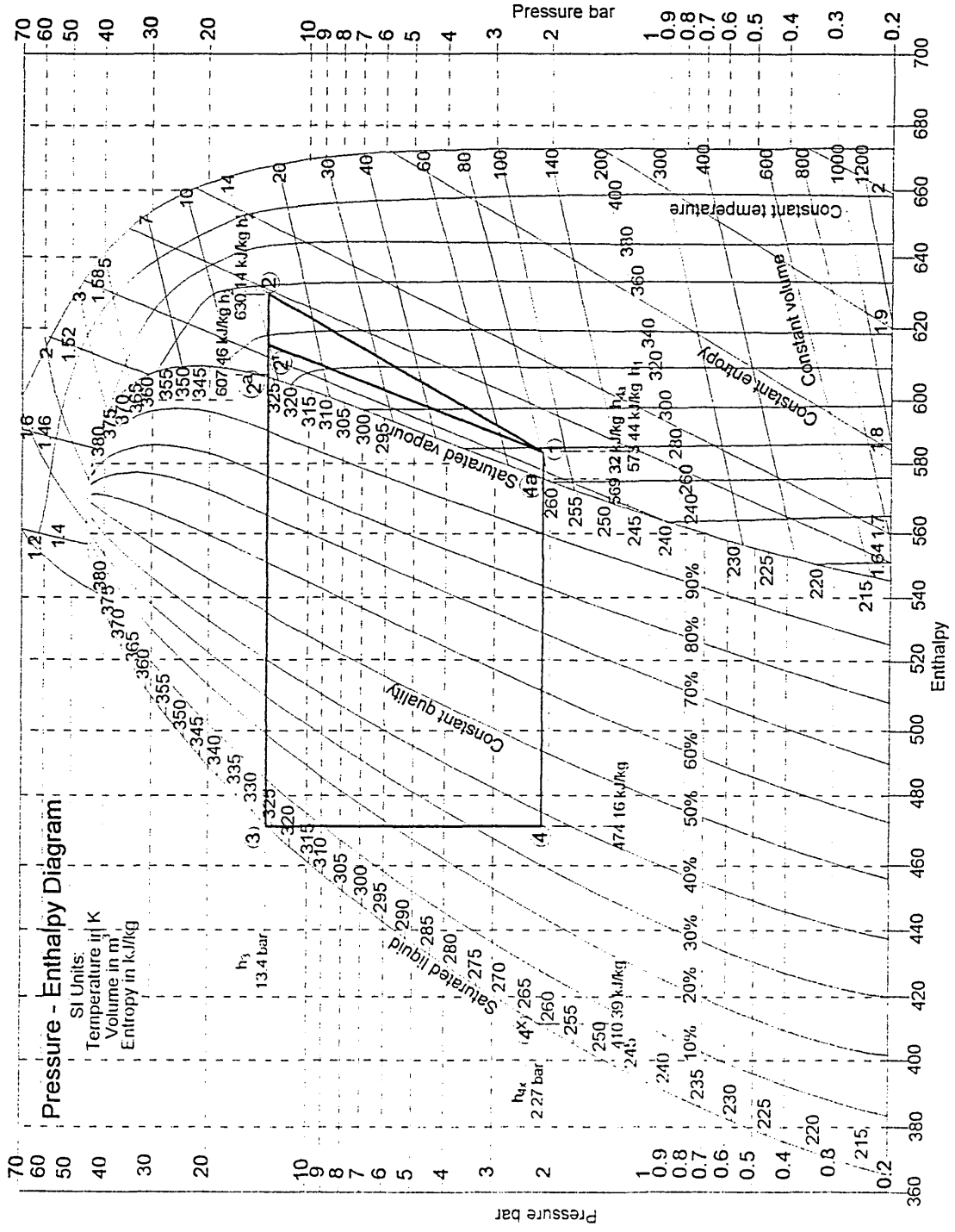


Figure 22

Values of enthalpy
R12 Refrigerant

Figure 23 shows a thermal performance chart of a heat pump compressor for a range of evaporating and condensing temperatures. It is representative of performance data presented by manufacturer. The mathematical model allows for an open compressor whereas the data shown in Figure 23 is for the hermetically sealed compressor normally used for heat pumps applied to domestic space heating systems. The performance of the hermetically sealed compressor is discussed later.

### 3.5.2 Compressor Efficiency at Part Load Conditions.

A calculation has already been made of the compressor isentropic efficiency at design load conditions, but it would be an advantage to survey manufacturer's data to find the compressor with the highest seasonal efficiency. The process by which this is done is by the use of compression efficiency maps as suggested by Gluckman [35]. For the compressor being considered, the illustrated contours of constant isentropic efficiency plotted against condenser and evaporator temperatures, enabling the whole range of operating conditions to be studied is shown in Figure 24. The efficiency contours are shown for two reciprocating compressors, similarly sized, 'A' being semi-hermetic and 'B; open. It was noted by the editor of reference [35], that, in this case, the open compressor was shown to be the higher efficient machine and was also cheaper. The approach using lines of constant compressor isentropic efficiency to calculate heat pump efficiency at varying atmospheric temperatures can be made. The total, annual duration of any particular load condition may be obtained from the heating analysis chart.

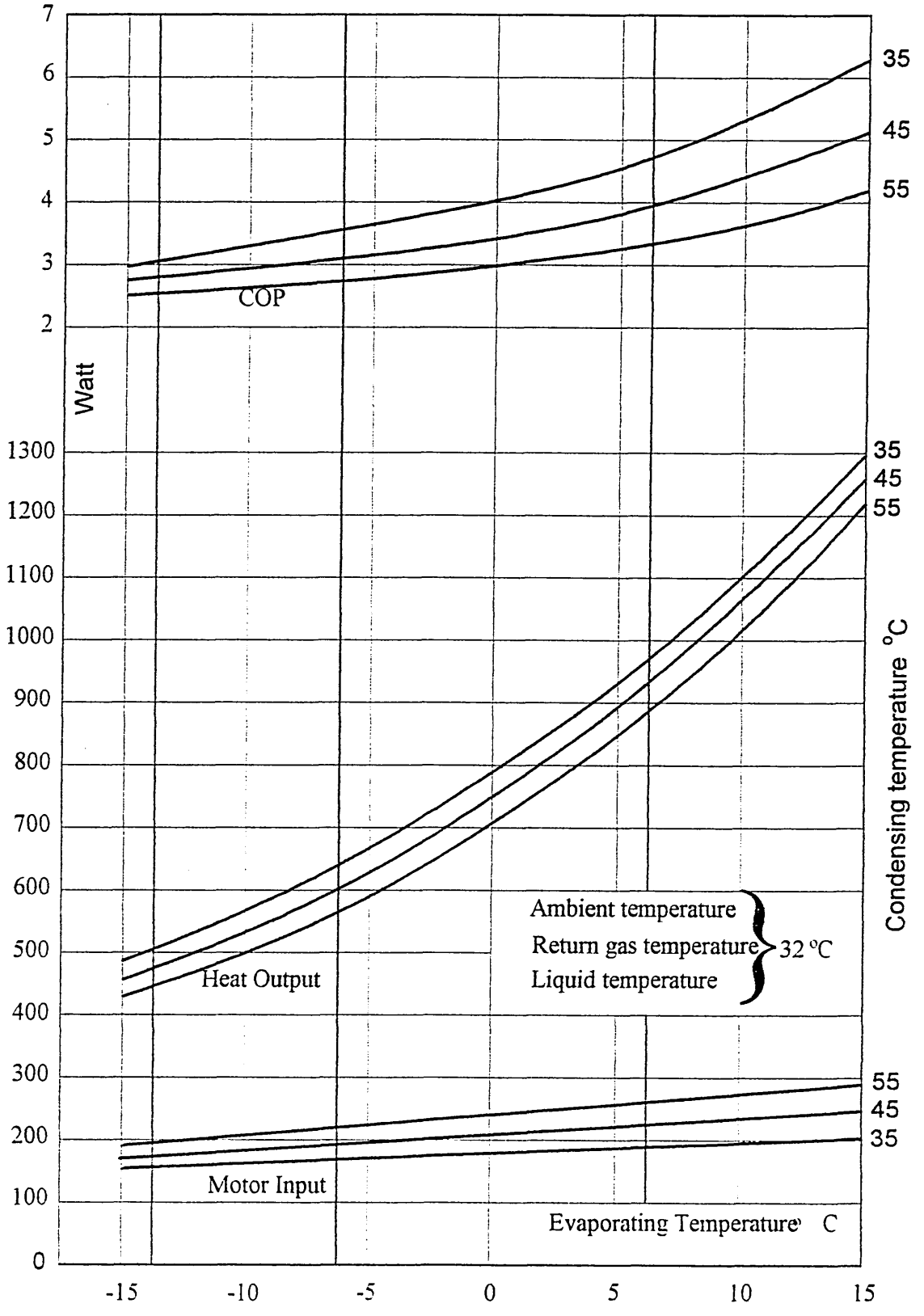


FIGURE 23 Thermodynamic Performance of a Hermetically Sealed Compressor

(Danfoss compressor FR7H)

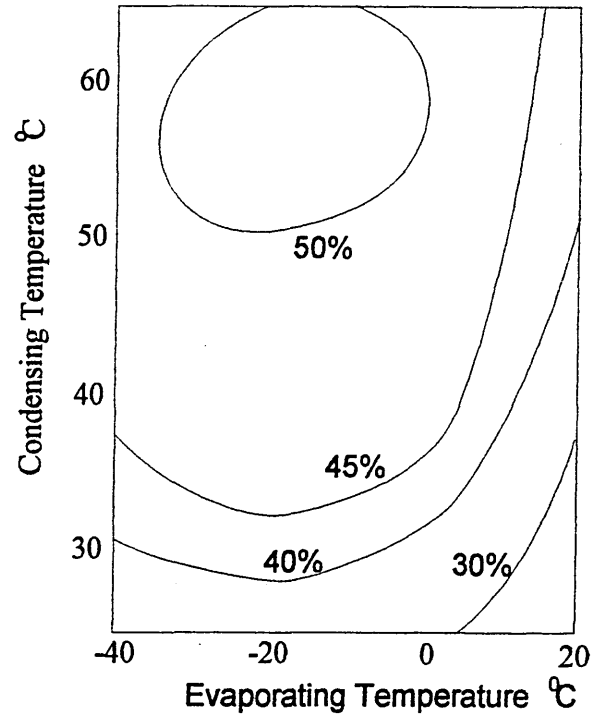


(a)

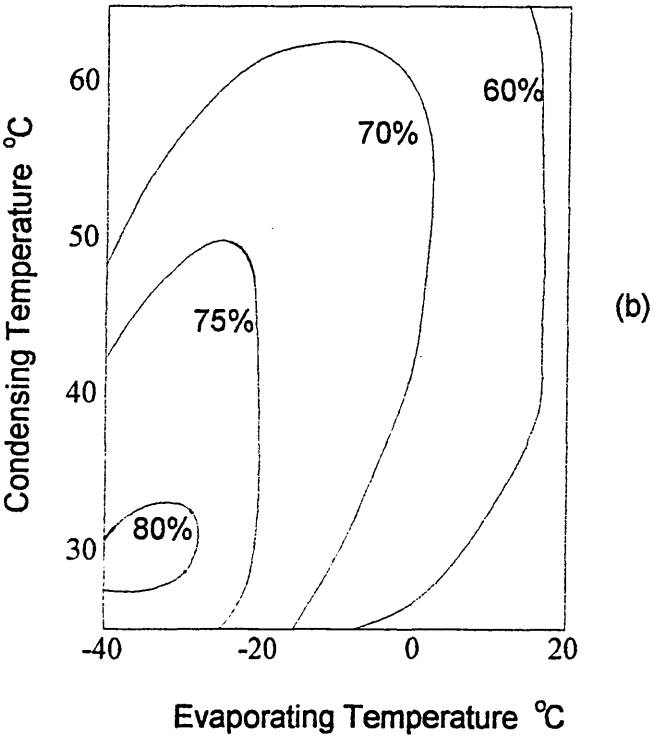


(b)

FIGURE 24 Compressor Efficiency Maps

Contours of Constant Isentropic Efficiency

### 3.5.3 Refrigerant Mass Flow

To enable the electrical input and thermal output of the compressor and the performance of the heat exchangers to be calculated, the refrigerant mass flow through the compressor must be calculated.

### 3.5.4 Heat Analysis Chart.

The effect of varying climatic conditions on heat pump performance may be acquired by study of a heat analysis chart. Charts are available covering weather for diverse locations in the U.K., Figure 25 being one example. Percentage heating demand for the heating season on the heating analysis chart was divided into six sections. Dotted lines from the x-axis to the y-axis enabled the number of days per annum in each section to be identified on the y-axis. The thick continuous lines in the middle of each section indicated on the x-axis, show the mean percentage load for that section. The increase of heat output caused by the rise of ambient temperatures above that of the design load, need to be taken into account when operating times of the heat pump are calculated.

### 3.5.5 Thermodynamic Properties Input to Computer Program.

The properties of the thermodynamic values of the refrigerant R12 required for the computer program were taken primarily from tabulations by Raznjevic [36] and Wilson [37].

The mathematical model and computer program were intended, initially, to calculate the design and construction of the four main units making up the heat pump cycle at the design conditions. Following on from the initial calculations, the computer program was designed to calculate the changing performance, if, for example, the seasonal thermal performance of the heat pump was required.

To calculate the seasonal thermal performance of the heat pump, the changing thermodynamic properties of the refrigerant, due to changes of temperatures and pressures, need to be entered into the computer program. To comply with this requirement, the calculations would be made at design and part load conditions.

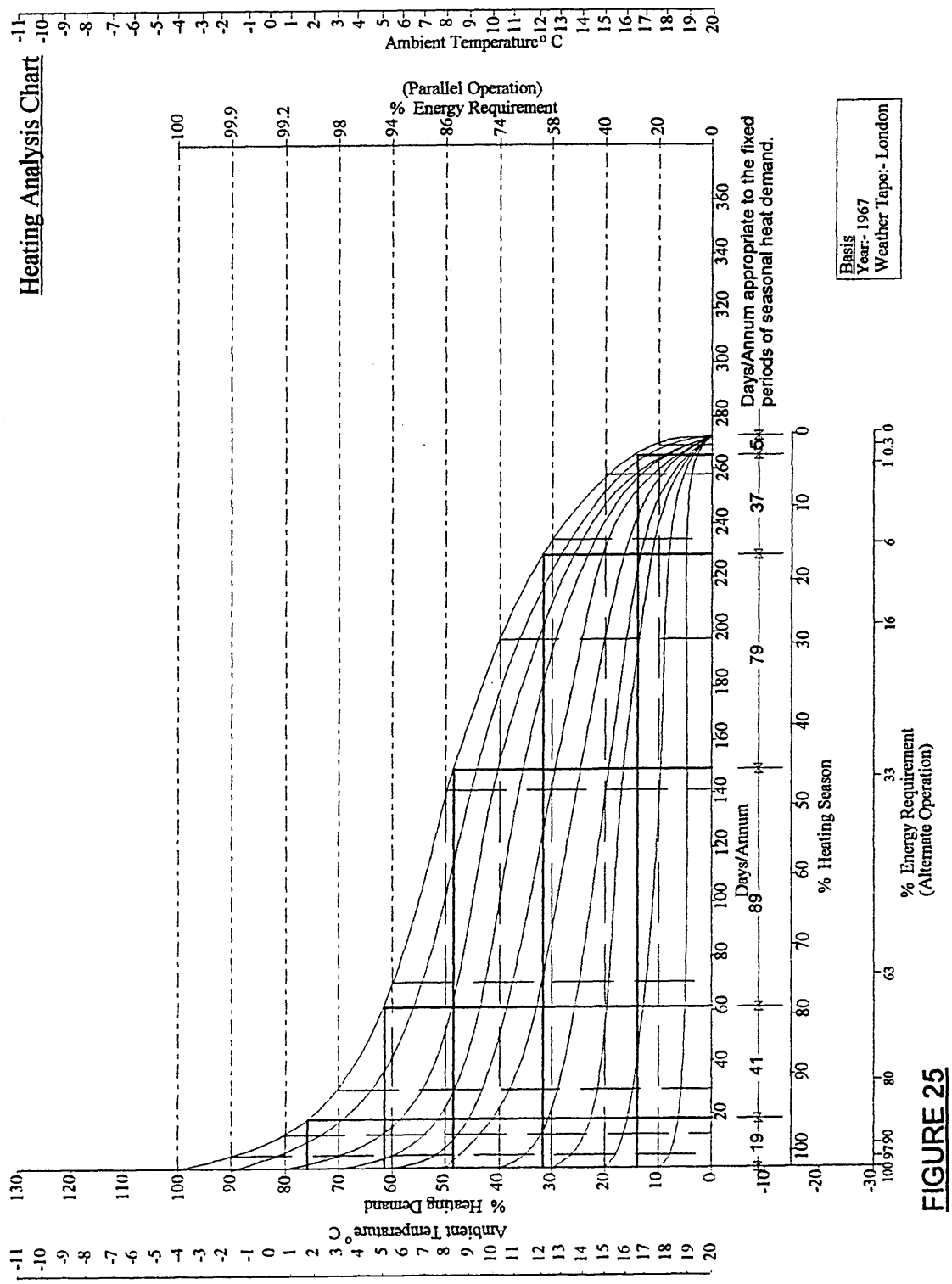
Heating Analysis Chart
Ambient Temperature° C
(Parallel Operation)
% Energy Requirement
Days/Annum appropriate to the fixed periods of seasonal heat demand.
Basis
Year:- 1967
Weather Tape:- London
% Heating Demand
Ambient Temperature° C
Days/Annum
% Heating Season
% Energy Requirement
(Alternate Operation)

FIGURE 25

It was found that changes in refrigerant thermodynamic properties was a time consuming process. With the objective of saving time when reprogramming the computer, techniques of obtaining equations were used, based on thermodynamic property tables for refrigerant R12. The techniques involved formulating equations for the whole range of operating conditions of the heat pump, to the accuracy required, once again were found to be time consuming and protracted [38] [39]. The method of simultaneous equations shown in appendix A3.5 were used with relatively simplified computer programs and time saved[54].

## 3.6 Summary of Heat Pump Performance Calculations

Development of the design procedures of the various parts, which when assembled, went together to form a domestic heat pump was an instructive exercise. From this, a clearer understanding was obtained of the heat exchangers and heat transfer and changes in state of the refrigerant within the thermodynamic cycle.

The refrigerant, upon which the above calculations were based being R12, was made redundant but the methods in the mathematical model and computer program are applicable to any refrigerant used for domestic heat pumps. When using any other than refrigerant R12, the appropriate properties of the adopted refrigerant being used, needs to be inserted into the computer program. This includes the appropriate values of the physical properties of the refrigerant at the working conditions of temperature and pressure. The process involved in the refrigerant change being first the development and selection of suitable replacement refrigerants and then the physical properties needed to be ascertained by the refrigerant manufacturers. For the design of a domestic heat pump using, what are now known as environmentally friendly refrigerants, the appropriate physical properties was needed to be applied. The refrigerant R134(a) was used in the future research, but at that time, the physical properties referred to above were not available.

A number of appendices regarding the domestic heat pump performance are included. The first being the basic mathematical model at steady state performance of the refrigerant cycle.

This is accompanied by three subsequent appendices providing additional information. Appendix A3.2 lists computer constants, where each item is numbered for identification in the computer program, together with the units used.

Correction factors for the mean temperature difference of cross flow through the evaporator of refrigerant and atmospheric air, can be obtained from graphical data in appendix A3.3. Factors for the correction components enabling the nucleate-boiling suppression factors to be obtained, are also included. Appendix A3.4 provides a copy of input and output data from the computer program.

Also listed in appendix A3.5, are the various equations intended to be used to calculate thermodynamic properties of the refrigerant from known values of refrigerant pressure and temperature [36] [37]. Progress was made, but in order to obtain equations with the necessary accuracy to cover the whole range of values of pressure and temperature required for the mathematical model, the task became extremely time consuming and, therefore, a distraction from the main objective of the research. This item was set aside for the present.

CONCLUSIONS

The steady state model enables a designer to see how changers in individual components affect the overall performance of the installation.

The compressor efficiency maps can be used to select a compressor which will operate efficiently for the required duty.

The model shows that the output from the heat pump varies considerably throughout the whole heating season. Similarly the heating load is weather dependent. Using a heating analysis chart and the steady state model the designer can predict the cycling of the heat pump system thoughtout the season.

# CHAPTER 4 - DESIGN OF THE SPACE HEATING SYSTEM

## 4.1 INTRODUCTION

This chapter discusses ways in which the thermal efficiency of the space heating system may be adversely affected if the heat distribution system and its controls are not properly designed and installed. This principally entails matching thermal output of the heat distribution system, which consists of the water distribution pipework and heat emitters, to the space heating load. Thermal performance of the space heating system was studied for the following periods:

(i) prior to occupation during the preheat period, and

(ii) during the period of occupation when the comfort conditions are being maintained.

UK climatic conditions were studied together with the thermal effects of the building construction. This included a study of the provision of additional heat to supplement heat pump thermal output on very cold days.

## 4.2 MATCHING HEAT PUMP OUTPUT TO THE LOAD

The water circulation system transports heat from the heat pump to the emitters within the heated space. Both the water circulation system and the heat emitters need to be sized and designed to match the thermal performance of the heat pump. Matching heat supply to the thermal load poses some problems, because of the rise of atmospheric air temperature above the design point condition, causing the heat pump output to increase, as discussed in Chapter 3. The space heating load reduces under the same change of atmospheric conditions. The anomaly is compounded, because, whilst changes of atmospheric temperature alters heat pump thermal output, the output of the distribution system remains ostensibly the same.

In commercial office buildings, the energy used to preheat the building prior to occupation can be up to 50% of the total space heating energy consumption. Because of the different mode of occupation, the proportion of energy used to preheat domestic dwellings is generally lower than that for commercial offices, but it is considered that this subject is worthy of study.

### 4.2.1 Space Heating Prior to Occupation

Energy losses from the structure to the atmosphere are reduced by preheating the building in the shortest possible time. To do this the maximum possible thermal input rate is required. The sizing of the heat pump, the thermal emitters and the time control system were studied.

During the preheat period, at times of the year when atmospheric temperatures are above the design point, if the heat emitters are designed to match the heat pump output at design point, the full capacity of the heat pump is not realised. Under these conditions, COP will be reduced due to heat pump on/off cycling and the preheat period will be extended.

### 4.2.2 Space Heating During Occupation

Problems associated with matching output of the heat emitters to the heat pump during preheat, apply equally to the occupation period. In addition, a study was made of the water temperature control and capacity control systems. The speed of thermal response of the heat distribution system and on/off cycling frequency whilst controlling room temperature may adversely effect the efficiency of the installation.

## 4.3 DESIGN OF THE HEAT DISTRIBUTION SYSTEM

Losses caused by on/off cycling of the space heating system, as established by laboratory testing were discussed in chapter 2, paragraph 2.5. Cycling frequency is affected by the amplitude of the temperature fluctuations and by the speed of response to temperature change of the heat distribution and temperature control systems.

### 4.3.1 Notional Time Constant of Heat Distribution System

It was found in a study by Pepper and Smith [40] that a number of design features of the heat distribution system effect the notional time constant. This, in turn, effects the heat pump cycling

frequency and the efficiency of the installation. The main items of design effecting efficiency are flow/return water temperature difference, single or two pipe water distribution system and thermal storage within the water circulation system.

### 4.3.2 Temperature Difference - Water Circulation System

The notional time constant of a heat distribution system is increased by designing for an increased temperature differential through the heat emitters as shown in Figure 27. From this, it is ascertained that a design that provides an increased temperature drop through the system, reduces mass flow of the circulating media and reduces the cycling frequency. Increased temperature differential through the heat distribution system has the advantage of reducing the return water temperature to the heat pump. This increases the M.T.D. in the condenser and, therefore, increases the heat transfer.

If the condenser is designed for counterflow, the possible level of refrigerant sub-cooling is increased and the additional heat taken from the high pressure refrigerant increases the thermal output and COP of the heat pump.

### 4.3.3 Pipework Design - Water Circulation

From the data supplied on notional time constants, the thermal response of the two-pipe system would appear to be slower on start up than the single-pipe system. The single-pipe system has the advantage of a quicker response on start up but in continuous operation, the two pipe system provides a more unified distribution throughout the dwelling [40]. Therefore the choice of mode of circulation for a space heating system supplied from a heat pump favours the two-pipe water circulation system.

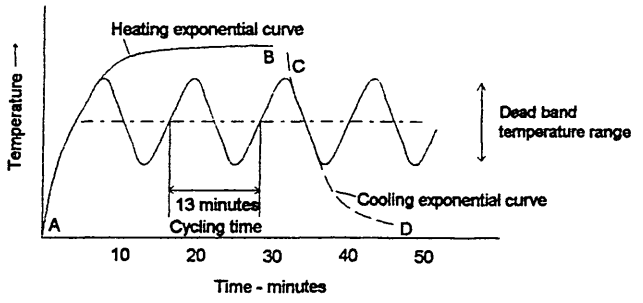


On / off cycling time
Notional time constant 4 minutes

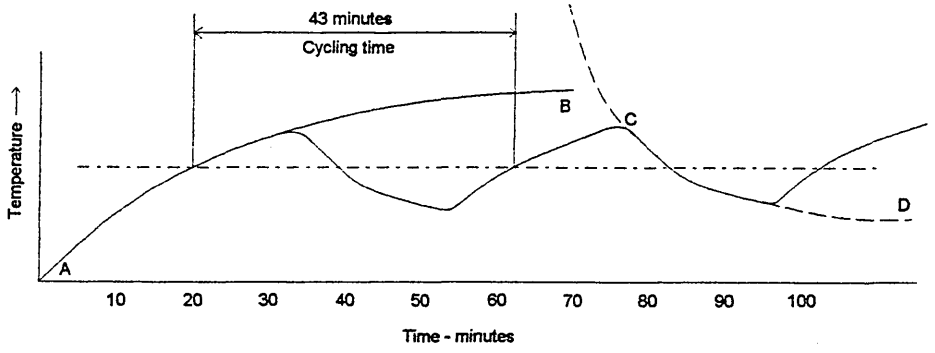


On / off cycling time
Notional time constant 20 minutes

Figure 27 Heating Notional Time Constant

### 4.3.4 Thermal Storage

To supplement the thermal storage that is normally inherent in the heat pump installation, additional storage may be built into the refrigerant circulation system. This may be either on the high or low temperature side of the heat pump [41], or alternatively into the water circulation system.

Increased thermal storage has the following advantages:

(i) storage of heat by use of the electricity at lower priced off peak tariff,

(ii) reduce the on/off switching frequency caused by the heat pump capacity control system,

(iii) to improving stability and energy balance of the installation, and

(iv) increase of COP and reduction of heat pump design capacity by levelling out peak loads.

## 4.4 TIME AND CAPACITY CONTROL

Automatic control systems are available to switch on the space heating system at the optimum time to preheat the domestic dwelling to comfort conditions ready for occupation. During the period of occupation, output of the space heating system is normally capacity controlled to the predetermined temperature fixed by the occupants. The optimum time taken to preheat the building for occupation varies due to changing external and internal temperatures throughout the heating season. An alternative to automatic control is for the occupant to manually adjust the start up time to the seasonal space heating requirements.

Dale and Crawshaw [42] discussed the advantages of a manual control loop process of observe, think, decide and, if necessary, act. In doing this and in the utilisation of previous experience, learning and memory are involved. They proposed the installation of a seven day time controller, with adjustable on/off time switch which is reviewed by the occupants. In the intervening years, this has been achieved whereby even domestic systems have programmable controllers.

Programmes for optimum start time control, monitor internal and external temperatures and switch on the heating system at a time calculated to preheat the building just in time for occupation. Time

taken for the preheat is monitored daily and the programme is automatically updated if necessary. There is always a temptation for the occupant to make adjustments to the space heating control system without sufficient knowledge of the outcome. To minimise the effects of this, the most simplified system of a seven day time controller that can be manually adjusted would be preferred, otherwise the automatic optimum time controller that is self correcting could be considered.

### 4.4.1 Heat Pump Capacity Control

Features of the thermostatic control that affect cycling frequency of the heat pump have been discussed in by Fitzgerald [43]. He produces data showing how cycling frequency varies due to changing load conditions. The author has taken the data of Fitzgerald to produce a typical set of curves, shown in Figure 28. This shows how the various design features of both the heat distribution system and room thermostat effect the cycling periodic time. This technical paper was produced to show how design of the heat distribution system and specification of the room thermostat effect the thermal output and COP of the heat pump installation.

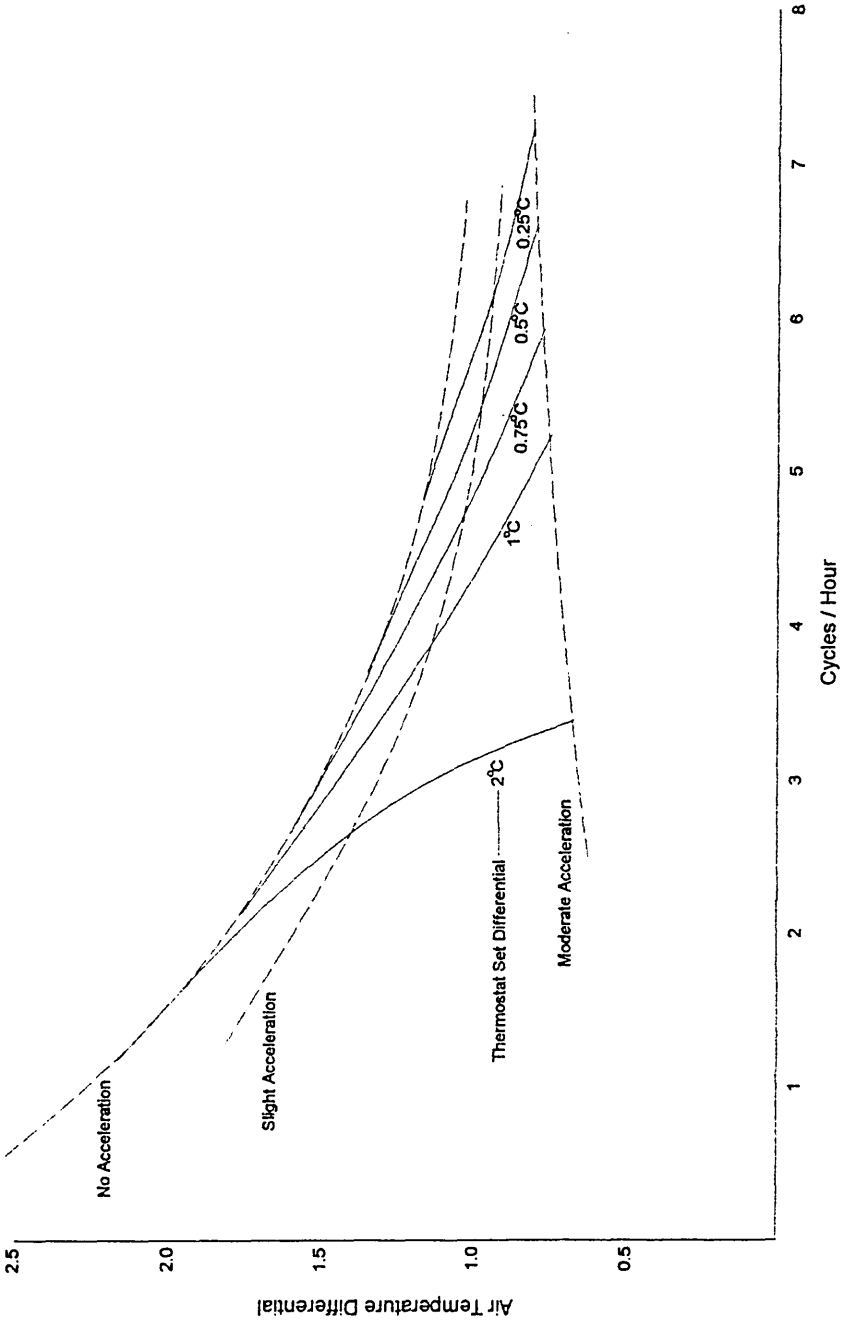


Figure 28 Room Thermostat - Performance at 50% Load

Dotted lines indicate how the cycles per hour increase due to increased acceleration and reduced set differential of the thermostat.

4.4.2 Water Temperature Control

The distribution system being studied below is the closed water circulation which transmits heat being transferred from the condenser, through the heat distribution system to heat emitters fitted within the heated accommodation.

When considering the steady state operation of the heat pump in Chapter 3 Figure 21, water in the heat distribution system was shown to be at a constant temperature, independent of rise of ambient temperature. It has been demonstrated previously that in conventional heat pumps, at part load conditions, the room thermostat causes the heat pump to operate intermitently. The water temperature therefore increases whilst the heat pump is operational and reduces when inoperative. The indicated water temperature shown in Figure 21 represents what may be considered to be the mean temperature.

Output capacity of the heat emitters within the heated space would normally be matched to the heat pump output at design conditions. When atmospheric temperature rises above the designed condition, the heat pump is therefore switched on/off under the control of the room thermostat according to the set temperature differential. This causes both flow and return water temperatures to increase but they are limited by the room thermostat which switches the heat pump on/off due to the increase or reduction of room temperature. In addition to the room thermostat, whilst the heat pump is controlled in operation, at all times the refrigerant cycle is controlled to by the degree of superheat at the compressor suction.

The part load operations discussed above were known to be caused by reduced heat pump efficiency and therefore were studied further in the laboratory research discussed in Chapter 7.

## 4.5 APPLICATION OF THE HEAT PUMP TO UK DWELLINGS AND CLIMATIC CONDITIONS\

For the analysis of heat pump seasonal performance, it was decided to take published monthly averages of daily maximum and minimum dry bulb temperatures. Calculations of hourly variations were based on the assumption that temperatures varied sinusoidally throughout the day. Study of the application of heat pumps to domestic dwellings in the UK were made comparing buildings of light and heavy construction. Domestic accommodations contain a wide variety of complex human activities and therefore optimum 'comfort' conditions span a wide range. It was found that the design of internal environmental conditions can be allowed to swing about a mean temperature.

### 4.5.1 Thermal Response of the Building Structure

Research into the effects of change throughout the daily cycle of atmospheric conditions was carried out at the Electricity Council Research Centre, Capenhurst [44]. A mathematical model of the behaviour of heavy and light constructions was used to calculate and compare the thermal performance. Both dwellings were insulated to the same high level. The time taken to preheat a building of heavy construction during the average January conditions was shorter due to less overnight cooling than with the light construction, however the daily fuel consumption of the heavy house was in the order of 10% greater. These trials show that for two walls of the same overall level of thermal insulation, the heavy construction provided lower levels of temperature deviation throughout the day when compared to the light construction building.

Computer calculations made by the UK Electricity Council Research Centre [45] report that if plant is oversized by 40%, then this will lower the seasonal COP by 12%. The heat supplied to the building will drop by 10%, but energy input to the heat pump increases by only 2%. The lowering of the COP caused by oversized plant is attributed to heat pump cycling. Reduction of the heat demand is considered to be due to a reduced preheat period. It was also shown that a heat pump can operate with a higher effective COP in a heavy building when compared to a lighter one.

A further series of calculations by the Electricity Council Research Centre [45] assessed the effect of building mass on the seasonal performance of heat pumps with regard to the heat pump size and seasonal COP. Calculations made with this programme indicate that higher COP does not necessarily produce lower energy consumption. The higher COP from a building of heavy construction resulted in a higher input of energy. The lower COP resulting from plant oversize is accompanied by a lower energy consumption and lower heat supply to the building. This is attributed to energy saved by reduced preheat periods.

4.5.2 UK Climatic Conditions

Heat transfer in the evaporator from atmospheric air flow to the refrigerant is affected by both temperature and humidity levels. The influence of moisture in atmospheric air is an important factor, because up to 15% of the collected heat may arise through the latent heat of condensation of water vapour [41]. An equation given by Jones [46] provides temperature variations of ambient air throughout the diurnal cycle:

$$t = t_{15} - \frac{D}{2} \times \left[1 - \sin\left(\frac{\phi\pi - 9\pi}{12}\right)\right]$$

where:

t = temperature at various times of the day,

$t_{15}$ = peak temperature occurring at 15.00 hrs sun time,

D = diurnal temperature range, and

$\phi$ = hours - time of day.

This equation is based on the assumption that temperatures vary sinusoidally throughout the day, the minimum night time temperature being at 03.00 hrs and peak day time at 15.00 hrs. It was decided that an equation of this type would simplify the specification of dry bulb temperature at any time throughout the space heating season. The use of an equation made it necessary to only input monthly, average, maximum temperatures and diurnal temperature range into the computer.

In the UK, the minimum diurnal temperatures and maximum humidity are normally assumed to occur one hour before dawn. For the purpose of this project this convention was included, the one equation being replaced by the following three equations:

A method which has been used extensively in the design of space heating systems and air conditioning, assumes that the maximum daytime atmospheric air temperature occurs at 3pm, as described above. However, the minimum daytime temperature occurs one hour before dawn. For the purpose of this project, this convention was, therefore, adopted and equations were developed to replace the above equation by Jones [46].

The calculation was made for the twenty four hours, starting at 1am, through to midnight on the same day. One equation was developed to cover the whole period as follows:

$$Y = A - B / 2 \times (1 - \sin E)$$

This equation calculates atmospheric temperature 'Y' at times on the hour throughout the day. 'A' is the maximum temperature, taken to be at 3pm. 'B' is the diurnal temperature range through the 24 hour day. The variable 'E' has three calculated values, one for each of the three periods determined by the following equations:

(i) from 1am to the minimum daytime temperature:

$$E = ( ( X + 9 ) / ( D + 9 ) + 2.5) \times \pi$$

(ii) from minimum am to maximum pm temperature:

$$E = ( ( X - D ) / ( 15 - D ) + 1.5 ) \times \pi$$

(iii) from maximum pm to midnight temperature:

$$E = ( ( X - 15 ) / ( D + 9 ) + 2.5 ) \times \pi$$

where: X = hour - times through the 24 hour day

D = time of the day when the minimum atmospheric temperature occurs.

Mean dry bulb air temperatures and dew-point at each hour during each day for the month of the year are given in graphical form [47]. The properties of humid air are given for a range of dry bulb temperatures and humidity levels appropriate to each month of the heating season can be obtained.

Seasonal thermal performance of the heat pump and variation of space heating load will be based on the above equations. The monthly average of maximum daytime and diurnal variation for the sinusoidal curves will be obtained for each month throughout the space heating season.

## 4.6 THERMAL COMFORT IN DOMESTIC ACCOMMODATION

As a result of the wide variety of complex activities carried out in domestic dwellings and clothing levels of the building's occupants, optimum conditions span a wide range. The acceptable internal environmental temperature is 20°C, based on a combination of one third mean radiant and two thirds air temperature [48]. Allowing a wide range of room temperature differential by the thermostat, producing a fresh and more stimulating internal environment [49]. Domestic space heating systems fitted with a room thermostat are flexible in their temperature control. The occupants may find themselves satisfied with a lower room temperature and a lower 'percentage of people dissatisfied' than in a factory or office, as they have to pay the space heating fuel bill personally.

## 4.7 SUPPLEMENTARY HEATING

The installation, capital and maintenance costs of a space heating system are frequently greater than that of a conventional installation. One method of reducing the capital cost is to reduce the size of heat pump and then provide supplementary heat. This reduces the capital cost, but may increase the running costs. The supplementary heat, when operating in parallel with the heat pump, needs to be thermostatically controlled. It may be preferable, therefore, that electricity is used to provide the supplementary heat as this is easily and efficiently controlled by the thermostat. The

heat pump would be controlled by a room thermostat and the supplementary heat only being supplied at low atmospheric temperature, below the balance point, when the outside thermostat calls for additional space heating. The quantity of supplementary heat required would be the thermal variance between the heat pump output and the space heating load as shown in Figure 29. The varying locations of the balance point due to varying heat pump size are shown in Figure 30. It is preferable that the low temperature capacity control on/off switching should be of supplementary heat supply only. An on/off time control, to supply heat only when the heat pump is operative, and an outside thermostat, to activate the supplementary heat supply only when outside temperatures are below the balance point temperature of the heat pump are included.

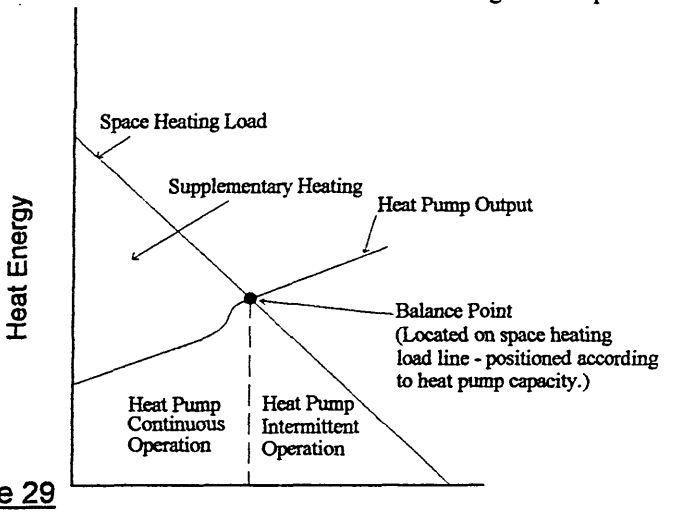


Figure 29

Identification Of Modes Of Energy Supply To The Heating System

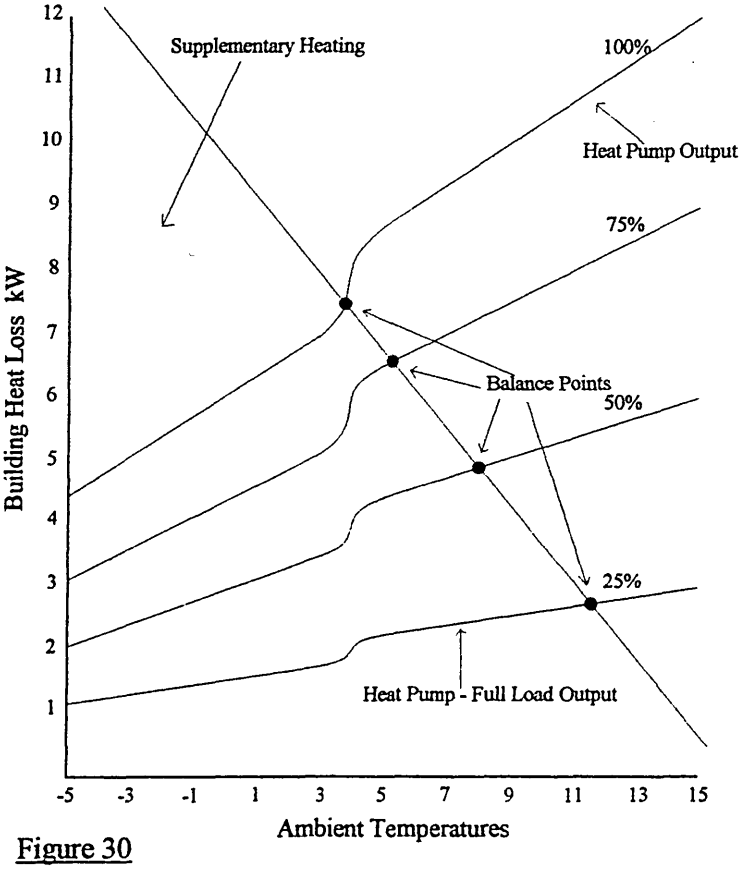


Figure 30

Heat Pump Energy Output And Supplementary Heating

4.7.1 Thermodynamics of the Combined Performance of the Heat Pump and Supplementary Heat.

The relationship between building heat loss, ambient temperature, space heating load and heat pump output is indicated graphically at Figure 31. Space heating load, heat pump performance and other values on which this graph is produced, are taken from the technical paper by Foxley and Weaver [25]. This publication provides data based on laboratory and field trials and pump performance for both steady state and at part load conditions when on / off cycling. Using this data and a heating analysis chart for London, Figure 25, the seasonal performance when operating in conjunction with supplementary heating was made. The first calculation , Appendix A4.1 Table 3 as made with a heat pump sized to meet the space heating load at the balance point at 4°C, this being in accordance with the data produced by Foxley and Weaver. Three further calculations were made to show the increased demand for supplementary heat when three graduated reductions of 25% of thermal capacity of the heat pump were made, at Appendices 4.1 at Tables 4, 5 and 6. A summary of results are shown at Appendix 4.1 Table.7.

The heat pump designed to meet the space heating load at the balance point of 4°C is attributed to have 100% load output. A total of four individual capacity ratings of heat pump were identified, each reducing in capacity by 25%. Reduction of heat pump capacity increases the balance temperature above that of the previous model, see Figure 30. Energy used jointly by the heat pump and supplementary heating are shown on the graph in Figure 31.

This shows how the reduction of heat pump capacity increases the proportion of heat pump continuous operation, therefore, saving fuel. The simultaneous increase of supplementary heat required, more than offsets any energy saved, however.

Reduction of heat pump output capacity at low ambient temperature is caused by ice formation on the evaporator heat transfer surfaces. When the ambient temperatures are above that of the balance point, heat pump operation is intermittent to reduce thermal output to that of the space heating

load. Ambient temperatures below that of the balance point, allow the heat pump to operate continuously. Any deficiency between the heat pump output and the requirements of the space heating load is supplied by the supplementary heat.

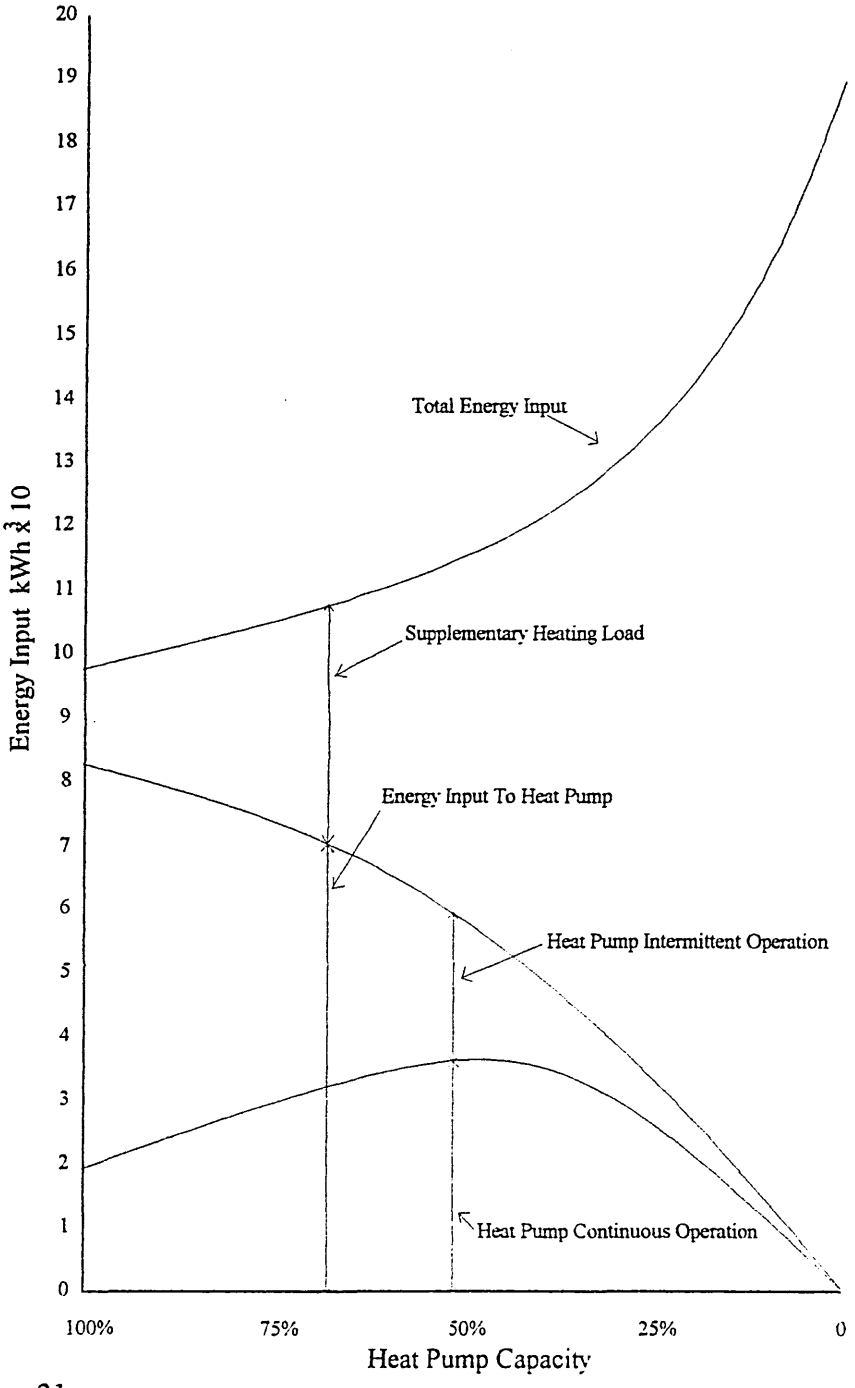


Figure 31

Heat Pump Operation With Supplementary Heating

# CHAPTER 5. LABORATORY RESEARCH - HEAT PUMP TEST RIG REFRIGERANT R12

## 5.1 INTRODUCTION.

Contact was maintained with the chemical industry and refrigerant compressor manufacturers throughout the practical phase of this research, regarding the change from the established refrigerants in general use at that time, to the environmentally friendly refrigerants. Development of a suitable environmentally friendly refrigerant was complete, however, development work by the manufacturers of a compressor suitable for this research project and the environmentally friendly refrigerant, were still to be completed. The refrigerant industry was still in the midst of the change of refrigerants and it was clear that there would be a time delay before environmentally friendly refrigerants could be used on this research project.

In the light of these circumstances, it was decided to undertake laboratory research, using refrigerant R12. The use of this refrigerant was soon to be prohibited and the research using it was, therefore, geared to the techniques of design and construction of the heat pump, also to the gaining operational experience that could later be applied to domestic heat pumps using an environmentally friendly refrigerant.

With the objective of preparation for the future test using environmentally friendly refrigerants, it was decided to build and put into operation a water to water heat pump test rig using Refrigerant R12. Laboratory research specifically applicable to the thermodynamic performance of Refrigerant R12. would be avoided. The advantages of using a water-to-water heat pump were that changes of the evaporation temperature could be made without the use of the environmental chamber. The use of this facility being in full demand by others.

## 5.2 BRIEF DESCRIPTION OF TEST RIG ASSEMBLY.

A schematic diagram of the water to water heat pump test rig, using refrigerant R12, as constructed in the laboratories of Sheffield Hallam University for this part of the research, is shown at Figure 35.

For the purposes of this research project, the type of heat pump being studied transfers heat from air to water. The objectives in building the refrigerant R12 test rig made it desirable at this stage to construct a water to water heat pump. The parts for a water to water heat pump were more readily available and this would fully serve the purpose of the laboratory trials at this stage. The refrigerant circulation was powered by an electrically driven, hermetically sealed compressor. This discharges first to the cylindrical shell of the water cooled condenser, then to the refrigerant control expansion valve and finally, returning to the compressor at low pressure through the heat evaporator exchange coil immersed in a water filled tank. The condenser water circulation system consisted principally of a water storage tank and water outflow tank. When the water circulation reached the control temperature the control valve measuring the flow temperature to the condenser diverted a proportion of return water from the condenser to the outflow tank.

Inflow of cold water through the ball valve maintained the water level and reduced the temperature to the set point temperature. The electrical immersion heaters were used to reduce the warm up period when starting up the heat pump from cold. Water temperature in the evaporator tank was controlled using an on-off thermostat in the electrical supply to the immersion heater. The agitator, in the same fitting as the thermostat and water heater, operated continuously to maintain a uniform water temperature and to enhance heat transfer from water to the refrigerant. The evaporator tank contained an auxiliary heater to manually adjust the water temperature when necessary.

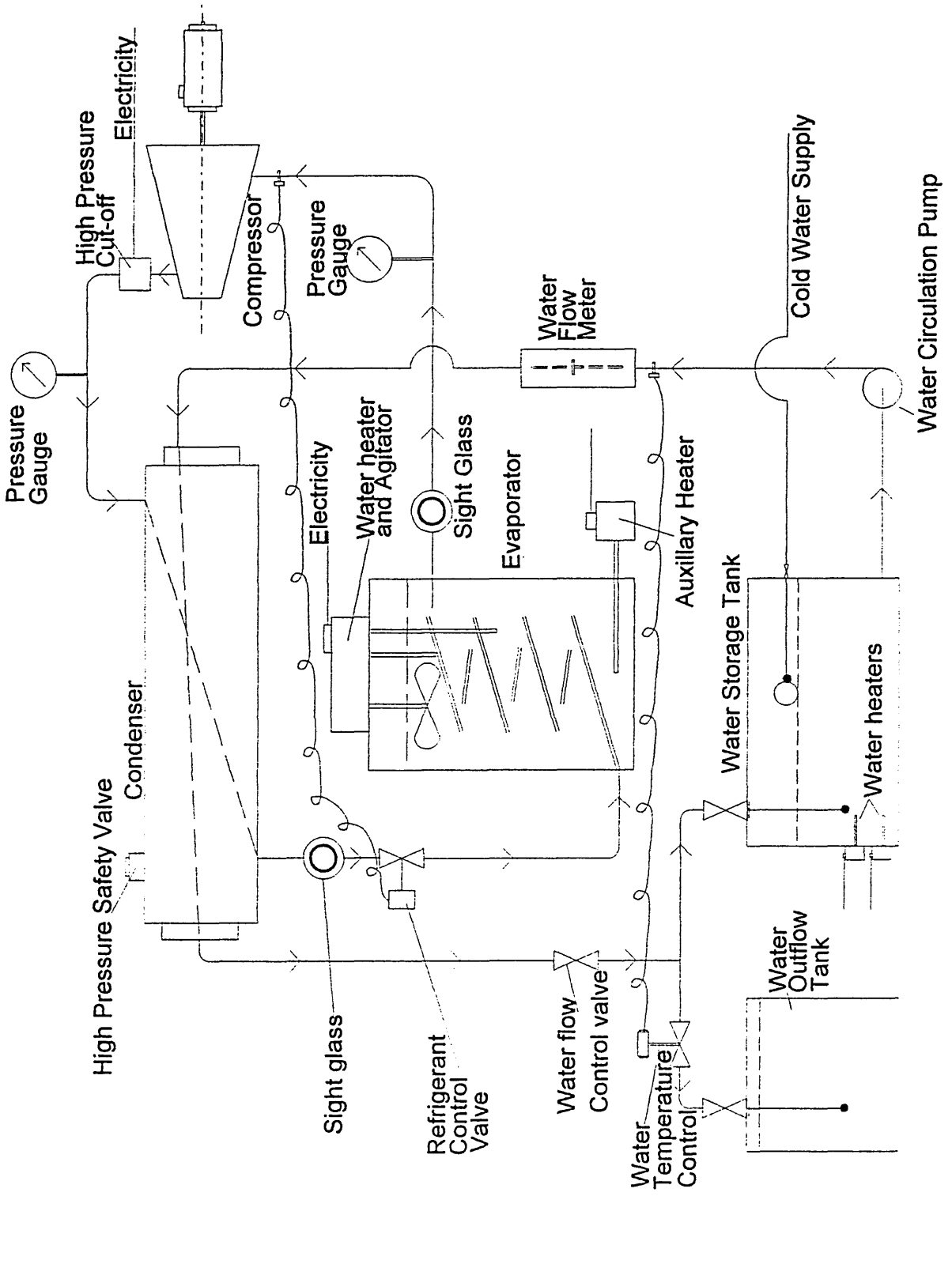


Heat Pump Test Rig
Water to Water - refrigerant R12

FIGURE 35

## 5.3 BUILDING THE TEST RIG.

### 5.3.1 Safety Procedures.

The heat pump was mounted onto a steel frame, which was purposely designed and constructed to support all of the equipment correctly. The largest concentration of weight was in the water tanks which were fitted at low level on the rig. The frame and all metallic parts of the fittings were electrically earthed, then checked and certified to be safe by a competent person. Working pressures of the equipment were checked against the maximum cut out pressures of the heat pump.

### 5.3.2 Condenser Design.

The condenser consisted of a mild steel shell containing both liquid and vapour refrigerant. Refrigerant to water heat exchanger tubes were mounted horizontally between tube plates and headers at each end of the shell. The copper tubes, running the full length of the shell, were arranged for three pass water flow. Outside the heat exchanger tubes the upper part of the condenser shell contained vapour whilst the lower part accumulated the necessary reserve liquid refrigerant storage.

A spring loaded pressure relief valve was fitted into the condenser shell. This was designed to relieve refrigerant to atmosphere and reduce pressure in the event of the refrigerant pressure rising above 10 bar (gauge). In addition, the pipework supplying high pressure refrigerant from the compressor to the condenser were fitted with a high pressure control to switch off the compressor at a slightly lower pressure than the set pressure of the condenser high pressure relief valve. The objective of the compressor high pressure switch off control was to reduce the possibility of the release of refrigerant vapour to the atmosphere.

5.3.3 Compressor

The compressor used was a Danfoss FR7H, hermetically sealed, with a displacement of 6.93 $cm^3$/rev. This was driven by a 170 W electric motor. The thermal output stated by the manufacturer, when evaporating at 0°C and condensing at 55°C, was specified to be 770 W. This performance was obtained from laboratory trials made by the manufacturer. The test conditions used were those specified by the European Committee of Manufacturers of Refrigeration equipment, Brussels, Belgium (hereafter referred to as CECOMAF). The test procedures followed were as specified in the International Standard ISO 917:1989(E) and the British Standard Specification BS3122 Part 1. This international standard specifies methods of test for performance, determination of refrigerant capacity and of volumetric efficiency. Also determination of power, isentropic efficiency and coefficient of performance of refrigerant compressors.

5.3.4 Refrigerant Control Valve

The valve controlling pressure, refrigerant mass flow and the degree of superheat of the compressor suction, was fitted in the pipework at the refrigerant outlet from the condenser.

5.3.5 Thermal Insulation

To minimise thermal losses from the heat pump. thermal lagging was applied. The surfaces thermally insulated included the refrigerant pipework on the high pressure side of the compressor. A removable muff made from glass fibre inside a plastic wrapping was made to insulate the condenser shell. The rectangular evaporator water storage tank was thermally insulated using polystyrene slabs approximately 45mm thick.

5.3.6 Instrumentation.

Ten thermocouples were used to automatically scan and record temperatures at fixed points on the test rig. Eight were fitted to the refrigerant cycle whilst the remaining two were fitted to record inlet and outlet water temperatures at the condenser. Both the time taken to measure temperature,

(named the pause), and the time between scans, (named the dwell), were adjusted to create the required scan frequency. Scanning frequencies were varied between two and five minutes, depending on the varying requirements of the study. The location of the thermocouples on the rig are shown on an outline sketch of the refrigerant cycle in Figure 36.

Readings from Bourdon type pressure gauges, evaporator water temperature, the condenser water flow rate and the refrigerant levels in the sight glasses were taken and recorded manually at times coincidental with the automatic temperature scan.

## 5.4 COMMISSIONING THE TEST RIG.

### 5.4.1 Purging the Refrigerant Circulation System

After completing the test rig construction, hoses of the Gould System Analyser were connected to the heat pump test rig to facilitate the purging of the refrigerant system. Hoses from the analyser manifold were connected to the R12 refrigerant storage bottle, to the vacuum pump and then from the manifold to the suction and delivery pipework of the compressor, as shown in Figure 37. The vacuum pump first purged air from the hoses of the analyser, then the heat pump system after which a small charge of refrigerant was transferred from the storage bottle to pressurise the test rig. The analyser was then disconnected from the test rig.

At all times during the heat pump commissioning and testing, care was taken to keep the evaporator above atmospheric pressure to safeguard against the ingress of air into the system. During the commissioning period, when connecting the system analyser to replenish refrigerant leakage, the hoses were purged before tightening at the heat pump end of the connection.

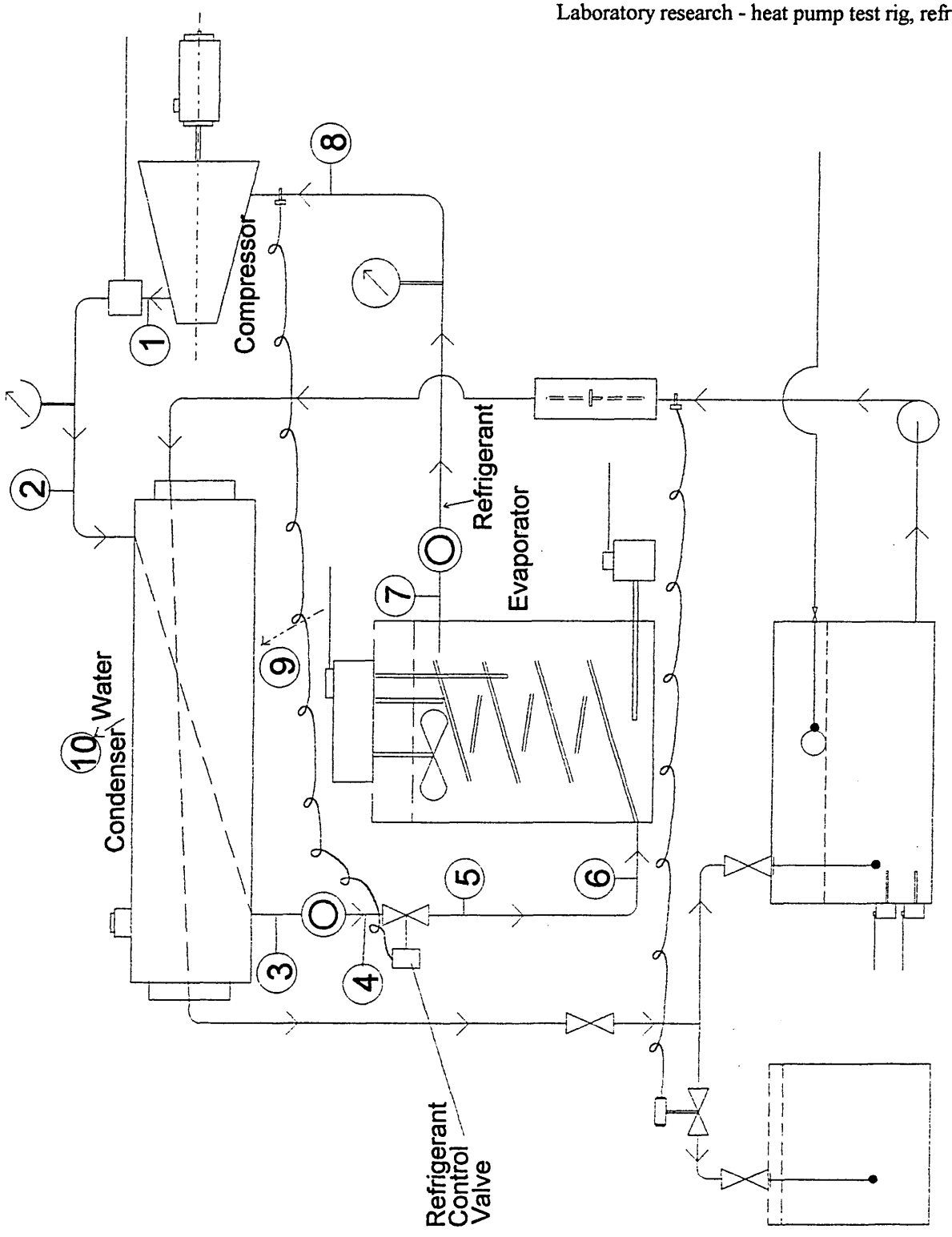


FIGURE 36 Locations of thermocouples in R12 test rig

TO PURGE HOSES: open valves C and D. Connect hoses 1, 3 and 4 as shown, but not tightened at the other end from the manifold. Open valve G to begin the purge.

TO PURGE THE SYSTEM: close valves C and . Connect hoses 1 and 3. Connect hose 2 to the manifold and direct the oposite end to the vent. Crack open valves H and L Crack open valves C and D to begin the purge.

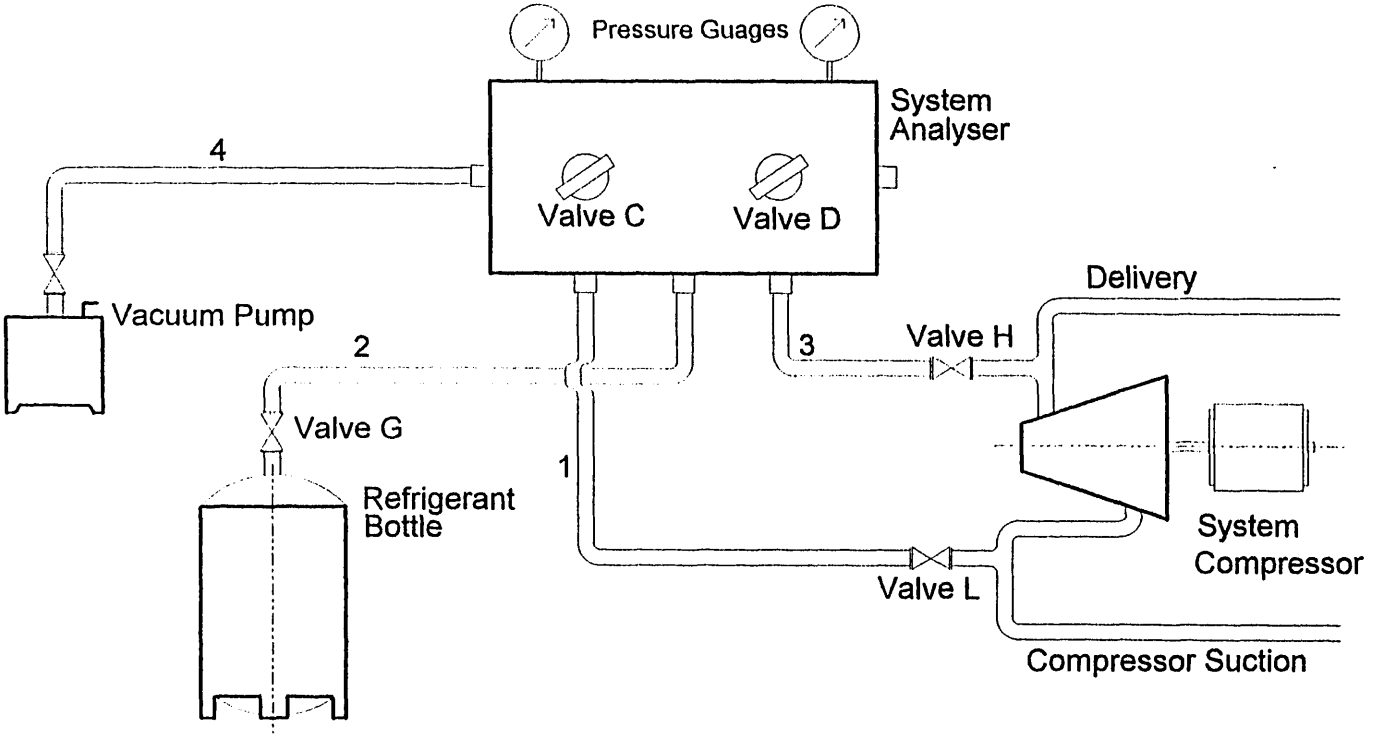


TO CHARGE THE REFRIGERANT INTO SUCTION SIDE OF COMPRESSOR: close valves C and D. Connect hoses 1, 2 and 3 as shown. Crack open valve H and open valve L to mid position. Open valve C and regulate the flow.

Figure 37

Purging the System and Charging Refrigerant

5.4.2 Refrigerant Leakage Testing

A leakage check was made using the bubble test. A mixture of soft soap and water was brushed onto the outer surface of the joints in order that if there was a leakage of refrigerant, bubbles would form on the outer surface. Leakages were found from the compression joints in the pipework. The compression joints were tightened and the leakage stopped. It was then found that disturbance of the pipework had caused other leaks to occur. This procedure was protracted and joints that had once been made tight, were again found to be leaking. To solve this problem the pipework was completely dismantled and rebuilt brazing all joints.

Originally compression joints were used, because it was considered that they would be satisfactory for the pressures involved and time would be saved on the construction and dismantling of the rig. The reason for the failure of the compression joint fittings is not known with any degree of certainty. The pipework layout in question was compact in the vicinity of the compressor therefore the pipework thermal expansion and contraction together with the vibrations from the compressor, could have been a contributory cause of the leakages. The pipework was reconstructed replacing the compression fittings with braised joints, which proved to be satisfactory.

Calculations were made with the object of appraising the extent of refrigerant leakage when not in use using the ideal gas law: $pV = mRT$.

Calculations indicated extremely low vapour loss of 0.00284kg of refrigerant in three days. It was concluded that the heat pump pressure was being maintained by vaporisation of the small amount of liquid refrigerant in the condenser shell. The bubble test, described above was found to be the most reliable indicator of refrigerant leakage when the heat pump was not in use, as it not only indicating that there was a leakage, but also located it. The loss of refrigerant was also indicated by reduced thermal output. For acceptable heat pump thermal performance it was found to be essential that the sight glass on the outlet from the condenser was vapour free.

5.4.3 Refrigerant Sight Glasses

Two sight glasses were fitted into the refrigerant circulation system, one in the compressor suction and the other at the refrigerant output from the condenser. The compressor was designed for a pressure increase and volume reduction of the refrigerant as it passed between inlet and outlet valves. It could not safely operate with liquid refrigerant because it would not have the same volume reduction. The sight glass at the compressor suction may show traces of oil, but otherwise it must be free of refrigerant liquid.

When adjustments were made to either the heat pump controlled temperature or the pressure settings, observations at the sight glass fitted into the compressor suction were made. For the safe operation of the heat pump frequent observations of the sight glass needed to be made at the time and for a period following any control adjustment. The second sight glass which was fitted at the condenser refrigerant outlet provided an alternative approach to assessing leakage of the refrigerant using the universal gas equation. For the satisfactory operation of the heat pump the refrigerant must be fully liquefied before leaving the condenser and this should be evident by observations at the sight glass. Refrigerant loss from the system was indicated if the refrigerant was not completely liquefied and there was a flow of vapour through the sight glass. When the sight glass was passing both vapour and liquid the liquid surface line was clearly visible. If the sight glass was running full, there was no indication to differentiate between vapour or liquid flow. In these circumstances, a small circle drawn on a piece of paper, when viewed through the sight glass flowing full of liquid, was distorted to an ellipse.

5.4.4 Condenser Water Circulation System.

The pumped water circulation rate through the condenser was controlled by taking readings from the variable-area flowmeter and making manual adjustments of a globe valve fitted at the condenser outlet. The inlet water temperature to the condenser was controlled by automatic

adjustment of the water thermostatic control valve. Rise of water temperature at the inlet to the condenser caused the water temperature control valve to open and divert the water flow to the water outflow tank. Cold water added to the water storage tank reduced the condenser inlet water temperature.

It was found that modulation of the water temperature control valve affected the pressure drop through the water circulation system and therefore affected the rate. This necessitated frequent checks to be made of the water flow rate. Modifications to this arrangement were needed when the heat pump was rebuilt for tests involving the environmentally friendly refrigerants.

Heat losses from the water storage tank and the pipework caused the amount of water flowing to the water outflow tank to be very small. The control valve was characterised for linear flow control, however, this was found to be oversized and lacking in valve authority. As a result of this, frequent readings of the water circulation rate and temperatures needed to be taken.

## 5.5 REFRIGERANT COMPRESSOR - THERMODYNAMIC PERFORMANCE

Domestic heat pumps used for space heating are most frequently fitted with a hermetical compressor. A major advantage of this type of compressor is that a large proportion of the heat given off by the electrically driven motor is retained in the refrigerant. A small proportion of this heat transferred to the compressor suction is lost by heat emission from the outer shell, but in the open type compressor the whole of this heat would be lost to atmosphere.

A hermetically sealed compressor gains useful heat energy input to the compressor suction, but also introduces an additional series of physical actions into the refrigeration cycle that otherwise would not need to be considered. The temperature and pressure at which the refrigerant enters the inlet valves would normally be known, as in the open type compressor, but with a hermetically sealed compressor, the values known by the designer are those at the inlet to the compressor shell. These features of the hermetically sealed compressor may have a minimal effect on the heat pump

performance, but it should be kept in mind that they do exist. Due to the physical design of the hermetically sealed compressor, the manufacturer's performance test data is normally based on the physical conditions of the refrigerant entering the outer shell of the compressor.

In order to properly design other operative units within the thermodynamic cycle, the refrigerant mass flow that will be produced by the compressor needs to be known. This can be acquired by firstly calculating the flow volume at the compressor suction from which the refrigerant mass flow can be obtained. Further information of the correlation between these values was supplied by Faithfull [50] in which volumetric efficiency of the compressor as a function of pressure ratio, clearance volume and index of the compression process is given.

The compressor performance tests adopted by the manufacturer are based on the CECOMAF test procedures, where, in place of the heat exchangers, a calorimeter is used. These tests are made with a high level of superheat at the compressor suction. Test conditions of the manufacturer need to be converted to the operating conditions required by the user, a procedure which, for domestic heat pumps, would normally include a change of thermal output and a reduction in the compressor suction superheat.

### 5.5.1 Manufacturers Performance Testing

The 'National Foreword' to British Standard Specification 3122, Part 2, states that due to the large variation of applications and operating conditions for which refrigerant compressors are used, the European Committee of Manufacturers produced a standard specification for performance trials. This was not based on any practical application. The International Standard Specification published by CECOMAF, applies to tests carried out at the manufacturers works and was intended to provide test results of sufficient accuracy to assess the suitability of a compressor for any refrigeration installation. Details of the EEC Committee that produced the International Standard

Specification, the foundation, aims and members are to be found in the International Organisation Year Book [51]. The test procedures are detailed in the International Standard ISO917:1989. The equivalent British Standard Specification is BS3122 Part 1 and the procedures for presentation of performance data is BS3122 Part 2.

In place of heat exchangers that are normally used in the heat pump construction, the compressor manufacturer's test procedures use a calorimeter to measure the performance of the compressor. The calorimeter enabled the refrigerant vapour return temperature to the compressor and the liquid temperature, to be the same as ambient temperature, that is 32°C. The intending user of the compressor selects from the manufacturer's brochure a compressor output that can provide the thermal performance, with refrigerant suction and delivery pressures, that are required. Also the thermal output, as measured by the manufacturer's CECOMAF tests needs to be the same as, or near to, the output capacity required. The change of state conditions from the 'measured conditions' as adopted by the compressor manufacturer, to the sought conditions by the user are shown on the pressure enthalpy diagram in Figure 38.

For the study of change from the manufacturer's test conditions to those required by a user, a range of evaporation temperatures between +15°C and -15°C were examined. The values adopted for the refrigerant saturation temperatures were those given in the thermophysical property tables. The fixed compressor suction temperature is 32°C, as shown in the manufacturer's brochure, an abstract from which is shown at Figure 39. The superheat entering the compressor shell is between 17K and 47K. The normal practice in the U.K. would be to design for the compressor suction of 5K superheat [52] to produce the optimum heat pump performance and safeguard against liquid entering the compressor cylinders. It is necessary, therefore, to convert from the manufacturer,s test conditions test to the operating conditions required.

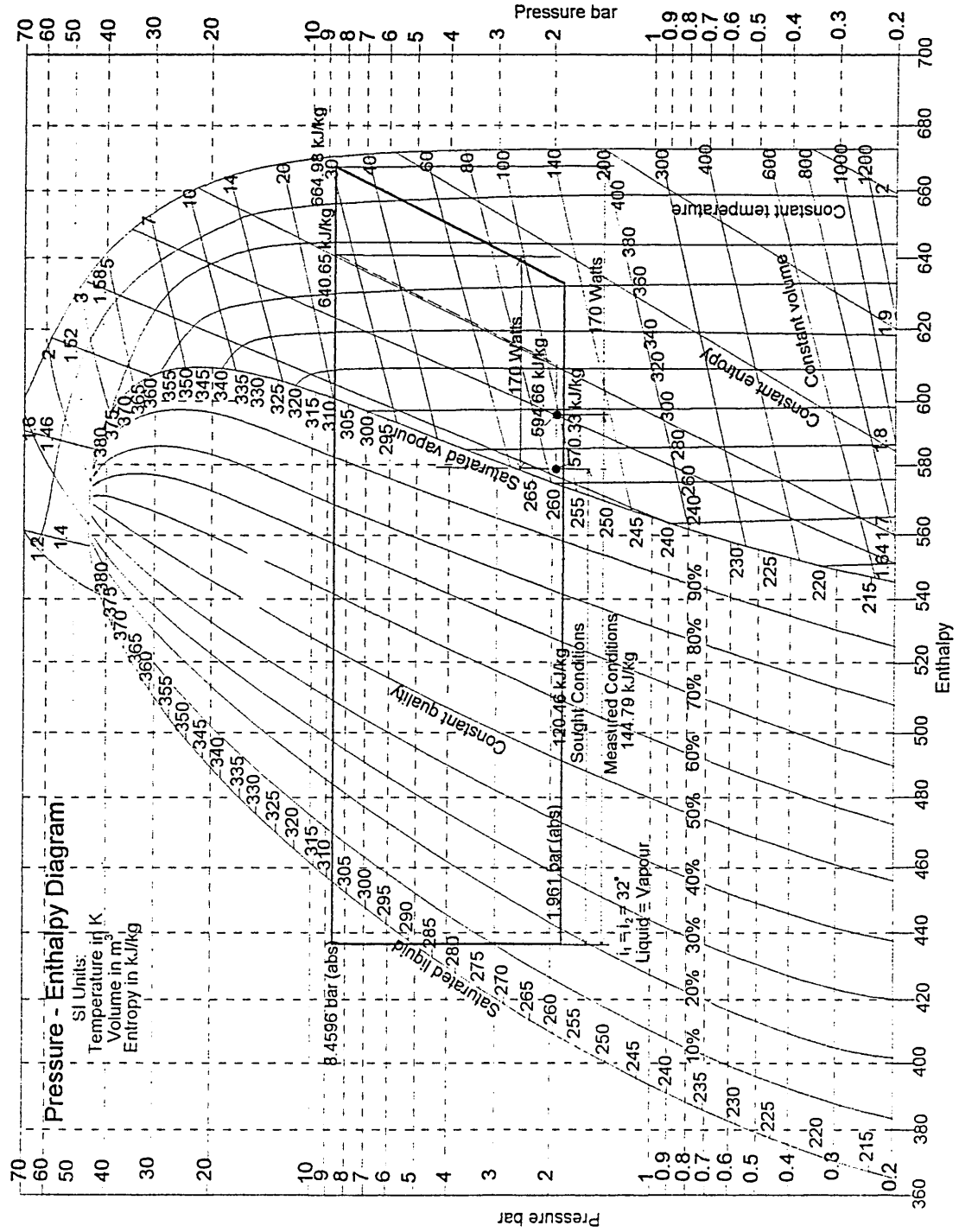


Figure 38 Compressor - Change of State Conditions

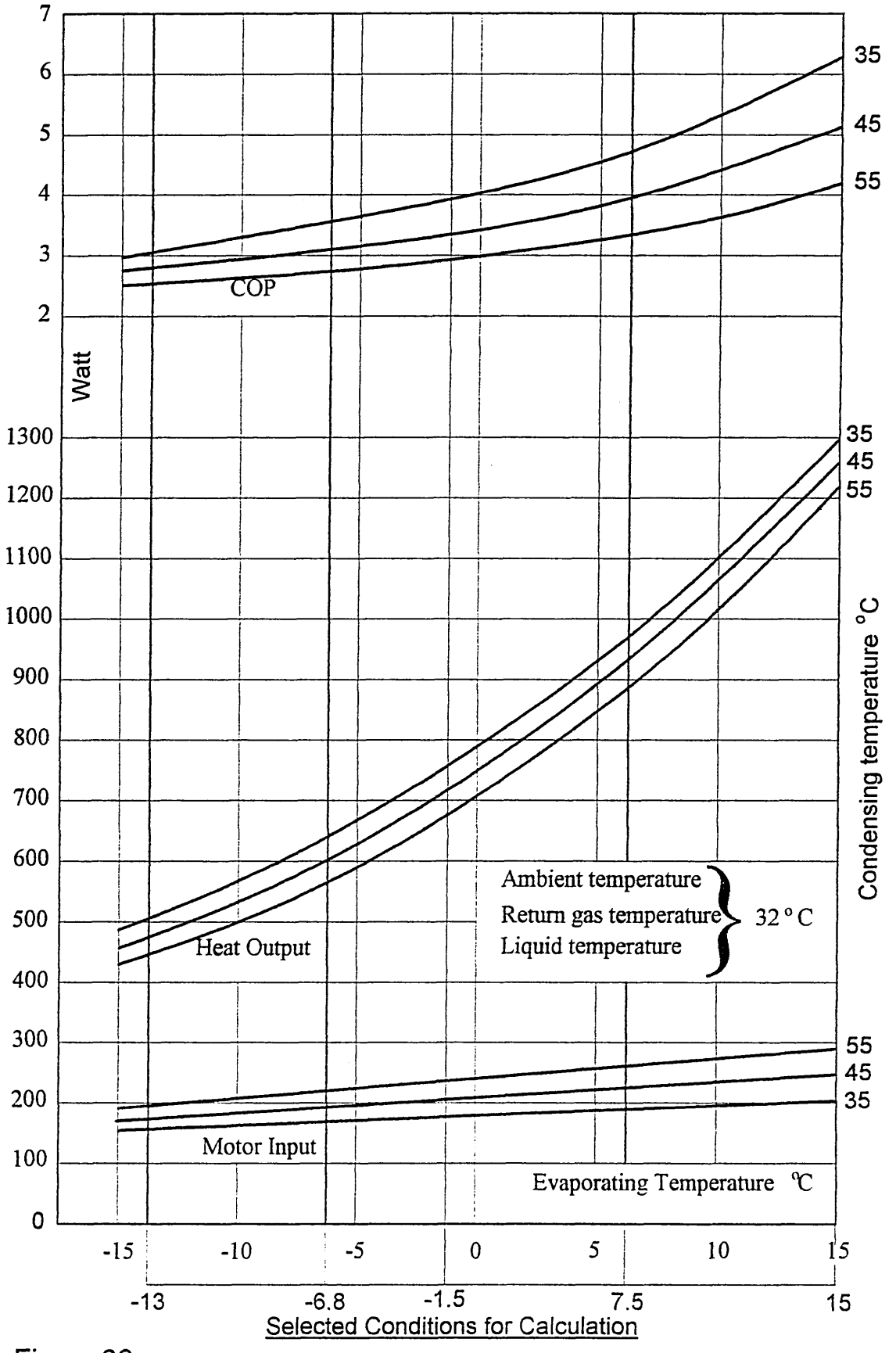


Figure 39

Thermodynamic Performance of a Hermetically Sealed Compressor

Based on the manufacturer's test results, the selected fifteen sets of test conditions were transferred to the pressure enthalpy chart shown at Figure 40. Also, Figure 41 shows CECOMAF test conditions plotted against compressor pressure differential and refrigerant mass flow. The objective of this exercise was to gain a clearer understanding of the manufacturer's test conditions and the conversion from these to those required by the user.

The compressor performance calculations of the selected test conditions are included at appendix A5.1. Tables 8, 9 and 10 contain the individual calculations. Table 8, has five evaporation temperatures -13°C to 15°C and the condensing temperature for all of these tests is 35°C. Tables 4 and 5 have the same evaporation temperatures but condensing at 45°C and 55°C respectively. The mathematical procedures, as shown on Table 11, Appendix A5.1, detail the first set of results on the first page, this being a typical calculation used for all the tests in this appendix.

All of the fifteen calculations in Appendix A5.1 are at the manufacturer's test conditions, but additional values of refrigerant mass flow, volumetric efficiency and isentropic efficiency are calculated. An abstract from the manufacturer's brochure on the method by which the compressor performance provided by the chart to the conditions required by the user is shown in Appendix A5.2..

For all the calculations made in the above appendix, the thermophysical data of the refrigerant used was taken at those conditions evident at the compressor shell inlet. All the physical or thermal changes taking place inside the compressor shell were considered to be part of the compressor operation. Tables of refrigerant R12 thermodynamic data used are given by Raznjevig [36].

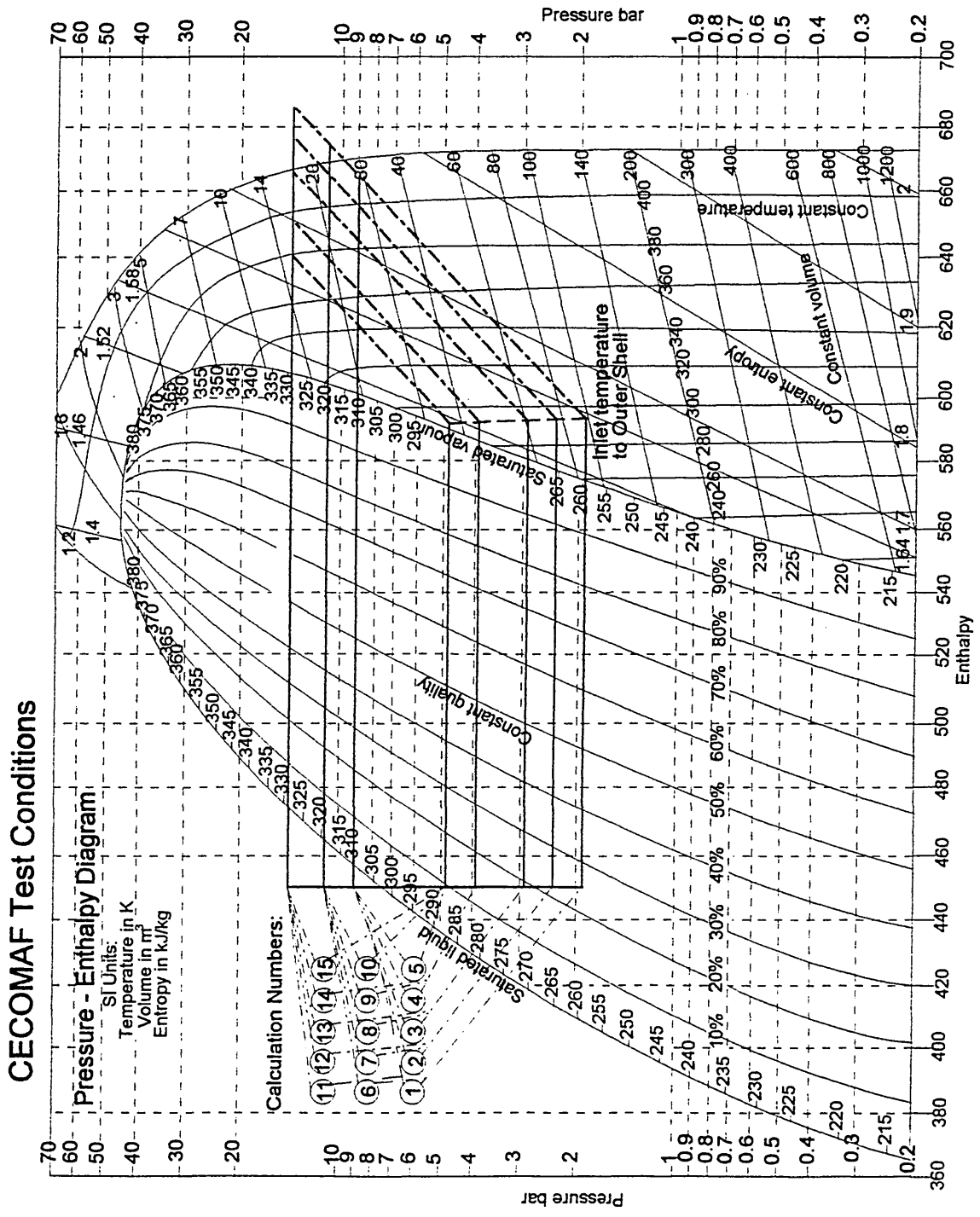


Figure 40 Pressure - Enthalpy Chart for Refrigerant R12

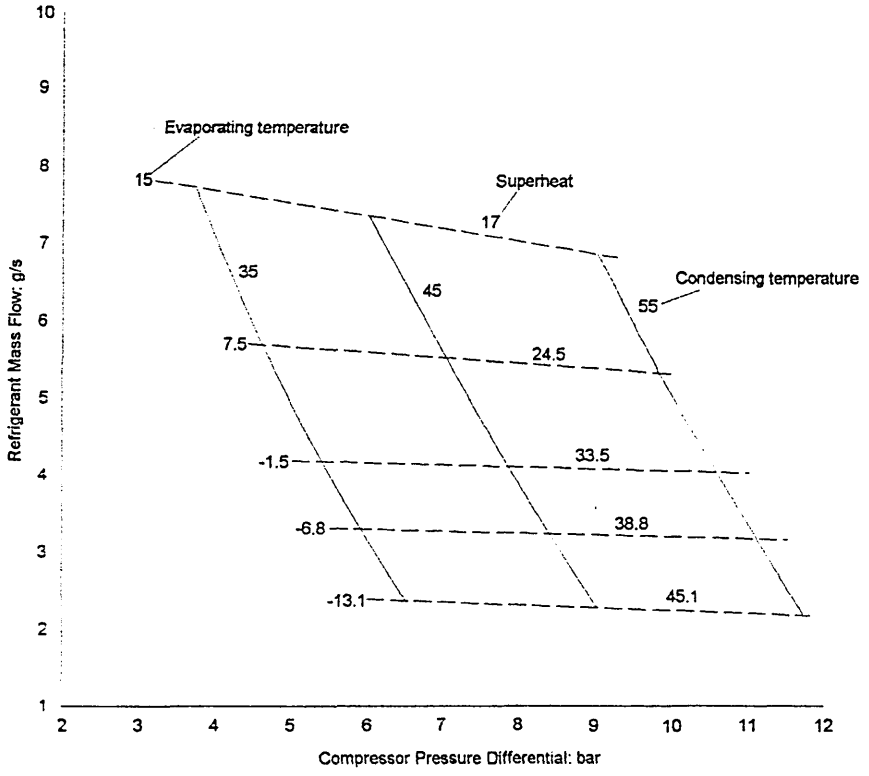


Figure 41 Influence of Pressure Differential on Refrigerant Mass Flow

The manufacturer's calculation procedures, referred to above, provide a method by which the selection of compressor may be made, but before procuring the other components making up the refrigerant cycle, it was found that a more detailed approach is required. Determination of compressor capacity for varying operating conditions is only correctly obtained by study of the combined effects of the factors governing the change, the principle factor in the change of compressor performance being volumetric efficiency, from which refrigerant mass flow may be obtained. It is stated by Dossat [53] that in laboratory tests, volumetric efficiency is primarily a function of the compression ratio which remains practically constant, regardless of the operating range.

The manufacturer's calculation procedures state that any change that takes place outside the compressor has no influence on the quantity of refrigerant circulated and both the text and the diagram, associated with this statement, show a decrease of superheat at the compressor suction. This change of refrigerant temperature and, therefore, specific volume of the refrigerant is outside the compressor and does, according to the theories advanced by Dossat, effect compressor performance. Differences were found in the calculated heat pump capacity and volumetric efficiency. This may be admissible for sizing the compressor, but when sizing the heat exchangers, volumetric efficiency and refrigerant mass flow need to be considered further.

Calculations were made by firstly applying the manufacturer's data as shown in Appendix A5.1 and then by following the principles of Dossat [53] as shown in Appendix 5.3, in that volumetric efficiency and therefore refrigerant mass flow are varied and are dependent upon the compression ratio.

For other designs of refrigerant compressor, for example an open compressor. this data would be taken immediately prior to the inlet to the suction valve, but in the hermetically sealed compressor, because the provision is not normally provided to measure temperatures and pressures inside the compressor shell, location of the point of and that of the open compressor do

not coincide. The added heat to the refrigerant after entering the compressor shell must affect the value of volumetric efficiency, but providing that the temperature sensor is similarly located in practice to that of the compressor trials, it must be assumed at this stage that this procedure is acceptable.

A graph of volumetric efficiency against compression ratio for the fifteen calculations in Appendix A5.1, is shown in Figure 42. The regression curve is the average condition calculated to the equation: $Y = 100.2013 - 11.9967X + 1.3744X^2 - 0.063889X^3$

Where: $Y =$ percentage volumetric efficiency, and

$X =$ compression ratio of pressure increase between the refrigerant inlet and outlet connections of the compressor outer shell.

The manufacturer's calculation procedure of change of state, indicates no change of electrical input to the compressor motor when the superheat is reduced from the CECOMAF test to the normal operating conditions. A graphic representing this is shown at Figure 42. These calculations follow those recommended by the manufacturer assuming that reduction of superheat does not change the refrigerant mass flow through the heat pump cycle. These factors, along with others, was studied in this chapter by reviewing the change of state calculations from the CECOMAF test conditions compared to the those obtained in normal practice. The derived data has been obtained using refrigerant R12. The refrigerant being considered in the next chapter will be the environmentally friendly refrigerant R134(a). The methodology for obtaining data will still apply for the new refrigerant.

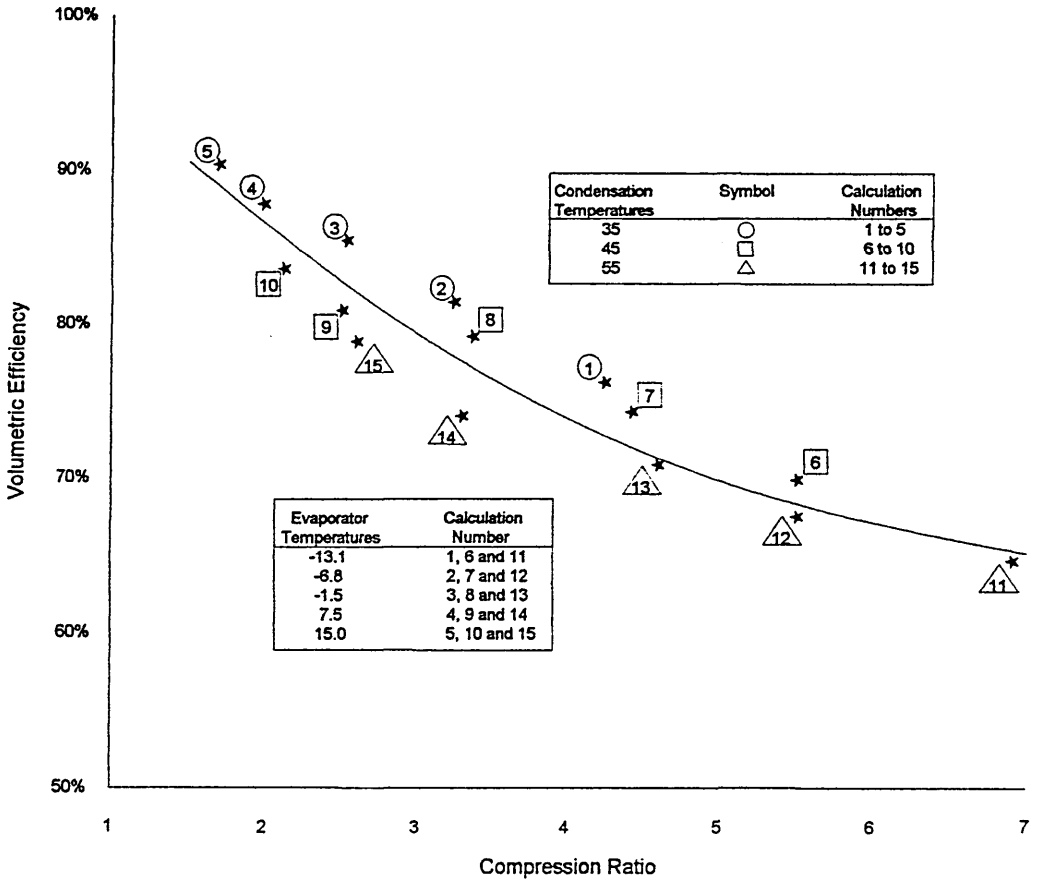


Figure 42 Volumetric Efficiency based on the Compression Ratio of refrigerant Compressor

5.5.2 Conversion from Test Results to the User Conditions.

Heat pump performance calculated covered in Appendix A5.3, are in two parts, the first based on the CECOMAF conditions which are normally adopted by compressor manufacturers performance tests. The second part calculates performance when superheat at the compressor shell was reduced to 5K. The second calculation follows the theories detailed by Dossat, referred to previously in this chapter, using the fixed relationships between compression ratio and volumetric efficiency of the compressor. The fifteen calculations are listed in Tables 12 to 15, the first three tables cover the calculations, and details of the methods used are shown in Table 15.

Unless noted otherwise, the calculation and row numbers below, refer to Appendix A5.2. Procedures detailed by the manufacturer were followed, as shown in rows {8} to {12}. For the purpose of these calculations, the refrigerant mass flow rate is not changed from those of the test conditions. The reduced superheat calculated in rows (13) to (19). The values of refrigerant specific volume at the compressor suction is shown to be reduced from that of the CECOMAF performance tests to a superheat of 5K..

Calculations shown in rows {13} to {19} are based on the theory given by Dossat, were the volumetric efficiency is a function of compression ratio. There is no change of compression ratio and, therefore, in the refrigerant flow volume at the compressor suction, which is in keeping with the publication by Dossat. The refrigerant mass flow shown in row 12, being that obtained in the manufacturer's performance tests is shown to be increased in row 16, that being calculated to be obtained with 5K compressor suction.

5.5.3 Operating Conditions - Heat Pump Output Capacity

The change of conditions assumed for these calculations was that superheat at the refrigerant input to the compressor shell was produced from the test conditions as 5K superheat. In concurrence

with the above, it was accepted that during the change to operating conditions, there was no change of electrical input. In order that a understanding could be reached of the processes of change of state and the quantity of refrigerant in circulation, an alternative approach to the quantity of refrigerant circulated was made.

5.5.4 Compressor Volumetric Efficiency.

Calculation of the volumetric efficiency following the reduction of refrigerant superheat to 5K, was established in appendix A5.3 by first following the manufacturer's method of calculation as shown in appendix A5.2. and then by calculations on change of volumetric efficiency. The second calculation takes into account the increased density of the refrigerant due to temperature reduction. From these two calculations the differing volumetric efficiency is shown in appendix A3 between the two calculations in the rows numbered {12a} and {23}. It follows that if the second calculation is accepted, that in addition to the increased volumetric efficiency, the refrigerant mass flow and thermal output of the heat pump is underrated in the first calculation.

It follows from the theory advanced by Dossat, that if there is no change of compression ratio, there is no change of compressor suction volume. Reduction of the superheat at the compressor suction causes an increased specific enthalpy of the refrigerant, which increases the anticipated thermal output of the heat pump.

5.5.5 Influence of Lubricating Oil on Heat Pump Performance

Whilst the heat pump compressor is in operation. it is probable that lubricating oil is being carried over from the compressor along with the refrigerant and passing through the heat exchangers. An investigation into the effects of oil using a refrigerant R12 heat pump was made by McMullan, Murphy and Hughes [34]. Abandoning of refrigerant R12 and the development of

environmentally friendly refrigerants causes the experimental results of this research to be outdated to some extent, but there are items that are deserving of discussion.

There is a section in the above report that discusses the refrigerant mass flow rate. At the beginning of this particular subject there is a statement that, "the refrigerant mass flow is the product of refrigerant density and the compressor displacement." This statement is followed by a graph, based on the experimental results obtained from varying degrees of superheat at the compressor suction and the resultant varying levels of refrigerant mass flow. The results indicated a linear relationship between the degree of superheat and refrigerant mass flow. The refrigerant mass flow is reduced with increasing levels of superheat. During this particular trial, there was no oil passing through the evaporator.

Reference is made in the above technical paper on the effects on the heat pump efficiency of high levels of oil in circulation and low levels of superheat at the compressor suction. It is possible for both the condenser and evaporator to act as heat rejectors with 25% oil in the refrigerant to oil mixture and low levels of superheat.

### 5.5.6 Hermetically Sealed Compressors - Energy Flow inside Shell

In order to further study the performance of the hermetically sealed compressor, the thermal actions as described by Dossat were considered in greater detail. The performance data used by the manufacturer was obtained from the physical testing of the compressor with a high level of superheat at the compressor suction. There are, therefore, two adjustments to performance of the compressor to be made. Firstly, it was necessary to reduce the compressor superheat to 5K and secondly, to change operating conditions to match those of the user.

For the continued study of the hermetically sealed compressor a flow diagram of thermal reactions inside the compressor shell is included at Figure 44. The compressor shell loses energy due to heat emission to the surroundings, but before entering the compression cylinder, energy is transferred

to the refrigerant from the motor windings. The energy input to the compressor may be divided into three parts, firstly heat energy to the compressor suction, secondly to the heat emission from the compressor shell and finally to the mechanical energy driving the compressor. Between the discharge of the high pressure refrigerant from the compression cylinder and its discharge from the outer shell, there is a temperature difference which allows heat to be transferred from the high temperature to the low temperature liquid. In addition, heat is emitted from the metal parts of the compressor to the low pressure refrigerant within the shell. This causes the recycling of energy which is shown in the diagram labelled as high temperature heat transfer. The thermal processes are shown within the boundaries in which they operate, namely, the compressor outer shell, electrical motor, and compression cylinder. At this stage the diagram is not to scale as it was only drawn to demonstrate an outline of energy flow.

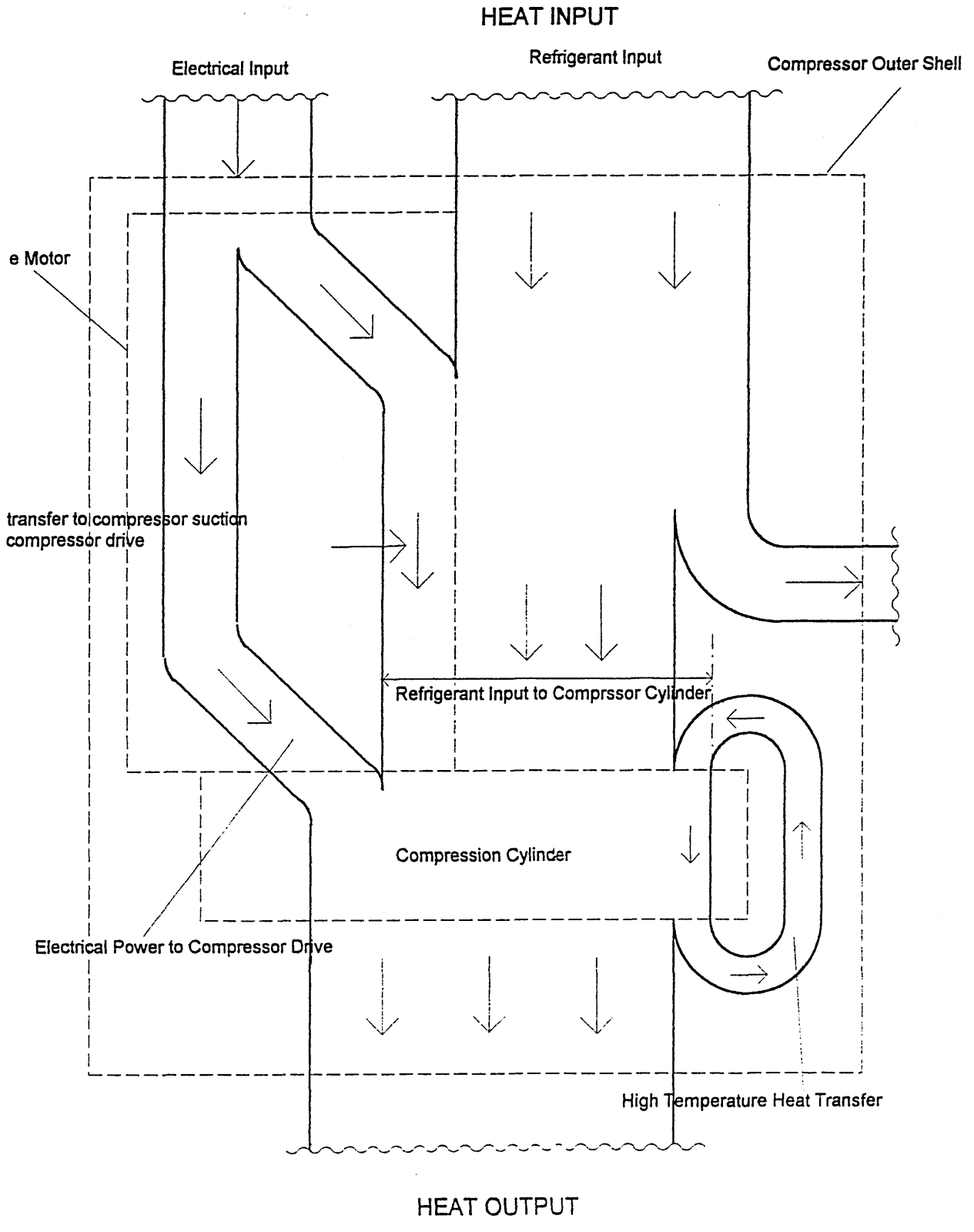


FIGURE 44

Heat Energy Flow Inside Compressor Shell

Hermetically Sealed Compressor

Within the compressor shell heat energy is conserved by flow from higher to lower temperature refrigerant. Heat energy from the motor and compressor passes to the refrigerant and heat from the high temperature side is recycled from the delivery back to the suction. To research fully the thermal performance of the compressor, it would be necessary to insert a thermocouple inside of the compressor shell. As this is not possible, it was decided that, when testing using refrigerant R134(a), a thermocouple would be secured to the outer surface of the compressor shell. This would enable a calculation of the heat loss to atmosphere to be made.

## 5.6 PERFORMANCE TESTS - TEST RIG USING REFRIGERANT R12.

Following the building, testing and setting to work of the test rig, a series of tests were made using the water to water heat pump rig. Initially, all observations were made and recorded manually after commissioning, however, temperature was measured and recorded using a ten point recorder. Synchronisation between the temperature scan and the manual recording of the observations were made by keeping a record of the time. The temperature scan was normally set to operate at five minute intervals and the manual readings were made to coincide. The positive benefits obtained from this part of the research were gained mainly from the practical applications of the previously known basic procedures. The thermodynamic performance data obtained had little originality and was, therefore, of little benefit to this research. A clearer understanding was obtained in the practical understanding of the operation and control of domestic heat pumps in general and of the compressor performance in particular.

## 5.7 CONCLUSIONS - HEAT PUMP DESIGN, CONSTRUCTION AND OPERATION

The test rig, using refrigerant R12, was designed, built, commissioned and operated with the object of research for items applicable when using the environmentally friendly refrigerant R134(a).

5.7.1 Obstacle found whilst building the test rig.

Whilst building the test rig, due to the compact arrangement of the refrigerant pipework, it was found necessary to braise the pipe joints. The movement whilst heating and cooling caused recurring joint leakage when using compression fittings, otherwise, after solving the refrigerant leakage problem, the test rig operated satisfactorily.

5.7.2 Safeguards whilst heat pump was in operation.

The high pressure cut off safety control operated in accordance to the designed safety procedures, so that, at no time was the high pressure relief valve caused to operate. An added item towards the safe operation of the heat pump were the two sight glasses. Firstly, whilst commissioning the test rig, a watch was kept on the sight glass at the compressor suction so that liquid was not carried over into the compressor shell. Also, whilst the heat pump was in operation, the refrigerant leakage losses could be quickly observed, because the sight glass on the outlet from the evaporator would not be running full of liquid.

5.7.3 Control of compressor suction superheat.

Control of the superheat was made by the temperature adjustment screw on the thermostatic control valve and by fitting varying sized orifices see Figure 16. No difficulty was experienced in adjustment of superheat, but at all times the danger of liquid refrigerant entry into the compression cylinder was kept in mind, and avoided.

For the hermetically sealed compressor to be controlled in the same way as for an open compressor the suction temperature control would need to be installed inside the compressor shell, adjacent to the compressor suction valve. In practice, this is not the case, as the location of the temperature control sensor is normally mounted on the pipework immediately prior to entering the outer shell of the compressor. After passing the temperature sensor, the refrigerant is subject to a temperature increase before entering the compression cylinder.

5.7.4 Manufacturer's test procedures.

The CECOMAF test procedure adopted by the compressor manufactuer mounts the compressor suction temperature control sensor at the inlet to the compressor shell. Tests were made with superheat control temperatures varying from 17K to 45K, dependent on evaporating temperatures. Refrigerant temperature is increased further by heat transfer from the motor windings before entering the compressor chamber with a heretically sealed compressor.

Further research needed to be undertaken on the energy distribution inside the compressor shell. It would appear that the calculation procedures proposed by the manufacturer for change of state, are intended for that purpose and no more. The calculation of refrigerant mass flow for design of the heat exchangers must be subject to other mathematical procedures.

5.7.5 Change of state calculations.

Additional superheat gained by heat transfer from the motor windings increases the specific volume of the refrigerant entering the compressor. In the normal operation of the heat pump, superheat is controlled at 5K, at the refrigerant entry to the compressor shell. Invariably, therefore, the change of state calculations will include this reduction of superheat, but also an increase of energy per unit volume of refrigerant, for a domestic heat pump.

For example, at a pressure of 1.47 bar(abs) with a saturation temperature of -20.7°C the vapour returning at 32°C, will produces a superheat at the inlet to the shell of 52.7K. This would normally be reduced to 5K in normal practice. Reduction of superheat at the compressor suction does not produce any change of compression ratio and therefore the compressor suction volume remains unchanged. Energy variation per unit volume, based on unit volume of refrigerant, is calculated as follows:

| | | | |
|---|---|---|---|
| From: | Heat Energy at 32°C | = | 52.7K Superheat |
| | 595.66 kJ/kg x 7.1588 kg/m$^3$ | = | 4264 kJ/m$^3$ |
| To: | Heat Energy at -15.7°C | = | 5K Superheat |
| | 567.00 kJ/kg x 8.632 kg/m$^3$ | = | 4894 kJ/m$^3$ |

Due to the reduction of superheat, there is a consequential reduction of enthalpy from 595.66 kJ/kg to 567.00 kJ/kg, which reduces the energy input to the compressor. The temperature reduction also produces a higher density refrigerant, which increases density from 7.184 kg/m$^3$ to 8.632 kg/m$^3$. Reduction of enthalpy reduces the energy flow by 4.7 % but increase of the refrigerant mass flow reverses the loss to a gain of 14.7 % at the input to the compressor.

Due to a lack of funds, there was no refrigerant flow meter available to be fitted to the R12 test rig. As a result of this, the refrigerant mass flow was calculated by equating the electrical energy input to the compressor to the enthalpy gain across the compressor to determine the mass flow rate.

Heat losses to the atmosphere from the compressor shell are not included at this stage, because of the lack of performance data obtained from the laboratory trials. Provision for this will be made in the next chapter when a thermocouple was fitted to the compressor outer shell. In order to obtain the temperature of the refrigerant within the shell, the thermocouple was enclosed by thermal insulation material.

# CHAPTER 6 LABORATORY RESEARCH - DESIGN OF MODULAR HEAT PUMP

## 6.1 INTRODUCTION.

The change over from refrigerant R12 to R134(a) was carried out successfully. The environmentally friendly refrigerant R134(a) and a matching compressor became available and were used for the remaining research. Using this newly introduced refrigerant, a modular designed air to water heat pump for the space heating of domestic dwellings was investigated. The objective of this was to provide an improvement in the seasonal performance of the heat pump by reducing energy used in the on/off cycling, whilst matching the heat pump output to meet the space heating load.

The heat pump test rig previously built for refrigerant R12 was completely dismantled. Using the supporting frame and condenser from the redundant test rig, a heat pump suitable for the environmentally friendly R134(a), was designed, built and commissioned. Whilst making the above changes, the heat source for the heat pump was also changed from water to atmospheric air. Parts of the refrigerant R12 test rig that were nominated for reuse were both physically and chemically cleaned. The controls and instrumentation were properly checked for accuracy before being fitted. Preliminary tests were made, after which, the test rig was loaded into the environmental chamber.

Laboratory research was made to simulate one of a number of modular units that in practice would operate in parallel. Following on from the study of heat pump performance made in chapter 5, the tests in this chapter included a thermocouple that was placed on the outer face of the compressor shell to enable an assessment to be made of the energy distribution within the compressor shell and the thermal conditions of the compression process.

On completion, commissioning and loading of the heat pump test rig into the environmental chamber, the next objective was to make a full analysis of the energy gain and loss, individually, by air, refrigerant and water.

Exhaustive efforts were made into the calculation of a thermal balance between air, refrigerant and water, but satisfactory results could not be obtained. Following repeated calculations it became evident that an alternative approach needed to be made.

The instrumentation used for recording the modulation of temperatures and pressures of the refrigerant, were checked before installation. The meter measuring electrical input to the compressor had also been checked before installation. The above instrumentation enabled the heat pump performance to be measured throughout the whole refrigerant cycle. Refrigerant mass flow was obtained by calculation described at the end of the previous chapter, clause 5.75, chapter 5.

## 6.2 THE AIR TO WATER HEAT PUMP.

In order to illustrate the design principles being considered, a diagrammatic arrangement of one possible layout using four modular units operating in parallel is shown in Figure 45. The water circulation system for three modular units is shown, the refrigerant circulation for one modular unit only is shown. The next stage of testing was to determine the characteristics of a single modular unit using an air to water system. At this stage, the refrigerant was changed to R134(a).

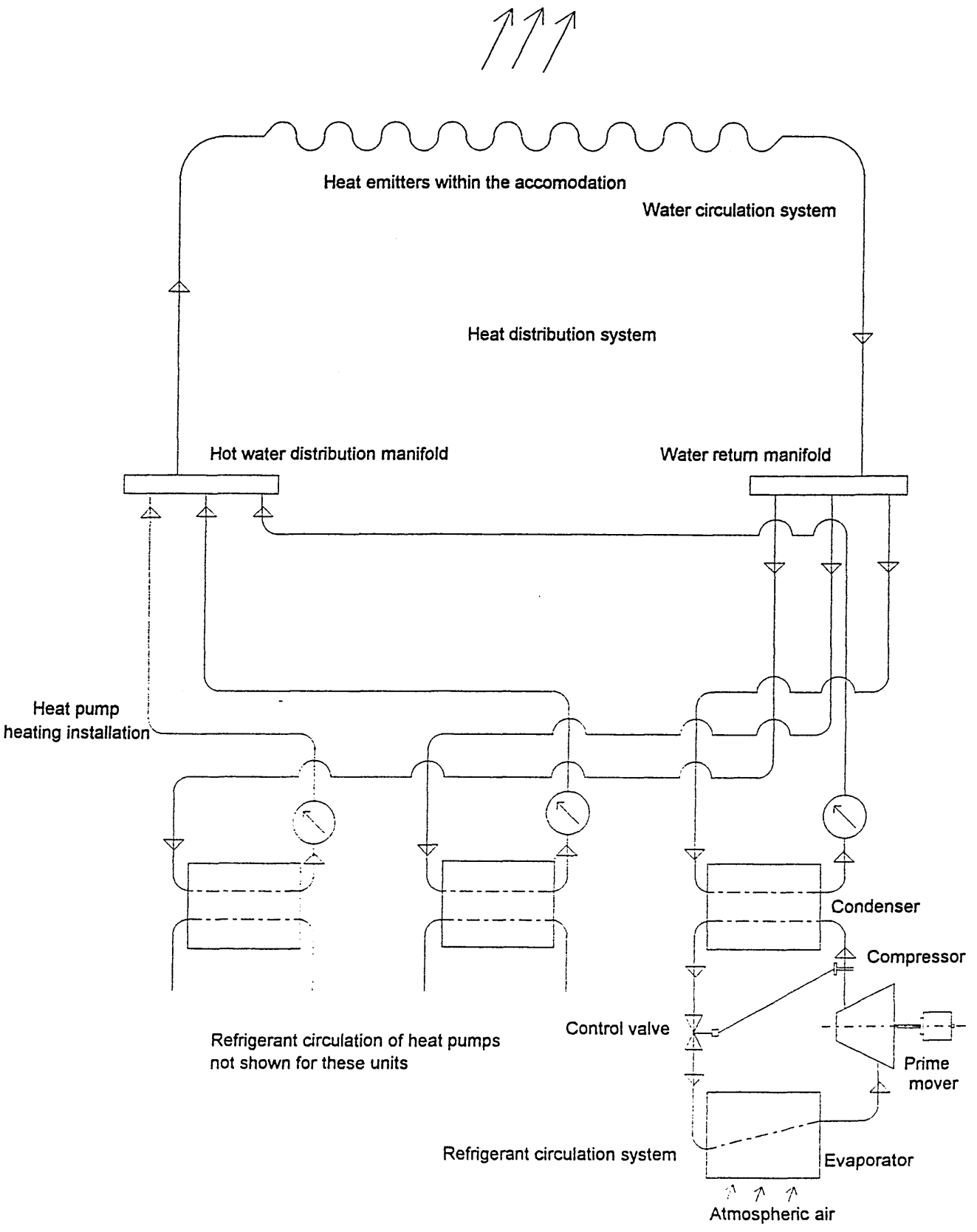


FIGURE 45 Diagramatic layout of modular heat pump installation for domestic space heating

Refrigerant R12, was widely used when the move to HFCs, environmentally friendly refrigerants including refrigerant R134(a), became more widespread. Pressures to make the change were gradual over an extended period at the start, until it became clear to most of the world's governments, that acceptance of change was essential. Once that change became inevitable, pressures were put upon the chemical and engineering industry to produce and develop the use of environmentally friendly refrigerants in the shortest possible period of time. The latter part of the laboratory research for this thesis was undertaken at the latter stages of the development of refrigerant R134(a). This refrigerant was accepted in general use with the knowledge that the global warming potential was less than a tenth of that of refrigerant R12, but there was still some anxiety and doubts regarding the use of HCFC refrigerants in the long term.

### 6.2.1 Development of Refrigerant R134(a)

Events leading to the adoption of refrigerant R134(a) in place of the established refrigerant R12 started in earnest in 1974 at the University of California, when CFCs were linked to a depletion of stratospheric ozone. An international agreement in 1987, the Montreal Protocol, ratified these concerns and called for a freeze in the production and consumption of CFCs [55]. The meeting in 1993 at Copenhagen brought forward the ban of CFCs from the year of 2000 to the 1st January 1996 [56].

Replacement by HCFCs by HFCs as refrigerants was not considered by some to be a satisfactory solution to the environmental damage problems. The UK Government legislated that the use of HFCs were to be reduced to 1990 levels by the year 2000 [57].

Objectives of this research were discussed with the refrigerant manufacturer who recommended the use of Refrigerant R134(a).

Gu Refrigerants and the Gu Thermodynamic Cycle

The Gu refrigerants have been developed to operate in conjunction with the Gu thermodynamic cycle to replace the refrigerants now being used [58]. This was produced over a number of years by research, with the objective of producing more environmentally friendly plant operation and increased thermal efficiency from both refrigeration and air conditioning plants.

In order to assess the level of atmospheric contamination on the Gu cycle when compared against established refrigerants, it was proposed that a worksheet be produce to compare values based on 'Total Equivalent Warning Impact' (TEWI). The calculated value of TEWI is the sum total of both the direct and indirect effects. Direct effect is based on the annual refrigerant loss by leakage, multiplied by the GWP. The indirect effects are based on the plant efficiency and annual power consumption.

6.2.2 Thermodynamic Properties of Refrigerant R134(a).

A consideration of the performance of environmentally friendly refrigerants was found in the technical paper Experimental Performance of Ozone-Safe Alternatives [59]. This paper lists the global warming potential of CFC and Alternative Refrigerants. The following data was extracted from Table 1 and Table 3A of the above technical paper;

| Refrigerant | Formula | COP.H | GWP |
|---|---|---|---|
| R12 | $CCL_2F_2$ | 2.32 | 3.10 |
| R134(a) | $CF_3CH_2F$ | 2.3 | 0.30 |

Where;

COP.H = Coefficient of Performance - Heating.

GWP = Global Warming Potential. (R11 = 1.0, Scientific Assessment of ozone: 1989)

From the above test results the thermodynamic performance appears to show little difference between R12 and R134(a), but the environmentally harmful effects of R134(a) were reported to be a tenth of the harmful effects of refrigerant R12.

Industrial change over to the use of environmentally friendly refrigerants was undertaken by manufacturers under the pressure of demands for quick results. Decisions as to the type and chemical composition of the environmentally friendly refrigerants had to be finalised first. Thermodynamic properties of the liquid, vapour and superheat states needed to be properly designed for their use.

Thermal properties of refrigerant R134(a) were issued by the manufacturer, but a number of revisions had to be made. Clearly the data had been produced quickly, but with too much haste at the cost of a reduction in accuracy. Repeated updating of the thermodynamic data became a difficulty, but finally the data was distributed on a computer disk. This provided a quick method by which data could be loaded into the computer.

### 6.2.3 Compressor

The compressor used was hermetically sealed and generally similar in basic design to that used for R12, described in Chapter 5, other than it's suitability for use with the refrigerant R134(a). The compressor used was a Danfoss SC15GH, code number 104G8560, displacement 15.3cm$^3$/rev.

Manufacturer's CECOMAF Test Results:

Condensing temperature: 55°C

Ambient temperature: 32°C

Suction gas temperature: 32°C

Liquid temperature: 55°C

220 V. 50Hz.

Fan cooling at 32°C Ambient Temperature.

Heat output = capacity + power consumption.

Capacity Watts.

| Evaporating Temp: | °C | -15 | -10 | -5 | 0 | +5 | +10 | +15 |
|---|---|---|---|---|---|---|---|---|
| Capacity : | Watts | 435 | 570 | 730 | 900 | 1140 | 1420 | 1730 |
| Power Consumption: | Watts | | 420 | | | 575 | | |

Power consumption was given only for evaporating temperatures -10°C and +5°C. Other values, were assumed to be in a linear relationship to those given.

6.2.4 Condenser

The condenser used previously for R12 was cleansed from contamination left from previous use by using the Retrofit Flushing Programme, specified by the refrigerant manufacturer. The cleanser used was Hexene which involved vaporised toxicity hazards from the acid, which were a danger if inhaled or to the eyes and exposed skin. The cleansing procedures were discussed and agreed in detail with the University Safety Officer prior to action being taken. The whole action, including the disposal of the used acid, was safely completed. The cleansing procedure was performed by a Senior Technician of the university staff in the presence of and to the complete satisfaction of the Safety Officer.

The manufacturer's R12 System Retrofit was used prior to loading Ester KLEA134(a) refrigerant, with the object of cleansing any contamination of the condenser and in particular to remove the mineral oil.

### 6.2.5 Condenser - Water Circulation System

During the previous R12 heat pump test programme, it was found that operation of the water temperature control valve adversely affected the pressure drop through the system. This caused variations of the mass flow rate. When the R12 test rig was in operation the water flow had to be frequently reset by manually adjusting the globe valve. For continuity of the tests it was desirable to maintain constant flow, and, therefore, the globe valve was replaced by a needle valve and an automatic temperature control valve was fitted to regulate the inlet temperature to the condenser.

To overcome the problem of stabilising condenser water flow a water separating tank was installed into the system, as shown in Figure 46. High water temperature at the condenser inlet caused a proportion of the hot water flow to be drained off to the overflow tank. Cold water make up reduced the water temperature in the water storage tank. Electric immersion heaters were fitted into the water storage tank to reduce the heat up period on start up.

### 6.2.6 Evaporator

In addition to the change of refrigerant from R12 to R134(a), the heat pump evaporator was changed in design from water to air heat source. This involved dealing with ice formation on the air side of the heat exchanger. The complete heat pump construction was loaded into an Environmental Chamber where air temperature and humidity were controlled. Previous laboratory research had been chiefly directed towards steady state operation of the heat pump.

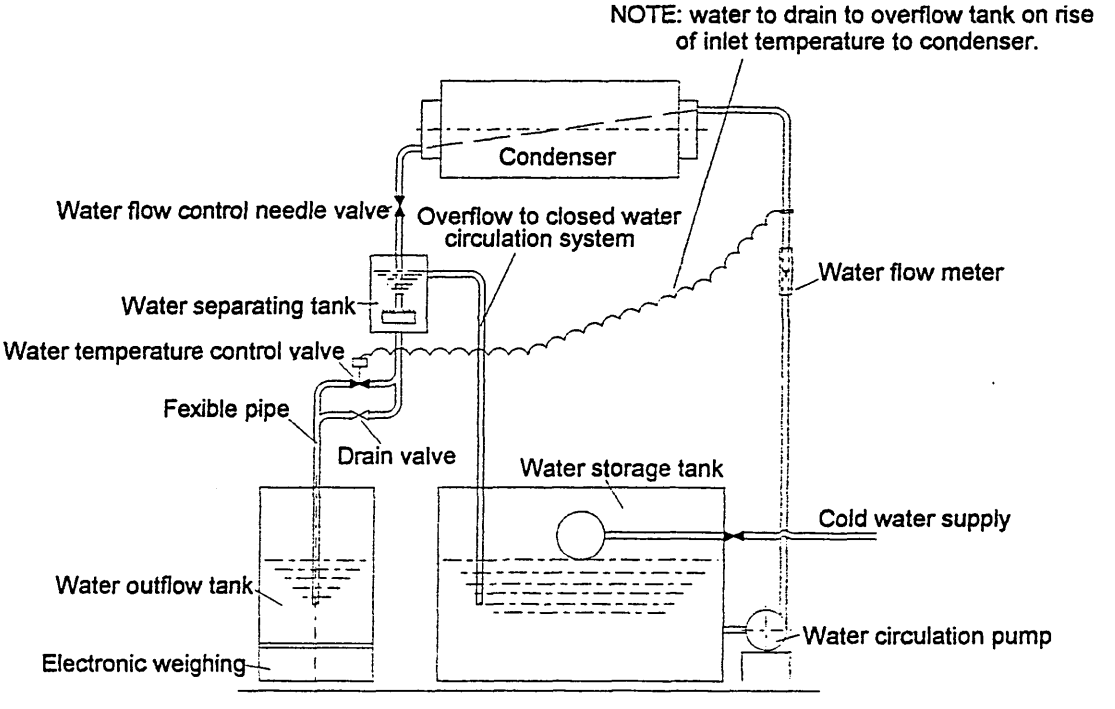


FIGURE 46 Addition of water separation tank and modification of water circulation pipework

The evaporator heat exchanger coil was mounted inside a rigid plastic container. Air intake was in the end, at high level in the container, passing down over the heat exchanger coil. The outflow from the evaporator discharged in the direction of the compressor. Air discharged from the evaporator container was utilised as supplementary cooling of the compressor outer shell. The air flow was activated by an axial flow fan at the air inlet to the evaporator. Air flow volume was controlled by a hand operated damper at the air outlet. Plate P1 shows the test rig before being transferred into the test chamber. A schematic diagram of the major components of the test rig is shown at Figure 47. This diagram indicates the major items of the test rig in a similar relative position when viewed from the front and slightly to the left of the photographer.

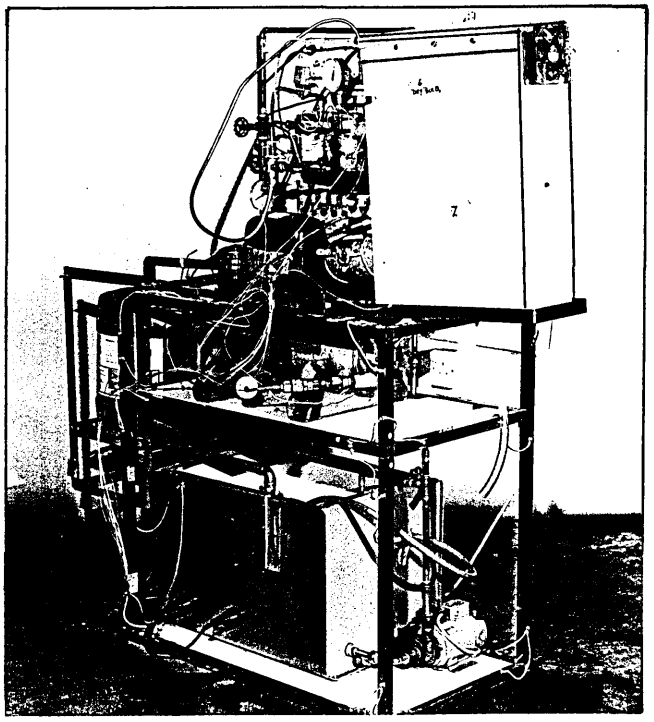

Plate P1

Test rig prior to loading into the

Environmental Chamber

6.2.7 Environmental Chamber.

The internal dimensions of the chamber were 1.95m width x 3.05m length x 2.02m height. Total volume was approximately $12m^3$. The air conditioning plant included the following:

(a) Refrigeration Plant,

(b) Internal Space Heating,

(c) Hygromatik Steam Injection Humidifier,

(d) Evaporative Humidifier,

(e) Air Injection Fan, and

(f) Air Circulation Fan.

With an ambient air temperature of 20°C and without any heating load inside the chamber, the refrigeration plant was capable of reducing the chamber temperature to -20°C. After loading the heat pump test rig into the chamber and in operation, the heating load reduced the minimum chamber temperature to -5°C. With steam injection, when making trials with high humidity inside the chamber, the minimum temperature was raised to -1°C. These temperatures were accepted as the lowest whilst making tests simulating seasonal atmospheric conditions.

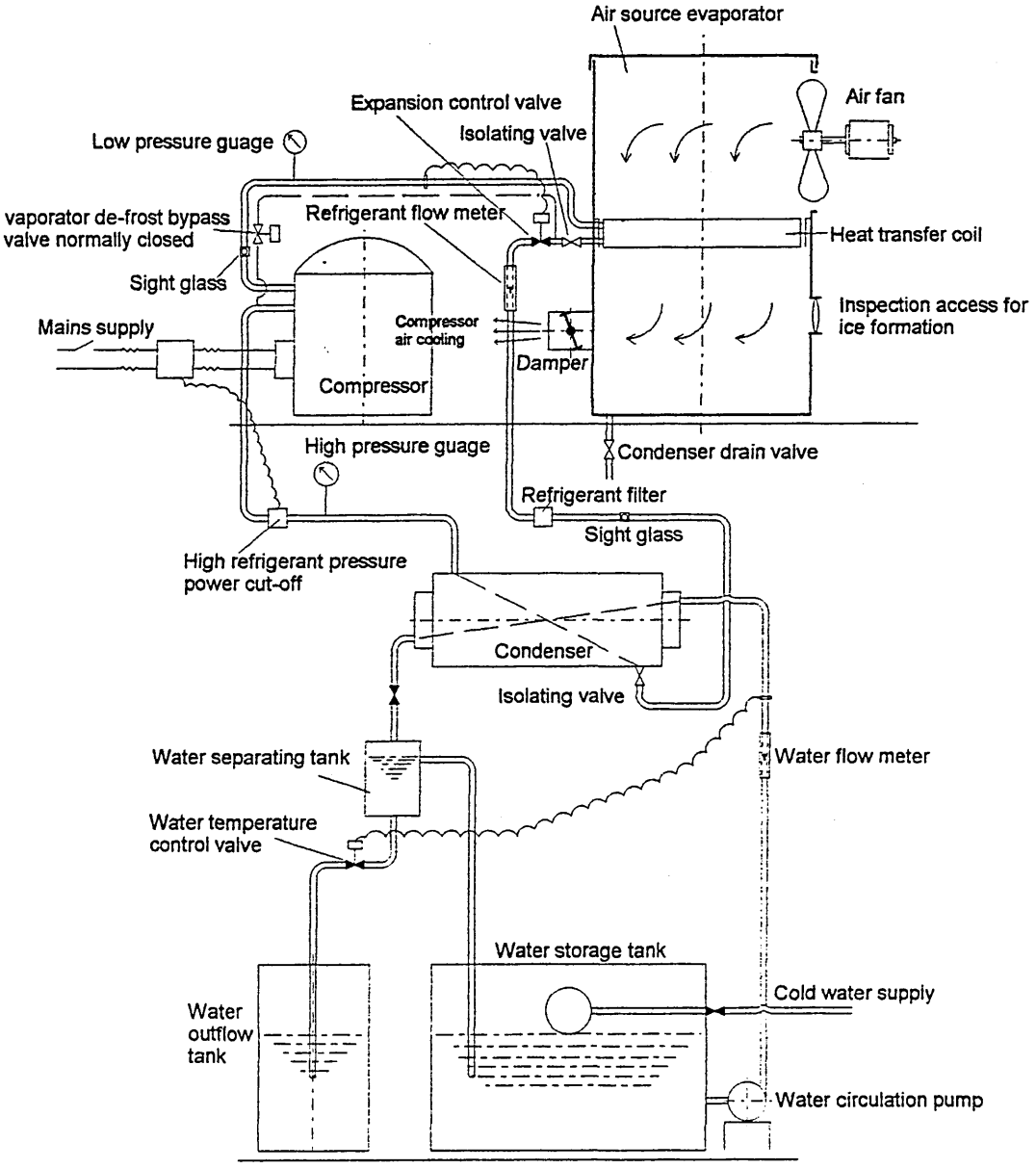


Figure 47 Schematic diagram - domestic heat pump test rig
Refrigerant R123(a)

The plate P2, taken from the front of the chamber shows the door open and the evaporative humidifier in position. When the chamber was built no provision was made for power supply cables, control cables or piped services into or out of the chamber. To overcome this, a temporary thermally insulated door, free of hinges, with apertures for the service cables and pipes was fitted.

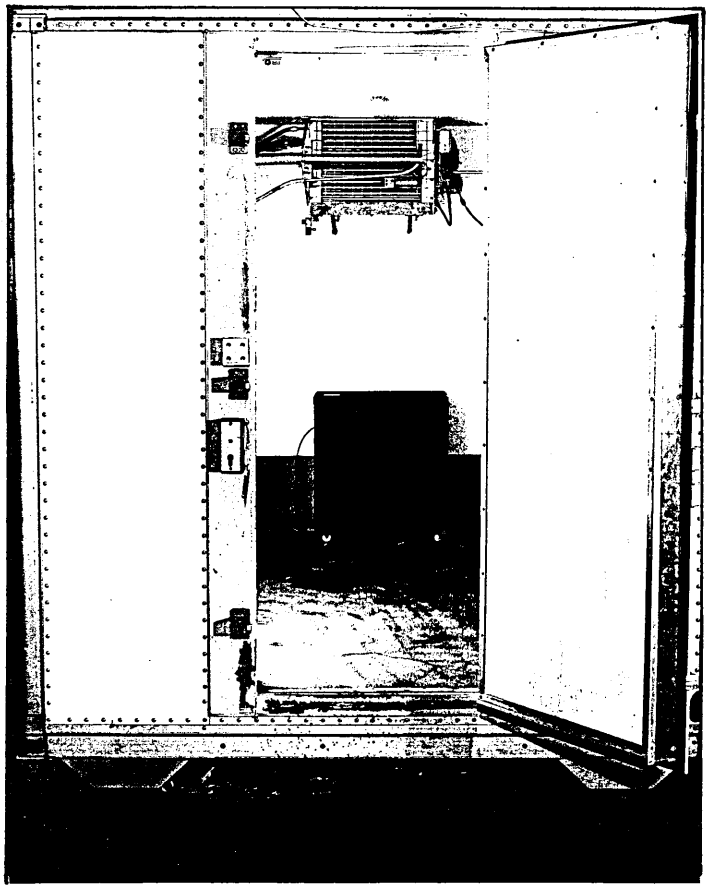

Plate P2

Front view of the Environmental Chamber

6.2.8 Instrumentation

Layout of the ten thermocouples, were generally similar to that of the R12 test rig, modifications being made to accommodate the change of the heat source from water to atmospheric air. A total of three thermocouples were fitted to the air side of the evaporator inlet, one dry bulb, one wet bulb on the air inlet and one dry bulb on the air outlet.

A thermocouple was also fitted to the external surface of the compressor shell in order to estimate to refrigerant temperature entering the compressor cylinder. It was not considered appropriate to open up the sealed compressor casing or to drill the shell for the insertion of a thermocouple.

6.2.9 Instrumentation Plates.

P3: Comark 6601, ten channel electronic thermocouple meter which was programmed to scan the thermocouples fitted to the test rig.

P4: Epson LX800 Printer, used to record the temperatures in co-ordination with the ten channel electronic thermocouple meter.

P5: Electrical input power to the heat pump test rig, compressor motor, Electronic Wattmeter Feedback EW 604.

P6: 300 DC Power supply to the Hygromatik Humidifier, controlling the rate of evaporation and steam injection to the Environmental Chamber.

P7: Eurotherm 91E, Controlling the power supply and temperature of the heater fitted inside the Environmental Chamber.

P8: 30 Volt. electrical supply to measure refrigerant pressures.

P9: Farnell E30/1 to Gould Bryan's three pen recorder. Used for recording, through a transducer, the compressor suction and delivery pressures of the test rig. Two channels were used.

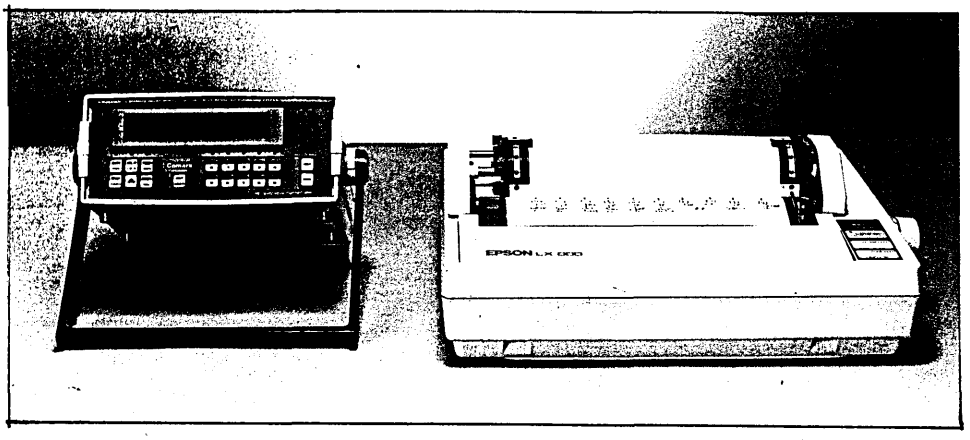


P3 P4

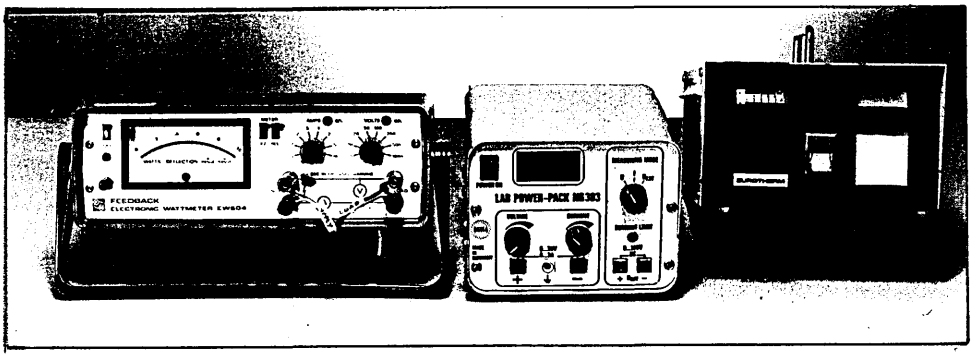


P5 P6 P7

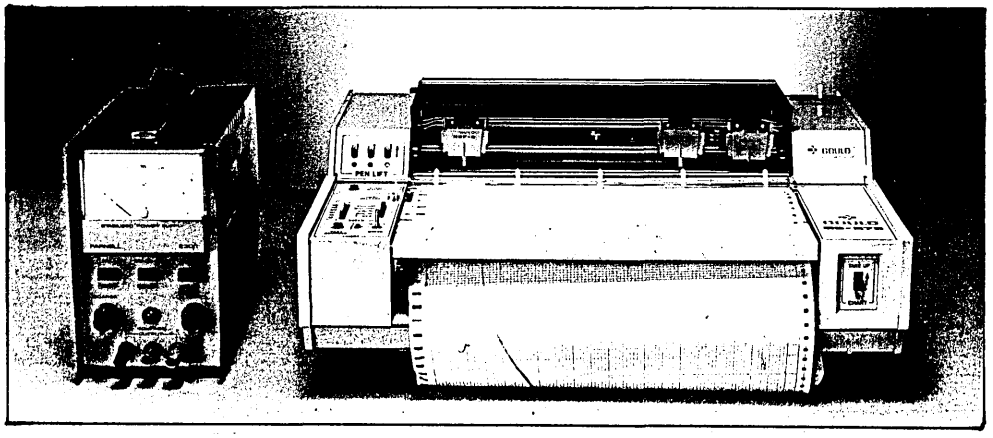


P8 P9

Plates P3 to P9 - Instrumentation of the Test Rig

6.2.10 Defrosting of the Evaporator.

Ice, which for the purposes of this project originated as moisture in the atmospheric air, was deposited on the heating surfaces of the evaporator due to low atmospheric temperature. It is the heat exchanger surface temperature in contact with the atmospheric air that governs the extent by which icing takes place. Dependent upon the heat exchanger design, ice formation normally begins to form at air temperatures of 3°C or 5°C.

An investigation into the factors influencing the thermal performance due to ice formation on the heat exchanger coil was made by Bouma [60]. This research concludes that the insulating effect of the layers of ice only slightly affects the thermal capacity of the evaporator. Tests were made with fin spacing of 1.9 mm, which is smaller than normally used. The major affect of icing found when the fin spacing are small, is that the air volume flow rate is reduced due to the diminishing air passage area. Fins providing the extended heating surface on the air side spaced at 4.5mm pitch between individual fins, were found to be the minimum acceptable.

It was found by the Electricity Association [61], from tests with ambient temperatures of -1°C, that effects on the seasonal COP caused by the defrosting requirement was insignificant, but the reduced heat pump thermal output at times of peak demand could be a disadvantage. It was found that at the same temperature, -1°C, the reverse-cycle defrost reduced the heating capacity by 19% and the hot-gas defrosting system by 25%. The reduction of heating capacity became significantly less at higher temperatures and at 3°C ambient was found to be marginal. Seasonal energy loss due to the icing was found to be an insignificant proportion of the annual energy costs, but it was concluded by the Electricity Association that allowance should be made when sizing the heat pump to maintain comfort conditions at times when they are most needed. This causes an increase of heat pump capacity up to 25% .

Formation of ice on the fins reduces the cross sectional area available for air flow, thus reducing the air flow volume and heat flow through the heat exchanger. Fins placed closer together reduce the time interval in which the deterioration of heat pump thermal output occurs.

At other times, when the seasonal atmospheric temperatures are above those at which ice is being formed, the heat pump would normally be oversized, but if extra capacity is allowed to cover the short period of reduction of capacity due to icing, the heat pump would be further oversized. Heat pump performance with supplementary heating making allowance for the reduction of heat pump output incurred due to ice formation, as shown previously in Figure 30.

The fin coil evaporator for this research had one refrigerant stream through 18 tubes, six wide and three deep with 0.37m between end plates and 5mm spacing between fins. For this project, defrosting the evaporator by a hot vapour bypass was used. This involved a refrigerant bypass fitted from the compressor output to the evaporator input. The automatic defrosting on/off control was an electronic timer unit activating a solenoid valve fitted into the refrigerant bypass. An alternative manual control of defrosting periods, from outside the environmental chamber, was fitted.

### 6.2.11 Refrigerant Flow Meter.

The advantages of installing a refrigerant flow meter into the refrigeration circulation system was realised whilst running the refrigerant R12 test rig. There was not a suitable meter available in the laboratory, the necessary calculations to size the meter were made. The thermodynamic data upon which the calculations were made was the latest available prior to writing the specification of the refrigerant flow meter.

The first stage of the calculations to specify the operating conditions for the refrigerant flow meter were based on the compressor manufacturer's performance data, as shown in appendix A6.1. These calculate the refrigerant mass flow, compressor suction volume and volumetric efficiency

and are based on superheat at the compressor suction between 17K and 47K. Appendix A6.2 recalculates the same operating conditions of pressure and temperature as appendix A6.1, but the superheat for the whole range of results are calculated for a 5K superheat. Appendix A6.3 takes into account the changing conditions between appendices A6.1 and A6.2 and recalculates the thermal performance at the operating conditions of 5K superheat.

The object in making both calculations was to observe the difference in values, so that the results of both conditions were within the operating range of both calculations. The certificate of calibration from the meter manufacturer, specified a range of operation from 0.16 to 1.6 l/min.

The flow rate indicated by the refrigerant flow meter is only true when the fluid density is that at which the meter was calibrated. Any deviation of fluid density may be corrected by the procedures detailed in appendix A6.4. Due to changing condenser pressure and resulting change of fluid density in practice, these calculations need to be followed.

### 6.2.12 Evaporator - Measurement of Air Flow.

The air flow volume obtained from the axial flow fan mounted at the air inlet was measured before mounting the evaporator onto the test rig. A 100mm diameter metal tube was fitted, with a test point two thirds down stream from the air outlet connection onto the evaporator casing. To properly locate the test probe, calculations were made of the internal cross sectional area of the tube which was divided into three equal concentric areas. The three centres of area each side of the tube centre, giving a total of six test points, were nominated.

Two series of tests measuring air velocities were made using the alternatively the Pitot Tube and the Hot Wire air flow meters. The Pitot Tube gave a slightly lower velocity which concurred when checked against the data provided by the air fan manufacturer. At a temperature of 18°C the air volume was found to be $95m^3$/hour, the value which was included in the heat pump performance calculations.

## 6.3 COMMISSIONING AND OPERATION OF THE R134(a) TEST RIG.

After first purging the refrigerant circulation system it was pressurised using refrigerant R134(a) and refrigerant leakage tests were made. Preliminary trials were made to establish the correct liquid refrigerant charge within the condenser. This was made by the observing the liquid and vapour refrigerant flow through the sight glasses. The refrigerant charge was increased until the sight glass installed at the condenser discharge was running full of liquid. Both of the high pressure safety cut off controls, the pressure relief valve and the automatic high pressure cut off were then set and tested. The vapour defrosting bypass was installed and tested.

Prior to loading the heat pump test rig into the environmental chamber, preliminary tests were made from which results and observations of performance and calculations were obtained. It was found that there were two items of malfunction, these being the refrigerant flow meter and the condenser water circulation system. The approach made to the calculations was to check the heat pump thermal performance for the whole of the heating cycle, as far as practicable. The performance calculations were found to be unsatisfactory, because the values of energy input to energy output, did not equate.

Detailed calculations from the initial test run are included in Appendix A6.5. The thermal performance calculated here was found to be inaccurate, but the detailed study of the performance calculations were found to be useful. The most significant item being that, if there is no sub-cooling of the condenser liquid, the refrigerant saturated temperature at the condenser output and evaporator input, does not give any indication of enthalpy at these points. This item may be considered to be elementary, but it is important to know if, for any reason, the designed thermal performance of the heat exchangers is not being fully produced.

The manufacturer's of the refrigerant flow meter were contacted regarding this, who asked for the meter to be returned for recalibration. Due to the extensive refurbishing of the university buildings, the laboratories were soon to be demolished and rehoused making recalibration

FIGURE 48 Calculation of Refrigerant Mass Flow

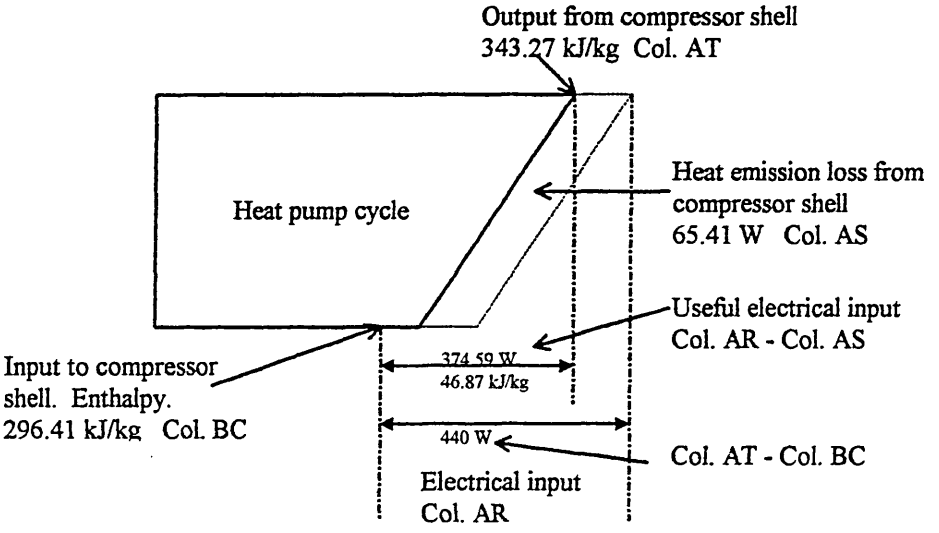


Data from: Analysis of heat pump thermal performance, steady state operation, Scan 20.

| Input kJ/min | = | Output kJ/min |
|---|---|---|
| $\frac{374.59 \times 60}{1000}$ | = | 46.87 kJ/kg x M kg/min |
| M kg/min | = | $\frac{22.475 \text{ kJ/min}}{46.87 \text{ kJ/kg}}$ |
| Refrigerant mass flow | = | 0.480 kg/min Col. BE |

Col. Indicates the column from which the data was abstracted.

## Calculation of Compressor Performance

Equations of state.

| Data | | Units |
|---|---|---|
| A | = Electrical input to compressor | Watts |
| B | = Refrigerant mass flow | kg/min |
| C | = Specific enthalpy | kJ/kg |

Where the value of two of the above items are known, the third is calculated as follows:

To calculate electrical input 'A':

A = B x C
= kg/min x kJ/kg = kJ/min
= kJ/min x 1000/60 = J/s

To calculate refrigerant mass flow 'B':

B = A/C
= J/s / kJ/kg
= (J/s / kJ/kg) x 60/1000 = kg/min

To calculate specific enthalpy 'C':

C = A/B
= J/s / kg/min
= (J/s / kg/min) x 60/1000 = kJ/kg

impossible. Use of the refrigerant flow meter was, therefore, abandoned. Calculation of the refrigerant mass flow was made using the existing instrumentation. The method used is shown in Figure 48.

The condenser water circulation system at the condenser outlet was modified by the addition of a water tank as shown in Figure 46. The layout of the pipework was amended and an additional water tank fitted to divert away from the storage tank when the inlet temperature to the condenser increased above the set temperature. The water flow rate was adjusted by a manually operated needle control valve at the condenser outlet, after which it entered an open topped water separating tank. The addition of the water separating tank enabled the condenser to operate at a controlled temperature and constant pressure.

### 6.3.1 Steady State Operation of the Test Rig

Following the fitting of the water separation tank and modification of the pipework, the condenser water circulation system proved to operate satisfactorily. The heat pump was then loaded into the environmental chamber. It was found that the previous calculations, made to size the refrigerant flow meter, could not be used as originally intended. The previously made flow meter calculations were used, as shown in both Appendix A6.1, based on the CECOMAF manufacturer's performance tests and Appendix A6.3, where allowance was made of differing operating conditions of the test rig. These were used as a guide to the steady state thermal performance of the test rig.

Heat pump thermal output, Appendix A6.1, row 15, and compression ratio, row 33, were utilised to represent performance based on the manufacturer's performance trials. The results are shown as curve 'B' in Figure 49. Locations of the thermocouples are shown numbered on Figure 50.

Points indicated by an 'x' on Figure 49, are the results of a steady state trial run of the heat pump test rig operating in the environmental test chamber. Three sets of results from the laboratory trials and the methods used for the calculations, are shown in Appendix A6.6. The complete set of results calculated from the tests are shown on the graph of compression ratio and thermal output in Figure 49. It was not possible to obtain test results to cover the whole range of the graph using the test rig, due to the fact that the maximum condenser pressure was 10 bar (abs). With regard to the graph in Figure 49 and the test rig results, it was observed that there were deviations above and below the curve, but the trend was to follow curve 'B'.

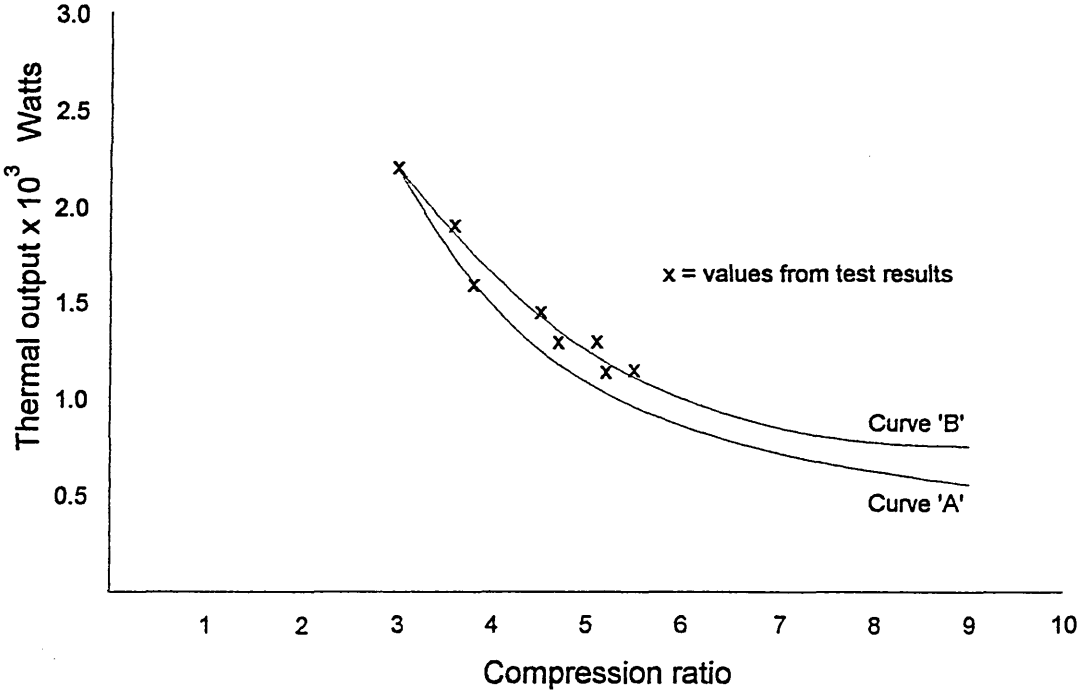


FIGURE 49 Thermal output of heat pump test rig plotted against compression ratio.

Calculation from:
Curve 'A' - manufacturer's CECOMAF performance test results,
Curve 'B' - refrigerant R134(a) test rig performance, based on CECOMAF tests, but with adjustments made for the reduction of superheat at the compressor suction to 5K,
'X' - results from laboratory trials.

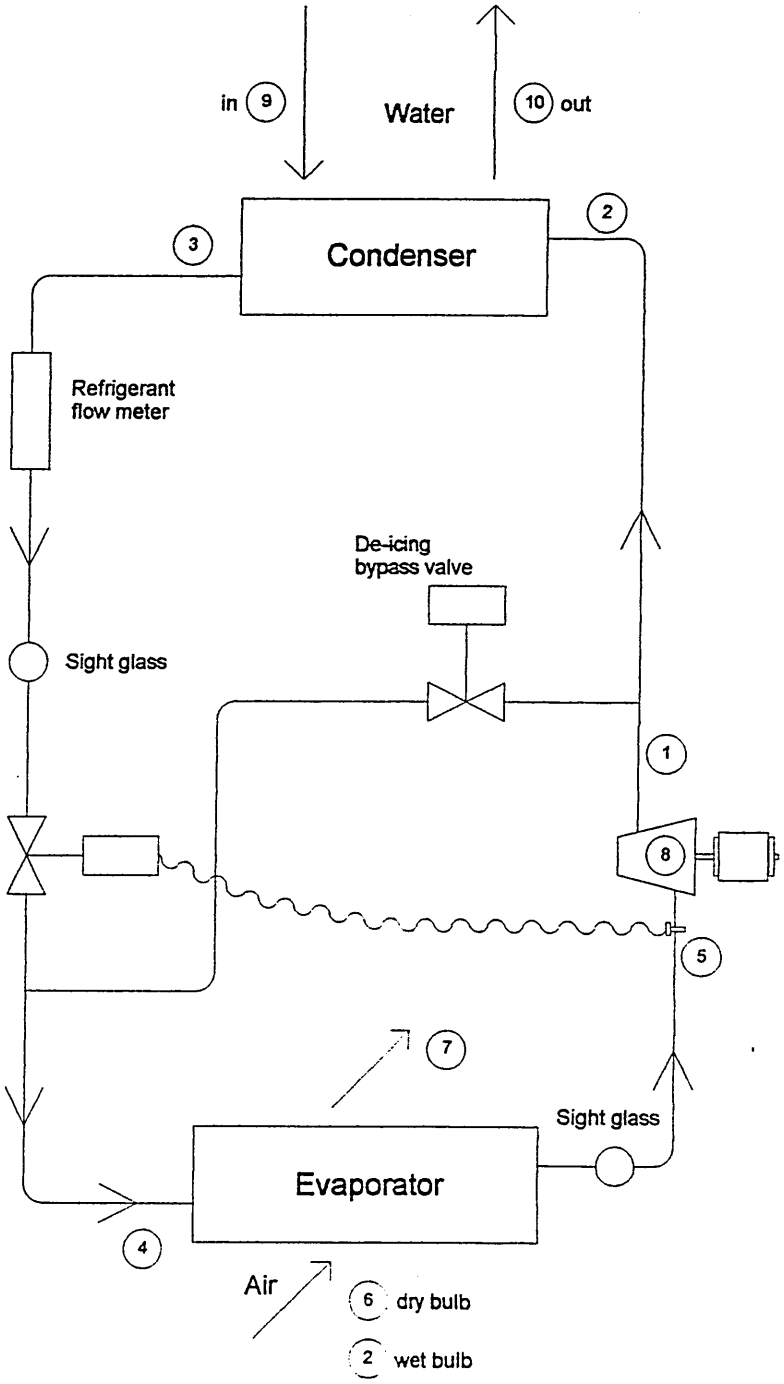


Figure 50 Refrigerant cycle - R134(a)
Showing locations of thermocouples and de-icing bypass

### 6.3.2 Energy Distribution Inside the Compressor Shell

A better understanding of the changing conditions of temperature and pressure inside the compressor shell was required. During the laboratory research it was realised that the true superheat of the refrigerant entering the compressor cylinders was not known, neither was it published by the compressor manufacturer. Isentropic efficiency was calculated on the value entering the shell of the compressor which normally produced a result in the order of 60 to 70%. This does not include for the additional heat gain due to heat given off by the compressor and motors before the refrigerant enters the compression cylinders

The objective of this particular investigation was to obtain the refrigerant vapour temperature at the point, as near as possible, to that where the refrigerant enters the compressor cylinder. Drilling the compressor shell to fix a thermocouple inside the shell was impractical and therefore a thermocouple was fixed in a mid position vertically on the outer surface of the compressor shell. After cleaning the surface, the thermocouple (number 8), was secured to the surface and then covered locally with a pad of thermal insulation material. Locations of the ten thermocouples being used are shown in Figure 50.

Calculation of the degree of superheat entering the compressor was obtained first. Appendix A6.5, column K gives the refrigerant saturated temperature through the evaporator. Column O records the temperature at which the refrigerant enters the compressor shell, given by column P. The temperature at column P being assumed to be equal to that inside the compressor shell.

The saturated refrigerant temperatures of the evaporator are shown, in column K, to be below zero. The total degrees of superheat entering the compressor cylinder would be given by the addition of columns K and P.

The average superheat for the whole of the eighteen sets of results shown in Appendix A6.5, was found to be 37.7K. When the isentropic efficiency was calculated from the above data, it was found that it produced an efficiency greater than 100%. Delivery temperature from the compressor was measured by thermocouple 1 and it was questioned if there was a loss from the refrigerant high pressure to the low pressure refrigerant between the output from the compression cylinder and the point of temperature measurement. Heat energy return from the high pressure to the low pressure side of the compressor is shown in the previous chapter, the heat energy flow chart, Figure 44.

## 6.4 HEAT PUMP CAPACITY CONTROL.

Atmospheric air is the most universally obtainable heat source of low grade heat and, therefore, is used as the heat source for this study of space heating domestic dwellings using heat pumps. When operating at design conditions, the domestic space heating installation must produce sufficient heat to meet the space heating load. When atmospheric temperature falls below the design temperature, air to water heat pump thermal output is reduced, but the space heating load increases. To maintain the same level of thermal comfort conditions as previously discussed, supplementary heat needs to be provided.

Increase of atmospheric temperature causes a reversal of the above conditions. The space heating load diminishes and the increased thermal output of the heat pump needs to be reduced to properly simulate the space heating requirements. The most frequently used capacity control system for the heat pump is the utilisation of a wall mounted room thermostat or thermostatic radiator valve to activate, or switch off, the heat pump on rise and fall of room temperature. Increased atmospheric temperature reduces the space heating load, but the reduced

temperature.difference between condensing and evaporating increases the potential continuous load output of the heat pump.

Variable Speed Drives for Capacity Control of Heat Pumps

The methods by which the rotation speed of electrically driven motors may be varied, has been developed over a number of years. Since the 1980s, at a time when domestic space heating using a heat pump lost favour, the performance of variable speed drives have continued to improve on other applications. The market by which the control of mass flow of the refrigerant in circulation is varied to match heat pump output to the space heating load is, for the present, very small.

The operation of conventional heat pumps used for domestic space heating have cycling losses that are significant. The variable speed drive needs to provide a controlled capacity reduction of thermal output from the heat pump. In addition, the electrical input to the compressor motor needs to be reduced, as near as possible, in the same ratio as the thermal output from the heat pump, and for other functions including the lubrication of the compressor to operate satisfactorily at all levels of thermal output control.

Seasonal Operation of Modular Units

The system of capacity control studied in this project was made by the use of modular units. Operation of both the conventional and modular heat pumps is shown in Figure 51, where the oversizing of the heat pumps above the design point varies between the two arrangements.

The amount by which the heat output of the heat pump is in excess to that required for both of the above procedures is shown in the charts in the figure referred to above. Clearly the proportion by which the excess heat pump capacity, shown by the cross hatching, is significantly reduced by the use of modular units. To determine the amount by which the coefficient of performance may be increased by the use of modulator heat pumps needs to be based on field trials. It would haveeen preferable to use the data for refrigerant R134(a), but it was found convenient to use the published

results of field trials by Foxley and Weaver [25]. The data produced in this paper involves a total of forty installations in Europe, but the analysis for estimation of heat pump seasonal COP is based on the climate in SE England. These calculations do not fully produce the increased heat pump performance obtained by the use of a modular units, but they have been utilised to indicate the gains obtained by reducing the effects of on / off cycling.

Calculations of the conventional and modular design heat pump are shown in Appendix A6.7. Sheets one and two of this appendix describes each item in the modular design. Details of the equations used are included in sheet 3, which shows the calculation of seasonal performance using five modular units. Sheet four is the calculation of the thermal performance of a conventional heat pump producing the same seasonal heat input to the building, as that for the five unit modular design.

The building heat loss is unchanged from the field conditions detailed by Foxley and Weaver, but it was decided to have five modular units, each 25% of the heat pump output capacity used in the technical paper. This change provides increased thermal input to the building which at low atmospheric temperatures, reduces the requirement for supplementary heat. The COP for operation at both part and full loads were as used and unchanged from the values given in the technical paper. The calculations in the above appendix show that an increase of 10% COP is obtained, due to the reduction of the effects of an on / off cycling by using a heat pump of modular design. The loss of energy due to intermittent operation of the heat pump at part load conditions was calculated, but the savings that could be made from the loss of energy due to oversizing of the heat pump at light load conditions was not determined.

For example, at an atmospheric temperature of 13°C, the energy supply to the space heating system by conventional heat pump would be 11.4 kW to meet a space heating load of 1.86kW, more than six times oversized.

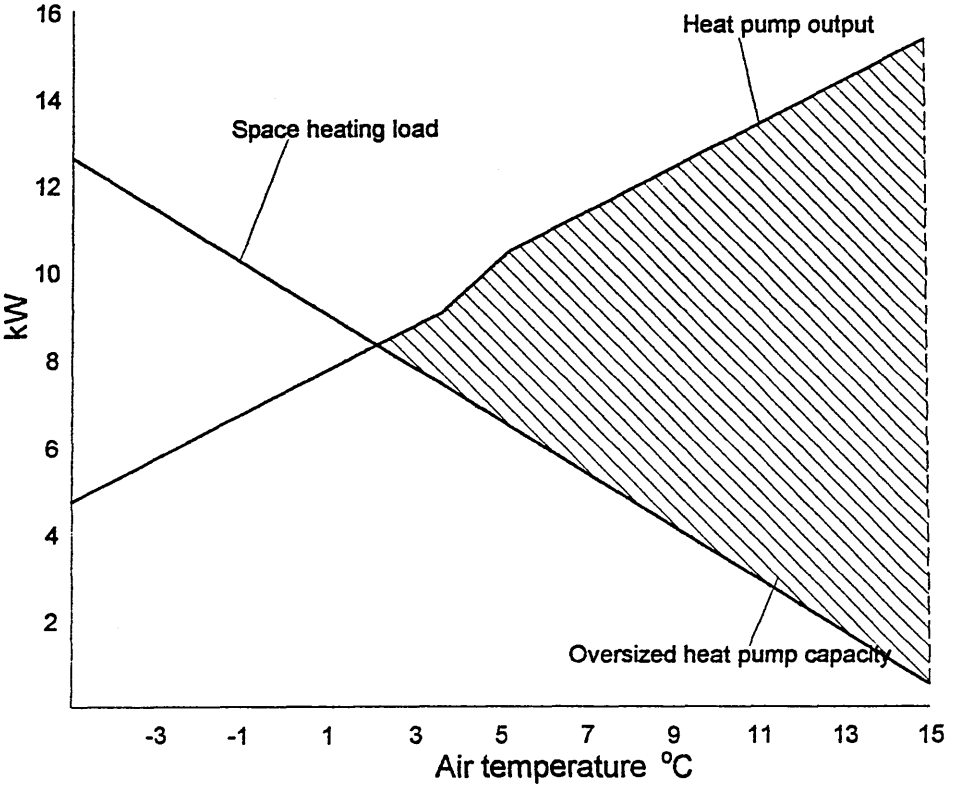


Conventional Heat Pump

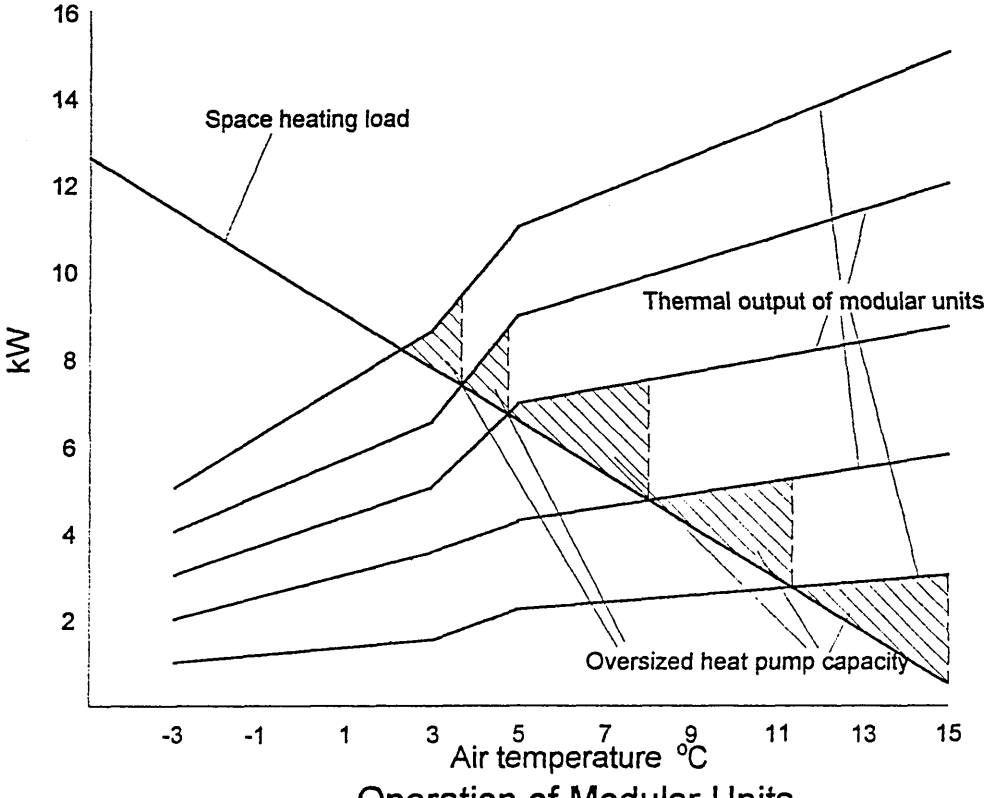


Operation of Modular Units

FIGURE 51 Seasonal operation of conventional and modular designed heat pumps

A modular designed heat pump would only operate one of the five units, reducing producing the overload to 60%. The calculations took into account that, at any time, of the number of units necessary to fulfil the requirements of the space heating load, one unit only would be on / off cycling. For example, if four units were in operation, three units would be operating continuously and the other being the only one cycling. Figure 51 shows that, in a conventional heat pump, between full load conditions at the balance point and no load due to increasing atmospheric temperature, oversizing varies between zero and full load of the heat pump. The modular design thaned heat pump operates in a similar mode, but in five small stages, the overload never being above the thermal output of one modular unit. The etched area indicates oversizing for each arrangement and shows that the modular design is reduces this to 15% of the conventional heat pump.

Calculations conducted by the Electricity Council Research Centre [61], show that oversizing of the heat pump in domestic installations by 20% and 40% reduce the seasonal COP by 8% and 14% respectively. This report and the technical paper by Foxley and Weaver, are not directly related to modular designed heat pumps, therefore, the calculations based on their results only cover part of the change in design. It is considered that in practice the energy savings would be further increased above the 10% figure calculated by the improved matching between heat pump output to the space heating load.

The performance of a modular designed heat pump is studied by dividing the changing load conditions into three zones. The first to be studied is the low atmospheric temperature zone, that is with air temperatures of 3°C and below. This zone includes the balance point, the air temperature below which the demand for space heating is increased, but the heat output is reduced. Lessening of the continuous thermal output of the heat pump is caused by the reduced atmospheric air temperatures and also to the freezing of air moisture onto the heat exchange surfaces in the evaporator.

An advantage of the modular designed heat pump is the flexibility of design which allows provision to be made for extra units to be fitted if the installed heat pump capacity is inadequate. Referring to appendix A6.7, calculations not included in the script show that thermal output of the fifth unit increases the heat pump output by less than 4%, but the contribution is 18% in this low temperature zone considered above.

The heating analysis chart shows, that in the UK, from the total of 272 days in the heating season, that atmospheric temperatures are below 3°C approximately 30 days per annum. Also the number of days that temperatures are above 13°C is a similar period. For 212 days, which is a large proportion of the heating season, atmospheric temperatures are within this temperature range. For almost 80% of the running time in the heating season, the heat pump is operating within the centre zone. The modular design of heat pump is shown to increase the COP above that of the conventional heat pump, but field trials would be required to obtain the full extent of savings.

In the light load zone of operation, the oversizing of the conventional heat pump is at its greatest. In field trials, this zone needs to be researched in detail, because the losses caused by on / off cycling and the large degree of capacity oversizing is pertinent to energy losses. The test data [25] used shows that COP is reduced in this zone to 20% of the value produced by the continuous operation due to on / off cycling. The full extent by which the COP can be improved needs to be investigated.

# CHAPTER 7. RESULTS FROM LABORATORY TRIALS

## 7.1 APPRAISAL OF THE LABORATORY RESEARCH

### 7.1.1 Introduction.

Earlier tests [19] had shown that heat pumps were not performing well in field trials. This was due to on/off cycling. An investigation was conducted during this research to determine the nature of the energy losses during cycling.

Immediately that the refrigerant R134(a) and a suitable refrigerant compressor became available, construction of the heat pump test rig was started. At that time, the thermodynamic property data for refrigerant R134(a) was available, to enable the thermal performance of the test rig to be calculated, but the physical properties to allow the heat exchangers to be properly designed was to be supplied later. There were other setbacks to follow, because the thermodynamic property data for R134(a) was published in haste and was subject to a number of updates and corrections.

In the effort to make the best use of time available and also to cope with limited funding, existing heat exchangers available from the stores at the university were used. At that time, the performance could not be calculated, because of a lack of heat transfer data of the refrigerant R134(a). The test rig was constructed and the laboratory trials were made. A series of trial runs

were carried out, but apart from the initial test runs whilst commissioning the test rig, performance calculations were, by necessity, delayed until after completion of the laboratory trials. Following the analysis given in Appendix 6.5, it was further observed, that the thermal output was lower than expected and also that the refrigerant flow meter produced a reading only slightly above zero. The false results of thermal performance were found to be caused by malfunction of the water flow through the condenser. This was corrected prior to further trials being made and alternative means of evaluating the refrigerant mass flow through the circulation system were used.

## 7.2 TEST RIG THERMAL PERFORMANCE

Whilst making the subsequent heat pump trial runs, the changing refrigerant conditions of temperature, pressure and enthalpy within the heat pump cycle, with particular reference to those between condenser outlet and evaporator inlet, are of significance. In normal practice, refrigerant discharged from the condenser would be at point 'A' on the pressure / enthalpy diagram as shown in Figure 52. Sub-cooling would be evident by the temperature drop shown at point 'B'. The refrigerant is not fully condensed as at point 'C', thermal output of the heat pump is reduced, but this is not shown by any change of temperature.

If there is any question regarding the thermal output of the heat pump, it can be checked by obtaining the temperature difference of water flow compared to the return, multiplied by the mass flow of water in circulation. At constant pressure, enthalpy changes are not accompanied by a corresponding temperature change within the latent heat zone.

This demonstrates the impracticalities of calculating thermal performance from the refrigerant cycle. The most appropriate method by which the thermal performance of heat pump is monitored, is by the calculation of heat transfer through the water circulation system.

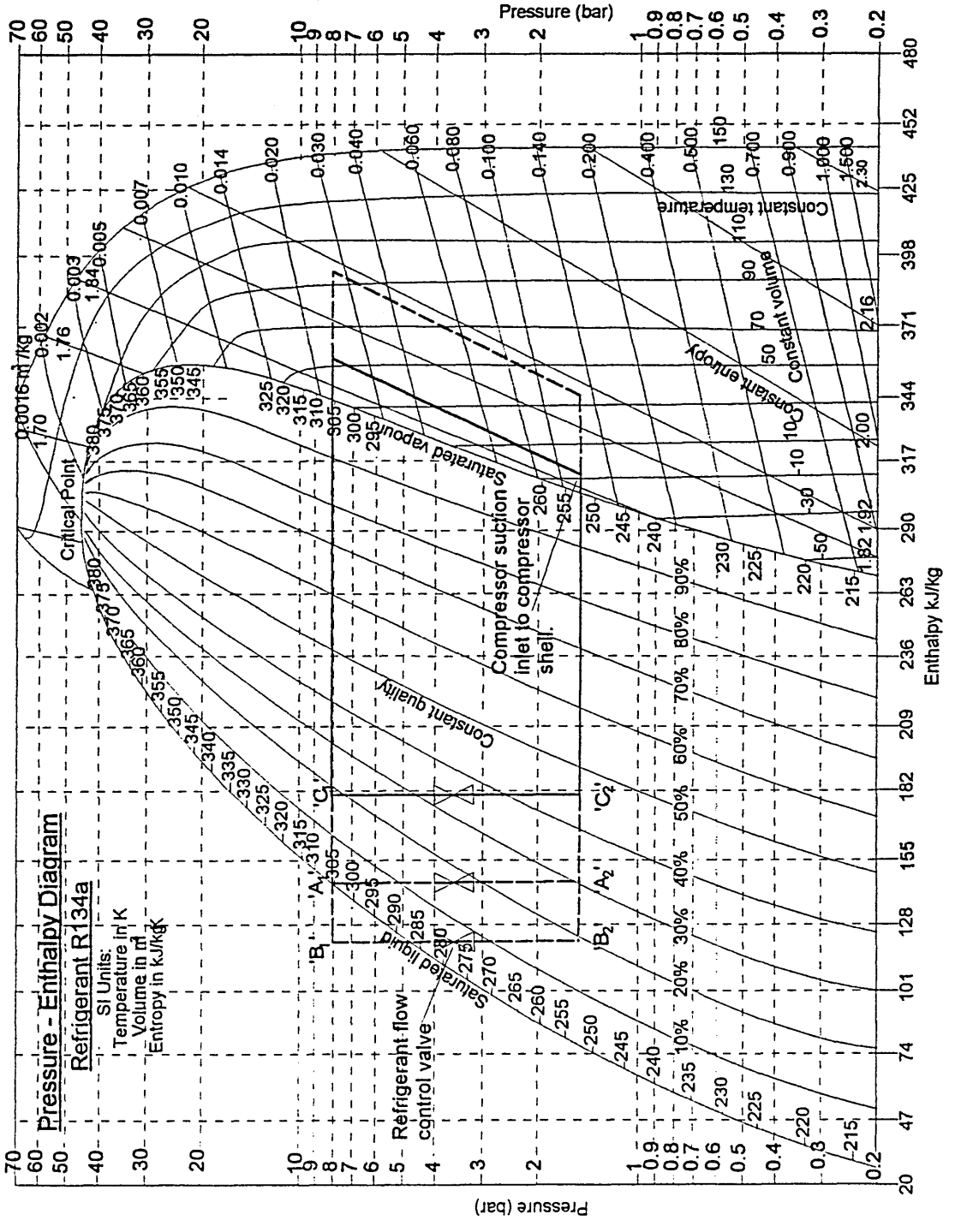


FIGURE 52 Refrigerant Condensation. Improvement and deteriation of Compressor Thermal Output by Sub-Cooling or Incomplete Liquidation of Refrigerant.

It is of significance, therefore, that thermal output of the heat pump can be below the required performance, due to the incomplete liquification of the refrigerant leaving the condenser. When designing and installing a heat pump for domestic space heating, the thermal performance heat output needs to be properly designed and the thermal input and output certified in the commissioning tests must be properly recorded. The air, water and refrigerant flow velocities effect heat transfer and are of importance. When installing and commissioning a domestic heat pump, a water flow meter should be installed in the water distribution system with thermometer pockets in the flow and return pipework.

## 7.3 TEST RIG PERFORMANCE - STEADY STATE OPERATION.

The test rig was designed to simulate the part of a domestic space heating system using refrigerant R134(a). One of the number of units contained in a modular heat pump was represented by the test rig. During the trials, the environmental chamber suction temperatures were reduced in order to obtain the compressor suction temperatures as shown in appendix A7.1, column B.

Appendix A7.1 reports three sets of results for each of the four occasions on which, as near as possible, stable conditions were obtained. The operating pressure range of the heat pump condenser was limited to that shown in column E. Due to the maximum safe working pressure of the condenser being 10 bar (abs), the maximum working pressure was not allowed to exceed 9.6 bar (abs). The locations of the thermocouples during the trials are shown in Figure 53.

Refrigerant temperatures and pressures are shown in the first section, columns B to H. The second section, columns L to P, provide values of enthalpy which were obtained from the thermodynamic property equations supplied by the refrigerant supplier. The equation to obtain the enthalpy of the

saturated liquid at the condenser discharge required that values of 'X', shown in column N, be used in column O.

In connection with the compressor, the electrical supply was metered and listed in section 3, column T. The compressor shell temperature, column U, along with that of the ambient air inside the chamber, column V, were measured so that, in the absence of a refrigerant flow meter, the refrigerant mass flow, column Y, was calculated.

Calculation of refrigerant mass flow through the heat pump, section 4, column AC, was based on observations of thermal input and thermal output. A second calculation, based on the manufacturer's set procedure produces an average for the twelve sets of results, 10% higher. Values of energy input and output of the compressor were utilised to calculate the values of refrigerant mass flow through the heat pump.

The lower refrigerant mass flow found in the laboratory trials would cause difficulties due to loss of heat transfer where heat exchanger design was based on the higher velocities shown in column AD. Otherwise, the energy input, shown in column AE, heat output, shown in column AF and the resulting C.O.P., shown in column AG, appear to be satisfactory. The resulting difference of performance caused by the above difference of refrigerant mass flow was found in previous trials and is shown in Figure 49.

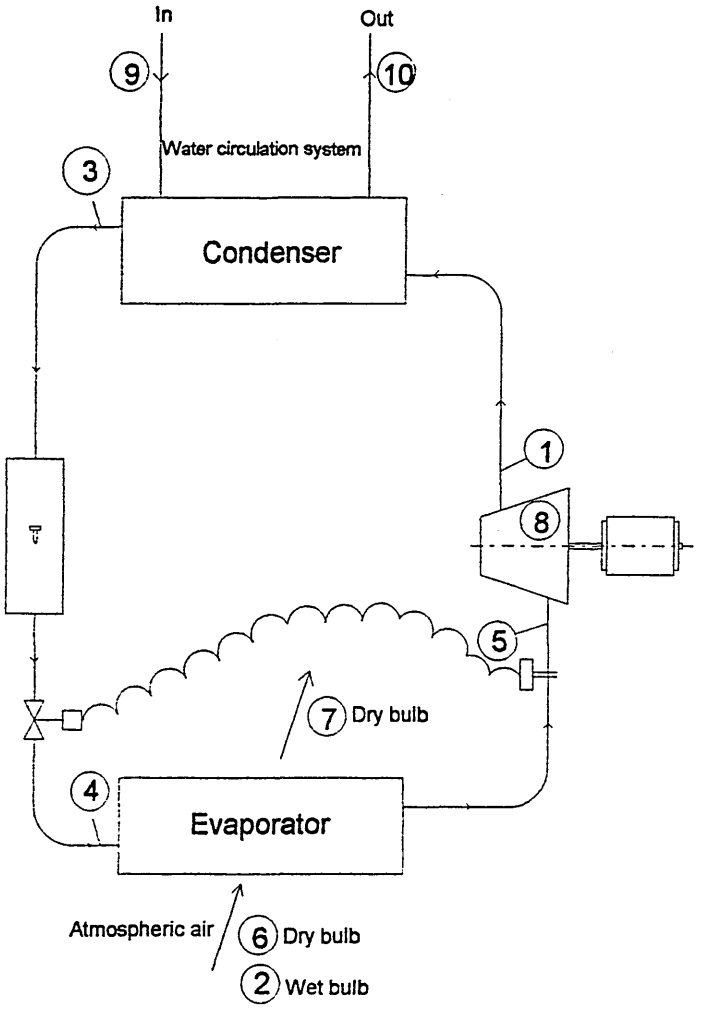


Figure 53 Thermocouple locations on Refrigerant Cycle

7.3.1 Compressor - Isentropic Efficiency.

Using data from scan 346, appendix A7.1, calculation of isentropic efficiency is as follows;

Isentropic Efficiency = Isentropic Output / Indicated Output.

$= (h_2' - h_1) / (h_2 - h_1)$

where,

$h_1$ = Enthalpy at Compressor Suction.

$h_2$ = Delivery.

$h_2'$ = Constant Entropy Output.

$= (325.97 - 295.19) / (338.05 - 295.19)$

Isentropic Efficiency = 72 %

The above calculation produces values of isentropic efficiency for a totally enclosed refrigerant compressor that is comparable to other compressors of similar design. This procedure could be useful whilst selecting the most efficient compressor to meet the working conditions. When the selection of compressor has been made, it is necessary to know the refrigerant mass flow rate through the closed cycle of the heat pump. An important item in the design is to size the heat exchangers to the velocity necessary to obtain satisfactory heat transfer.

Distribution of heat energy within the compressor shell was discussed previously, from which the refrigerant mass flow was obtained by equating the input to the compressor in Watts, against the output of kilojoules per kilogram.

Trials of the test rig provided a period of steady state operation shown in Appendix A7.1, the findings from which enabled a further research to be made into the subject of heat distribution within the outer shell of the totally enclosed refrigerant compressor.

## 7.4 TEST RIG PERFORMANCE - UNSTEADY STATE.

There is only a very short period annually that thermal output from the heat pump and the space heating load are in balance. The period when atmospheric temperatures are above the balance point and the thermal output from the heat pump needed to be reduced, were studied.

An important item in the application of heat pumps to domestic space heating is the affect of intermittent operation on the seasonal thermal performance. In order to observe the effects of intermittent operation whilst the test rig was in the environmental chamber. The compressor was switched on and off for varying lengths of time whilst observations were made, particularly when idling. The condenser air fan and the water circulating pump operated continuously throughout the trial. The principle item in this part of the study was to ascertain the energy loss due to the compressor being switched off and then in restoring the test rig to the conditions immediately prior to switching off.

### 7.4.1 Laboratory Trials - Intermittent Operation.

To simulate the conditions being studied, the heat pump was started up and operated continuously for a warm up period. Following this, the compressor was intermittently switched on and off. At the beginning of the test, the compressor was switched off for observation of the changing conditions for a period of one hour. It was realised that this was a longer period of shut off than would normally be expected in practice, but the object of a longer period of compressor shut off was to allow the trends of the changing conditions to become more apparent. Following on from this, the switching was made to simulate, as near as possible, the intermittent operation pertaining to normal practice.

The test rig was constructed to simulate, as closely as possible, the normal heat distribution system that circulates water between the heat pump condenser and the heating surface within the heated space. In a practical application, water would absorb heat whilst passing through the condenser and be cooled by giving off heat from heat emitters within the dwelling. The test rig was sized to represent one unit of a modular designed heat pump and, therefore, the thermal input and output was much less than that of the conventional domestic heat pump. Otherwise, the performance represents that of a standard unit.

7.4.2 Heat Flow to Domestic Accommodation.

The objective of focusing initially on this part of the study was to display the reasons why on and off switching of the compressor used for a capacity control system, reduced the heat pump efficiency. The study was directed to the connection between the heat pump and the heat emitters within the heated space, that being the only path of the heat flow in question. Following on from this, research was directed to the on / off cycling frequency and the loss of temperature difference between condenser and evaporator whilst the compressor is inoperative.

The following discussion is based on data obtained during laboratory trials. In this section. Figure 54 provides the performance data. In the graph, the time was shown on the X axis and the Y axis shows the heat flow to and from the heat pump and the space heating system. Water flow and return temperatures were measured by the Comark ten channel electric thermocouple meter for the scans shown on the X axis. The water mass flow was measured by a glass tube variable area flow meter. The heat transferred was obtained by equating water mass flow and the differential temperature.

During the first part of the test, the compressor was made inactive for one hour and followed later by the compressor being inoperative for periods of five and ten minutes respectively. The graph represents useful thermal performance of the heat pump as positive and negative values in Watts. Positive values represent heat flow from the heat pump to the dwelling. Negative values indicate the heat flow from the dwelling to the heat pump. The reversed flow heat occurred when the water return temperature to the heat pump was at a higher temperature than the flow.

### 7.4.3 Intermittent Operation - results from Laboratory Trials

The first stage of the following laboratory research was made to examine heat transfer between the heat pump and heat distributing system whilst the heat pump was operating under manual on / off intermittent operation of the compressor. The results are shown in graphical form in Figures 54 and 55. This shows that when the compressor was switched off, there was, not only heat transfer to the space heating system, but there were traces of heat being transferred from the dwelling back to the heat pump. Following on from this study, the research was directed to the heat pump refrigerant and the effects of the capacity control on the condenser and evaporator temperatures and pressures.

### 7.4.4 Intermittent Operation - Heat Flow from the Heat Pump to the Heat Distribution System

The graph in Figure 54 shows the heat transferred to and from the heating system in the first run and the high rate at which the energy output to the space heating system is reduced. Also, at the end of a long shut off period, the test rig temperature quickly recovers to approximately 60% output, after which an extended warm up period would be required to reinstate the normal operating conditions.

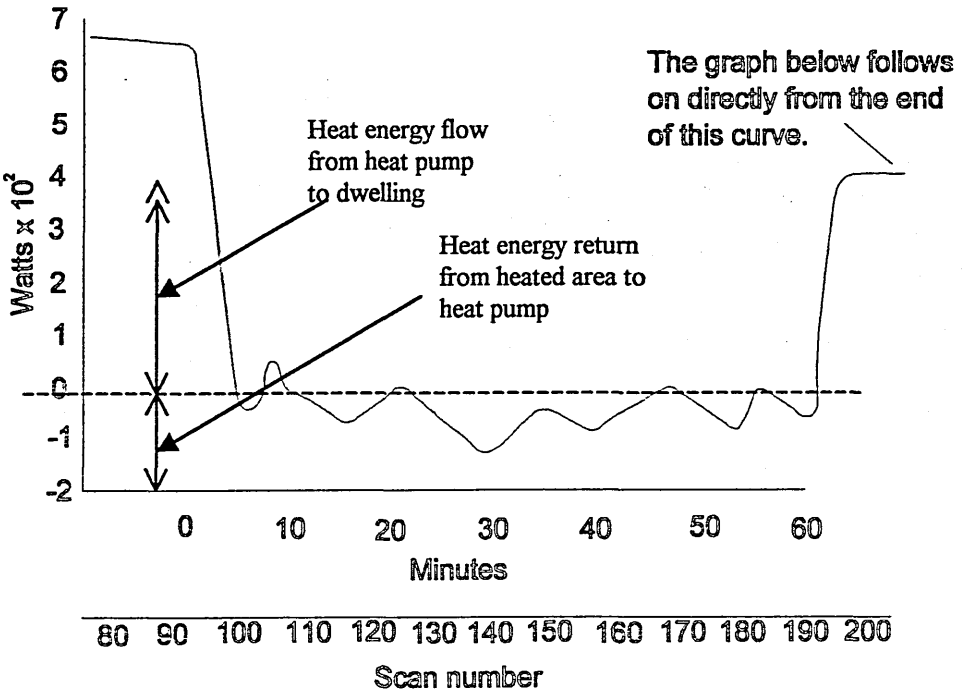


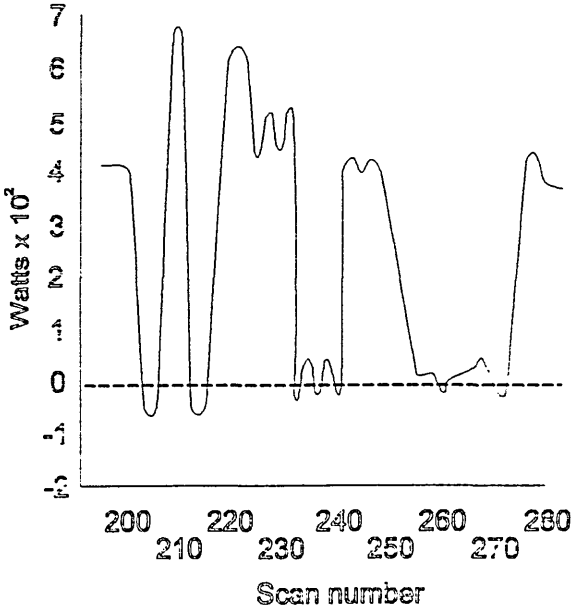


FIGURE 54 Heat Flow Between Heat Pump and Space Heating System

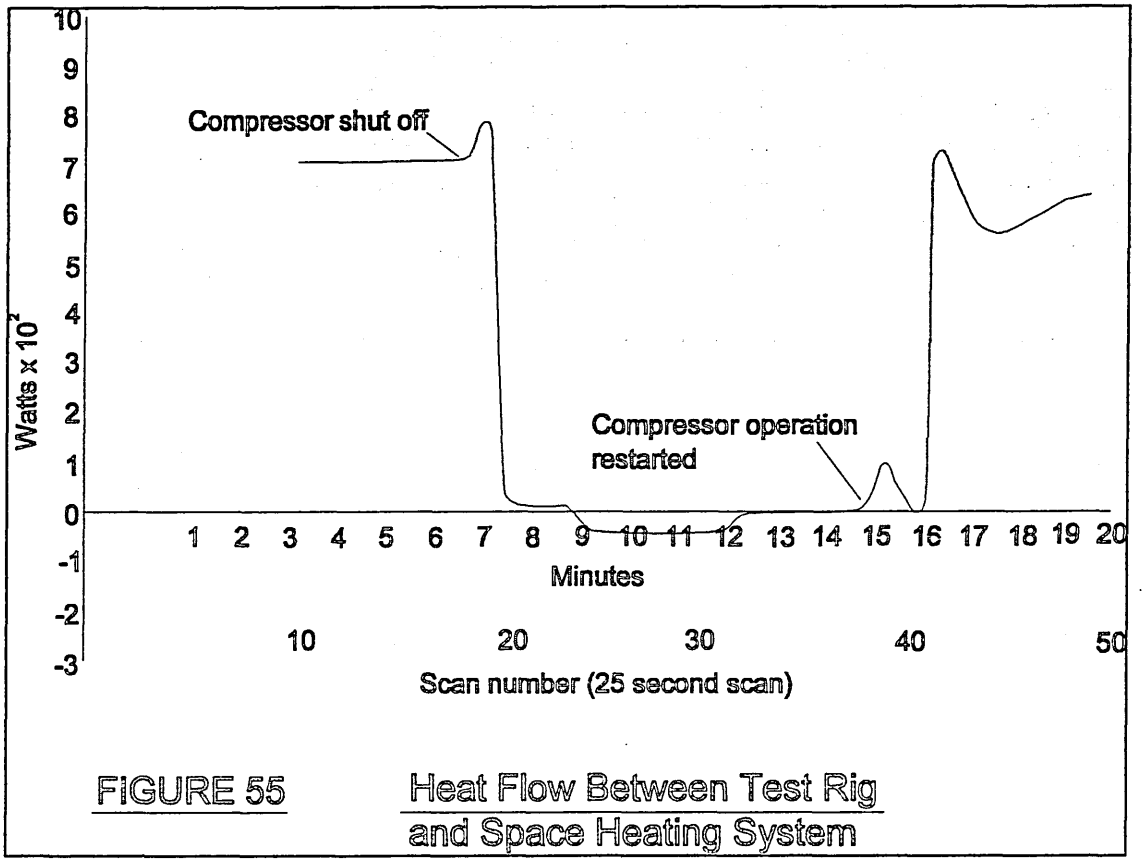


FIGURE 55 Heat Flow Between Test Rig and Space Heating System

In the period of scan 190 to 230, it is shown on the graph Figure 54, that the heat pump was twice switched off. This switching was made to observe the heat flow for short periods that the compressor was switching off. Heat flow between the condenser and space heating system was reversed by the on / off switching. The positive energy flow when the compressor was operative and greater value during this period, than would be otherwise expected. It was observed that towards the end of the previous one hour period, that the compressor had been idle. Ice had been deposited on the air side of the evaporator.

In normal practice, the heat pump operates at full output below the balance point which eliminates the need for capacity control. In the laboratory trials, the on / off cycling of the compressor was

manually controlled and, therefore, the balance point was none existent. Similarly, the one hour shut off period made it convenient to observe the performance for a longer period and at any time during this period the compressor could have been restarted without any change to what had gone before.

Following on from scan 230, there were two periods during which the compressor was switched off. The thermal output was, however, 60% of the rated capacity, there being a time delay before the heat pump was operating at normal operation conditions.

The period of one hour shut off is a longer time than would be expected in normal practice and, therefore, for the second phase of the trial, the heat pump was switched off for twenty minutes only. The results for this are shown in Figure 54 & 55. Characteristics of the heat flow between the heat pump and the heat distribution system were found to be generally similar, but independent of the length of time that the compressor was inactive, as shown in Figures 56 and 57. Turning to the conditions within the heat pump when the compressor was inactive, it was found that the cycling frequency and length of compressor shut off time did have an effect on the thermal efficiency, because of the energy consumption of the compressor whilst restoring the normal working conditions of the heat pump cycle.

### 7.4.5 Intermittent Operation - Heat Pump Temperatures and Pressures

During the one hour shut off, the pressure and temperature differences between condenser and pressure was found to reduce. The reduction of pressure difference was caused by a pressure drop of the condenser and a rise in pressure of the evaporator immediately after shut off was of major significance, because of the energy required to reinstate normal operating conditions.

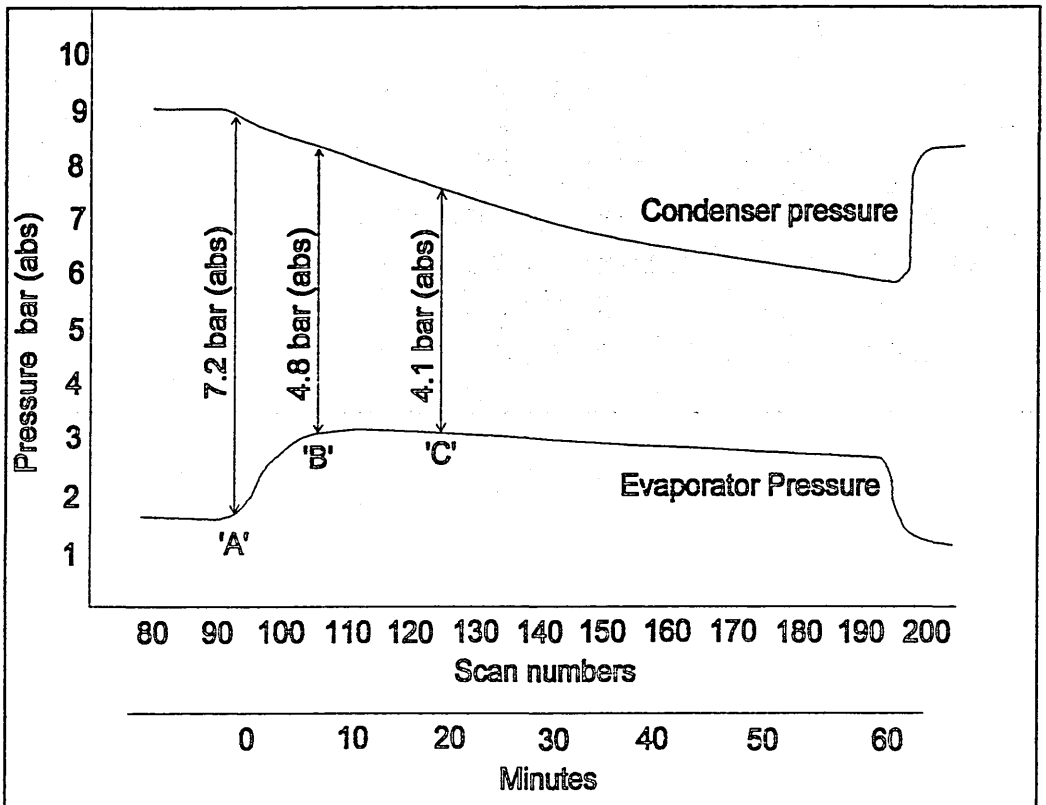


FIGURE 56 Instability of Refrigerant Pressures During One Hour Shut Off of Compressor

The pressure difference of the heat pump throughout the one hour shut off period is shown in Figure 56. When the heat pump was operating at a frequency of 1.5 cycles per hour, with a twenty minute off period per cycle, the compressor was inoperative between positions 'A' and 'C' on the graph. The work done to restore the pressure to the normal working conditions would be:

$1.5 \times (7.2 - 4.1) = 4.65$ bar

If the cycling frequency was raised to three cycles per hour, the compressor being inoperative between the positions 'A' and 'B', the pressure difference through which the compressor would need to recover would be:

$3 \times (7.2 - 4.8) = 7.2$ bar

The increased cycling frequency increases the work done by the compressor by 35%. There is energy to be saved by reducing the cycling frequency.

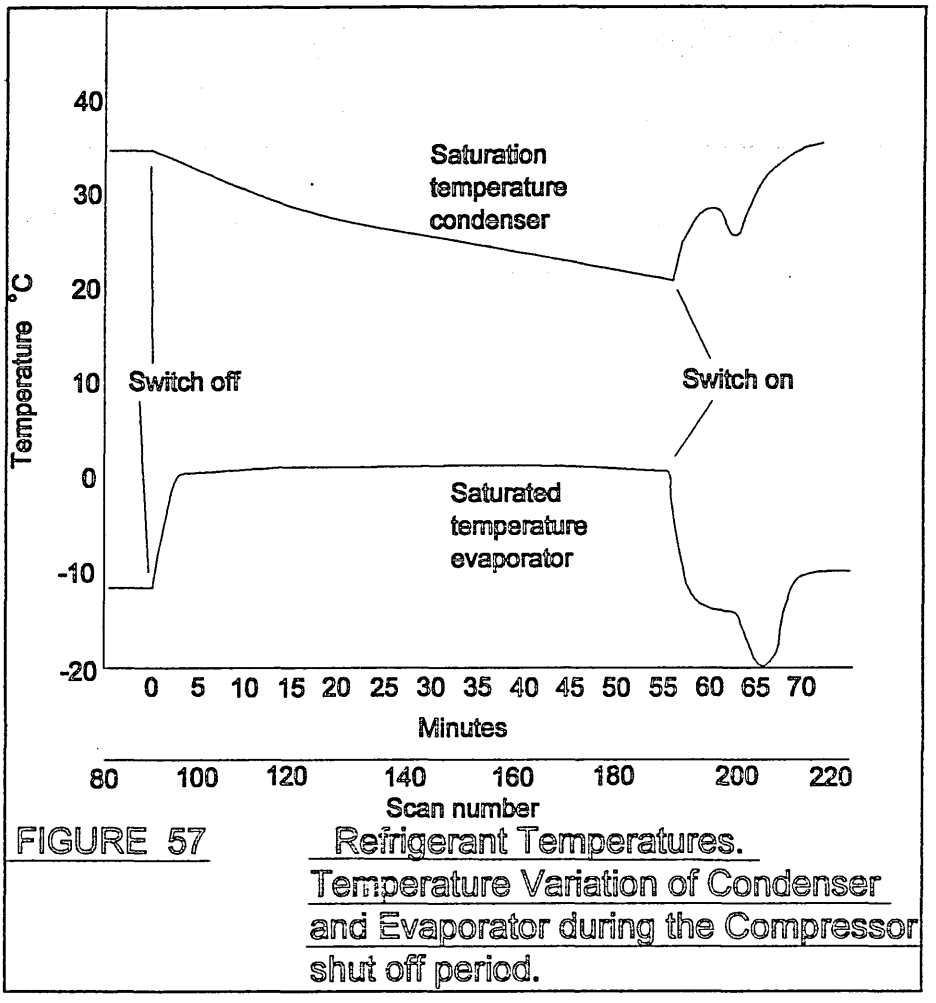


FIGURE 57 Refrigerant Temperatures. Temperature Variation of Condenser and Evaporator during the Compressor shut off period.

The following graphs display a similarity between the curves formed by pressure in Figure 56 and temperature in Figure 57, whilst the compressor was inoperative. The following graphs were made of the refrigerant temperatures only, but are intended to represent the changing conditions of both temperature and pressure. To obtain a clearer illustration of the changing conditions, Figure 58 plots the differential in one curve which was previously shown on two.

The curve at Figure 58 shows that immediately after the compressor switch off, there is a period in which the temperature difference reduces quickly. The dotted line on the graph shows how the rapid temperature reduction occurs after approximately five minutes, the cooling rate is then reduced. The cycling frequency needs to be kept to a minimum consistent with maintaining comfort periods within the dwelling. If the heat pump capacity control causes on / off switching at frequent and short intervals, energy input to the compressor would be greatly increased.

### 7.4.6 De-icing of the Evaporator.

When atmospheric temperatures fall below 3°C, the air temperature is reduced and moisture contained in the air passing through the evaporator freezes, thus forming ice on the heat transfer surfaces of the evaporator. Ice formation restricts the air flow through the evaporator and therefore needs to be removed periodically. The method used to de-ice the test rig consisted of a condenser bypass, delivering the high temperature vapour directly from the compressor to the evaporator inlet, see Figure 59 . A valve was fitted into the bypass which was normally closed. This was opened periodically for short periods to melt the ice. During the de-icing refrigerant flow through the condenser is not cut off, but the resistance to refrigerant flow through the condenser is greater than that of the de-icing bypass. The majority of refrigerant heat flow is, therefore, direct from the compressor to the evaporator. It may be seen from Figure 59, that the heat flow to the dwelling is interrupted during the bypass process, but this was for a short period only. The bypass valve was opened twice with a short period in-between, the second being to affirm or otherwise, the findings in the first.

### 7.4.7 Laboratory Research - Summary of Findings.

Understanding of the physical response that was displayed in the figures associated with this chapter, produced a better understanding of the heat pump operation. The study of energy flow

from electrical input and from the environment to the heated space enabled the finer details of this process to be more clearly understood. Energy used in creating the conditions of pressure and temperature within the refrigerant cycle were lost every time that the compressor was switched off. Methods by which the extent of the losses could be reduced were researched.

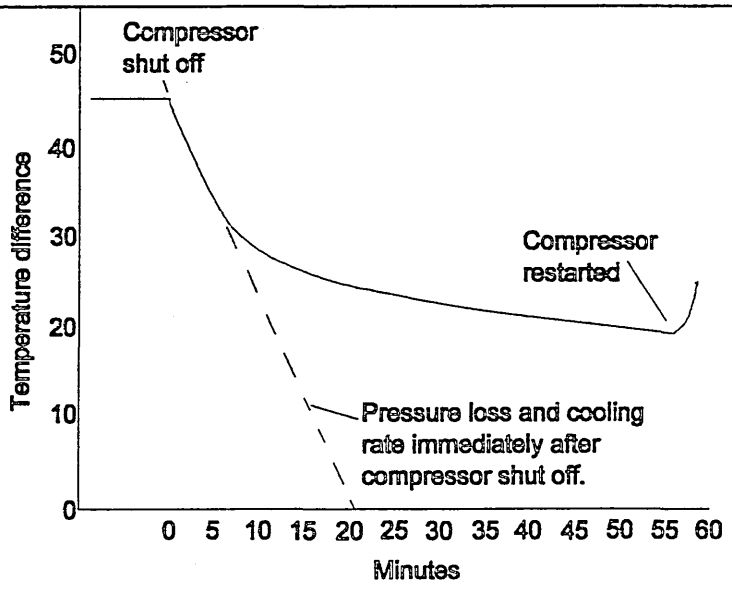


FIGURE 58 Refrigerant Saturated Temperature Difference Between Condenser and Evaporator.

There was only one heat flow path between the condenser and the heaters within the heated space. Whilst the compressor was inactive there was no outflow along this path, but there was a tendency for the heat to flow in the reverse direction. That was from the space heating system, back to the heat pump. Dependant upon the length of time that the compressor had been idle, there was a time delay after start up before the full capacity of heat was transferred to the space heating system. Clearly that the energy used to repressurise the refrigerant cycle could not be recovered from that direction. During the de-icing, the small reduction of pressure difference between the evaporator

and condenser was quickly recovered. Immediately that the de-icing bypass was closed, the energy flow to the space heating system was restored.

The most pertinent outcome from this research was in the realisation that there was a short coming in the analysis of the heat pump performance following the laboratory research. The ease by which the heat pump may be allowed to operate without extracting the whole of the latent heat from the refrigerant was shown. The crucial point of this is, that this could happen without any indication being observed by checking the refrigerant temperatures and pressures. When commissioning the domestic heat pump, the contractually specified thermal output being transferred from the heat pump to the space heating system should be demonstrated.

## 7.5 MODULAR HEAT PUMP - OBJECTIVE.

The capacity control of the modular designed heat pump would be obtained by having only the required number of units in operation, to meet the space heating load. Further site trials need to be made, but it is considered that the modular heat pump would eliminate all on/off cycling losses. If comfort conditions within the dwelling were not being maintained, an additional unit could be brought into operation. If necessary, one unit could automatically be operated for capacity control. In light load conditions of the intermediate seasons, the necessary background heat could be supplied by only one unit being in operation. In these conditions, one unit operating at full load producing three kilowatts, for example, would be of a higher thermal efficiency than a unit capable of five times the capacity operating for twelve minutes an hour.

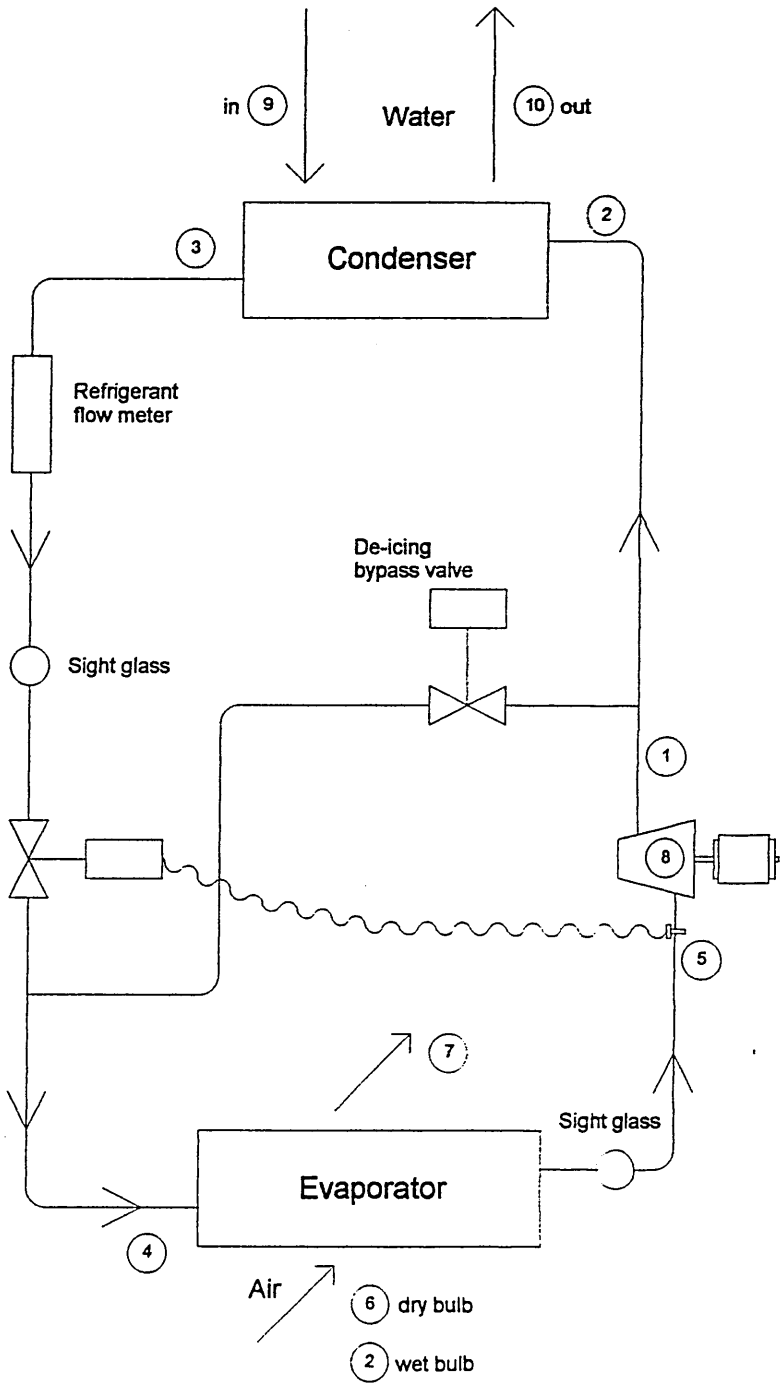


Figure 59 Refrigerant cycle - R134(a)
Showing locations of thermocouples and de-icing bypass

It was visualised that for the modular heat pump to be commercially acceptable, standardised and factory assembled units, would need to be produced. The number of standard sized low cost units necessary to meet the space heating full load would be installed. Standardisation of the unit design and complete factory assembly would reduce costs. Factory assembly being cheaper than site work would enable the modular units to be assembled and tested at lower cost, with the correct managerial control. In the event of a major fault on any unit, it could be replaced and returned to the factory for maintenance. With this arrangement, experienced engineers, properly equipped, would undertake the necessary service.

When the heat pump is operating at maximum space heating load and under freezing atmospheric conditions, the condensers of the individual units may be de-iced in sequence. An additional unit may be installed to cope with space heating load under these conditions. This would allow for one unit to be off load for de-icing or maintenance at any time and yet the full space heating load could still be met.

# CHAPTER 8. CONCLUSIONS AND RECOMMENDATIONS FOR FURTHER RESEARCH

## 8.1 INTRODUCTION

In the 1980's, there was an increase in the number of heat pumps being installed in the UK for domestic space heating. In the most of these cases, the heat pump replaced a fossil fuel fired boiler. There followed a period of dissatisfaction, mainly as a result of the fact that the heat pump installations did not fulfil expectations. It has been clearly demonstrated that when cycling, the overall coefficient of performance of the heat pump is greatly reduced. The modular heat pump was studied with the objective of overcoming this problem. The graphs in Figure 51 show both the existing and proposed operational procedures.

## 8.2 APPLICATION OF MODULAR HEAT PUMPS.

The thermodynamic cycle used in the domestic heat pump studied in this research was basically the same as that used for refrigeration and, in particular, domestic refrigerators. These generally operate without any routine or break down maintenance for the whole of their existence and it is suggested that, whilst the domestic heat pump may require annual maintenance, there is every reason why the performance should approach that of the refrigerator.

A modular heat pump could be manufactured as a standard thermal unit, the number of units being supplied to meet the space heating load. Each unit of the modular heat pump would be factory manufactured, tested and packaged there, so that, on site the only connections required would be electricity, water flow and return. It would be an advantage for the hydraulic pressure loss through the heat distribution system to be specified by the client and the water circulation pump to be

supplied by the manufacturer. This would enable the correct water flow volume required for the condenser to provide the necessary heat transfer.

The above procedures, would reduce the costs of the heat pump installation by reducing the work on site. Work in the factory may be increased, but it does provide the manufacturer with a method by which the performance of the compressor and heat exchangers meet the requirements of the physical and thermal conditions on site.

## 8.3 INSTALLATION OF THE MODULAR HEAT PUMP

A diagrammatic layout on site of the modular heat pump and the heat distribution system is shown in Figure 45. It was not possible to consider all of the alternatives and, therefore, the ideal water circulation system needs to be proved on site.

The modular designed heat pump provides advantages against the conventional heat pump. When on light loads in the intermediate seasons, the conventional pump is grossly overloaded. The modular heat pump would be able to operate with only one unit and a second unit brought into operation if the thermal output from the first is insufficient. It is considered that, at part load, the on / off cycling may be completely eliminated, but this is another item to be proved by trials on site. It was found in the laboratory trials that the heat loss from the heat pump and associated pipework, to the atmosphere were negligible.

When sizing and selecting the heat exchangers, the basic principles associated with the open compressors of suction volume against pressure increase, could not be followed. Due to preheat of the refrigerant after entering the compressor shell, the suction temperature into the compressor

cylinder was not known for some performances. The CECOMAF test results provided useful information, but for sizing the heat exchangers, additional data was required.

## 8.4 CHANGE OF REFRIGERANTS

Producing the mathematical model for performance of the whole cycle provided an explicit understanding of heat pump performance, although changing the types of refrigerants inhibited the use of the program developed for R12.

At the time of the research in this area the full thermodynamic data for R134(a) was not available and there were a numerous changes made to the initially published data. Now that definitive data is available the program could be modified for use with R134(a) or other environmentally friendly refrigerant.

## 8.5 FUTURE RESEARCH

To make further progress, field trials of a modular designed heat pump would be required. The production of a number of modular units would be needed, with a proved thermal efficiency and performance before installation into a domestic dwelling. The heat pump and heat emitters within the heated space need to be an integrated design. At the design conditions, water flow temperatures and temperature rise through the heat pump design conditions must be matched by the same temperature and temperature drop through the space heating system.

It has become apparent whilst researching the design and use of heat pumps for domestic heating, that there is little or no demand at present, but this is a time of change and if and when suitable reliable sources of energy or nuclear power becomes predominant for electrical power generation there will be great advantages in using heat pumps to replace fossil fuels for heating domestic dwellings.

APPENDIX A3.1

MATHEMATICAL MODEL OF STEADY STATE CONDITIONS: REFRIGERANT R12



SECTION 1: COMPRESSOR

1.1 Thermal Performance

| | | |
|---|---|---|
| Suction Pressure: $P_1$ (1) | = | 2.27 bar (abs.) |
| Delivery Pressure: $P_2$ (2) | = | 13.6 bar (abs.) |
| Evaporator Saturation Temp: $t_4$ (3) | = | -9°C |
| Superheat Section Temp: $t_1$ (4) | = | -2°C |
| Compressor Inlet Specific Enthalpy: $h_1$ (5) | = | 573.44 kJ/kg |
| Entropy at Inlet: $s_1$ (6) | = | 4.7736 kJ/kg.K |
| Isentropic Output: $h_2'$ (7) | = | 607.46 kJ/kg |
| Isentropic Efficiency : $\eta$ (8) | = | 0.60 |
| | = | Isentropic Thermal Input. / Indicated Thermal Input |
| | = | $(h_2' - h_1) / (h_2 - h_1)$ |

where h = Specific Enthalpy, and subscript numbers are points on the refrigeration cycle.
See Figure 22.

Specific Enthalpy Compressor Discharge: $h_2$ (9)= $(h_2' - h_1) / n + h_1$
= (607.46 - 573.44) / 0.60 + 573.44
= 630.14 kJ/kg

1.2 Mechanical Performance

At this stage, thermal output of the heat pump is unknown. A Compressor Piston Displacement Volume $V_p$ (11) of 0.0103 cubic meters used in this model is based on preliminary calculations provided for a thermal output of 12kW.

The volume of refrigerant passing through the compressor varies due to the changing pressure ratio. A tabulation of volumetric efficiency against this pressure ratio, (Dossat R.J., Principles Of Refrigeration, 1961. Pub. John Wiley and Sons, Inc. London) was used to produce at a cubic equation using pressure ratio to obtain volumetric efficiency.

Compressor- Pressure Ratio: $C_R$ (10) = $P_2 / P_1$
= 13.6 / 2.27
= 5.99

Volumetric Efficiency = 63.5%

Piston Displacement Volume: $V_p$ (11) = 0.0103 $m^3$

Suction Volume: $V_1$ (12) = $\frac{\text{Disp. Volume} \times \text{Vol. Effy.}}{100}$
= $\frac{0.0103 \times 63.5}{100}$
= 0.00654 $m^3$

Specific Volume Refrigerant Suction: $V_{1s}$ (13)= 0.0778 $m^3/kg$

Refrigerant Mass Flow: $\dot{m}$ (14) = $\frac{\text{Suction Volume.}}{\text{Specific Volume}}$
= $\frac{0.00654}{0.0778}$
= 0.084 kg/s

Mechanical Work Input: $W_m$ (15) = $(h_2 - h_1) \times \dot{m}$
= (630.14 - 573.44) 0.084
= 4.764 kW

where $h_2$ and $h_1$ are Suction and Delivery Values of Specific Enthalpy.

SECTION 2: CONDENSER

The condenser consists of one heat exchanger, but for the purpose of calculation it is considered in two parts, namely the Desuperheating Zone and the Condensing Zone. These are calculated individually and in sequence. Refrigerant leaving the condenser is wet saturated. The refrigerant and water streams run in counterflow. See Figure 15.

Note: All heat transfer calculations for condenser and evaporator designs omit fouling resistances.
Pressure drop on the refrigerant side is assumed to be concentrated at the pressure control valve.
The condenser is formed from two concentric tubes. Refrigerant in the inner tube flowing counter to water in the annular space between the inner and outer tubes.
First to be calculated is the water heat transfer coefficient which is the same value in both the desuperheating zone and the condensing zone.

2.1 Water Side - Heat Transfer Coefficient

Specific Enthalpy Refrigerant Inlet: $h_2(9)$= 630.14 kJ/kg

Specific Enthalpy Outlet: $h_3$ (16) = 474.14 kJ/kg

Heat Transfer to Water: $Q_w$ (17) = $(h_2 - h_3) \times \dot{m}$

= (630.14 - 474.14) × 0.084

= 13.11 kW

Water Flow Temp. (to system): $t_{w1}$ (18) = 50°C

Water Return Temp: $t_{w2}$ (19) = 45°C

Heating Temp. Range: $A_d$ (20) = 50 - 45

= 5°C

Inside Diameter of Outer Tube: $D_1$ (21) = 0.056 m

Outside Diameter of Inner Tube: $D_2$ (22)= 0.0254 m

Number of Tubes in Parallel: N (23) = 1

Cross Sectional Area to Flow: A (24) = $0.7854 (0.056^2 - 0.0254^2)$

= $0.001956\ m^2$

Water Specific Heat: C (25) = 4182 J/kg.K

Density:ρ (26) = $989\ kg/m^3$

Water Flow Rate: $V_f$ (27) = $(Q_w \times 10^3) / (C \times A_d \times \rho)$

= $(13110 \times 10^3) / ((4182 \times 5 \times 989)$

= 0.634 l/s

Water Velocity: $V_w$ (28) = $V_f / A$

= $(0.634 \times 10^{-3}) / (1.956 \times 10^{-3})$

= 0.324 m/s

Characteristic Length: l (29) = 0.056 - 0.0254

= 0.0306 m

For annular flow, the characteristic length is equal to external diameter minus the internal diameter. Calculation procedure of the following heat-transfer coeficient was based upon reference [29] Example 1 page 35. Details of the equations used on pages 4 & 5.

Water Viscosity: μ (30) = $0.0005756\ Ns/m^2$

Reynolds Number: Re (31) [eq. 10] = $\rho V_W l / \mu$

$$= \frac{989 \times 0.324 \times 0.0306}{0.0005756}$$

= 17040

Thermal Conductivity: k (32) = 0.658 W/mK

Prandtl Number: $P_r$ (33) [eq. 11] = $C\mu / k$

$$= \frac{4182 \times 0.0005756}{0.658}$$

= 3.658

Correlation Parameter: E (34) [eq. 18] = $0.0225 \exp [ -0.0225 (\ln Pr)^2]$

= $0.0225 \exp [ -0.0225 (\ln 3.658)^2]$

= 0.02166

Stanton Number: St (35) [eq. 17] = $E\ Re^{-0.205}\ Pr^{0.505}$

= $0.02166 \times 17040^{-0.205} \times 3.658^{-0.505}$

= 0.00153

Heat Transfer Coefficient: $\alpha_w$ (36) [eq. 16]= $St.\rho\ V_w\ C$

= $989 \times 0.324 \times 4182 \times 0.00153$

= $2047\ W/m^2 k$

2.2 Desuperheat Zone

2.2.1 Refrigerant Side - Heat Transfer Coefficient

Inside Diameter of Inner Tube: $D_3$ (37) = 0.0203 m

Outside Diameter of Inner Tube: $D_2$ (22) = 0.0254m

Mean Tube Diameter of Inner Tube: $D_w$(38)= 0.02285m

Number of Tubes in Parallel: N (23) = 1

Cross Sectional Area to Flow: $A_s$ (39) = $0.7854 \times D_3^2$

= $0.7854 \times 0.0203^2$

= $0.00032366\ m^2$

Refrigerant Density: $\rho_r$ (40) = $66.94\ kg/m^3$

Refrigerant Velocity: $U_r$ (41) = $\dot{m} / (A_s \times \rho_s)$

= $0.084/(0.00032366 \times 66.94)$

= 3.878 m/s

Refrigerant Viscosity: $\mu_r$ (42) = $1.39 \times 10^{-5}\ Ns/m^2$

Characteristic Length: l (43) = 0.0203 m

Reynolds Number: Re [eq. 10] = $\rho_s V_r l / \mu_s$

= $(66.94 \times 3.878 \times 0.0203) / 0.0000139$

= 379118

Refrigerant Specific Heat: $C_r$ (44) = 779 J/kg.K

Refrigerant Thermal Conductivity: $k_r$ (45)= 0.01273 W/mK

Prandtl's number: Pr (46) [eq. 11] = $C_r \mu_r / k_r$

= $(779 \times 1.39 \times 10^{-5}) / 0.01273$

= 0.851

Correlation Parameter: E (47) [eq. 18] = $0.0225 \exp[-0.0225 (\ln Pr)^2]$

= $0.0225 \times \exp[-0.0225 (\ln 0.851)^2]$

= 0.0225

Stanton Number: St (48) [eq. 17] = $E\ Re^{-0.205}\ Pr^{-0.505}$

= $0.0225 \times 379118^{-0.205} \times 0.851^{-0.505}$

= 0.001754

Heat Transfer Coefficient: $\alpha_i$ (49) [eq.16]= $\rho_s \mu C_s St$

(based on inner tube diameter) = $66.94 \times 3.878 \times 779 \times 0.001754$

= $354.699\ W/m^2K$

Heat Transfer Coefficient: $\alpha_o$ (50) = $\alpha_i \times D_3 / D_2$

(based on outside diameter of tube) = $\frac{354.699 \times 0.0203}{0.0254}$

= $283.48\ W/m^2K$

2.2.2 Overall Heat Transfer Coefficient

Tube Wall Thickness: $y_w$ (51) = $(D_2 - D_3) / 2$

= $\frac{0.0254 - 0.0203}{2}$

= 0.00255 m

Tube Wall Mean Diameter: $D_w$ (38) = $(D_2 - D_3) / 2$

= $\frac{0.0254 + 0.0203}{2}$

= 0.02285 m

Wall Thermal Conductivity: $k_w$ (52) = 45 W/m.K

Overall Heat Transfer Coefficient: $1/U_d$ (53)= $1/\alpha_w + 1/\alpha_0 + (y_w/k_w \times D_2/D_w)$

[eq. 40a] = $\dfrac{1}{2047} + \dfrac{1}{283.48} + \dfrac{0.00255 \times 0.0254}{45 \times 0.02285}$

$\therefore U_d$ = 245.15 W/m$^2$K

2.2.3 Heat Transfer Area

Specific Enthalpy Point 2A: $h_{2a}$ (54) = 595.04 kJ/kg

Heat Gain Desuperheating: $Q_{sh}$ (55) = $(h_2 - h_{2a})\,\dot{m}$

= (630.14 - 595.04) 0.084

= 2.95 kW

Water Temp. Entering Desuperheater: $t_s$ (56)= $50 - 5 \times \left(\dfrac{h_2 - h_{2a}}{h_2 - h_3}\right)$

= $50 - 5 \times \left(\dfrac{630.14 - 595.04}{630.14 - 474.14}\right)$

= 48.88°C

Refrigerant Inlet Temp: $T_2$ (57) = 103°C

Condensing Temp. : $T_s$ (58) = 55°C

Log. M.T.D.: $Q_{in}$ (59) = $\dfrac{(T_2 - t_2) - (T_s - t_s)}{\ln\left[(T_2 - t_2)/(T_s - t_s)\right]}$

= $\dfrac{(103 - 50) - (55 - 48.88)}{\ln [(103\ 50)/(55 - 48.88)]}$

= 21.7 °C

Desuperheat Zone Heating Surface: $A_d$ (60) [eq. 46]= $Q_{sh}/(Q_{in} \times U_d)$

= $\dfrac{2.95 \times 1000.}{245.15 \times 21.7}$

= 0.555 m$^2$

2.3 Condensing Zone

2.3.1 Refrigerant Side - Heat Transfer Coefficient

Tube length (estimated): $L_c$ (61) = 21.52 m

Note: For the computer calculation, the tube length (61) needed to be estimated. The value is later corrected by mathematical iteration. The corrected value obtained previously from computer calculations is used here.

Condensation rate: $\Gamma$ [kg/m refrigerant mass flow divided by tube length] = $\dot{m}/L_c$

= $\dfrac{0.084}{21.52}$

= 0.00391 kg/ms

Refrigerant Liquid Density: $\rho_L$ (62) = 1189 kg/m$^3$

Vapour Density: $\rho_G$ (63) = 75.98 kg/m$^3$

Gravitational Constant: g (64) = 9.81 m/s$^2$

Liquid Viscosity: $\mu_L$ (65) = 0.0001554 Ns/m$^2$

Thermal Conductivity: $k_L$ (66) = 0.0758 W/mK

Heat Transfer Coefficient: $\alpha_o$ (67) [eq. 35]= $0.951 k_L \left( \frac{\rho_L (\rho_L - \rho_G) g}{\mu_L \Gamma'} \right)^{\frac{1}{3}}$

$= 0.951 \times 0.0758 \times \left( \frac{1189 \times (1189 - 75.98) \times 9.81}{0.0001554 \times 0.00391} \right)^{\frac{1}{3}}$

$= 2001 \text{ W/m}^2\text{K}$

Heat Transfer Coefficient: $\alpha_i$ (68) $= (2001 \times 0.8) \times \frac{0.0203}{0.0254}$

(See note below.) $= 1279 \text{ W/m}^2\text{K}$

Note: The Heat Transfer Coefficient was first calculated for condensation on the external surface of the tube and 0.8 to compensate for condensation inside. 0.0203/0.0254 for the reduced area.

2.3.2 Overall Heat Transfer Coefficient

Overall Heat Transfer Coefficient: $U_C$ (69) [eq. 40a]

$$\frac{1}{U_c} = \frac{1}{\alpha_w} + \frac{1}{\alpha_i} + \frac{y_w \times D_2}{k_w \times D_w}$$

$$U_c = \frac{1}{\frac{1}{2047} + \frac{1}{1279} + \frac{0.00255 \times 0.0254}{45 \times 0.02285}}$$

$= 748.98 \text{ W/m}^2\text{K}$

2.3.3 Heat Transfer Area

Heat Gain Change Condensing Zone: $Q_C$ (70)= $(h_{2a} - h_3) \times \dot{m}$

$= (594.04 - 474.14) \times 0.084$

$= 10.16 \text{ kW}$ (or 10160 W)

Log. M.T.D.: $\theta_{ln}$ (71) $= \frac{(T_s - t_s) - (T_s - t_r)}{\ln\left[(T_s - t_s) / (T_s - t_r)\right]}$

(see condenser design data sheet No. 2) $= \frac{(55 - 45) - (55 - 48.88)}{\ln [(55-45) / (55 - 48.88)]}$

$= 7.9°\text{C}$

Heat Transfer Area: $A_c$ (72) $= UA_T\theta$

(Condensing Zone ) $= \frac{10160}{749.98 \times 7.9}$

$= 1.715 \text{ m}^2$

Calculated Tube Length: $L_c$ (73) $= \frac{1.715}{3.1416 \times 0.0254}$

$= 21.52 \text{ m}$

Calculated tube length confirms the estimated tube length (61 - page 5). At this stage, the computer was programmed to compute iteration calculations, modifying the estimated tube length until it was the same as the calculated value .

2.4 Condensate Sub-Cooling

The condensate leaving the condenser was assumed to be liquid at saturated temperature and pressure. There was, therefore, no advantage taken of refrigerant sub-cooling.

2.5 Total Heat Transfer Area

Condenser Total Heat Transfer Area: $A_T$ (74)=Area Condensing Zone +Area Desuperheating Zone

$= 1.715 + 0.555$

$= 2.27\ m^2$

Condenser Total Tube Length: $L_T$ (75) $= \dfrac{2.27}{3.14159 \times 0.0254}$

$= 28.45\ m$

SECTION 3: REFRIGERANT THERMAL CONTROL VALVE

3.1 Controlled Expansion

The Refrigerant Thermal Control Valve regulates the pressure drop, restricting flow with the object of giving a constant degree of superheat entering the compressor. In practice there are frictional and radiation losses, but in the computer programme the expansion is assumed to be adiabatic.

SECTION 4: EVAPORATOR

4.1 Air Side Heat Transfer Coefficient

Air Approach Velocity: $U_a$ (76) = 5 m/s

Tube Centres: $Y_f$ (77) = 0.0572 m

Tube Outside Diameter: $D_o$ (78) = 0.0254 m

Velocity at Minimum Area: $U_m$ (79) $= \dfrac{0.0572 \times 5}{0.0572 - 0.0254}$

$= 8.99$ m/s

Physical Properties of Air (Mean Temperature -2°C):

Density: $\rho_a$ (80) = 1.263 kg/m$^3$

Viscosity: $\mu_a$ (81) = 0.000017338 Ns/m$^2$

Thermal Conductivity: $k_a$ (82) = 0.0236 W/mK

Specific Heat: $C_a$ (83) = 1010 J/kgK

Reynolds Number: Re (84) = $\rho_a u_a l_a / \mu_a$

[eq. 10] $= \dfrac{1.263 \times 0.0254 \times 8.99}{0.000017338}$

$= 16634$

Prandtl Number: Pr (85) = $(C_a \times \mu_a) / k_a$

[eq. 11] $= \dfrac{1010 \times 0.000017338}{0.0236}$

$= 0.742$

Extended Heating Surface Dimensions:

Fin Pitch: $Y_F$ (86) = 0.0043 m

Height: $H_F$ (87) = 0.0158 m

Thickness: $\delta_F$ (88) = 0.000381 m

Fin Pitch is limited to 0.0043 m, which equates to a maximum of 6 fins per inch to reduce the adverse effects on the air flow at low temperatures when ice may be formed due to freezing atmospheric humidity.

Nusselt Number: Nu (89) [eq. 26] = $0.134\ Re_c^{0.681}\ Pr^{0.33}\ F_N$

Heat Transfer Correction Factor for Tube arrangement: $F_N$ [eq. 26]$= \left(\frac{y_F}{H_F}\right)^{0.2} \times \left(\frac{y_F}{\delta_F}\right)^{0.1134}$

(Tubes in Line) $Nu = 0.134\,Re_c^{0.681}\ Pr^{0.33}\left(\frac{y_F}{H_F}\right)^{0.2}\left(\frac{y_F}{\delta_F}\right)^{0.1134}$

$$= 0.134 \times 16634^{0.681} \times 0.742^{0.33} \times \left(\frac{0.0043}{0.0158}\right)^{0.2} \times \left(\frac{0.043}{0.000381}\right)^{0.1134}$$

$= 92.291$

Heat Transfer Coefficient: $\alpha$ (90) [eq. 9]

$Nu = \alpha l / k_a$

$\therefore \alpha = (Nu \times k_a) / l$

$= \frac{92.291 \times 0.0236}{0.0254}$

$= 85.75\ W/m^2K$

Area of Fin: $A_f$: (91) $= (3.1416 \times 2/4) \times (D_f^2 - D_0^2)$

$= (3.1416 \times 2/4) \times (0.057^2 - 0.0254^2)$

$= 0.00409\ m^2$

External Tube Area Per Fin: $A_0$ (92) $= D_2 \times 3.1416 \times y_f$

$= 0.0254 \times 3.1416 \times 0.0043$

$= 0.000343\ m^2$

Fin Efficiency: $A_x$ (93) = 95%

Heat Transfer Coefficient: $\alpha_A$ (94)

(based on outside of tube) $= 0.95 \times \alpha \times A_f/A_0$

$= \frac{0.95 \times 85.75 \times 0.00409}{0.000343}$

$= 971\ W/m^2K$

## 4.2 Evaporating Zone

### 4.2.1 Refrigerant Side - Heat Transfer Coefficient

Heat transfer by forced convective boiling is considered in two additive parts, namely the convective component and the nucleate boiling component. The convective component is first calculated as though there is only liquid flowing in the tube then it is corrected for two phase heat transfer.

Heating Surface Arrangement and Mass Flow

Tube Inside Diameter: $D_i$ (95) = 0.0203 m

Number of Tubes in Parallel: N (23) = 1

Note: There is only one refrigerant flow path in the following calculation. Array (129) is included in the computer programme for use in later calculations.

Refrigerant Flow Velocity: G (96) $= \dot{m} / (0.7854 \times D_i)$

$= \frac{0.084}{0.7854 \times 0.0203^2}$

$= 259.54\ kg/m^2s$

Convective Component

Specific enthalpy at dry points on the refrigerant circulation system are established on the pressure enthalpy chart Figure 22.

Vapour Fraction: X (97) = $(h_4 - h_{4x}) / (h_{4A} - h_{4x})$

= (474.16 - 410.39) / (569.32 - 410.39)

= 0.401

Viscosity: $\mu_L$ (98) = 0.00030842 Ns/m$^2$

Reynolds Number (Liquid): Re (99) [eq. 31] = $\dfrac{(1-X)GD_i}{\mu_L}$

= $\dfrac{(1 - 0.401) \times 259.54 \times 0.0203}{0.00030842}$

= 10233

Specific Heat: $C_L$ = 913.4 J/kgK

Thermal Conductivity: $k_L$ (100) = 0.1 W/mK

Prandtl Number (Liquid): Pr (101) [eq.12] = $C_L \mu_L / k_L$

= $\dfrac{913.4 \times 0.00030842}{0.1}$

= 2.817

Nusselt Number: Nu (102) = $0.023 \times Re^{0.8} \times Pr^{0.4}$

= $0.023 \times 10233^{0.8} \times 2.817^{0.4}$

= 55.18

Heat Transfer Coefficient. Convective Component: $\alpha_{DB}$ (103)

Nu = $\alpha_{DB}\, l / k_L$

$\therefore \alpha_{DB}$ = $(k_L \times Nu) / l$

= $(0.1 \times 55.18) / 0.0203$

= 271.8 W/m$^2$K

Correction for Two Phase Heat Transfer

Liquid Density: $\rho_L$ (104) = 1422 kg/m$^3$

Vapour Density: $\rho_G$ (105) = 13.23 kg/m$^3$

Vapour Viscosity: $\mu_G$ (106) = $1.133 \times 10^{-5}$ Ns/m$^2$

Two Phase Flow Parameter: $\dfrac{1}{X_{tt}}$ (107) [eq. 33] = $\left(\dfrac{\chi}{1-\chi}\right)^{0.9} \times \left(\dfrac{\rho_L}{\rho_G}\right)^{0.5} \times \left(\dfrac{\mu_G}{\mu_L}\right)^{0.1}$

= $\left(\dfrac{0.401}{0.599}\right)^{0.9} \times \left(\dfrac{1422}{13.23}\right)^{0.5} \times \left(\dfrac{0.00001133}{0.00030842}\right)^{0.1}$

= 5.191

Convective Correction Factor: $F_c$ (108)

The following formula is derived from calculations made by a supplementary computer programme, data is from Figure 13, Appendix 4.

$F_c$ = $1.3961 + 1.3458X - 0.03781X^2 + 0.0005844X^3$

(where X = 5.191)

= 7.45

Convective Component: $\alpha_{con}$ (109) = $F_c \times \alpha_{DB}$

= $7.45 \times 271.8$

= 2025 W/m$^2$K

Nucleation Suppression Factor: $S_c$ (110) = $Re_L F_c^{1.25}$

= $10233 \times 7.45^{1.25}$

= $12.595 \times 10^4$

The following formula is from Data Ref. 1, Fig.14, Supplementary Computer Program Number 3.

$X = Re_L \times F_c^{1.25} / 10^4$

$S_c = 0.9227 - 0.083198X + 0.0033124X^2 - 0.000047713X^3$

= 0.3051

Surface Tension: $\sigma$ (111) = 0.01296 N/m

Liquid Phase Viscosity: $\mu_L$ (98) = 0.00030842 $N_s/m^2$

Latent Heat of Evaporation: $\lambda$ (112) = 158931 J/kg

Vapour Density: $\rho_G$ (105) = 13.23 $kg/m^3$

Fluid Temperature Adjacent to Tube Wall: $T_w$ (134)= -6.74 °C

Refrigerant Saturation Temperature: $t_4$ (3)= -9 °C

Corresponding Pressure to $T_w$: $p_w$ (114) = 245593 $N/m^2$

Saturation Pressure: $p_1$ (1) = 227000 $N/m^2$

Heat Transfer Coefficient: $\alpha_{FZ}$ (115) [eq. 27]

$$=0.00122 \times \left( \frac{k_L^{0.79} \times C_L^{0.45} \times p_L^{0.49}}{\sigma^{0.5} \times \mu_L^{0.29} \times \lambda p_s^{0.24}} \right) \times (T_w - T_s)^{0.24} \times (p_w - p_s)^{0.75}$$

$$=0.00122 \times \left( \frac{0.10^{0.79} \times 913.4^{0.45} \times 1422^{0.49}}{0.01296^{0.5} \times 0.00030842^{0.29} \times (158931 \times 13.24)^{0.24}} \right)$$

$$\times \left(-6.735 - (-9)\right)^{0.24} \times (245593 - 227000)^{0.75}$$

$\alpha_{FZ}$ = 803.73 $W/m^2K$

Nucleate Component

Heat Transfer Coefficient: $\alpha_{nuc}$ (116) = $\alpha_{FZ} \times S_c$

= $803.73 \times 0.3051$

= 245.2 $W/m^2K$

Heat Transfer Coefficient

Heat Transfer Coefficient: $\alpha_o$ (117) = $(\alpha_{nuc} + \alpha_{con}) \times D_1 / D_0$

(Based on Outside Area of Tube)= H.T. Coeff. Nucleate + H.T. Coeff. Convective Component

= $(245.2 + 2052) \times (0.0203 / 0.0254)$

= 1836 $W/m^2K$

Overall Heat Transfer Coefficient: $U_B$

$$\frac{1}{U_B} = \frac{1}{\alpha_A} + \frac{1}{\alpha_0} + \frac{y_w \times D_0}{k_w \times D_w}$$

$$\therefore U_B = \frac{1}{\frac{1}{971} + \frac{1}{1836} + \frac{0.0025 \times 0.0254}{45 \times 0.0229}}$$

= 661.2 $W/m^2K$

4.2.2 Heat Transfer Area

Air Inlet Temperature: $T_{AI}$ (118) = 0 °C

Air Outlet Temperature: $T_A$ (119) = -4 °C

See evaporator design sheet No. 3, Figure 26.

Log M.T.D.: $\theta_{in}$ (120) = $$\frac{(T_{A1} - t_s) - (T_{A0} - t_s)}{\ln\left[(T_{A1} - t_s) / (T_{A0} - t_s)\right]}$$

= $\frac{[0 - (-9)] - [-4 - (-9)]}{\ln [0 - (-9)] / [-4 - (-9)]}$

= 6.81°C

Heat Transfer Forced Convective Boiling: $Q_B$ (121)= $(h_{4a} - h_4) \times \dot{m}$

= $(569.32 - 474.14) \times 0.084$

= 7.997 kW

Heat Transfer Area: $A_{CB}$ (122) = $Q_B \times 10^3 / (\theta_{in} \times U_B)$

= $7997 / (6.81 \times 611.2)$

= 1.921 $m^2$

4.3 Superheating Zone

4.3.1 Refrigerant Side - Heat Transfer Coefficient

Superheat - Specific Volume: $V_r$ (123) = 13.02 $kg/m^3$

Flow Area: $s_r$ (124) = 3.24 $10^{-4}$ $m^2$

Velocity: $u_r$ (125) = $\dot{m} / (s \times \rho)$

= $0.084 / (0.000324 \times 13.02)$

= 19.91 m/s

Viscosity: $\mu_r$ (126) = 0.000011435 $Ns/m^2$

Specific Heat Capacity: $C_r$ (127) = 604 J/kgK

Thermal Conductivity: $k_r$ (128) = 0.00784 W/mK

Reynolds Number: Re (129) = $\rho ul / \mu$

[eq. 10] = $\frac{13.02 \times 19.91 \times 0.0203}{0.000011435}$

= 460796

Prandtl Number: Pr (130) = $C\mu / k$

[eq. 11] = $\frac{604 \times 0.000011435}{0.00784}$

= 0.881

Correction Parameter: E (131) = $0.0225 \text{ Exp } (-0.0225 (\ln 0.881)^2)$

[eq. 18] = 0.022

Stanton Number: St (132) = $E \, Re^{-0.205} \, Pr^{-0.505}$

[eq. 17] = $0.022 \times 460796^{-0.205} \times 0.881^{-0.505}$

= 0.002

Heat Transfer Coefficient: $\alpha_r$ (133) [eq. 16]= $\rho uCSt$

(based on internal tube area) = $13.02 \times 19.91 \times 604 \times 0.002$

= 313.15 $W/m^2K$

Heat Transfer Coefficient: $\alpha_{rl}$ (134) = $313.15 \times \frac{0.0203}{0.0254}$

(based on external tube area)

= 250.3 $W/m^2K$

4.3.2 Overall Heat Transfer Coefficient

Superheater Zone: $U_s$ (135) : $1/U_s$ = $\frac{1}{\alpha_A} + \frac{1}{\alpha_i} + \frac{y_w \times D_0}{k_w \times D_w}$

$\therefore U_s$ = $\frac{1}{\frac{1}{971} + \frac{1}{250.3} + \frac{0.0025 \times 0.0254}{45 \times 0.0229}}$

= 196.59 W/m$^2$K

4.3.3 Heat Transfer Area

Heat Transfer - Superheat Zone: $Q_s$ (136)= $(h_1 - h_{4a}) / \dot{m}$

= $(573.44 - 569.32) \times 0.084$

= 0.346 kW

Log. Mean Temperature Difference

Corrected for Cross Flow: P(137)[eq. 58]= $\frac{t_{out} - t_{in}}{T_{in} - t_{in}}$

= $\frac{-2 - (-9)}{0 - (-9)}$

= 0.78

R (138) [eq. 59]= $\frac{T_{in} - T_{out}}{t_{out} - t_{in}}$

= $\frac{0 - (-4)}{-2 - (-9)}$

= 0.57

From Graph 41. Appendix 4.: $F_T$(139) = 0.8

Log. M.T.D.: $\theta_{in}$ (71) = $\frac{5 - 2}{\ln(5/2)} \times 0.8$

= 2.62°C

Heating Surface Area - Superheating Zone: $A_s$ (140)= $Q_S / (U \times \theta)$

= $0.346 \times 1000 / (196.59 \times 2.62)$

= 0.672 m$^2$

Total Heating Surface - Area Evaporator: $A_E$(141)= 1.921 + 0.672

= 2.593 m$^2$

Total Tube Length Evaporator: T (142) = $2.593 / (3.14159 \times 0.0254)$

= 32.495 m

Total Heat to Evaporator: $Q_E$ (143) = Area Evaporating Zone + Area Superheating Zone

= $(573.44 - 474.14) \times 0.084$

= 8.343 kW

4.4 Total Air Volume

Air Density: $\rho_a$ (80) = 1.263 kg/m$^3$

Air Specific Heat Capacity: $C_a$ (83) = 1.0038 kJ/kgK

Air Temperature Drop Through Evaporator= 0 - (-4)

= 4 °C

Total Air Volume - Evaporator: $V_a$ (144)= $Q_E / (\rho_a \times C_a \times \Delta_t)$

= 8.341 / (1.263 × 1.0038 × 4)
= 1.645 $m^3/s$

SECTION 5: SUMMARY OF CALCULATED RESULTS

Thermal Input

Power Input - Compressor: $Q_m$ (15) = 4.762 kW

Heat Input - Evaporator: $Q_E$ (143) = 8.343 kW

[The calculations neglect radiation and friction losses and they also do not include the power consumed by the air fan.]

Energy Input to Heat Pump: (145) = 4.7642 + 8.343
= 13.11 kW

Thermal Output

Heat Transfer to Water: $Q_w$ (17) = 13.11 kW

Coefficient of Performance (COP)

Calculated COP: (146) = $\frac{\text{Heat Output}}{\text{Input to Compressor}}$
= $\frac{13.11}{4.7642}$
= 2.75

Carnot Theoretical Performance:

Condensing Temperature: $T_h$ (147) = 273 + 55
= 328K

Evaporating Temperature: $T_c$ (148) = 273 + (-9)
= 264K

Carnot COP (149) = $T_h / T_h - T_c$
= $\frac{328}{328 - 264}$
= 5.125

Vapour Compression Performance:

Specific Enthalpy Compressor Inlet: $h_1$ (5)= 573.44 kJ/kg.

Specific Enthalpy Compressor Outlet: $h_2$ (9)= 630.14 kJ/kg.

Specific Enthalpy Condenser Output: $h_3$ (16)= 474.14 kJ/kg.

Heat Pump COP (150) = $(h_2 - h_3) / (h_2 - h_1)$
= $\frac{630.14 - 474.14}{630.14 - 573.44}$
= 2.75

Carnot Efficiency: (151)

Carnot Efficiency = $\frac{\text{Calculated COP} \times 100}{\text{Carnot COP}}$
= $\frac{2.75 \times 100}{5.125}$
= 54%

APPENDIX A3.2

Computer array numbers

| Computer Constant | Symbol used in script | Description | Units |
|---|---|---|---|
| 1 | $P_1$ | Suction Pressure | bar (abs) |
| 2 | $P_2$ | Delivery Pressure | bar (abs) |
| 3 | $t_4$ | Evaporator Saturation Temperature | °C |
| 4 | $t_1$ | Superheat Suction Temperature | °C |
| 5 | $h_1$ | Compressor Inlet Specific Enthalpy | kJ/kg |
| 6 | $s_1$ | Specific Entropy at Inlet | kJ/kgK |
| 7 | $h_2'$ | Specific Enthalpy Output | kJ/kg |
| 8 | $\eta$ | Efficiency | |
| 9 | $h_2$ | Specific Enthalpy Compressor Discharge | kJ/kg |
| 10 | $C_R$ | Compressor-Compression Ratio | |
| 11 | $V_P$ | Piston Displacement Volume | $m^3/s$ |
| 12 | $V_1$ | Compressor Suction Volume | $m^3/s$ |
| 13 | $V_{1s}$ | Specific Volume Refrigerant Suction | $m^3/kg$ |
| 14 | $\dot{m}$ | Refrigerant Mass Flow | kg/s |
| 15 | $Q_m$ | Mechanical Work Input to Compressor | kW |
| 16 | $h_3$ | Specific Enthalpy | kJ/kg |
| 17 | $Q_w$ | Heat Transfer to Water | kW |
| 18 | $t_{w1}$ | Water Flow Temperature (To System) | °C |
| 19 | $t_{w2}$ | Water Return Temperature (From System) | °C |
| 20 | $A_d$ | Heating Temperature Range | °C |
| 21 | $D_1$ | External Tube, Internal Diameter | m |
| 22 | $D_2$ | Internal Tube, External Diameter | m |
| 23 | N | Number of Tubes in Parallel | |
| 24 | A | Cross Sectional Area to Flow | $m^2$ |
| 25 | C | Specific Heat | J/kgK |
| 26 | $\rho$ | Density | $kg/m^3$ |
| 27 | $V_f$ | Water Flow Rate | l/s |
| 28 | $V_w$ | Water Mean Velocity | m/s |
| 29 | l | Characteristic Length | m |
| 30 | $\mu$ | Viscosity | $Ns/m^2$ |
| 31 | Re | Reynold's Number | |
| 32 | k | Thermal Conductivity | W/mK |
| 33 | Pr | Prandtl Number | |
| 34 | E | Correlation Parameter | |
| 35 | St | Stanton Number | |
| 36 | $\alpha_w$ | Heat Transfer Coefficient (Water Side) | $W/m^2K$ |
| 37 | $D_3$ | Internal Tube, Internal Diameter | m |
| 38 | $D_w$ | Mean Tube Diameter of Inner Tube | m |
| 39 | $A_s$ | Cross Sectional Area to Flow | $m^2$ |
| 40 | $\rho_r$ | Refrigerant Density | $kg/m^3$ |
| 41 | $U_r$ | Refrigerant Mean Velocity | m/s |
| 42 | $\mu_r$ | Refrigerant Viscosity | $Ns/m^2$ |
| 43 | l | Characteristic Length | m |
| 44 | $C_r$ | Refrigerant Specific Heat | J/kgK |
| 45 | $k_r$ | Refrigerant Thermal Conductivity | W/mK |

| | | | |
|---|---|---|---|
| 46 | Pr | Prandtl's number | |
| 47 | E | Correlation Parameter | |
| 48 | St | Stanton Number | |
| 49 | $\alpha_i$ | Heat Transfer Coefficient ($D_i$) | $W/m^2K$ |
| 50 | $\alpha_o$ | Heat Transfer Coefficient ($D_o$) | $W/m^2K$ |
| 51 | $y_w$ | Tube Wall Thickness | m |
| 52 | $k_w$ | Wall Thermal Conductivity | W/mK |
| 53 | $U_d$ | Overall Heat Transfer Coefficient | $W/m^2K$ |
| 54 | $h_{2a}$ | Specific Enthalpy Dry Saturation Point 2A | kJ/kg |
| 55 | $Q_{sh}$ | Heat Gain Desuperheating | kW |
| 56 | $t_s$ | Temperature Entering Desuperheater | °C |
| 57 | $T_2$ | Refrigerant Inlet Temperature | °C |
| 58 | $T_s$ | Condensing Temperature | °C |
| 59 | $Q_{in}$ | Log M.T.D. (Desuperheat Zone) | |
| 60 | $A_d$ | Heat transfer area | $m^2$ |
| 61 | $L_c$ | Tube Length | m |
| 62 | $\rho_L$ | Liquid Density | $kg/m^3$ |
| 63 | $\rho_G$ | Vapour Density | $kg/m^3$ |
| 64 | g | Gravitational Constant | $m/s^2$ |
| 65 | $\mu_L$ | Liquid Viscosity | $N/m^2$ |
| 66 | $k_L$ | Thermal Conductivity | W/mK |
| 67 | $\alpha_o$ | Heat Transfer Coefficient | $W/m^2K$ |
| 68 | $\alpha_I$ | Heat Transfer Coefficient | $W/m^2K$ |
| 69 | $U_c$ | Overall Heat Transfer Coefficient (Condensing Zone) | $W/m^2K$ |
| 70 | $Q_c$ | Heat Transferred Condensing Zone | kW |
| 71 | $\theta_{in}$ | Log M.T.D. (Condensing Zone) | °C |
| 72 | $A_c$ | Condensing Zone Heat Transfer Area | $m^2$ |
| 73 | l | Calculated tube length | m |
| 74 | $A_T$ | Condenser Total Heat Transfer Area | $m^2$ |
| 75 | $L_T$ | Condenser Total Tube Length | m |
| 76 | $U_a$ | Air Approach Velocity | m/s |
| 77 | $Y_f$ | Tube Pitch Centres | m |
| 78 | $D_o$ | Tube Outside Diameter | m |
| 79 | $U_m$ | Velocity at Minimum Area | m/s |
| 80 | $\rho_a$ | Air Density | $kg/m^3$ |
| 81 | $\mu_a$ | Air Viscosity | $Ns/m^2$ |
| 82 | $k_a$ | Air Thermal Conductivity | W/mK |
| 83 | $C_a$ | Air Specific Heat | J/kgK |
| 84 | Re | Reynold's number | |
| 85 | Pr | Prandtl number | |
| 86 | $Y_F$ | Fin Pitch | m |
| 87 | $H_F$ | Fin Height | m |
| 88 | $\delta_F$ | Fin Thickness | m |
| 89 | Nu | Nusselt Number | |
| 90 | $\alpha$ | Heat Transfer Coefficient (Outside Plane Tubes) | $W/m^2K$ |
| 91 | $A_f$ | Fin Area | $m^2$ |
| 92 | $A_o$ | External Tube Area Per Fin | $m^2$ |
| 93 | $A_x$ | Fin Efficiency | |
| 94 | $\alpha_A$ | Heat Transfer Coefficient (Outside Finned Tubes) | $W/m^2K$ |
| 95 | $D_i$ | Tube Inside Diameter | m |
| 96 | G | Refrigerant Flow Velocity | $kg/m^2s$ |
| 97 | X | Vapour Fraction | decimal |
| 98 | $\mu_L$ | Liquid Viscosity | $Ns/m^2$ |
| 99 | Re | Reynold's number | |

| | | | |
|---|---|---|---|
| 100 | $k_L$ | Liquid Thermal Conductivity | W/mK |
| 101 | Pr | Prandtl number | |
| 102 | Nu | Nusselt's number | |
| 103 | $\alpha_{DB}$ | Heat Transfer Coefficient (Dittus-Boelter Method) | |
| 104 | $\rho_L$ | Liquid Density | $kg/m^3$ |
| 105 | $\rho_G$ | Vapour Density | $kg/m^3$ |
| 106 | $\mu_G$ | Vapour Viscosity | $Ns/m^2$ |
| 107 | $1/X_{tt}$ | Two Phase Flow Parameter | |
| 108 | $F_c$ | Convective Boiling Correction Factor | |
| 109 | $\alpha_{con}$ | Heat Transfer Coefficient, Convective Component | |
| 110 | $S_c$ | Nucleation Suppression Factor | |
| 111 | $\sigma$ | Surface Tension | N/m |
| 112 | $\lambda$ | Latent Heat of Evaporation | J/kg |
| 113 | $T_w$ | Tube Wall Temperature | °C |
| 114 | $p_w$ | Corresponding Pressure at Saturated Wall Temperature | |
| 115 | $\alpha_{FZ}$ | Heat Transfer Coefficient (Foster-Zuber) | $W/m^2K$ |
| 116 | $\alpha_{nuc}$ | Nucleate Compression Convective Boiling | $W/m^2K$ |
| 117 | $\alpha_o$ | Heat Transfer Coefficient | $W/m^2K$ |
| 118 | $T_{A1}$ | Air Inlet Temperature | °C |
| 119 | $T_A$ | Air Outlet Temperature | °C |
| 120 | $\theta_{in}$ | Log M.T.D. | °C |
| 121 | $Q_B$ | Heat Transfer, Forced Convective Boiling | kW |
| 122 | $A_{CB}$ | Heat Transfer Area (Evaporator Zone) | $m^2$ |
| 123 | $V_r$ | Refrigerant Superheated Specific Volume | $kJ/m^3$ |
| 124 | $s_r$ | Refrigerant Flow Area | $m^2$ |
| 125 | $u_r$ | Refrigerant Velocity | m/s |
| 126 | $\mu_r$ | Refrigeration Viscosity | $Ns/m^2$ |
| 127 | $C_r$ | Refrigerant Specific Heat Capacity | J/kgK |
| 128 | $k_r$ | Refrigerant Thermal Conductivity | W/mK |
| 129 | Re | Reynold's number | |
| 130 | Pr | Prandtl's number | |
| 131 | E | Correlation Parameter | |
| 132 | St | Stanton Number | |
| 133 | $\alpha_r$ | Refrigerant Heat Transfer Coefficient (on Internal Tube Area) | |
| 134 | $\alpha_{rl}$ | Refrigerant Heat Transfer Coefficient (on External Tube Area) | |
| 135 | $U_s$ | Overall Coefficient of Efficiency (Superheat Zone) | |
| 136 | $Q_s$ | Heat Transfer (Superheat Zone) | kW |
| 137 | P | Constant Derived From Graph | |
| 138 | R | Constant Derived From Graph | |
| 139 | $F_T$ | Correction Factor Derived From Graph | |
| 140 | $A_s$ | Heat Transfer Area (Superheat Zone) | $m^2$ |
| 141 | $A_E$ | Evaporator Total Heating Area | $m^2$ |
| 142 | T | Evaporator Total Tube Length | m |
| 143 | $Q_E$ | Total Heat to Evaporator | kW |
| 144 | $V_a$ | Air Volume | $m^3$ |
| 145 | | Energy Input to Heat Pump | kW |
| 146 | | Calculated Coefficient of Performance | |
| 147 | $T_h$ | Condensing Temperature | °C |
| 148 | $T_c$ | Evaporating Temperature | °C |
| 149 | | Carnot Coefficient of Performance | |
| 150 | | Heat Pump Coefficient of Performance | |

APPENDIX A3.3

GRAPHICAL DATA FOR MATHEMATICAL MODEL

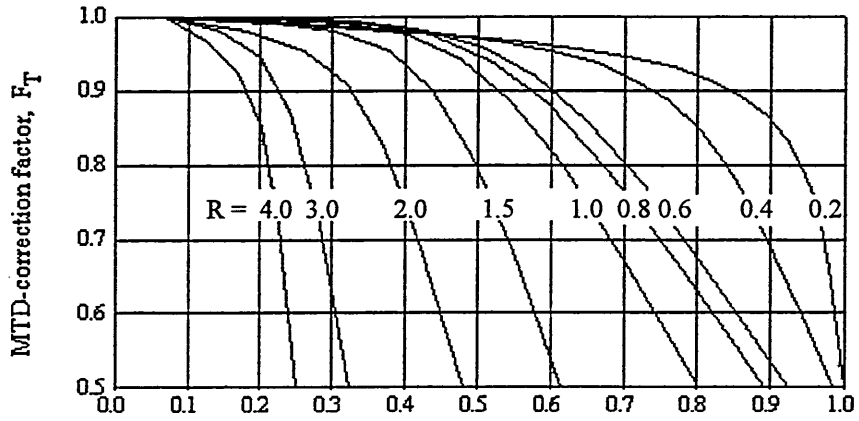


$$P = \frac{t_{out} - t_{in}}{T_{in} - t_{in}}$$

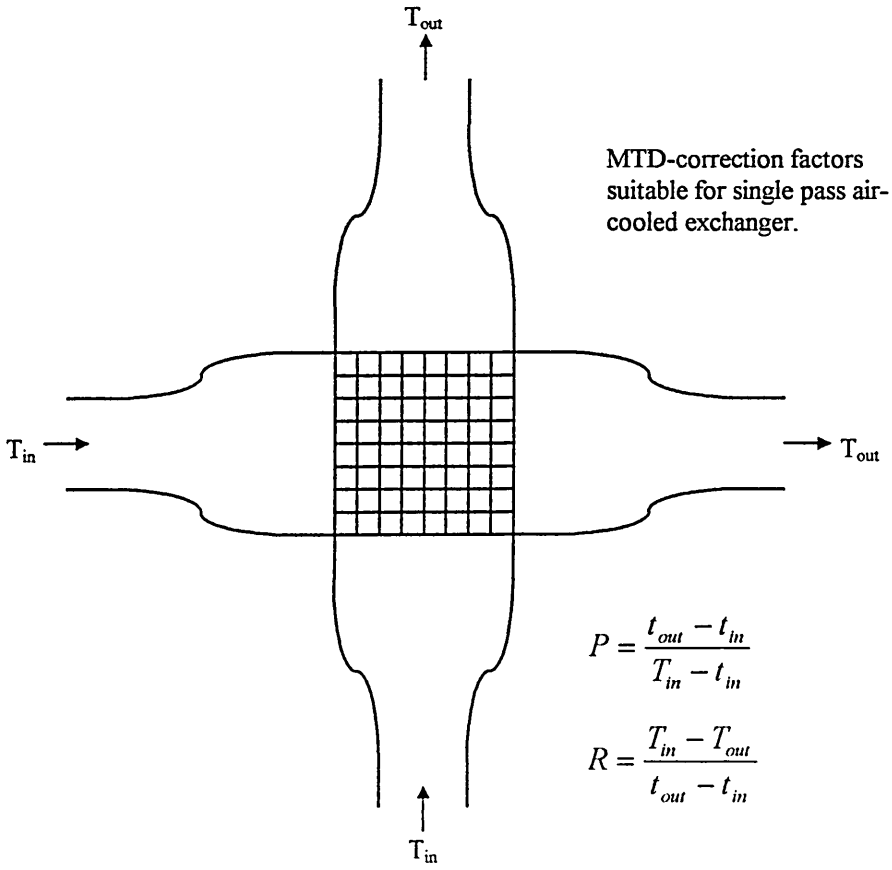


MTD-correction factors suitable for single pass air-cooled exchanger.

$$P = \frac{t_{out} - t_{in}}{T_{in} - t_{in}}$$

$$R = \frac{T_{in} - T_{out}}{t_{out} - t_{in}}$$

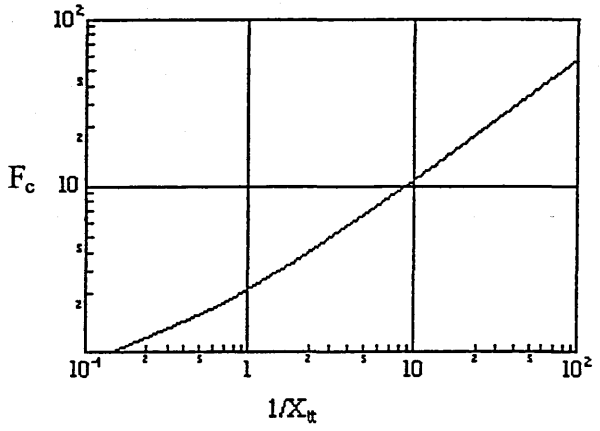


Chen (1966) correlation: convective component correction factor

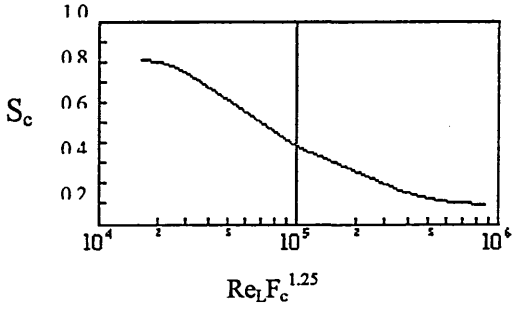


Chen (1966) correlation: nucleate-boiling suppression factor

APPENDIX A3.4

COMPUTER PRINT OUT - HEAT PUMP DESIGN

CALCULATION NUMBER 506

| Item No. | Description | Units | Input Data | Output Data |
|---|---|---|---|---|
| 1 | Suction Pressure | bar (abs) | 2.27 | |
| 2 | Delivery Pressure | bar (abs) | 13.6 | |
| 3 | Evaporator saturation temperature | °C | -9 | |
| 4 | Superheat Suction temperature | °C | -2 | |
| 5 | Compressor inlet specific enthalpy | kJ/kg | 573.44 | |
| 6 | Specific entropy at inlet | kJ/kg | 4.773 | |
| 7 | Specific enthalpy output | kJ/kg | 607.46 | |
| 8 | Compressor isentropic efficiency | (%) | 60 | |
| 9 | Specific enthalpy compressor discharge | kJ/kg | | 630.14 |
| 10 | Compressor/Compression ratio | | | 5.99 |
| 11 | Piston displacement volume | $m^3/s$ | 0.0103 | |
| 12 | Compressor suction volume | $m^3/kg$ | 0.0778 | |
| 13 | Suction volume refrigerant suction | $m^3/s$ | | 0.00654 |
| 14 | Refrigerant mass flow | kg/s | | 0.084 |
| 15 | Mechanical work to compressor | kW | | 4.764 |
| 16 | Specific enthalpy | kJ/kg | 474.14 | |
| 17 | Heat transfer to water | kW | | 13.11 |
| 18 | Water flow temperature (to system) | °C | 50 | |
| 19 | Water return temp. (from system) | °C | 45 | |
| 20 | Heating temperature range | °C | | 5 |
| 21 | Inside diameter of outer tube | m | 0.056 | |
| 22 | Outside diameter of inner tube | m | 0.0254 | |
| 23 | Number of tubes in parallel | 1 | | |
| 24 | Cross section area to water flow | $m^2$ | | $1.956 \times 10^{-3}$ |
| 25 | Water specific heat | kJ/kg | 4182 | |
| 26 | Water density | $kg/m^3$ | 989 | |
| 27 | Water flow rate | l/s | 0.634 | |
| 28 | Water mean velocity | m/s | | 0.324 |
| 29 | Characteristic length | m | | 0.0306 |
| 30 | Viscosity | $Ns/m^2$ | $5.756 \times 10^{-4}$ | |
| 31 | Reynold's number | | | 17040 |
| 32 | Thermal Conductivity | W/mK | 0.658 | |
| 33 | Prandtl number | | | 3.658 |
| 34 | Correlation parameter | | | $2.166 \times 10^{-2}$ |
| 35 | Stanton number | | | $1.53 \times 10^{-3}$ |
| 36 | H.T. coefficient (water side) | $W/m^2K$ | | 2047 |
| 37 | Inside diameter of inner tube | m | 0.0203 | |
| 38 | Mean diameter of inner tube | m | 0.02285 | |
| 39 | C.S.A. refrigerant side | $m^2$ | | $3.236 \times 10^{-4}$ |
| 40 | Refrigerant density | $kg/m^3$ | 66.94 | |
| 41 | Refrigerant mean velocity | m/s | | 3.878 |
| 42 | Refrigerant viscosity | $Ns/m^2$ | 0.0000139 | |
| 43 | Characteristic length | m | | 0.0203 |
| 44 | Refrigerant specific heat | J/kgK | 779 | |
| 45 | Refrigerant thermal conductivity | W/mK | 0.01273 | |
| 46 | Prandtl's number | | | 0.851 |
| 47 | Correlation parameter | | | $2.25 \times 10^{-2}$ |

| Item No. | Description | Units | Input Data | Output Data |
|---|---|---|---|---|
| 48 | Stanton number | | | $1.754 \times 10^{-3}$ |
| 49 | H.T. coeff ($D_i$) | $W/m^2K$ | | 354.699 |
| 50 | H.T. coeff ($D_o$) | $W/m^2K$ | | 283.48 |
| 51 | Tube Wall thickness | m | | $2.585 \times 10^{-3}$ |
| 52 | Wall thermal conductivity | W/mK | 45 | |
| 53 | Overall heat transfer coefficient | $W/m^2K$ | | 245.15 |
| 54 | Specific enthalpy | kJ/kg | 595.04 | |
| 55 | Heat gain Desuperheat | kW | 2.95 | |
| 56 | Water temp. entering desuperheater | °C | | 48.88 |
| 57 | Refrigerator inlet temperature | °C | 103 | |
| 58 | Condensing temperature | °C | 55 | |
| 59 | Log M.T.D. | °C | | 21.7 |
| 60 | Heat transfer area | $m^2$ | | 0.555 |
| 61 | Tube length (estimated) | m | 21.52 | |
| 62 | Refrigerant liquid density | $kg/m^3$ | 1189 | |
| 63 | Refrigerant vapour density | $kg/m^3$ | 75.98 | |
| 64 | Gravitational constant | $m/s^2$ | 9.81 | |
| 65 | Liquid viscosity | $Ns/m^2$ | $1.554 \times 10^{-4}$ | |
| 66 | Thermal conductivity | W/mK | 0.0758 | |
| 67 | Heat transfer coefficient ($\alpha_o$) | $W/m^2K$ | | 2001 |
| 68 | Heat transfer coefficient ($\alpha_l$) | $W/m^2K$ | | 1279 |
| 69 | Overall H.T. coefficient | $W/m^2K$ | | 748.98 |
| 70 | Heat gain change, condensing zone | kW | | 10.16 |
| 71 | Log M.T.D. | °C | | 7.9 |
| 72 | H.T. area condensing zone | $m^2$ | | 1.715 |
| 73 | Calculated tube length | m | | 21.52 |
| 74 | Total condenser H.T. area | $m^2$ | | 2.27 |
| 75 | Total condenser tube | m | | 28.45 |
| 76 | Air approach velocity | m/s | 5 | |
| 77 | Tube pitch centres | m | 0.0572 | |
| 78 | Outside diameter tubes | m | 0.0254 | |
| 79 | Velocity at minimum area | m/s | | 8.99 |
| 80 | Air density | $kg/m^3$ | 1.263 | |
| 81 | Air viscosity | $Ns/m^2$ | $1.7338 \times 10^{-5}$ | |
| 82 | Air thermal conductivity | W/mK | $2.36 \times 10^{-2}$ | |
| 83 | Air specific heat | J/kgK | 1010 | |
| 84 | Reynold's number | | | 16634 |
| 85 | Prandtl number | | | $7.42 \times 10^{-2}$ |
| 86 | Fin pitch | m | $4.3 \times 10^{-3}$ | |
| 87 | Fin height | m | $1.58 \times 10^{-2}$ | |
| 88 | Fin thickness | m | $3.81 \times 10^{-4}$ | |
| 89 | Nusselt number | | | 92.291 |
| 90 | Heat transfer coefficient | $W/m^2K$ | | 85.75 |
| 91 | Fin area | $m^2$ | | $4.09 \times 10^{-3}$ |
| 92 | Tube H.T. areas | $m^2$ | | $3.43 \times 10^{-4}$ |
| 93 | Fin efficiency | (%) | 95 | |
| 94 | H.T. coeff (based on tube ex. surface) | $W/m^2K$ | | 971 |
| 95 | Inside diameter tubes | m | $2.03 \times 10^{-2}$ | |
| 96 | Refrigerant flow velocity | $kg/m^2s$ | | 259.54 |
| 97 | Mass fraction of vapour | | | 0.401 |
| 98 | Refrigerant liquid viscosity | $Ns/m^2$ | $3.0842 \times 10^{-4}$ | |
| 99 | Reynold's number (liquid) | | | 10233 |
| 100 | Thermal conductivity | W/mK | 0.1 | |

| Item No. | Description | Units | Input Data | Output Data |
|---|---|---|---|---|
| 101 | Prandtl number (liquid) | | | 2.817 |
| 102 | Nusselt's number | | | 55.18 |
| 103 | H.T. coeff ($\alpha_{DB}$) | $W/m^2K$ | | 271.8 |
| 104 | Liquid density | $kg/m^3$ | 1422 | |
| 105 | Vapour density | $kg/m^3$ | 13.23 | |
| 106 | Vapour viscosity | $Ns/m^2$ | $1.133 \times 10^{-5}$ | |
| 107 | Two phase flow parameter | | | 5.191 |
| 108 | Convective correction factor $F_c$ | | | 7.45 |
| 109 | Convective component of boiling | $W/m^2K$ | | 2025 |
| 110 | Nucleation suppression factor | | | 0.3051 |
| 111 | Surface tension | N/m | 0.01296 | |
| 112 | Latent heat of evaporation | J/kg | 158931 | |
| 113 | Tube wall temperature | °C | -6.74 | |
| 114 | Revised value sat. press. corresponding to wall temp. | | | 245593 |
| 115 | Heat transfer coefficient ($\alpha_{FZ}$) | $W/m^2K$ | | 803.73 |
| 116 | Heat transfer coefficient ($\alpha_{nuc}$) | $W/m^2K$ | | 245.2 |
| 117 | Heat transfer coefficient ($\alpha_o$) | $W/m^2K$ | | 1836 |
| 118 | Air inlet temperature | °C | 0 | |
| 119 | Air outlet temperature | °C | -4 | |
| 120 | Log M.T.D. | °C | | 6.81 |
| 121 | Heat transfer forced conv. boiling | kW | | 7.997 |
| 122 | H.T. area, evaporating zone | $m^2$ | | 1.921 |
| 123 | Mean refrigerant density | $kg/m^3$ | 13.02 | |
| 124 | Refrigerant flow areas | $m^2$ | | $3.24 \times 10^{-4}$ |
| 125 | Refrigerant velocity superheating | m/s | | 19.91 |
| 126 | Refrigerant viscosity | $Ns/m^2$ | | $1.1435 \times 10^{-5}$ |
| 127 | Specific heat capacity | J/kgK | 604 | |
| 128 | Thermal conductivity | W/mK | 0.00784 | |
| 129 | Reynold's number | | | 460796 |
| 130 | Prandtl number | | | 0.881 |
| 131 | Correction parameter | | | 0.022 |
| 132 | Stanton number | | | 0.002 |
| 133 | Heat transfer coefficient ($\alpha_r$) | $W/m^2K$ | | 313.15 |
| 134 | Heat transfer coefficient ($\alpha_{r1}$) | $W/m^2K$ | | 250.3 |
| 135 | Overall H.T. coefficient | $W/m^2K$ | | 196.59 |
| 136 | Evaporator superheat | kW | | 0.346 |
| 137 | Correction factor P | | 0.78 | |
| 138 | Correction factor R | | 0.57 | |
| 139 | Correction factor $F_T$ | | 0.8 | |
| 140 | H.T. area, evap. superheating zone | $m^2$ | | 0.672 |
| 141 | Evaporator total area | $m^2$ | | 2.593 |
| 142 | Evaporator tube length | m | | 32.495 |
| 143 | Total heat to evaporator | kW | | 8.343 |
| 144 | Total air volume through evaporator | $m^3/s$ | | 1.645 |
| 145 | Energy input to heat pump | kW | | 13.11 |
| 146 | Calculated C.O.P. | | | 2.75 |
| 147 | Condensing temperature | K | | 328 |
| 148 | Evaporating temperature | K | | 264 |
| 149 | Carnot C.O.P. | | | 5.125 |
| 150 | Thermal performance C.O.P. | | | 2.75 |
| 151 | Carnot efficiency | | | 54% |

APPENDIX A3.5

EQUATIONS USED IN REGRESSIONAL CALCULATIONS

Linear Equation

(i) $an + b\Sigma x = \Sigma y$

(ii) $a\Sigma x + b\Sigma x^2 = \Sigma yx$

Regressional equation $y = a + bx$

Quadratic Equation

(i) $an + b\Sigma x + c\Sigma x^2 = \Sigma y$

(ii) $a\Sigma x + b\Sigma x^2 + c\Sigma x^3 = \Sigma yx$

(iii) $a\Sigma x^2 + b\Sigma x^3 + c\Sigma x^4 = \Sigma yx^2$

Regressional equation $y = a + bx + cx^2$

Cubic Equation

(i) $an + b\Sigma x + c\Sigma x^2 + d\Sigma x^3 = \Sigma y$

(ii) $a\Sigma x + b\Sigma x^2 + c\Sigma x^3 + d\Sigma x^4 = \Sigma yx$

(iii) $a\Sigma x^2 + b\Sigma x^3 + c\Sigma x^4 + d\Sigma x^5 = \Sigma yx^2$

(iv) $a\Sigma x^3 + b\Sigma x^4 + c\Sigma x^5 + d\Sigma x^6 = \Sigma yx^3$

Regressional equation $y = a + bx + cx^2 + dx^3$

Quartic Equation

(i) $an + b\Sigma x + c\Sigma x^2 + d\Sigma x^3 + e\Sigma x^4 = \Sigma y$

(ii) $a\Sigma x + b\Sigma x^2 + c\Sigma x^3 + d\Sigma x^4 + e\Sigma x^5 = \Sigma yx$

(iii) $a\Sigma x^2 + b\Sigma x^3 + c\Sigma x^4 + d\Sigma x^5 + e\Sigma x^6 = \Sigma yx^2$

(iv) $a\Sigma x^3 + b\Sigma x^4 + c\Sigma x^5 + d\Sigma x^6 + e\Sigma x^7 = \Sigma yx^3$

(v) $a\Sigma x^4 + b\Sigma x^5 + c\Sigma x^6 + d\Sigma x^7 + e\Sigma x^8 = \Sigma yx^4$

Regressional equation $y = a + bx + cx^2 + dx^3 + ex^4$

Three Variables

(i) $an + b\Sigma x + c\Sigma y = \Sigma z$

(ii) $a\Sigma x + b\Sigma x^2 + c\Sigma yx = \Sigma zx$

(iii) $a\Sigma y + b\Sigma yx + c\Sigma y^2 = \Sigma zy$

Regressional equation $z = a + bx + cy$

APPENDIX A4.1

SUPPLEMENTARY HEATING CALCULATIONS

The following figures show the calculations performed for the supplementary heating,

They are broken down as follows:-

| 100% Heat Pump Capacity | | | | | | | | | | | | | |
|---|---|---|---|---|---|---|---|---|---|---|---|---|---|
| A | C | E | G | I | J | K | | M | N | P | | R | T |
| Ambient Temp. °C | Building Loss kW | Heating days/annum | Heat Req'd (14th day) kWh/annum | Heat Pump Capacity kW | Heat Pump Maximum Output kWh | Heat Pump Useful Output kWh | | COP Full Load | COP Part Load | Heat Pump Input | | Supp. Heat kWh | Heat Pump Energy Input 8417 kWh |
| 15 | 0.62 | 26 | 226 | 12.1 | 4404 | 226 | | 3.13 | 1.31 | 172 | | | 601kWdays/ht. season |
| 13 | 1.86 | 25 | 651 | 11.4 | 3990 | 651 | Part Load 13878 | 3 | 1.71 | 381 | Part Load 6569 | | |
| 11 | 3.1 | 34 | 1476 | 10.7 | 5093 | 1476 | | 2.86 | 1.96 | 753 | | | 6569kWh above bal point |
| 9 | 4.34 | 42 | 2552 | 10 | 5880 | 2552 | | 2.72 | 2.12 | 1204 | | | 469kWdays/ht. season |
| 7 | 5.58 | 66 | 5156 | 9.3 | 8593 | 5156 | | 2.58 | 2.19 | 2354 | | | |
| 5 | 6.82 | 40 | 3819 | 8.7 | 4872 | 3819 | | 2.44 | 2.24 | 1705 | | | 1848kWh below bal point |
| 3 | 8.06 | 20 | 2257 | 7 | 1960 | 1960 | Full Load 3637 | 2.06 | 2.06 | 951 | Full Load 1848 | 297 | 132kWdays/ht. season |
| 1 | 9.3 | 12 | 1562 | 6.3 | 1058 | 1058 | | 1.93 | 1.93 | 548 | | 504 | |
| -1 | 10.54 | 6 | 885 | 5.7 | 479 | 479 | | 1.81 | 1.81 | 265 | | 407 | 1397kWh Supp. Heat |
| -3 | 11.78 | 2 | 330 | 5 | 140 | 140 | | 1.68 | 1.68 | 83 | | 190 | 100kWdays/ht. season |
| | | Sum: 273 | Sum: 18914 | | | Sum, kWh: 17517 | | | | Sum, kWh: 8417 | | Sum: 1397 | |

TABLE 3

| 75% Heat Pump Capacity | | | | | | | | | | | | | |
|---|---|---|---|---|---|---|---|---|---|---|---|---|---|
| A | C | E | G | I | J | K | | M | N | P | | R | T |
| Ambient Temp. °C | Building Loss kW | Heating days/annum | Heat Req'd (14th day) kWh/annum | Heat Pump Capacity kW | Heat Pump Maximum Output kWh | Heat Pump Useful Output kWh | | COP Full Load | COP Part Load | Heat Pump Input | | Supp. Heat kWh | Heat Pump Energy Input 7747 kWh |
| 15 | 0.62 | 26 | 226 | 9.1 | 3303 | 226 | | 3.13 | 1.31 | 172 | | | 553kWdays/ht. season |
| 13 | 1.86 | 25 | 651 | 8.6 | 2993 | 651 | Part Load 10060 | 3 | 1.71 | 381 | Part Load 4864 | | |
| 11 | 3.1 | 34 | 1476 | 8 | 3820 | 1476 | | 2.86 | 1.96 | 753 | | | 4864kWh above bal point |
| 9 | 4.34 | 42 | 2552 | 7.5 | 4410 | 2552 | | 2.72 | 2.12 | 1204 | | | 347kWdays/ht. season |
| 7 | 5.58 | 66 | 5156 | 7 | 6445 | 5156 | | 2.58 | 2.19 | 2354 | | | |
| 5 | 6.82 | 40 | 3819 | 6.5 | 3654 | 3654 | | 2.44 | 2.24 | 1498 | | 165 | 2883kWh below bal point |
| 3 | 8.06 | 20 | 2257 | 5.3 | 1470 | 1470 | | 2.06 | 2.06 | 714 | | 787 | 206kWdays/ht. season |
| 1 | 9.3 | 12 | 1562 | 4.7 | 794 | 794 | Full Load 6382 | 1.93 | 1.93 | 411 | Full Load 2883 | 769 | |
| -1 | 10.54 | 6 | 885 | 4.3 | 359 | 359 | | 1.81 | 1.81 | 198 | | 526 | 2472kWh Supp. Heat |
| -3 | 11.78 | 2 | 330 | 3.8 | 105 | 105 | | 1.68 | 1.68 | 63 | | 225 | 177kWdays/ht. season |
| | | Sum: 273 | Sum: 18914 | | | Sum, kWh: 16442 | | | | Sum, kWh: 7747 | | Sum: 2472 | |

TABLE 4

| 50% Heat Pump Capacity | | | | | | | | | | | | | |
|---|---|---|---|---|---|---|---|---|---|---|---|---|---|
| A | C | E | G | I | J | K | | M | N | P | | R | T |
| Ambient Temp. °C | Building Loss kW | Heating days/annum | Heat Req'd (14th day) kWh/annum | Heat Pump Capacity kW | Heat Pump Maximum Output kWh | Heat Pump Useful Output kWh | | COP Full Load | COP Part Load | Heat Pump Input | | Supp. Heat kWh | Heat Pump Energy Input 6097 kWh |
| 15 | 0.62 | 26 | 226 | 6.1 | 2202 | 226 | | 3.13 | 1.31 | 172 | | | 436kWdays/ht. season |
| 13 | 1.86 | 25 | 651 | 5.7 | 1995 | 651 | Part Load 4904 | 3 | 1.71 | 381 | Part Load 2510 | | |
| 11 | 3.1 | 34 | 1476 | 5.4 | 2547 | 1476 | | 2.86 | 1.96 | 753 | | | 2510kWh above bal point |
| 9 | 4.34 | 42 | 2552 | 5 | 2940 | 2552 | | 2.72 | 2.12 | 1204 | | | 179kWdays/ht. season |
| 7 | 5.58 | 66 | 5156 | 4.7 | 4297 | 4297 | | 2.58 | 2.19 | 1665 | | 859 | |
| 5 | 6.82 | 40 | 3819 | 4.4 | 2436 | 2436 | Full Load 8551 | 2.44 | 2.24 | 998 | Full Load 3588 | 1383 | 3588kWh below bal point |
| 3 | 8.06 | 20 | 2257 | 3.5 | 980 | 980 | | 2.06 | 2.06 | 476 | | 1277 | 256kWdays/ht. season |
| 1 | 9.3 | 12 | 1562 | 3.2 | 529 | 529 | | 1.93 | 1.93 | 274 | | 1033 | |
| -1 | 10.54 | 6 | 885 | 2.9 | 239 | 239 | | 1.81 | 1.81 | 132 | | 646 | 5458kWh Supp. Heat |
| -3 | 11.78 | 2 | 330 | 2.5 | 70 | 70 | | 1.68 | 1.68 | 42 | | 260 | 390kWdays/ht. season |
| | | Sum: 273 | Sum: 18914 | | | Sum, kWh: 13455 | | | | Sum, kWh: 6097 | | Sum: 5458 | |

TABLE 5

| 25% Heat Pump Capacity | | | | | | | | | | | | | |
|---|---|---|---|---|---|---|---|---|---|---|---|---|---|
| A | C | E | G | I | J | K | | M | N | P | | R | T |
| Ambient Temp. °C | Building Loss kW | Heating days/annum | Heat Req'd (14th day) kWh/annum | Heat Pump Capacity kW | Heat Pump Maximum Output kWh | Heat Pump Useful Output kWh | | COP Full Load | COP Part Load | Heat Pump Input | | Supp. Heat kWh | Heat Pump Energy Input 3332 kWh |
| 15 | 0.62 | 26 | 226 | 3 | 1101 | 226 | Part Load 877 | 3.13 | 1.31 | 172 | Part Load 553 | | 238kWdays/ht. season |
| 13 | 1.86 | 25 | 651 | 2.9 | 998 | 651 | | 3 | 1.71 | 381 | | | |
| 11 | 3.1 | 34 | 1476 | 2.7 | 1273 | 1273 | | 2.86 | 1.96 | 445 | | 202 | 553kWh above bal point |
| 9 | 4.34 | 42 | 2552 | 2.5 | 1470 | 1470 | | 2.72 | 2.12 | 540 | | 1082 | 40kWdays/ht. season |
| 7 | 5.58 | 66 | 5156 | 2.3 | 2148 | 2148 | Full Load 7019 | 2.58 | 2.19 | 833 | Full Load 2779 | 3008 | |
| 5 | 6.82 | 40 | 3819 | 2.2 | 1218 | 1218 | | 2.44 | 2.24 | 499 | | 2601 | 2779kWh below bal point |
| 3 | 8.06 | 20 | 2257 | 1.8 | 490 | 490 | | 2.06 | 2.06 | 238 | | 1767 | 199kWdays/ht. season |
| 1 | 9.3 | 12 | 1562 | 1.6 | 265 | 265 | | 1.93 | 1.93 | 137 | | 1298 | |
| -1 | 10.54 | 6 | 885 | 1.4 | 120 | 120 | | 1.81 | 1.81 | 66 | | 766 | 11018kWh Supp. Heat |
| -3 | 11.78 | 2 | 330 | 1.3 | 35 | 35 | | 1.68 | 1.68 | 21 | | 295 | 787kWdays/ht. season |
| | | Sum: 273 | Sum: 18914 | | | Sum, kWh: 7896 | | | | Sum, kWh: 3332 | | Sum: 11018 | |

TABLE 6

| Heat pump installation plus supplementary heating | | | | | |
|---|---|---|---|---|---|
| Heat pump performance | | | | | |
| Row | | | | | |
| A | Percentage heat pump capacity | 100 | 75 | 50 | 25 |
| B | Intermittent heat pump operation | | | | |
| C | Seasonal input kWh x $10^{-3}$ | 6.57 | 4.86 | 2.51 | 0.55 |
| D | Seasonal output kWh x $10^{-3}$ | 13.88 | 10.06 | 4.9 | 0.88 |
| E | Continuous heat pump operation | | | | |
| F | Seasonal input kWh x $10^{-3}$ | 1.85 | 2.88 | 3.59 | 2.78 |
| G | Seasonal output kWh x $10^{-3}$ | 3.64 | 6.38 | 8.55 | 7.02 |
| H | Total heat pump input | 8.42 | 7.74 | 6.1 | 3.33 |
| J | Total heat pump output | 17.52 | 16.44 | 13.45 | 7.9 |
| | Seasonal coefficient of performance | | | | |
| K | Intermittent heat pump operation | 2.11 | 2.07 | 1.95 | 1.6 |
| L | Continuous heat pump operation | 1.97 | 2.22 | 2.38 | 2.53 |
| M | Overall heat pump operation | 2.08 | 2.12 | 2.2 | 2.37 |
| N | Supplementary heat kWh x $10^{-3}$ | 1.4 | 2.47 | 5.46 | 11.02 |
| | Total seasonal energy heat pump plus supplementary | | | | |
| O | Input kWh x $10^{-3}$ | 9.82 | 10.21 | 11.56 | 14.35 |
| P | Output kWh x $10^{-3}$ | 18.91 | 18.91 | 18.91 | 18.91 |
| Q | Seasonal COP | 1.93 | 1.85 | 1.64 | 1.32 |

TABLE 7

SUMMARY OF RESULTS

APPENDIX A5.1

Compressor performance calculated at CECOMAF test conditions

Contents:

## COMPRESSOR PERFORMANCE CALCULATED AT CECOMAF TEST CONDITIONS

| Compressor swept volume: 0.000335m³/s | | | | | | |
|---|---|---|---|---|---|---|
| Condensing temperature: 35°C | | Pressure: 8.4596 bar (abs) | | | | |
| Row | Calculation number: | 1 | 2 | 3 | 4 | 5 |
| 1 | Evaporating temperature: °C | -13.1 | -6.8 | -1.5 | 7.5 | 15 |
| 2 | Pressure: bar (abs) | 1.961 | 2.452 | 2.942 | 3.923 | 4.903 |
| 3 | Superheat: K | 45.1 | 38.8 | 33.5 | 24.5 | 17 |
| 4 | Compressor pressure diff: bar | 6.499 | 6.008 | 5.518 | 4.537 | 3.557 |
| 5 | Compression ratio | 4.314 | 3.45 | 2.875 | 2.156 | 1.725 |
| 6 | Entropy: kJ/kg.K | 4.856 | 4.839 | 4.825 | 4.804 | 4.784 |
| 7 | Evaporator input: Watts | 350 | 480 | 590 | 810 | 1085 |
| 8 | Motor input: Watts | 170 | 180 | 190 | 195 | 200 |
| 9 | Output: Watts | 520 | 660 | 780 | 1005 | 1285 |
| 10 | Compressor suction enthalpy: kJ/kg | 594.66 | 594.11 | 593.49 | 592.36 | 591.11 |
| 11 | Evaporator input enthalpy: kJ/kg | 144.79 | 144.23 | 143.62 | 142.49 | 141.24 |
| 12 | Refrigerant mass flow: g/s | 2.417 | 3.328 | 4.108 | 5.685 | 7.682 |
| 13 | Compressor delivery: kJ/kg | 664.98 | 648.19 | 639.74 | 626.66 | 617.14 |
| 14 | Compressor isentropic delivery: kJ/kg | 626.3 | 620.14 | 612.75 | 608.17 | 601.57 |
| 15 | Specific volume: $m^3/kg$ | 0.1042 | 0.0818 | 0.0682 | 0.0504 | 0.0392 |
| 16 | Suction volume: $m^3/s \times 10^{-3}$ | 0.2519 | 0.2772 | 0.2802 | 0.2865 | 0.3011 |
| 17 | Volumetric Efficiency: % | 75.2 | 81.3 | 83.6 | 85.5 | 89.9 |
| 18 | Isentropic Efficiency: % | 45 | 48.1 | 41.6 | 46.1 | 40.2 |

| Summary of results | | | | | | |
|---|---|---|---|---|---|---|
| Heat output: | Watts | 520 | 660 | 780 | 1005 | 1285 |
| Coefficient of performance | | 3.06 | 3.67 | 4.11 | 5.15 | 6.43 |
| Refrigerant mass flow: | g/s | 2.417 | 3.328 | 4.108 | 5.685 | 7.682 |
| Volumetric efficiency: | % | 75.2 | 81.3 | 83.6 | 85.5 | 89.9 |
| Isentropic efficiency: | % | 45 | 48.1 | 41.6 | 46.1 | 40.2 |

Table 8

## COMPRESSOR PERFORMANCE CALCULATED AT CECOMAF TEST CONDITIONS

| Compressor swept volume: 0.000335$m^3/s$ | | | | | | |
|---|---|---|---|---|---|---|
| Condensing temperature: 45°C | | Pressure: 10.8099 bar (abs) | | | | |
| Row | Calculation number: | **6** | **7** | **8** | **9** | **10** |
| 1 | Evaporating temperature: °C | -13.1 | -6.8 | -1.5 | 7.5 | 15 |
| 2 | Pressure: bar (abs) | 1.961 | 2.452 | 2.942 | 3.923 | 4.903 |
| 3 | Superheat K | 45.1 | 38.8 | 33.5 | 24.5 | 17 |
| 4 | Compressor pressure diff: bar | 8.849 | 8.358 | 7.868 | 6.887 | 5.907 |
| 5 | Compression ratio | 5.512 | 4.409 | 3.674 | 2.756 | 2.205 |
| 6 | Entropy: kJ/kg.K | 4.856 | 4.839 | 4.825 | 4.804 | 4.786 |
| 7 | Evaporator input: Watts | 320 | 435 | 550 | 750 | 1000 |
| 8 | Motor input: Watts | 180 | 200 | 210 | 230 | 250 |
| 9 | Output: Watts | 500 | 635 | 760 | 980 | 1250 |
| 10 | Compressor suction enthalpy: kJ/kg | 594.66 | 594.11 | 593.49 | 592.36 | 591.11 |
| 11 | Evaporator input enthalpy: kJ/kg | 144.79 | 144.23 | 143.62 | 142.49 | 141.24 |
| 12 | Refrigerant mass flow: g/s | 2.21 | 3.016 | 3.829 | 5.263 | 7.08 |
| 13 | Compressor delivery: kJ/kg | 676.1 | 660.42 | 648.33 | 636.06 | 626.42 |
| 14 | Compressor isentropic delivery: kJ/kg | 626.3 | 624.28 | 620.35 | 613.17 | 606.57 |
| 15 | Specific volume: $m^3/kg$ | 0.1042 | 0.0818 | 0.0682 | 0.0504 | 0.0392 |
| 16 | Suction volume: $m^3/s \times 10^{-3}$ | 0.23 | 0.247 | 0.261 | 0.265 | 0.278 |
| 17 | Volumetric Efficiency: % | 68.7 | 73.6 | 78 | 79.2 | 82.8 |
| 18 | Isentropic Efficiency: % | 42.5 | 45.5 | 49 | 47.6 | 43.8 |

| Summary of results | | | | | | |
|---|---|---|---|---|---|---|
| Heat output: | Watts | 500 | 635 | 760 | 980 | 1250 |
| Coefficient of performance | | 2.78 | 3.18 | 3.62 | 4.26 | 5 |
| Refrigerant mass flow: | g/s | 2.21 | 3.016 | 3.829 | 5.263 | 7.08 |
| Volumetric efficiency: | % | 68.7 | 73.6 | 78 | 79.2 | 82.8 |
| Isentropic efficiency: | % | 42.5 | 45.5 | 49 | 47.6 | 43.8 |

Table 9

## COMPRESSOR PERFORMANCE CALCULATED AT CECOMAF TEST CONDITIONS

| Compressor swept volume: 0.000335$m^3/s$ | | | | | | |
|---|---|---|---|---|---|---|
| Condensing temperature: 55°C | | Pressure: 13.5999 bar (abs) | | | | |
| Row | Calculation number: | 11 | 12 | 13 | 14 | 15 |
| 1 | Evaporating temperature: °C | -13.1 | -6.8 | -1.5 | 7.5 | 15 |
| 2 | Pressure: bar (abs) | 1.961 | 2.452 | 2.942 | 3.923 | 4.903 |
| 3 | Superheat K | 45.1 | 38.8 | 33.5 | 24.5 | 17 |
| 4 | Compressor pressure diff: bar | 11.638 | 11.147 | 10.657 | 9.6769 | 8.6969 |
| 5 | Compression ratio | 6.935 | 5.546 | 4.622 | 3.466 | 2.774 |
| 6 | Entropy: kJ/kg.K | 4.856 | 4.839 | 4.825 | 4.804 | 4.786 |
| 7 | Evaporator input: Watts | 290 | 395 | 500 | 685 | 930 |
| 8 | Motor input: Watts | 190 | 220 | 240 | 260 | 290 |
| 9 | Output: Watts | 480 | 615 | 740 | 945 | 1220 |
| 10 | Compressor suction enthalpy: kJ/kg | 594.66 | 594.11 | 593.49 | 592.36 | 591.11 |
| 11 | Evaporator input enthalpy: kJ/kg | 144.79 | 144.23 | 143.62 | 142.49 | 141.24 |
| 12 | Refrigerant mass flow: g/s | 2.003 | 2.739 | 3.481 | 4.807 | 6.584 |
| 13 | Compressor delivery: kJ/kg | 689.52 | 674.43 | 662.43 | 646.44 | 635.15 |
| 14 | Compressor isentropic delivery: kJ/kg | 640.36 | 631 | 627.22 | 617.76 | 610.83 |
| 15 | Specific volume: $m^3/kg$ | 0.1042 | 0.0818 | 0.0682 | 0.0504 | 0.0392 |
| 16 | Suction volume: $m^3/s \times 10^{-3}$ | 0.2087 | 0.224 | 0.2374 | 0.2422 | 0.2581 |
| 17 | Volumetric Efficiency: % | 62.3 | 66.9 | 70.9 | 72.3 | 77 |
| 18 | Isentropic Efficiency: % | 48.2 | 45.9 | 48.9 | 47 | 44.8 |

| Summary of results | | | | | | |
|---|---|---|---|---|---|---|
| Heat output: | Watts | 480 | 615 | 740 | 945 | 1220 |
| Coefficient of performance | | 2.53 | 2.8 | 3.08 | 3.63 | 4.21 |
| Refrigerant mass flow: | g/s | 2.003 | 2.739 | 3.481 | 4.807 | 6.584 |
| Volumetric efficiency: | % | 62.3 | 66.9 | 70.9 | 72.3 | 77 |
| Isentropic efficiency: | % | 48.2 | 45.9 | 48.9 | 47 | 44.8 |

Table 10

## COMPRESSOR PERFORMANCE CALCULATED FROM CECOMAF DATA.

### Typical Calculation from Table 8 - Calculation number 1

The details below was included as typical Calculation of Tables 8, 9 &10.

| | | |
|---|---|---|
| 1 | Evaporating temperature | = -13.1°C |
| 2 | Evaporating pressure | = 1.961 bar (abs) |
| 3 | Compressor suction - superheat | = 45.1°C |
| 4 | Compression differential | = Condenser pressure - {2}<br>= 8.4596 - 1.961<br>= 6.499 bar (abs) |
| 5 | Compression ratio | = Condenser pressure / {2}<br>= 8.4596 / 1.961<br>= 4.314 bar (abs) |
| 6 | Entropy - compressor suction | = 4.856 kJ/kg.K |
| 7 | Evaporator input | = 350 W |
| 8 | Motor electrical input | = 170 W |
| 9 | Thermal output | = 520 W |
| 10 | Enthalpy - compressor suction | = 594.66 kJ/kg |
| 11 | Evaporator - enthalpy gain<br>Where R = 449.87 kJ/kg, the liquid return specific enthalpy to the evaporator | = {10} - R<br><br>= 594.66 - 449.87<br>= 144.79 kJ/kg |
| 12 | Refrigerant mass flow | = {7}J/s / {11}kJ/kg<br>= 350 / 144.79<br>= 2.417 g/s |
| 13 | Compressor discharge - specific enthalpy | = ({11} x {8} / {7}) + {10}<br>= (144.79 x 170 / 350) + 594.66<br>= 664.98 kJ/kg |
| 14 | Compressor delivery - isothermal compression | = 626.3 kJ/kg |
| 15 | Specific volume - compressor suction | = 0.1042 $m^3$/kg |
| 16 | Compressor suction volume | = {12} g/s x {15} $m^3$/kg<br>= (2.417 x 0.1042) / 1000<br>= 0.0002519 $m^3$/s |
| 17 | Volumetric efficiency | = {16} / Compressor swept volume<br>= (0.0002519 / 0.000335) x 100<br>= 75.2 % |
| 18 | Isentropic efficiency | = ({14} - {10}) x 100 / ({13} - {10})<br>= (626.3 - 594.66) x 100 / 664.98 - 594.66<br>= 45 % |

Table 11

APPENDIX A5.2 — Change of state
Manufacturer's calculation procedure

Conversion of heat putput

We would point out that the heat putput for a compressor is measured on a calorimeter at the stated gas and liquid temperatures.
The heat output is arrived at by adding the refrigeration capacity to the motor input.

If conversion to other states is required, this can be done by using the formula:

$$G = \frac{Q}{q_o}(kg/h)$$

where, Q is the refrigeration capacity read off from the calorimeter wattmeter, $q_o$ is the difference in the heat contents between the gas state $I_4$ and the liquid state $I_2$.

The refrigerant capacity Q can now be determined at another liquid or gas state using the formula:

$$\frac{Q_{measured}}{i_4 - i_2} = \frac{Q_{sought}}{i_3 - i_1} \qquad \text{or}$$

$$Q_{sought} = Q_{measured} \times \frac{i_3 - i_1}{i_4 - i_2}(Watts)$$

This change in state takes place outside the compressor and thus has no influence on the quantity of refrigerant circulated.
The heat contents are read off from a vapour table for the refrigerant in question.

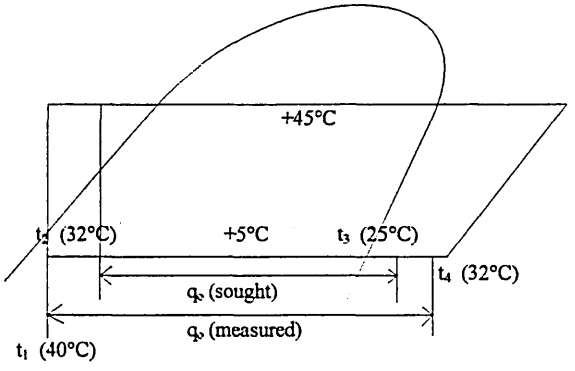


Example: What is the heat output for an SC10H compressor at +5°C evaporating temperature, 45°C liquid temperature and 25°C suction gas temperature?
For the SC10H compressor, the heat output is read off on page 7 as 1300 Watts and the energy consumption as 325 Watts at +5°C evaporating temperature and 45°C condensing temperature.
Thus, the refrigerant capacity constitutes:
1300 - 325 + 975 Watts

From a vapour table for refrigerant R12, the following heat content is read off at +5°C evaporating temperature:
$i_4$ = gas superheated to 32°C = 141.56 kcal/kg
$i_2$ = liquid sub-cooled to 32°C = 107.47 kcal/kg
$i_3$ = gas superheated to 25°C = 140.50 kcal/kg
$i_1$ = liquid sub-cooled to 40°C = 109.42 kcal/kg

$$Q_{sought} = 975 \times \frac{140.50 - 109.42}{141.56 - 107.47} = 889 Watts$$

Heat output = 889 + 325 = 1214 Watts

APPENDIX A5.3

Compressor and heat pump performance

Contents:

## COMPRESSOR AND HEAT PUMP PERFORMANCE

Compatibility between the manufacturer's CECOMAF calculations and those based on refrigerant mass flow.

For all calculations - compressor superheat 5K at shell inlet.

Specific enthalpy at evaporator inlet = 449.87 kJ/kg

| | Calculation number: | | 1 | 2 | 3 | 4 | 5 |
|---|---|---|---|---|---|---|---|
| Evaporator | | | | | | | |
| 1 | Pressure: | bar (abs) | 1.961 | 2.452 | 2.942 | 3.923 | 4.903 |
| 2 | Saturated temperature: | °C | -13.1 | -6.8 | -1.5 | 7.5 | 15 |
| 3 | Saturated temperature: | K | 260.05 | 266.35 | 271.65 | 280.65 | 288.15 |
| 4 | Compressor suction: | K | 265.05 | 271.35 | 276.65 | 285.65 | 293.15 |
| Condenser | | | | | | | |
| 5 | Pressure: | bar (abs) | 8.4596 | 8.4596 | 8.4596 | 8.4596 | 8.4596 |
| 6 | Saturated temperature: | °C | 35 | 35 | 35 | 35 | 35 |
| 7 | Compression ratio | | 4.314 | 3.45 | 2.875 | 2.156 | 1.725 |
| Calculation conforming to manufacturer's proposed procedure | | | | | | | |
| 8 | Enthalpy measured: | kJ/kg | 144.79 | 144.23 | 143.62 | 142.49 | 141.24 |
| 9 | Enthalpy sought: | kJ/kg | 120.46 | 123.47 | 126 | 130.19 | 133.6 |
| 10 | Evaporator heat gain: | W | 291 | 411 | 518 | 740 | 1026 |
| 11 | Heat output: | W | 461 | 591 | 708 | 935 | 1226 |
| 12 | Refrigerant mass flow: | g/s | 2.417 | 3.328 | 4.108 | 5.685 | 7.682 |
| 12a | Volumetric efficiency | | 63.9 | 71.3 | 74.3 | 78.9 | 86.5 |
| Calculation based on compressor volumetric efficiency | | | | | | | |
| 13 | Suction volume: | $m^3 \times 10^{-3}/s$ | 0.252 | 0.273 | 0.278 | 0.286 | 0.295 |
| 14 | Suction temperature: | K | 265.05 | 271.35 | 276.65 | 285.65 | 293.15 |
| 15 | Specific volume: | $m^3/kg$ | 0.0886 | 0.0718 | 0.0606 | 0.0465 | 0.0377 |
| 16 | Mass flow: | g/s | 2.843 | 3.806 | 4.582 | 6.158 | 7.827 |
| 17 | Enthalpy compressor suction: | kJ/kg | 570.33 | 573.34 | 575.87 | 580.06 | 583.47 |
| 18 | Evaporator enthalpy gain: | kJ/kg | 120.46 | 123.47 | 126 | 130.19 | 133.6 |
| 19 | Evaporator heat gain: | W | 342.5 | 470 | 577.3 | 801.8 | 1045.7 |
| Summary of results - based on compressor volumetric efficiency | | | | | | | |
| 20 | Heat output: | W | 512 | 650 | 767 | 997 | 1246 |
| 21 | Coefficient of performance | | 3.01 | 3.61 | 4.04 | 5.11 | 6.23 |
| 22 | Refrigerant mass flow: | g/s | 2.843 | 3.806 | 4.582 | 6.158 | 7.827 |
| 23 | Volumetric efficiency: | % | 75.2 | 81.3 | 83.6 | 85.5 | 89.9 |

Table 12

## COMPRESSOR AND HEAT PUMP PERFORMANCE

Compatibility between the manufacturer's CECOMAF calculations and those based on refrigerant mass flow.

For all calculations - compressor superheat 5K at shell inlet.

Specific enthalpy at evaporator inlet = 449.87 kJ/kg

| | Calculation number: | | 6 | 7 | 8 | 9 | 10 |
|---|---|---|---|---|---|---|---|
| Evaporator | | | | | | | |
| 1 | Pressure: | bar (abs) | 1.961 | 2.452 | 2.942 | 3.923 | 4.903 |
| 2 | Saturated temperature: | °C | -13.1 | -6.8 | -1.5 | 7.5 | 15 |
| 3 | Saturated temperature: | K | 260.05 | 266.35 | 271.65 | 280.65 | 288.15 |
| 4 | Compressor suction: | K | 265.05 | 271.35 | 276.65 | 285.65 | 293.15 |
| Condenser | | | | | | | |
| 5 | Pressure: | bar (abs) | 10.81 | 10.81 | 10.81 | 10.81 | 10.81 |
| 6 | Saturated temperature: | °C | 45 | 45 | 45 | 45 | 45 |
| 7 | Compression ratio | | 5.512 | 4.409 | 3.674 | 2.756 | 2.205 |
| Calculation conforming to manufacturer's proposed procedure | | | | | | | |
| 8 | Enthalpy measured: | kJ/kg | 144.79 | 144.23 | 143.62 | 142.49 | 141.24 |
| 9 | Enthalpy sought: | kJ/kg | 120.46 | 123.47 | 126 | 130.19 | 133.6 |
| 10 | Evaporator heat gain: | W | 266 | 372 | 483 | 658 | 946 |
| 11 | Heat output: | W | 446 | 572 | 693 | 888 | 1196 |
| 12 | Refrigerant mass flow: | g/s | 2.21 | 3.016 | 3.83 | 5.264 | 7.08 |
| 12a | Volumetric efficiency | | 58.5 | 64.6 | 69.3 | 73.1 | 79.7 |
| Calculation based on compressor volumetric efficiency | | | | | | | |
| 13 | Suction volume: | $m^3 \times 10^{-3}/s$ | 0.248 | 0.252 | 0.257 | 0.265 | 0.274 |
| 14 | Suction temperature: | K | 265.05 | 271.35 | 276.65 | 285.65 | 293.15 |
| 15 | Specific volume: | $m^3/kg$ | 0.0886 | 0.0718 | 0.0606 | 0.0465 | 0.0377 |
| 16 | Mass flow: | g/s | 2.7995 | 3.5153 | 4.2369 | 5.7091 | 7.2729 |
| 17 | Enthalpy compressor suction: | kJ/kg | 570.33 | 573.34 | 575.87 | 580.06 | 583.47 |
| 18 | Evaporator enthalpy gain: | kJ/kg | 120.46 | 123.47 | 126 | 130.19 | 133.6 |
| 19 | Evaporator heat gain: | W | 337.2 | 434 | 533.8 | 743.3 | 971.7 |
| Summary of results - based on compressor volumetric efficiency | | | | | | | |
| 20 | Heat output: | W | 507 | 614 | 724 | 919 | 1172 |
| 21 | Coefficient of performance | | 2.82 | 3.07 | 3.45 | 3.99 | 4.69 |
| 22 | Refrigerant mass flow: | g/s | 2.799 | 3.515 | 4.237 | 5.709 | 7.273 |
| 23 | Volumetric efficiency: | % | 68.7 | 73.6 | 78 | 79.2 | 82.8 |

Table 13

## COMPRESSOR AND HEAT PUMP PERFORMANCE

Compatibility between the manufacturer's CECOMAF calculations and those based on refrigerant mass flow.

For all calculations - compressor superheat 5K at shell inlet.

Specific enthalpy at evaporator inlet = 449.87 kJ/kg

| | Calculation number: | | 11 | 12 | 13 | 14 | 15 |
|---|---|---|---|---|---|---|---|
| Evaporator | | | | | | | |
| 1 | Pressure: | bar (abs) | 1.961 | 2.452 | 2.942 | 3.923 | 4.903 |
| 2 | Saturated temperature: | °C | -13.1 | -6.8 | -1.5 | 7.5 | 15 |
| 3 | Saturated temperature: | K | 260.05 | 266.35 | 271.65 | 280.65 | 288.15 |
| 4 | Compressor suction: | K | 265.05 | 271.35 | 276.65 | 285.65 | 293.15 |
| Condenser | | | | | | | |
| 5 | Pressure: | bar (abs) | 13.56 | 13.56 | 13.56 | 13.56 | 13.56 |
| 6 | Saturated temperature: | °C | 55 | 55 | 55 | 55 | 55 |
| 7 | Compression ratio | | 6.915 | 5.53 | 4.609 | 3.457 | 2.766 |
| Calculation conforming to manufacturer's proposed procedure | | | | | | | |
| 8 | Enthalpy measured: | kJ/kg | 144.79 | 144.23 | 143.62 | 142.49 | 141.24 |
| 9 | Enthalpy sought: | kJ/kg | 120.46 | 123.47 | 126 | 130.19 | 133.6 |
| 10 | Evaporator heat gain: | W | 241 | 338 | 439 | 626 | 880 |
| 11 | Heat output: | W | 431 | 558 | 679 | 886 | 1170 |
| 12 | Refrigerant mass flow: | g/s | 2.003 | 2.739 | 3.481 | 4.807 | 6.585 |
| 12a | Volumetric efficiency | | 53 | 58.7 | 63 | 66.7 | 74.1 |
| Calculation based on compressor volumetric efficiency | | | | | | | |
| 13 | Suction volume: | $m^3 \times 10^{-3}/s$ | 0.224 | 0.228 | 0.232 | 0.241 | 0.25 |
| 14 | Suction temperature: | K | 265.05 | 271.35 | 276.65 | 285.65 | 293.15 |
| 15 | Specific volume: | $m^3/kg$ | 0.0886 | 0.0718 | 0.0606 | 0.0465 | 0.0377 |
| 16 | Mass flow: | g/s | 2.5235 | 3.1748 | 3.8334 | 5.1834 | 6.6244 |
| 17 | Enthalpy compressor suction: | kJ/kg | 570.33 | 573.34 | 575.87 | 580.06 | 583.47 |
| 18 | Evaporator enthalpy gain: | kJ/kg | 120.46 | 123.47 | 126 | 130.19 | 133.6 |
| 19 | Evaporator heat gain: | W | 304 | 392 | 483 | 674.8 | 885 |
| Summary of results - based on compressor volumetric efficiency | | | | | | | |
| 20 | Heat output: | W | 494 | 612 | 723 | 935 | 1175 |
| 21 | Coefficient of performance | | 2.6 | 2.78 | 3.01 | 3.6 | 4.05 |
| 22 | Refrigerant mass flow: | g/s | 2.524 | 3.175 | 3.833 | 5.183 | 6.624 |
| 23 | Volumetric efficiency: | % | 62.3 | 66.9 | 70.9 | 72.3 | 77 |

Table 14

## CALCULATED PERFORMANCE - BASED ON COMPRESSOR SUCTION OF 5K SUPERHEAT

Typical Calculation from Table 12 - Calculation number 1

The Calculation below was included as typical Calculations of Tables 12,13 &14

| | | |
|---|---|---|
| Evaporator | | |
| 1 | Operating pressure | = 1.961 bar |
| 2 | Saturation temperature | = -13.1°C |
| 3 | Saturation temperature (abs) | = 260.05K |
| 4 | Compressor suction temperature (abs) | = 265.05K |
| Condenser | | |
| 5 | Operating pressure | = 8.4596 bar (abs) |
| 6 | Saturation temperature | = 35°C |
| Compressor | | |
| 7 | Compression ratio | = [5] / [1]<br>= 8.4596 / 1.961<br>= 4.314 bar |
| Calculation conforming to manufacturer's proposed procedure | | |
| 8 | Enthalpy gain measured<br>$(i^4 - i^2)$ | = {10} - 449.87 kJ/kg<br>= 594.66 - 449.87<br>= 144.79 kJ/kg |
| 9 | Enthalpy sought by user<br>Where E = specific enthalpy at 265.05K and 1.961 bar (abs) | = [E] - 449.87<br><br>= 570.33 - 449.87<br>= 120.46 kJ/kg |
| 10 | Refrigeration capacity | = ( [9] / [8] ) x {7}<br>= (120.46 / 144.79) x 350<br>= 291.19 W |
| 11 | Heat output | = [10] + {8}<br>= 291.19 + 170<br>= 461 W |
| 12 | Refrigerant mass flow | = [10] / [9]<br>= 291.19 / 120.46<br>= 2.417 g/s |
| 12a | Volumetric efficiency | = Suction volume / Swept volume<br>= ( [12] x [15] ) / (0.000335 x 10)<br>= (2.417 x 0.0886) / (0.00335)<br>= 63.9 % |

Continued on next page

| Calculation based on compressor volumetric efficiency | | |
|---|---|---|
| 13 | Compressor suction volume {16} | = 0.2519 x $10^{-3}$ $m^3/s$ |
| 14 | Compressor suction temperature [4] | = 265.05K |
| 15 | Compressor suction - specific volume (Value obtained from thermodynamic property data tables) | = 0.0886 $m^3/kg$ |
| 16 | Refrigerant mass flow | = [13] / [15]<br>= 0.0002519 / 0.0886<br>= 2.843 x $10^{-3}$ kg/s<br>= 2.843 g/s |
| 17 | Compressor suction - specific enthalpy (Value obtained from thermodynamic property data tables)<br>{1} pressure 1.961 bar (abs)<br>Temperature 5K superheat {4}<br>265.05K | = 570.33 kJ/kg |
| 18 | Evaporator enthalpy gain<br>(Specific enthalpy at inlet to the compressor shell minus the value at the inlet to the evaporator) | = 570.33 - 449.87<br>= 120.46 kJ/kg |
| 19 | Refrigeration heat gain through the evaporator<br>(Equal to the refrigerant enthalpy gain through the evaporator [kJ/kg] multiplied by the refrigerant mass flow [g/s] ) | = [18] x [16]<br>= 120.46 x 2.843<br>= 342.5 J/s<br>= 342.5 W |
| Summary of results - based on compressor volumetric efficiency | | |
| 20 | Heat pump - thermal output<br>(energy loss by heat emission from the compressor shell not deducted) | = [19] + [8]<br>= 342.5 + 170<br>= 512 W |
| 21 | Coefficient of performance | = [20] / [8]<br>= 512 / 170<br>= 3.02 |
| 22 | Refrigerant mass flow [16] | = 2.843 g/s |
| 23 | Volumetric efficiency of compressor<br>Where S = swept volume of compressor ($m^3/s$) | = ( [13] / S) x 100<br>= (0.0002519 / 0.000335) x 100<br>= 75.2 % |

Table 15

APPENDIX A6.1

Hermetic Compressor SC15GH using R134(a)

The calculations below were conducted utilising the Manufacturer's CECOMAF test results.
From these, the design data for other operating conditions was obtained.

| Row no. | Temperatures and Pressures | | | | | | |
|---|---|---|---|---|---|---|---|
| 7 | -15 | -10 | -5 | 0 | 5 | 10 | 15 |
| 8 | 47 | 42 | 37 | 32 | 27 | 22 | 17 |
| 9 | 258.15 | 263.15 | 268.15 | 273.15 | 278.15 | 283.15 | 288.15 |
| 10 | 1.639 | 2.005 | 2.432 | 2.925 | 3.492 | 4.139 | 4.873 |
| | Energy Input and Output - Thermodynamic Cycle | | | | | | |
| 13 | 0.435 | 0.570 | 0.730 | 0.900 | 1.140 | 1.420 | 1.730 |
| 14 | 0.368 | 0.420 | 0.472 | 0.523 | 0.575 | 0.627 | 0.678 |
| 15 | 0.803 | 0.990 | 1.202 | 1.423 | 1.715 | 2.047 | 2.408 |
| | COP Heating | | | | | | |
| 18 | 2.18 | 2.36 | 2.55 | 2.72 | 2.98 | 3.26 | 3.55 |
| | Specific Enthalpy Gain - Evaporator | | | | | | |
| 21 | 330.01 | 329.21 | 328.22 | 327.07 | 325.72 | 324.13 | 322.26 |
| 22 | 178.13 | 178.13 | 178.13 | 178.13 | 178.13 | 178.13 | 178.13 |
| 23 | 151.88 | 151.08 | 150.09 | 148.94 | 147.59 | 146.00 | 144.13 |
| | Refrigerant Mass Flow - kg/min | | | | | | |
| 26 | 0.17185 | 0.22637 | 0.29182 | 0.36256 | 0.46345 | 0.58356 | 0.72018 |
| 27 | 0.16098 | 0.21206 | 0.27337 | 0.33964 | 0.43414 | 0.54666 | 0.67464 |
| 28 | 0.14700 | 0.11920 | 0.09740 | 0.08010 | 0.06620 | 0.05500 | 0.04590 |
| | Compressor Suction Volume - $m^3$/min | | | | | | |
| 29 | 0.02526 | 0.02698 | 0.02842 | 0.02904 | 0.03068 | 0.03210 | 0.03306 |
| | Volumetric Efficiency and Compression Ratio | | | | | | |
| 32 | 56.93 | 60.81 | 64.06 | 65.45 | 69.15 | 72.34 | 74.50 |
| 33 | 9.05 | 7.40 | 6.10 | 5.07 | 4.25 | 3.59 | 3.05 |

Typical Calculation - calculation number one

| Row no. | | Calculations column |
|---|---|---|
| 7 | Evaporating temperature | -15°C |
| 8 | Superheat - compressor suction | 32 - (-15) = 47 K |
| 9 | Evaporating temperature (abs) | 258.15 K |
| 10 | Evaporator pressure | 1.639 bar (abs) |
| 13 | Capacity - (evaporator input) | 0.435 kW |
| 14 | Compressor power | 0.368 kW |
| 15 | Heat pump output | (13) + (14) = 0.803 kW |
| 18 | COP heating | (15) / (14) = 2.18 |
| 21 | Enthalpy - compressor suction | 330.01 kJ/kg |
| 22 | Enthalpy - entering evaporator | 178.13 kJ/kg |
| 23 | Specific enthalpy - evaporator | (21) - (22) = 151.88 kJ/kg |
| 26 | Refrigerant mass flow | [(13) / (23)] x 60 = 0.17185 kg/min |
| 27 | Liquid flow condenser outlet | (26) / 1.0675 = 0.16098 l/min |
| | where 1.0675 = refrigerant density kg/l | |
| 28 | Specific volume - compressor suction | 0.14700 $m^3$/kg |
| 29 | Compressor suction volume | (26) x (28) = 0.02526 l/min |
| 32 | Compressor - volumetric efficiency | [(29) / 0.04437] x 100 = 56.93% |
| | where 0.04437 $m^3$/min = displacement volume x RPM | |
| 33 | Compression ratio | 14.84 / (10) = 9.05 |
| | where 14.84 bar (abs) = condensing pressure | |

APPENDIX A6.2

Hermetic Compressor SC15GH using R134(a)

Calculation of refrigerant liquid flow - condenser discharge.
Refrigerant flow meter sizing.
These calculations are based on 5K superheat at the compressor suction.

| Row 1 | -15 | -10 | -5 | 0 | 5 | 10 | 15 |
|---|---|---|---|---|---|---|---|
| Compressor suction volume - $m^3/kg$ | | | | | | | |
| 2 | 0.02526 | 0.02698 | 0.02842 | 0.02904 | 0.03068 | 0.03210 | 0.03306 |
| 3 | 0.121192 | 0.10063 | 0.08376 | 0.07022 | 0.05932 | 0.05028 | 0.04291 |
| Refrigerant mass flow - kg/min | | | | | | | |
| 4 | 0.20720 | 0.26814 | 0.33935 | 0.41357 | 0.51720 | 0.63834 | 0.77037 |
| 5 | 1.0675 | 1.0675 | 1.0675 | 1.0675 | 1.0675 | 1.0675 | 1.0675 |
| Liquid refrigerant flow - l/min | | | | | | | |
| 6 | 0.1941 | 0.2512 | 0.3179 | 0.3874 | 0.4845 | 0.5980 | 0.7217 |
| Compression ratio | | | | | | | |
| 7 | 9.05 | 7.4 | 6.1 | 5.07 | 4.25 | 3.59 | 3.05 |

Alternative calculation with update of thermodynamic property data.
Rows 5 and 6 are recalculated in rows 5(a) and 6(a) below:

| | | | | | | | |
|---|---|---|---|---|---|---|---|
| 5(a) | 1.0788 | 1.0788 | 1.0788 | 1.0788 | 1.0788 | 1.0788 | 1.0788 |
| 6(a) | 0.1921 | 0.2486 | 0.3146 | 0.3834 | 0.4794 | 0.5917 | 0.7141 |

Typical calculation - calculation number one

| Row no. | Nomenclature | Calculation |
|---|---|---|
| 1 | Evaporating temperature | -15°C |
| 2 | Compressor suction volume (data taken from appendix 8, row 29) | 0.02526 $m^3$/min |
| 3 | Specific volume - compressor suction | 0.12192 $m^3/kg$ |
| 4 | Refrigerant mass flow | (2) $m^3$/min / (3) $m^3/kg$ = 0.20720 kg/min |
| 5 | Specific density - condenser discharge | 1.0675 kg/l |
| 6 | Liquid flow - condenser discharge | (4) / (5) = 0.19410 l/min |
| 7 | Compression ratio (data taken from appendix 9, row 33) | 9.05 |

APPENDIX A6.3

Hermetic compressor SC15GH using R134(a)

Calculations of refrigerant mass flow and heat output
based on 5K superheat at the compressor suction.

For all tests listed below, the condensing temperature iss 55°C and the pressure is 14.837 bar (abs). The refrigerant discharge from the caondenser is at a temperature of 328.15 K and the enthalpy is 179.13 kJ/kg.

| 1 | -15 | -10 | -5 | 0 | 5 | 10 | 15 |
|---|---|---|---|---|---|---|---|
| 2 | 1.639 | 2.005 | 2.432 | 2.925 | 3.492 | 4.139 | 4.873 |
| 3 | 263.15 | 268.15 | 273.15 | 278.15 | 283.15 | 288.15 | 293.15 |
| 4 | 293.36 | 296.49 | 299.56 | 302.61 | 305.62 | 308.58 | 311.48 |
| 5 | 114.23 | 117.36 | 120.43 | 123.48 | 126.49 | 129.45 | 132.35 |
| 6 | 0.2072 | 0.2681 | 0.3394 | 0.4136 | 0.5172 | 0.6383 | 0.7704 |
| 7 | 394 | 524 | 681 | 851 | 1090 | 1377 | 1699 |
| 8 | 368 | 420 | 472 | 523 | 575 | 627 | 678 |
| 9 | 762 | 944 | 1153 | 1374 | 1665 | 2004 | 2377 |
| 10 | 2.07 | 2.25 | 2.44 | 2.63 | 2.90 | 3.20 | 3.51 |
| 11 | 9.05 | 7.40 | 6.10 | 5.07 | 4.25 | 3.59 | 3.05 |

Typical calculation - calculation number one

Calculation based on 5K superheat at compressor suction.

| Row no. | Nomenclature | Calculation |
|---|---|---|
| 1 | Evaporating temperature | -15°C |
| 2 | Evaporator pressure | 1.639 bar (abs) |
| 3 | Compressor suction temperature | 263.36 K |
| 4 | Enthalpy compressor suction | 293.36 kJ/kg |
| 5 | Specific enthalpy gain - evaporator | (4) - 179.13 kJ/kg<br>= 114.23 kJ/kg |
| 6 | Refrigerant mass flow | 0.2072 l/min |
| 7 | Capacity - input to evaporator | (5) x (6) x 1000 / 60<br>= 114.23 x 0.2072 x 16.66<br>= 394 Watts |
| 8 | Compressor power consumption | 368 Watts |
| 9 | Heat pump output | (7) + (8)<br>= 394 + 368<br>+ 762 Watts |
| 10 | Coefficient of Performance (heating) | (9) / (8)<br>= 2.07 |
| 11 | Compression ratio | 14.837 / (2)<br>= 14.837 / 1.639<br>= 9.05 |

APPENDIX A6.4

## Refrigerant Flow Meter
## Series 250 Rotameter - variable flow meter - metal tube

Calculation of variant mass flow caused by the changing refrigerant density. Variations calculated are those due to changing refrigerant temperature and pressure. These are based on the publications and recommendations of the Meggitt Controls.
Calibration of refrigerant flow with varying liquid densities of condenser discharge.

$$F_2 = \frac{F_1}{\sqrt{(\sigma - \rho_1)\rho_2 / (\sigma - \rho_2)\rho_1}}$$

Where:

| | | |
|---|---|---|
| $F_1$ | = | volumetric flow - manufacturer's calibration |
| $F_2$ | = | volumetric flow - operating conditions |
| $\sigma$ | = | mean density of float |
| $\rho_1$ | = | fluid density - calibrated conditions |
| $\rho_2$ | = | fluid density - operating conditions |

Calibrated refrigerant liquid flow, $F_1$ = 0.16 l/min
Density of stainless steel alloy float = 7.96 g/cm$^3$
Calibrated density of refrigerant = 1.0675 l/min

Calculation of refrigerant liquid flow volume when 0.16 l/min is indicated by flowmeter.

| Condensing pressure | Saturation temp. | Refrigerant flow volume | Refrigerant mass flow |
|---|---|---|---|
| 5 bar (abs) | 15.80 °C | 0.147 l/min | 0.182 kg/min |
| 6 bar (abs) | 21.66 °C | 0.148 l/min | 0.180 kg/min |
| 7 bar (abs) | 26.82 °C | 0.150 l/min | 0.178 kg/min |
| 8 bar (abs) | 31.72 °C | 0.151 l/min | 0.178 kg/min |
| 9 bar (abs) | 35.67 °C | 0.152 l/min | 0.178 kg/min |
| 10 bar (abs) | 39.55 °C | 0.153 l/min | 0.176 kg/min |

The flow capacity of 0.16 l/min and the calibrated density of 1.0675 kg/l were adopted for the following calculations. The operating range of the flowmeter was 0.16 l/min to 1.6 l/min.

Nomenclature:
(1) Condenser - saturated liquid pressure - bar (abs)
(2) Condenser - condensing temperature - °C
(3) Condenser - operating liquid density - kg/l
(4) X - dimensionless constant
= [(7.96 - 1.0675) x D] / [(7.96 - D) x 1.0675]
= (6.8925 x D) / (8.4973 - 1.1396 x D)
where: D = refrigerant density - operating conditions - item 3 above
(5) Operating flow volume - Indicated flow volume / $X^{0.5}$ l/min
(6) R.M.F. - Refrigerant mass flow
= (3) x (5)

| Calculation number | 1 | 2 | 3 | 4 | 5 | 6 |
|---|---|---|---|---|---|---|
| (1) Pressure | 5 | 6 | 7 | 8 | 9 | 10 |
| (2) Temperature | 15.80 | 21.66 | 26.82 | 31.72 | 35.67 | 39.55 |
| (3) Density | 1.2407 | 1.2195 | 1.2001 | 1.1810 | 1.1651 | 1.1490 |
| (4) X | 1.1922 | 1.1681 | 1.1463 | 1.1248 | 1.1071 | 1.0892 |
| (5) Actual flow volume when indicated flow volume = 0.16 l/min | 0.147 | 0.148 | 0.149 | 0.151 | 0.152 | 0.153 |
| (6) R.M.F. (kg/min) | 0.182 | 0.181 | 0.179 | 0.178 | 0.177 | 0.176 |

To check the shortened equation for values of 'X', the densities 'D' for F = 0.16 l/min were inserted into the equation. The confirming value of X = 1 was obtained:

$$X = (6.8925 \times D) / (8.4973 - 1.1396 \times D)$$
$$= (6.9825 \times 1.0675) / ([(8.4973 - 1.1396) \times 1.0665]$$
$$= 7.3577 / (8.4973 - 1.1396)$$
$$= 1$$

$$F = 0.16 / 1 = 0.16 \text{ l/min}$$

| Indicated flow | Refrigerant relative density | | | | | |
|---|---|---|---|---|---|---|
| volume | 1.2407 | 1.2195 | 1.2001 | 1.1810 | 1.1651 | 1.1490 |

| Refrigerant flow volume l/min | | | | | | |
|---|---|---|---|---|---|---|
| 0.16 | 0.147 | 0.148 | 0.149 | 0.151 | 0.152 | 0.153 |
| 0.4 | 0.366 | 0.370 | 0.374 | 0.377 | 0.380 | 0.383 |
| 0.7 | 0.641 | 0.648 | 0.654 | 0.660 | 0.665 | 0.671 |
| 1.0 | 0.916 | 0.925 | 0.934 | 0.943 | 0.950 | 0.958 |
| 1.3 | 1.191 | 1.203 | 1.214 | 1.226 | 1.236 | 1.246 |
| 1.6 | 1.465 | 1.480 | 1.494 | 1.509 | 1.521 | 1.533 |

APPENDIX A6.5

## Heat pump test rig - performance calculations
## Summary of column headings

Following the laboratory trials using the R134(a) test rig, the calculations in this appendix were made to analyse the heat pump test rig performance. These calculations were made on the assumption that the condenser was fully condensing all of the refrigerant in circulation. Whilst the test rig was in operation, it was noted that the meter indicating the refrigerant mass flow and heat output was far lower than expected.

The details of the data in each column of the calculation are listed below.

| Column | Temperature units | Description |
|---|---|---|
| B | °C | Water output from the condenser |
| C | °C | Water input to the condenser |
| E | °C | Refrigerant - condenser discharge |
| F | K | Refrigerant - condenser discharge (absolute) |
| K | °C | Evaporator - refrigerant input temperature |
| L | K | Evaporator - refrigerant input temperature (absolute) |
| O | °C | Refrigerant input to compressor shell |
| P | °C | Refrigerant input to compressor cylinders |
| S | K | Refrigerant superheat entering compressor shell |
| W | K | Refrigerant superheat entering compressor cylinders |
| AB | °C | Compressor discharge |
| AC | K | Compressor discharge (absolute) |
| AF | K | Condenser - saturated vapour |
| AG | K | Superheat at compressor discharge |
| AN | K | Sub-cooling of condenser discharge |
| BR | °C | Air - dry bulb |
| BS | °C | Air - wet bulb |

| Column | Pressure units | Decription |
|---|---|---|
| AD | bar (abs) | Compressor suction |
| AE | bar (abs) | Compressor discharge |
| BT | mbar | Saturated pressure - wet bulb |
| BU | mbar | Saturated pressure - dry bulb |
| BV | mbar | Saturated pressure - vapour |

| Column | Enthalpy units | Description |
|---|---|---|
| H | kJ/kg | Refrigerant - enthalpy at condenser discharge |
| N & AW | kJ/kg | Refrigerant total latent heat at evaporating pressure |
| AM | kJ/kg | Latent heat - condenser |
| AO | kJ/kg | Condenser sub-cooling |
| AT | kJ/kg | Compressor discharge |
| AV | kJ/kg | Evaporator - saturated liquid heat |
| AX | kJ/kg | Evaporator - latent heat content |
| BA | kJ/kg | Compressor suction - inlet to cylinder |
| BC | kJ/kg | Compressor suction - inlet to shell |
| BD | kJ/kg | Refrigerant heat input - compressor cylinder |

| Column | Superheat units | Description |
|---|---|---|
| T | kJ/kg.K | Specific heat - refrigerant entering compressor shell |
| U | kJ/kg.K | Superheat - refrigerant entering compressor shell |
| X | kJ/kg.K | Specific heat - refrigerant entering compressor cylinder |
| Y | kJ/kg.K | Superheat - refrigerant entering compressor cylinder |
| AJ | kJ/kg.K | Specific heat - refrigerant compressor discharge |
| AK | kJ/kg.K | Superheat - refrigerant compressor discharge |

| Column | Watts units | Description |
|---|---|---|
| D | Watts | Heat output of the condenser |
| AR & BL | Watts | Compressor - electrical input |
| AS | Watts | Heat loss from compressor shell |
| BJ | Watts | Condenser refrigerant output |
| BK | Watts | Evaporator heat gain |
| BN | Watts | Heat input from air |
| BM | Watts | Condenser heat gain by water |
| BO | Watts | Heat energy difference - condenser to evaporator |
| CA | Watts | Refrigerant gain from motor armature |
| CB | Watts | Shell emission loss |
| CC | Watts | Energy input to compressor cylinder |
| CE | Watts | Energy input to evaporator |
| CI | Watts | Condenser - heat gain from water |
| CJ | Watts | Condenser - heat output from refrigerant |
| CM | Watts | Evaporator - heat air input |
| CN | Watts | Evaporator - heat input to refrigerant |

| Column | Other item units | Description |
|---|---|---|
| BB | % | Refrigerant dryness factor - evaporator inlet |
| BE | kJ/min | Refrigerant mass flow |
| BF | ratio | Refrigerant compression ratio |
| BG | | Coefficient of performance |
| BW | | Air - relative humidity |
| CK | | Condenser percentage heat loss |
| CL | | Evaporator percentage heat gain |

| | B | C | D | E | F | G | H |
|---|---|---|---|---|---|---|---|
| Scan number | Water out | Water in | Heat output - condenser | Temp. (3) | Temp. (3) | X | Enthalpy - condenser discharge |
| | °C | °C | Watts | °C | K | Constant | kJ/kg |
| 16 | 32.3 | 30.0 | 963.7 | 32.5 | 305.7 | 0.568 | 145.27 |
| 17 | 34.5 | 32.7 | 754.2 | 33.7 | 306.9 | 0.564 | 147.01 |
| 19 | 36.4 | 34.5 | 796.1 | 35.7 | 308.9 | 0.559 | 149.92 |
| 20 | 36.4 | 34.7 | 712.3 | 35.6 | 308.8 | 0.559 | 149.78 |
| 21 | 36.3 | 34.8 | 628.5 | 35.6 | 308.8 | 0.559 | 149.78 |
| 36 | 36.7 | 34.8 | 796.1 | 34.0 | 307.2 | 0.564 | 147.44 |
| 37 | 36.7 | 34.8 | 796.1 | 34.2 | 307.4 | 0.563 | 147.73 |
| 43 | 36.5 | 35.0 | 628.5 | 34.9 | 308.1 | 0.561 | 148.75 |
| 44 | 36.4 | 35.0 | 586.6 | 34.9 | 308.1 | 0.561 | 148.75 |
| 73 | 35.9 | 34.4 | 628.5 | 33.3 | 306.5 | 0.566 | 146.43 |
| 74 | 35.8 | 34.4 | 586.6 | 33.4 | 306.6 | 0.565 | 146.57 |
| 97 | 35.8 | 34.2 | 670.4 | 33.0 | 306.2 | 0.566 | 145.99 |
| 104 | 35.4 | 34.2 | 502.8 | 33.5 | 306.7 | 0.565 | 146.72 |
| 120 | 33.9 | 33.4 | 209.5 | 30.5 | 303.7 | 0.573 | 142.38 |
| 129 | 34.7 | 33.6 | 460.9 | 31.9 | 305.1 | 0.569 | 144.40 |
| 144 | 34.9 | 33.3 | 670.4 | 30.6 | 303.8 | 0.573 | 142.52 |
| 153 | 34.4 | 33.2 | 502.8 | 32.1 | 305.3 | 0.569 | 144.69 |
| 160 | 34.2 | 33.2 | 419.0 | 31.4 | 304.6 | 0.571 | 143.67 |
| 181 | 33.5 | 32.4 | 460.9 | 30.7 | 303.9 | 0.573 | 142.66 |

Identification of column data

For thermocouple locations, see Figure 57.

Column B — Water outlet from condenser — °C
Thermocouple number 10

C — Water inlet temperature to condenser — °C
Thermocouple number 9

D — Water - heat output from condenser — Watts
(col. B - col. C) x 6 x 4190 / 60 = (col. B - col. C) x 419

E — Refrigerant outlet temperature from condenser — °C
Thermocouple number 3

F — Refrigerant outlet temperature from condenser (absolute) — K
col. E + 273.15

G — Constant in equation to calculate enthalpy
$[1 - (\text{col F} / 374)^{0.333}]$

H — Enthalpy of refrigerant - condenser discharge — kJ/kg
$A + Bx + Cx^2 + Dx^3 + Ex^4$

| | K | L | M | N | O | P |
|---|---|---|---|---|---|---|
| Scan number | Refrigerant input to evaporator | Refrigerant absolute temperature | X | Latent heat | Temperature to shell | Temperature input to cylinder |
| | °C | K | Constant | kJ/kg | °C | °C |
| 16 | -4.2 | 268.8 | 0.655 | 201.45 | 0.4 | 23.8 |
| 17 | -4.0 | 269.0 | 0.655 | 201.30 | 0.6 | 25.0 |
| 19 | -9.4 | 263.6 | 0.666 | 205.28 | -3.8 | 25.7 |
| 20 | -10.3 | 262.7 | 0.668 | 205.94 | -4.5 | 25.7 |
| 21 | -10.4 | 262.6 | 0.668 | 206.01 | -3.8 | 25.6 |
| 36 | -6.8 | 266.2 | 0.661 | 203.38 | -1.9 | 14.8 |
| 37 | -7.3 | 265.7 | 0.662 | 203.75 | -2.0 | 14.8 |
| 43 | -10.5 | 262.5 | 0.668 | 206.08 | -5.4 | 15.1 |
| 44 | -10.7 | 262.3 | 0.669 | 206.23 | -5.2 | 15.2 |
| 73 | -10.9 | 262.1 | 0.669 | 206.37 | -6.5 | 16.0 |
| 74 | -11.6 | 261.4 | 0.670 | 206.87 | -6.8 | 16.1 |
| 97 | -9.6 | 263.4 | 0.667 | 205.43 | -3.8 | 11.8 |
| 104 | -13.1 | 259.9 | 0.673 | 207.95 | -6.5 | 11.9 |
| 120 | -1.5 | 271.5 | 0.650 | 199.41 | 1.9 | 13.0 |
| 129 | -14.3 | 258.7 | 0.676 | 208.80 | -7.9 | 12.5 |
| 144 | -8.5 | 264.5 | 0.664 | 204.63 | -0.1 | 10.6 |
| 153 | -14.5 | 258.5 | 0.676 | 208.94 | -7.0 | 10.8 |
| 160 | -9.3 | 263.7 | 0.666 | 205.21 | -2.8 | 11.6 |
| 181 | -16.4 | 256.6 | 0.680 | 210.28 | -8.1 | 12.2 |

Identification of column data

For thermocouple locations, see Figure 57.

| | | | |
|---|---|---|---|
| Column K | Evaporator - refrigerant inlet temperature<br>Thermocouple number 4 | °C |
| L | Evaporator - refrigerant inlet temperature<br>col. K + 273.15 | K |
| M | Calculation of constant for row N<br>Equation from R134(a) data sheet | |
| N | Total latent heat at evaporator pressure<br>Equation from R134(a) data sheet | kJ/kg |
| O | Refrigerant temperature - input to compressor shell<br>Thermocouple number 5 | °C |
| P | Temperature entering compression cylinder<br>Thermocouple number 8 | °C |

| | S/H entering compressor shell | | | S/H entering compressor cylinder | | |
|---|---|---|---|---|---|---|
| | S | T | U | W | X | Y |
| Scan number | Compressor suction | Specific heat | Superheat | Superheat input | Specific heat (8) | Superheat |
| | K | kJ/kg | kJ/kg | K | kJ/kg | kJ/kg |
| 16 | 4.6 | 0.78 | 3.58 | 28.0 | 0.74 | 20.85 |
| 17 | 4.6 | 0.78 | 3.59 | 29.0 | 0.74 | 21.60 |
| 19 | 5.6 | 0.77 | 4.31 | 35.1 | 0.74 | 25.86 |
| 20 | 5.8 | 0.77 | 4.45 | 36.0 | 0.74 | 26.48 |
| 21 | 6.6 | 0.77 | 5.07 | 36.0 | 0.74 | 26.47 |
| 36 | 4.9 | 0.77 | 3.79 | 21.6 | 0.74 | 16.00 |
| 37 | 5.3 | 0.77 | 4.10 | 22.1 | 0.74 | 16.35 |
| 43 | 5.1 | 0.77 | 3.91 | 25.6 | 0.74 | 18.82 |
| 44 | 5.5 | 0.77 | 4.22 | 25.9 | 0.73 | 19.03 |
| 73 | 4.4 | 0.77 | 3.37 | 26.9 | 0.73 | 19.76 |
| 74 | 4.8 | 0.77 | 3.67 | 27.7 | 0.73 | 2-.32 |
| 97 | 5.8 | 0.77 | 4.46 | 21.4 | 0.74 | 15.76 |
| 104 | 6.6 | 0.76 | 5.03 | 25.0 | 0.73 | 18.28 |
| 120 | 3.4 | 0.78 | 2.67 | 14.5 | 0.75 | 10.85 |
| 129 | 6.4 | 0.76 | 4.87 | 26.8 | 0.73 | 19.55 |
| 144 | 8.4 | 0.77 | 6.48 | 19.1 | 0.74 | 14.10 |
| 153 | 7.5 | 0.76 | 5.70 | 25.3 | 0.73 | 18.45 |
| 160 | 6.5 | 0.77 | 5.00 | 20.9 | 0.74 | 15.40 |
| 181 | 8.3 | 0.76 | 6.28 | 28.6 | 0.73 | 20.77 |

Identification of column data

For thermocouple locations, see Figure 57.

Column S refrigerant superheat entering compressor shell K
col. O - col. K

T Specific heat of superheated refrigerant entering compressor shell kJ/kg.K

Equation from R134(a) dtat sheet

U Superheat entering the compressor shell kJ/kg
col. S x col. T

W Degrees of superheat entering compressor cylinder K
col. P - col. K

X Specific heat of superheated refrigerant kJ/kg.K
Equation from R134(a) data sheet

Y Superheat entering compressor cylinder kJ/kg
col. W x col. X

| | AB | AC | AD | AE | AF | AG |
|---|---|---|---|---|---|---|
| Scan number | Compressor discharge temp. | Compressor discharge temp. (abs) | Compressor suction pressure | Compressor discharge pressure | Condenser saturated temp. | Superheat compressor discharge |
| | °C | K | bar (abs) | bar (abs) | K | °C |
| 16 | 60.8 | 334.0 | 2.35 | 8.40 | 306.5 | 27.4 |
| 17 | 63.0 | 336.0 | 2.35 | 8.80 | 308.0 | 28.0 |
| 19 | 65.3 | 338.3 | 2.00 | 9.30 | 310.0 | 28.3 |
| 20 | 66.0 | 339.0 | 1.85 | 9.25 | 309.5 | 29.5 |
| 21 | 66.0 | 339.0 | 1.85 | 9.25 | 309.5 | 29.5 |
| 36 | 50.1 | 323.1 | 2.05 | 9.45 | 310.5 | 12.6 |
| 37 | 50.5 | 323.5 | 2.05 | 9.40 | 310.3 | 13.2 |
| 43 | 52.5 | 325.5 | 1.85 | 9.35 | 310.2 | 15.3 |
| 44 | 52.7 | 325.7 | 1.70 | 9.30 | 310.0 | 15.7 |
| 73 | 52.1 | 325.1 | 1.80 | 9.25 | 309.5 | 15.6 |
| 74 | 52.7 | 325.7 | 1.75 | 9.20 | 309.3 | 16.4 |
| 97 | 45.7 | 318.7 | 2.00 | 9.25 | 309.5 | 9.2 |
| 104 | 47.7 | 320.7 | 1.80 | 9.20 | 309.3 | 11.4 |
| 120 | 31.6 | 304.6 | 2.80 | 8.10 | 305.0 | -0.4 |
| 129 | 45.8 | 318.8 | 2.05 | 9.00 | 309.0 | 9.8 |
| 144 | 44.2 | 317.2 | 2.10 | 9.10 | 309.1 | 8.1 |
| 153 | 46.0 | 319.0 | 1.70 | 8.90 | 308.0 | 11.0 |
| 160 | 39.3 | 312.3 | 2.70 | 7.90 | 304.3 | 8.0 |
| 181 | 46.4 | 319.4 | 1.70 | 8.80 | 308.0 | 11.4 |

Identification of column data

For thermocouple locations, see Figure 57.

| | | | |
|---|---|---|---|
| Column AB | Compressor discharge temperature<br>Thermocouple number 1 | °C |
| AC | Compressor discharge temperature (absolute)<br>col. AB + 273.15 | K |
| AD | Compressor suction pressure<br>Pressure reading from Bourdon pressure gauge | bar (abs) |
| AE | Compressor delivery pressure<br>Pressure reading from Bourdon pressure gauge | bar (abs) |
| AF | Condenser - saturated vapour temperature<br>Data from thermodynamic tables | K |
| AG | Superheat at compressor discharge<br>col. AC - col. AF | °C |

| | AJ | AK | AL | AM | AN | AO |
|---|---|---|---|---|---|---|
| Scan number | Specific heat compressor discharge | Superheat capacity | X | Condenser latent heat | Condenser sub-cooling temp drop | Condenser sub-cooling |
| | kJ/kg.K | kJ/kg | constant | kJ/kg | K | kJ/kg |
| 16 | 0.89 | 24.54 | 0.565 | 169.47 | 0.9 | 0.403 |
| 17 | 0.90 | 25.13 | 0.561 | 168.00 | 1.2 | 0.549 |
| 19 | 0.90 | 25.51 | 0.556 | 166.01 | 1.2 | 0.556 |
| 20 | 0.90 | 26.63 | 0.557 | 166.51 | 0.8 | 0.363 |
| 21 | 0.90 | 26.63 | 0.557 | 166.51 | 0.8 | 0.363 |
| 36 | 0.88 | 11.03 | 0.554 | 165.50 | 3.4 | 1.591 |
| 37 | 0.88 | 11.57 | 0.555 | 165.70 | 3.0 | 1.404 |
| 43 | 0.88 | 13.46 | 0.555 | 165.81 | 2.2 | 1.031 |
| 44 | 0.88 | 13.82 | 0.556 | 166.01 | 2.0 | 0.936 |
| 73 | 0.88 | 13.71 | 0.557 | 166.51 | 3.1 | 1.443 |
| 74 | 0.88 | 14.43 | 0.558 | 166.71 | 2.8 | 1.303 |
| 97 | 0.87 | 7.99 | 0.557 | 166.51 | 3.4 | 1.580 |
| 104 | 0.87 | 9.94 | 0.558 | 166.71 | 2.7 | 1.257 |
| 120 | 0.84 | -0.34 | 0.570 | 170.93 | 1.4 | 0.630 |
| 129 | 0.87 | 8.51 | 0.558 | 167.01 | 4.0 | 1.846 |
| 144 | 0.87 | 7.01 | 0.558 | 166.91 | 5.4 | 2.467 |
| 153 | 0.87 | 9.56 | 0.561 | 168.00 | 2.8 | 1.292 |
| 160 | 0.86 | 6.86 | 0.572 | 171.60 | -0.2 | -0.118 |
| 181 | 0.87 | 9.91 | 0.561 | 168.00 | 4.2 | 1.922 |

Identification of column data

| | | | |
|---|---|---|---|
| Column | AJ | Specific heat at compressor discharge<br>Equation from R134(a) data sheet | kJ/kg.K |
| | AK | Superheat at compressor discharge<br>col. AG x col. AF | kJ/kg |
| | AL | Calculation of constant for col. AM<br>Equation from R134(a) data sheet | |
| | AM | Condenser latent heat<br>Equation from R134(a) data sheet | kJ/kg |
| | AN | Temperature drop - sub-cooling of liquid<br>col. AF - col. F | K |
| | AO | Liquid sub-cooling at condenser outlet<br>(col. H x col. AN) / col. AF | kJ/kg |

| | AR | AS | AT | AU | AV | AW | AX |
|---|---|---|---|---|---|---|---|
| Scan number | Compressor electrical input | Compressor heat loss | Enthalpy compressor discharge | X | Evaporator liquid heat | Evaporator pressure of latent heat | Latent heat of evaporator |
| | Watts | Watts | kJ/kg | constant | kJ/kg | kJ/kg | kJ/kg |
| 16 | 430 | 60.71 | 339.69 | 0.655 | 94.13 | 201.45 | 150.31 |
| 17 | 430 | 63.67 | 340.69 | 0.655 | 94.40 | 201.30 | 148.69 |
| 19 | 410 | 65.41 | 342.00 | 0.666 | 87.21 | 205.28 | 142.57 |
| 20 | 440 | 65.41 | 343.27 | 0.668 | 86.02 | 205.94 | 142.18 |
| 21 | 440 | 65.16 | 343.27 | 0.668 | 85.89 | 206.01 | 142.12 |
| 36 | 440 | 39.54 | 325.57 | 0.661 | 90.66 | 203.38 | 146.60 |
| 37 | 440 | 39.54 | 326.41 | 0.662 | 90.00 | 203.75 | 146.01 |
| 43 | 440 | 40.21 | 329.05 | 0.668 | 85.76 | 206.08 | 143.08 |
| 44 | 440 | 40.44 | 329.51 | 0.669 | 85.49 | 206.23 | 142.96 |
| 73 | 440 | 42.25 | 328.09 | 0.669 | 85.23 | 206.37 | 145.17 |
| 74 | 440 | 42.47 | 329.02 | 0.670 | 84.30 | 206.87 | 144.60 |
| 97 | 390 | 32.92 | 322.07 | 0.667 | 86.95 | 205.43 | 146.38 |
| 104 | 430 | 33.14 | 324.62 | 0.673 | 82.32 | 207.95 | 143.56 |
| 120 | 430 | 35.54 | 313.60 | 0.650 | 97.75 | 199.41 | 154.78 |
| 129 | 430 | 34.44 | 321.76 | 0.676 | 80.75 | 208.80 | 145.15 |
| 144 | 390 | 30.34 | 318.91 | 0.664 | 88.41 | 204.63 | 150.51 |
| 153 | 390 | 30.77 | 323.54 | 0.676 | 80.48 | 208.94 | 144.74 |
| 160 | 400 | 32.49 | 322.01 | 0.666 | 87.34 | 205.21 | 148.88 |
| 181 | 410 | 33.79 | 322.50 | 0.680 | 77.99 | 210.28 | 145.61 |

Identification of column data

Column AR — Electrical input to compressor motor — Watts
Meter readings

AS — Heat emission from compressor shell — Watts
Heat convection and radiator losses

AT — Specific enthalpy - compressor discharge — kJ/kg
$(\text{col. H} + \text{col. AO} / 374)^{0.333}$

AU — Calculation of constant for column AV
$[1 - (\text{col. L} - 374)]^{0.333}$

AV — Enthalpy - saturated liquid at evaporation pressure — kJ/kg
Equation from R134(a) data sheet

AW — Total latent heat at evporation pressure — kJ/kg
Equation from R134(a) data sheet

AX — Evaporator - latent heat content — kJ/kg
col. AX + col. N - col. H

| | BA | BB | BC | BD | BE | BF | BG |
|---|---|---|---|---|---|---|---|
| Scan number | Enthalpy cylinder inlet | Dryness fraction - evaporator inlet | Enthalpy compressor suction | Heat input to compressor | Refrigerant mass flow | Compression ratio | Coefficient of perfomance |
| | kJ/kg | % | kJ/kg | kg/min | | | |
| 16 | 316.43 | 75 | 299.16 | 40.52 | 0.547 | 3.57 | 4.12 |
| 17 | 317.30 | 74 | 299.28 | 41.41 | 0.531 | 3.74 | 3.99 |
| 19 | 318.36 | 69 | 296.80 | 45.19 | 0.458 | 4.65 | 3.57 |
| 20 | 318.43 | 69 | 296.41 | 46.87 | 0.480 | 5.00 | 3.52 |
| 21 | 318.37 | 69 | 296.96 | 46.31 | 0.486 | 5.00 | 3.56 |
| 36 | 310.04 | 72 | 297.84 | 27.73 | 0.866 | 4.61 | 5.85 |
| 37 | 310.10 | 72 | 297.85 | 28.57 | 0.841 | 4.59 | 5.69 |
| 43 | 310.66 | 69 | 295.75 | 33.30 | 0.720 | 5.05 | 4.92 |
| 44 | 310.75 | 69 | 295.93 | 33.58 | 0.714 | 5.47 | 4.89 |
| 73 | 311.36 | 70 | 294.97 | 33.12 | 0.721 | 5.14 | 4.96 |
| 74 | 311.49 | 70 | 294.85 | 34.17 | 0.698 | 5.26 | 4.82 |
| 97 | 308.14 | 71 | 296.84 | 25.23 | 0.849 | 4.63 | 6.39 |
| 104 | 308.55 | 69 | 295.30 | 29.31 | 0.812 | 5.11 | 5.60 |
| 120 | 308.01 | 78 | 299.83 | 13.77 | 1.719 | 2.89 | 11.41 |
| 129 | 309.10 | 70 | 294.41 | 27.35 | 0.868 | 4.39 | 5.97 |
| 144 | 307.13 | 74 | 299.51 | 19.40 | 1.112 | 4.33 | 8.39 |
| 153 | 307.87 | 69 | 295.12 | 28.41 | 0.759 | 5.24 | 5.80 |
| 160 | 307.96 | 73 | 297.56 | 24.45 | 0.902 | 2.93 | 6.70 |
| 181 | 309.04 | 69 | 294.55 | 27.95 | 0.808 | 5.18 | 5.90 |

Identification of column data

Column BA Compressor - enthalpy at inlet to cylinder kJ/kg
col. AV + col. N + col. Y

BB Dryness fraction of refrigerant at evaporator inlet %
col. AX x 100 / col. N

BC Enthalpy at inlet to compressor shell kJ/kg
col. AV + col. AW + col. U

BD Specific enthalpy - useful energy input to compressor kJ/kg
col. AT - col. BC

BE Refrigerant mass flow through closed cycle kJ/kg
(col. AR - col. AS) x 60 / 1000 x col. BD

BF Compression ratio
col. AE / col. AD

BG Coefficient of performance
col. AJ / col. AR

| | BJ | BK | BL | BM | BN | BO |
|---|---|---|---|---|---|---|
| Scan number | Condenser refrigerant output | Evaporator refrigerant heat gain | Energy gain | Condenser water heat gain | Evaporator air input | Condenser / evaporator energy difference |
| | Watts | Watts | Watts | Watts | Watts | Watts |
| 16 | 1772 | 1403 | 430 | 964 | 651 | 312 |
| 17 | 1714 | 1347 | 430 | 754 | 658 | 96 |
| 19 | 1465 | 1120 | 410 | 796 | 577 | 219 |
| 20 | 1547 | 1172 | 440 | 712 | 567 | 145 |
| 21 | 1566 | 1191 | 440 | 629 | 561 | 68 |
| 36 | 2572 | 2172 | 440 | 796 | 386 | 411 |
| 37 | 2505 | 2104 | 440 | 796 | 399 | 398 |
| 43 | 2165 | 1765 | 440 | 629 | 467 | 162 |
| 44 | 2151 | 1751 | 440 | 587 | 476 | 110 |
| 73 | 2182 | 1784 | 440 | 629 | 421 | 207 |
| 74 | 2123 | 1725 | 440 | 587 | 441 | 146 |
| 97 | 2492 | 2135 | 390 | 670 | 350 | 320 |
| 104 | 2408 | 2012 | 430 | 503 | 431 | 72 |
| 120 | 4905 | 4511 | 430 | 210 | 146 | 64 |
| 129 | 2565 | 2170 | 430 | 461 | 428 | 33 |
| 144 | 3270 | 2911 | 390 | 670 | 246 | 424 |
| 153 | 2261 | 1902 | 390 | 503 | 408 | 95 |
| 160 | 2680 | 2313 | 400 | 419 | 159 | 260 |
| 181 | 2421 | 2044 | 410 | 461 | 421 | 40 |

Identification of column data

Column BJ Refrigerant - heat output from condenser Watts
(col. AT - col. H) x col. BE x 1000 / 60

BK Refrigerant - heat gain evaporator Watts
(col. BC - col. H) x col. BE x 1000 / 60

BL Electrical input to compressor Watts
col. BJ - col. BK + col. AS

BM Condenser water - heat gain Watts
Calculated sheet 1, column D

BN Air - heat input to evaporator Watts
1.026$m^3$/sec x 1227 J/$m^3$ x temp difference = 32.4 x temp difference

BO Energy difference - condenser to evaporator Watts
col. BM - col. BN

| | BR | BS | BT | BU | BV | BW |
|---|---|---|---|---|---|---|
| Scan number | Dry bulb temperature | Wet bulb temperature | Wet bulb saturated pressure | Dry bulb saturated pressure | Vapour pressure | Relative humidity |
| | °C | °C | mbar | mbar | mbar | % |
| 16 | 20.90 | 14.9 | 16.919 | 24.668 | 12.125 | 49 |
| 17 | 20.90 | 14.9 | 16.919 | 24.668 | 12.125 | 49 |
| 19 | 12.40 | 7.3 | 10.219 | 14.382 | 6.144 | 43 |
| 20 | 11.20 | 6.2 | 9.475 | 13.288 | 5.480 | 41 |
| 21 | 10.70 | 6.2 | 9.475 | 12.854 | 5.880 | 46 |
| 36 | 9.10 | 5.1 | 8.780 | 11.548 | 5.584 | 48 |
| 37 | 9.10 | 5.0 | 8.719 | 11.548 | 5.443 | 47 |
| 43 | 8.10 | 4.3 | 8.302 | 10.792 | 5.266 | 49 |
| 44 | 7.90 | 4.1 | 8.187 | 10.646 | 5.150 | 48 |
| 73 | 6.00 | 3.8 | 8.016 | 9.345 | 6.258 | 67 |
| 74 | 6.00 | 2.8 | 7.469 | 9.345 | 4.912 | 53 |
| 97 | 5.00 | 2.6 | 7.363 | 8.719 | 5.446 | 62 |
| 104 | 4.00 | 2.0 | 7.055 | 8.129 | 5.457 | 67 |
| 120 | 4.00 | 1.0 | 6.566 | 8.129 | 4.169 | 51 |
| 129 | 2.80 | 1.3 | 6.710 | 7.469 | 5.511 | 74 |
| 144 | 3.00 | 0.0 | 6.108 | 7.575 | 3.711 | 49 |
| 153 | 1.80 | 0.4 | 6.288 | 6.955 | 5.169 | 74 |
| 160 | 2.00 | 0.2 | 6.197 | 7.055 | 4.759 | 67 |
| 181 | 1.00 | 0.2 | 6.197 | 6.566 | 5.558 | 85 |

Identification of column data

For thermocouple locations, see Figure 57.

Column BR — Dry bulb air inlet temperature — °C
Thermocouple number 6

BS — Wet bulb inlet temperature — °C
Thermocouple number 2

BT — Wet bulb satruation pressure — mbar
6.108 x Exp. [(17.245 x col. BS) / (237.3 + col. BS)]

BU — Dry bulb saturation pressure — mbar
6.108 x Exp. [(17.245 x col. BR) / (237.3 + col. BR)]

BV — Vapour pressure — mbar
col. BT - [0.799 x (col. BR - col. BS)]

BW — Relative humidity — %
(col. BV / col. BU) x 100

| | CA | CB | CC | CE |
|---|---|---|---|---|
| Scan number | Gain from motor windings (8) - (5) | Shell emission loss | Energy input to compressor cylinder | Energy input to evaporator |
| | Watts | Watts | Watts | Watts |
| 16 | 157.33 | 60.71 | 211.97 | 1560 |
| 17 | 159.38 | 63.67 | 206.95 | 1507 |
| 19 | 164.35 | 65.41 | 180.24 | 1284 |
| 20 | 176.04 | 65.41 | 198.55 | 1348 |
| 21 | 173.26 | 65.16 | 201.58 | 1365 |
| 36 | 176.25 | 39.54 | 224.22 | 2348 |
| 37 | 171.80 | 39.54 | 228.67 | 2276 |
| 43 | 178.97 | 40.21 | 220.82 | 1944 |
| 44 | 176.29 | 40.44 | 223.28 | 1928 |
| 73 | 196.79 | 42.25 | 200.96 | 1981 |
| 74 | 193.66 | 42.47 | 203.86 | 1919 |
| 97 | 159.95 | 32.92 | 197.13 | 2295 |
| 104 | 179.37 | 33.14 | 217.49 | 2191 |
| 120 | 234.55 | 35.54 | 159.91 | 4745 |
| 129 | 212.37 | 34.44 | 183.19 | 2382 |
| 144 | 141.32 | 30.34 | 218.34 | 3052 |
| 153 | 161.19 | 30.77 | 198.04 | 2063 |
| 160 | 156.30 | 32.49 | 211.21 | 2469 |
| 181 | 195.08 | 33.79 | 181.13 | 2239 |

Identification of column data

| | | | |
|---|---|---|---|
| Column CA | Heat gain to refrigerant from motor windings<br>(col. BA - col. BC) x col. BE x 1000 / 60 | Watts |
| CB | Heat emitted from compressor shell<br>Previously calculated in col. AS | Watts |
| CC | Energy input to compressor cylinder<br>col. BL - col. CA - col. CB | Watts |
| CE | Energy input to refrigerant - evaporator<br>(col. BA - col. H) x col. BE x 1000 / 60 | Watts |

| | CI | CJ | CK | CM | CN | CO |
|---|---|---|---|---|---|---|
| | Condenser | | | Evaporator | | |
| Scan number | Water heat gain | Refrigerant heat output | Percentage heat loss | Heat input from air | Refrigerant heat gain | Percentage heat gain |
| | Watts | Watts | % | Watts | Watts | % |
| 16 | 964 | 1772 | 46 | 651 | 1560 | 58 |
| 17 | 754 | 1714 | 56 | 658 | 1507 | 56 |
| 19 | 796 | 1465 | 46 | 577 | 1284 | 55 |
| 20 | 712 | 1547 | 54 | 567 | 1348 | 58 |
| 21 | 629 | 1566 | 60 | 561 | 1365 | 59 |
| 36 | 796 | 2572 | 69 | 386 | 2348 | 84 |
| 37 | 796 | 2505 | 68 | 399 | 2276 | 82 |
| 43 | 629 | 2165 | 71 | 467 | 1944 | 76 |
| 44 | 587 | 2151 | 73 | 476 | 1928 | 75 |
| 73 | 629 | 2182 | 71 | 421 | 1981 | 79 |
| 74 | 587 | 2123 | 72 | 441 | 1919 | 77 |
| 97 | 670 | 2492 | 73 | 350 | 2295 | 85 |
| 104 | 503 | 2408 | 79 | 431 | 2191 | 80 |
| 120 | 210 | 4905 | 96 | 146 | 4745 | 97 |
| 129 | 461 | 2565 | 82 | 428 | 2382 | 82 |
| 144 | 670 | 3270 | 80 | 246 | 3052 | 92 |
| 153 | 503 | 2261 | 78 | 408 | 2063 | 80 |
| 160 | 419 | 2680 | 84 | 159 | 2469 | 94 |
| 181 | 461 | 2421 | 81 | 421 | 2239 | 81 |

Identification of column data

| | | | |
|---|---|---|---|
| Column | CI | Heat gain by water in the condenser<br>(col. B - col. C) x 419 | Watts |
| | CJ | Heat output from the refrigerant<br>(col. AO + col. AM) x col. BE x 1000 / 60 | Watts |
| | CK | Heat emitted to other sources<br>[(col. CJ - col. CI) / col. CJ] x 100 | % |
| | CM | Heat transfer from air in the evaporator<br>Calculated in col. BN | Watts |
| | CN | Heat gain by the refrigerant<br>Calculated in col. CE | Watts |
| | CO | Heat gain from other sources<br>[(col. CN - col. CM) / col. CN] x 100 | % |

APPENDIX A6.6

R134(a) refrigerant - test rig performance calculations

Based on the thermal perfomance of R134(a) test rig.

| Row number | Description | Calculation number 1 | 2 | 3 |
|---|---|---|---|---|
| 1 | Electrical input | 440 | 425 | 400 |
| 2 | Loss from shell | 45.69 | 66.59 | 78.16 |
| 3 | Useful electrical input | 394.31 | 358.59 | 321.84 |
| 4 | Thermocouple number 1 | 45.0 | 66.50 | 68.10 |
| 5 | Thermocouple number 3 | 29.7 | 32.70 | 32.20 |
| 6 | Thermocouple number 4 | -2.8 | -11.50 | -15.70 |
| 7 | Thermocouple number 5 | 13.5 | -3.70 | -5.30 |
| 8 | Thermocouple number 8 | 17.5 | 26.10 | 30.70 |
| 9 | Condenser pressure | 7.67 | 8.36 | 8.13 |
| 10 | Evaporator pressure | 2.62 | 1.85 | 1.57 |
| 11 | Compression ratio | 2.93 | 4.52 | 5.18 |
| 12 | Enthalpy - point 1 | 330.89 | 349.88 | 352.23 |
| 13 | Enthalpy - point 2 | 296.25 | 297.93 | 296.82 |
| 14 | Specific enthalpy gain - compressor | 34.64 | 51.95 | 55.41 |
| 15 | Refrigerant mass flow (kg/min) | 0.68 | 0.41 | 0.35 |
| 16 | Enthalpy - point 3 | 141.77 | 146.11 | 144.66 |
| 17 | Heat output (Watts) | 2153 | 1407 | 1206 |

| Summary of results | | | |
|---|---|---|---|
| Heat pump output (Watts) | 2153 | 1407 | 1206 |
| Refrigerant mass flow (kg/min) | 0.68 | 0.41 | 0.35 |
| Compression ratio | 2.93 | 4.52 | 5.18 |

Typical calculation - calculation number 1

Calculation based on 5K superheat at compressor suction and also that the refrigerant is completely liquified at the compressor discharge.

| Row number | | Details of calculation |
|---|---|---|
| 1 | Electrical supply to compressor | 440 Watts |
| 2 | Heat loss from shell<br>Radiant and convective heat loss calculation based on shell to room temperature difference | 45.69 Watts |
| 3 | Useful heat power input to the compressor | row (1) - row (2)<br>= 440 - 45.69 = 394.31 Watts |
| 4 to 8 | Temperature readings from thermocouples mounted on the test rig | |
| 9 | Absolute pressure - condenser | 7.67 bar (abs) |
| 10 | Absolute pressure - evaporator | 2.62 bar (abs) |
| 11 | Compression ratio | row (9) / row (10)<br>= 7.67 / 2.62 = 2.93 |
| 12 | Enthalpy of refrigerant at compressor delivery | 330.89 kJ/kg |
| 13 | Enthalpy of refrigerant at compressor suction | 296.25 kJ/kg |
| | Data for items (12) and (13) obtained from thermodynamic property tables | |
| 14 | Specific enthalpy gain of refrigerant flow through the compressor | row (12) - row (13)<br>= 330.89 - 296.25 = 34.64 kJ/kg |
| 15 | Refrigerant mass flow | row (3) / row (14) x 60 /1000<br>=394.31 / 34.64 x 60 / 1000<br>= 0.68 kg/min |
| 16 | Enthalpy of liqiud discharge from condenser<br>Obtained from thermodynamic tables | 141.77 kJ/kg |
| 17 | Heat pump output | [row (12) - row (16)] x row (15) x 1000 / 60<br>= [330.89 - 141.77] x 0.68 x 1000 / 60<br>= 2153 Watts |

APPENDIX A6.7

## Modular units - calculation of seasonal energy consumption
## Details of calculation procedures

| Column | |
|---|---|
| A | Atmospheric air pressure |
| B | Heat loss from buildings and heat required to maintain comfort conditions within the domestic dwelling |
| C | Thermal output from the heat pump from atmospheric air at temperature 'A' |
| D | Number of days in the heating season where, for a period of 14 days, when the average temperature 'A' pertained |
| E | Heat required to maintain comfort conditions within the domestic dwelling<br>col. B x col. D x 14 |
| F | Number of units operaitng to maintain the space heating load |
| G | Maximum continuous output per annum from operating units during the heating period<br>col. C x col. D x 14 x col. F |
| I | Atmospheric air temperature |
| J | Required heat output from heat pump<br>col. B x col. D x 14 |
| K | Number of operational hours to provide the required heat pump output<br>col. J / col. C |
| L | Unit load carried by each module of the heat pump<br>col. J x col. F / col. G |
| M | Number of modular units in operation in order to meet the space heating load |
| N | Coefficient of performance - unit operating continuously and at full load |
| O | Coefficient of performance - unit operating intermittently |
| R | Energy input - one unit - intermittent operation |

| A | B | C | D | E | F | G |
|---|---|---|---|---|---|---|
| Air temperature | Building loss | Heat pump output | Heating days per annum | Heat required per annum | Number of units operating | Maximum continuous output |
| °C | kW | kW | | kWh | | KWh |
| 15 | 0.62 | 3 | 26 | 226 | 1 | 1092 |
| 13 | 1.86 | 2.9 | 25 | 651 | 1 | 1015 |
| 11 | 3.1 | 2.7 | 34 | 1476 | 2 | 2570 |
| 9 | 4.34 | 2.5 | 42 | 2552 | 2 | 2940 |
| 7 | 5.58 | 2.3 | 66 | 5156 | 3 | 6376 |
| 5 | 6.82 | 2.2 | 40 | 3819 | 4 | 4928 |
| 3 | 8.06 | 1.8 | 20 | 2257 | 5 | 2520 |
| 1 | 9.03 | 1.6 | 12 | 1517 | 5 | 1344 |
| -1 | 10.54 | 1.4 | 6 | 885 | 5 | 588 |
| -3 | 11.76 | 1.3 | 2 | 329 | 5 | 182 |

| I | J | K | L | M | N | O |
|---|---|---|---|---|---|---|
| Air temperature | Required heat output | Operational hours | Load on each unit | Number of units operating | C.O.P. full load | C.O.P. part load |
| °C | kWh | | | | | |
| 15 | 226 | 75 | 0.207 | 1 | 3.13 | 1.31 |
| 13 | 651 | 224 | 0.641 | 1 | 3.00 | 1.71 |
| 11 | 1476 | 547 | 1.148 | 2 | 2.86 | 1.96 |
| 9 | 2552 | 1021 | 1.736 | 2 | 2.72 | 2.12 |
| 7 | 5156 | 2242 | 2.426 | 3 | 2.58 | 2.19 |
| 5 | 3819 | 1736 | 3.100 | 4 | 2.44 | 2.24 |
| 3 | 2257 | 1254 | 4.478 | 5 | 2.06 | 2.06 |
| 1 | 1517 | 948 | 5.000 | 5 | 1.96 | 1.93 |
| -1 | 885 | 632 | 5.000 | 5 | 1.81 | 1.81 |
| -3 | 329 | 253 | 5.000 | 5 | 1.68 | 1.68 |

| Q | R | S | T | U | V | W | X |
|---|---|---|---|---|---|---|---|
| Air temperature | Intermittent operation input | Input to units in continuous operation 1 | 2 | 3 | 4 | 5 | Total power Input |
| °C | | | | | | | |
| 15 | 172 | | | | | | 172 |
| 13 | 381 | | | | | | 381 |
| 11 | 97 | 449 | | | | | 546 |
| 9 | 510 | 540 | | | | | 1051 |
| 7 | 413 | | 1648 | | | | 2061 |
| 5 | 55 | | | 1515 | | | 1570 |
| 3 | 117 | | | | 979 | | 1096 |
| 1 | | | | | | 774 | 774 |
| -1 | | | | | | 489 | 489 |
| -3 | | | | | | 196 | 196 |
| | | | | | | Total input: | 8336 |

APPENDIX A7.1

## HEAT PUMP TEST RIG R134(A) THERMAL PERFORMANCE

### STEADY STATE OPERATION

### Details of calculation procedures

All of the following items refer to the refrigerant within the closed cycle. All of the data is based on laboratory trials where the heat pump was used within the environmental chamber.

| Column | | | |
|---|---|---|---|
| | | SECTION 1 | |
| B | Temperature | - inlet to compressor shell | °C |
| C | Pressure | - evaporator | bar (abs) |
| D | Temperature | - compressor delivery | °C |
| E | Pressure | - condenser inlet | bar (abs) |
| F | Temperature | - evaporator saturation vapour | °C |
| G | Temperature | - condenser saturated liquid | °C |
| H | Temperature | - compressor superheat, input to shell | K |
| | | SECTION 2 | |
| L | Enthalpy | - compressor suction | kJ/kg |
| M | Enthalpy | - compressor delivery | kJ/kg |
| N | Constant for equation col. O | | |
| | col. $N = X = [1 - ((G + 273.15) / 374.15)^{\frac{1}{3}}$ | | |
| O | Enthalpy | - output from condenser | kJ/kg |
| | col. $O = A + Bx + Cx^2 + Dx^3 + Ex^4$ | | |
| P | Compression ratio | | |
| | col. E / col. C | | |
| | | SECTION 3 | |
| T | Meter reading, electrical input | | Watts |
| U | Temperature (8), outer surface of conpressor shell | | |
| V | Air temperature inside the environmental chamber | | |
| W | Heat loss from compressor shell | | Watts |
| X | Useful heat input to compressor | | |
| | col. T - col. W | | |
| Y | Refrigerant mass flow | | kg/min |
| | col. $Y = (X \times 60) / [(\text{col. M} - \text{col. L}) \times 10^3]$ | | |
| | | SECTION 4 | |
| AB | Compression ratio | | |
| | col. E / col. C | | |
| AC | Refrigerant mass flow, obtained from laboratory trials | | kg/min |
| AD | Refrigerant mass flow, obtained from manufacturer's CECOMAF tests | | |
| AE | Electrical input to compressor, obtained from meter readings | | Watts |
| AF | Heat pump thermal output | | |
| | col. $AF = [\text{col. AC} \times (\text{col. M} - \text{col. O}) \times 10^3] / 60$ | | |
| AG | Coefficient of performance | | |
| | col. AF / col. AE | | |

Heat Pump Test Rig R134(a) - Thermal Performance
Steady State Operation

SECTION 1

| Column: | B | C | D | E | F | G | H |
|---|---|---|---|---|---|---|---|
| | Compressor Suction | | Compressor Delivery | | | | |
| Scan number: | Temperature °C | Pressure bar (abs) | Temperature °C | Pressure bar (abs) | Evaporator Saturated Temperature °C | Condenser Saturated Temperature °C | Compressor Suction at Superheat K |
| 11 | 0.4 | 2.30 | 65.1 | 9.1 | -6.40 | 36.07 | 6.80 |
| 12 | 0.9 | 2.40 | 67.4 | 9.3 | -5.35 | 36.86 | 6.25 |
| 13 | 1.0 | 2.40 | 68.6 | 9.6 | -5.35 | 38.03 | 6.35 |
| 18 | 2.5 | 2.40 | 61.4 | 8.9 | -5.35 | 35.06 | 7.85 |
| 19 | 2.4 | 2.40 | 65.0 | 9.2 | -5.35 | 36.47 | 7.75 |
| 20 | 2.5 | 2.40 | 65.1 | 9.1 | -5.35 | 36.07 | 7.85 |
| 70 | -3.1 | 1.95 | 54.0 | 8.9 | -10.71 | 35.26 | 7.61 |
| 80 | -4.6 | 1.85 | 57.4 | 8.9 | -11.99 | 35.26 | 7.39 |
| 90 | -5.0 | 1.80 | 60.0 | 8.9 | -12.71 | 35.26 | 7.71 |
| 345 | -7.7 | 1.70 | 54.9 | 7.2 | -14.10 | 25.50 | 6.40 |
| 346 | -7.6 | 1.70 | 55.2 | 7.2 | -14.00 | 25.50 | 6.40 |
| 347 | -7.6 | 1.70 | 55.5 | 7.2 | -14.00 | 25.50 | 6.40 |

Refrigerant input data for ensuing calculations

SECTION 2

| Column: | L | M | N | O | P |
|---|---|---|---|---|---|
| | Specific Enthalpy | | | | |
| Scan number: | Compressor Suction kJ/kg | Compressor Delivery kJ/kg | Values of X | Refrigerant Condenser Discharge kJ/kg | Compression Ratio |
| 11 | 300.28 | 348.16 | 0.56 | 150.4 | 4.0 |
| 12 | 300.44 | 350.47 | 0.56 | 151.6 | 3.9 |
| 13 | 300.53 | 350.99 | 0.55 | 153.3 | 4.0 |
| 18 | 303.38 | 344.75 | 0.56 | 149.0 | 3.7 |
| 19 | 301.75 | 347.89 | 0.56 | 151.0 | 3.8 |
| 20 | 303.38 | 348.16 | 0.56 | 150.4 | 3.8 |
| 70 | 298.26 | 337.00 | 0.56 | 149.3 | 4.6 |
| 80 | 297.27 | 340.12 | 0.56 | 149.3 | 4.8 |
| 90 | 297.08 | 343.26 | 0.56 | 149.3 | 4.9 |
| 345 | 295.10 | 340.95 | 0.59 | 135.2 | 4.2 |
| 346 | 295.19 | 341.25 | 0.59 | 135.2 | 4.2 |
| 347 | 295.19 | 341.55 | 0.59 | 135.2 | 4.2 |

Calculation of refrigerant mass flow based on the thermal input and output of the compressor

SECTION 3

| Column: | T | U | V | W | X | Y |
|---|---|---|---|---|---|---|
| Scan number: | Electrical input to compressor<br>Watts | Compressor shell temperature<br>(8)<br>°C | Ambient air temperature<br>(6)<br>°C | Heat loss from shell<br>Watts | Useful shell input<br>Watts | Refrigerant mass flow<br>kg/min |
| 11 | 430 | 26.9 | 21.8 | 43.6 | 386.43 | 0.48 |
| 12 | 430 | 28.2 | 21.9 | 46.1 | 383.89 | 0.46 |
| 13 | 440 | 28.9 | 22.0 | 47.5 | 382.51 | 0.45 |
| 18 | 420 | 23.9 | 22.2 | 37.9 | 402.13 | 0.58 |
| 19 | 400 | 26.2 | 22.4 | 42.3 | 377.72 | 0.49 |
| 20 | 400 | 26.4 | 22.4 | 42.7 | 357.33 | 0.48 |
| 70 | 400 | 16.4 | 8.9 | 23.2 | 376.77 | 0.58 |
| 75 | 400 | 18.1 | 7.6 | 26.0 | 373.99 | 0.52 |
| 80 | 400 | 20.2 | 6.8 | 29.6 | 370.45 | 0.48 |
| 345 | 380 | 17.4 | 3.6 | 24.5 | 355.49 | 0.47 |
| 346 | 380 | 17.6 | 3.7 | 24.9 | 355.15 | 0.46 |
| 347 | 380 | 17.8 | 3.8 | 25.2 | 354.81 | 0.46 |

Summary of results - Heat pump test rig

SECTION 4

| Column: | AB | AC | AD | AE | AF | AG |
|---|---|---|---|---|---|---|
| Scan number: | Compression ratio | 'A' Refrigerant mass flow kg/min | 'B' Refrigerant mass flow kg/min | Energy input<br>Watts | Heat output<br>Watts | Coefficient of performance |
| 11 | 4.0 | 0.48 | 0.56 | 430 | 1596 | 3.7 |
| 12 | 3.9 | 0.46 | 0.58 | 430 | 1526 | 3.5 |
| 13 | 4.0 | 0.45 | 0.56 | 430 | 1498 | 3.5 |
| 18 | 3.7 | 0.58 | 0.62 | 440 | 1903 | 4.3 |
| 19 | 3.8 | 0.49 | 0.60 | 420 | 1612 | 3.8 |
| 20 | 3.8 | 0.48 | 0.60 | 400 | 1578 | 3.9 |
| 70 | 4.6 | 0.58 | 0.47 | 400 | 1826 | 4.6 |
| 80 | 4.8 | 0.52 | 0.45 | 400 | 1666 | 4.2 |
| 90 | 4.9 | 0.48 | 0.44 | 400 | 1556 | 3.9 |
| 345 | 4.2 | 0.47 | 0.53 | 380 | 1595 | 4.2 |
| 346 | 4.2 | 0.46 | 0.53 | 380 | 1589 | 4.2 |
| 347 | 4.2 | 0.46 | 0.53 | 380 | 1579 | 4.2 |

REFERENCES


1. McMullan JT, Morgan R and Murray RB.
School of Physical Sciences,
New University of Ulster,
Energy Resources. Second Edition 1983. Chapter 1.
Edward Arnold (Publishers) Ltd. London.

2. Energy Trends - September 1994
Publication of the Government Statistical Service,
Department of Trade and Industry,
London SW1E 5HE.

3. Steven H and Lindley A,
"The race to seal the ozone hole."
I.C.I. Industrial Chemists,
New Scientist, 16th June 1990.

4. Cambell C J,
'Oil Shock'
Energy World, No. 240, June 1996, pp7,
The Magazine of the Institute of Energy.

5. Jennings J S,
'The Millenium and Beyond,
Energy World, No. 240, June 1996, pp13,
The Magazine of the Institute of Energy.

6. Kenney J F,
'Impending shortages of Petroleum Re-evaluated,
Energy World, No. 240, June 1996, pp16,
The Magazine of the Institute of Energy.

7. Odell P R,
'Oil Shock - a Rejoiner.'
Energy World, No. 247, March 1997, pp11,
The Magazine of the Institute of Energy.

8. Houghton J
Meteorological Office, Bracknell,
Report Prepared for the Intergovernmental Panel on Climatic Change,
Working Group 1. June 1990.

9. Leggett J,
Global Warming - The Greenpeace Report, 1990,
Oxford University Press.

10. Woodwell GM,
"The effects of Global Warming."
The Greenpeace Report, Global Warming, 1990,
Oxford University Press.

11. Scientific Assessment of Climatic Change,
Intergovernmental Panel on Climatic Change,
Report Prepared for I.P.C.C. by Working Group 1, June 1990.

12. Editorial, Building Services, The C.I.B.S.E. Journal
Volume 13, Number 12, December 1991.

13. "Guidelines on Environmental Issues."
Sponsored by Lloyd's Register and Department of the Environment
for Development
and Publishing of the 'Code of Professional Practice'
by the Engineering Council
Published by the Engineering Council, London, 1994.

14. "Institute of Mechanical Engineers calls for new Nuclear
Power Stations."
Professional Engineering
Volume 7, Number 17,pp4 October 1994.

15. Barthorpe F,
"Getting Switched onto Heat and Power."
Professional Engineering
Institute of Mechanical Engineers Magazine,
Volume 8, Number 4, March 1995.

16. Neal E,
"Heat pumps - Applications for Heating Conservation and
Heat Recovery." 1983.
Program Energy Combustion Science, Volume 9, pp179-197.

17. Lewitt EH,
"Thermodynamics Applied to Heat Engines."
Publisher - Sir Isaac Pitman and Sons Ltd. London.
4th Edition, 1949, pp24.

18. Braham GD,
Future Prospects for Heat Pumps, A Personal View,
Publisher - The Electricity Association
30 Mill Bank, London. 1985.

19. Private Communication,
Electricity Council.

20. Reay DA and MacMichael DBA
"Heat Pumps - Design and Application."
Publisher - Pergamon Press, Oxford, 1979.

21. Lewitt EH,
"Thermodynamics Applied to Heat Engines."
Publisher - Sir Isaac Pitman and Sons Ltd. London,
4th Edition, 1949, pp48.

22. Domestic Heat Pump Field Trials.
Made Available in Private Communications.

23. Faithful DC,
Operator's Manual - Air and Water Heat Pump.
P.A. Hilton Ltd., June 1981.
Stockbridge, Hants.

24. Raznjevig K,
Handbook of Thermodynamic Tables and Charts.
Publisher - Metran Hill, 1976.

25. Foxley DM and Weaver DR,
Laboratory Testing of Heat Pumps to Seasonal Coefficients of Performance,
Conference on New Energy Conservation Technologies and Their Commercialisation,
Berlin, 6-10 April 1981.

26. James RW, Marshall SA and Saluja BN,
Heat Pump as a Means of Utilising Low Grade Heat Energy
Polytechnic of the South Bank, London
Journal of the Institute of Heating and Ventilation Engineers,
Volume 43, January 1976.

27. Domanski PA and McLinen MO,
A Simplified Cycle Simulation Model for the Performance Rating of Refrigerants and Refrigerant Mixtures,
Building Environment Division, 1990.
National Institute of Standards and Technology
Gaithersburg, USA.

28. Ahrens FW,
Heat Pump Modelling, Simulation and Design,
Heat Pump Fundamentals, Edited by Berghmans J.
NATO Advanced Study Institutes Series,1983.
Publisher - Martinus Nijhoff, The Hague.

29. Butterworth D,
Introduction to Heat Transfer,
Engineering Design Guide Number 18,
Published for the Design Council and British Standards Institution,
Publisher - Oxford University Press, 1977.

30. Hewitt GF and Hall-Taylor NS,
Annular Two-Phase Flow,
Chemical Engineering Division, A.E.R.E., Harwell,
Publisher - Pergamon Press, Oxford, 1970.

31. Dossat RJ
Priciples of refrigeration, second edition, 1981, pp284
Publisher - John Wiley & Sons, New York.

32. McMullan JT, Masson A, Murphy N and Hewitt N,
Improvement of COP of Vapour Compression Heat Pumps
by Using a New Cycle, Final Report,
Centre for Research, University of Ulster, 1990.
Publisher - Commission of European Communities, Luxembourg.

33. Rogers GFC and Mayhew YR,
Engineering Thermodynamic Work and Heat Transfer
3rd Edition, 1980,
Publisher - Longman Group Limited, Harlow, Essex.

34. McMullan JT, Murphy N and Hughes DW
The effect of oil on the performance of heat pumps and refrigerators
Part 2, Experimental Results
Heat Recovery systems & C.H.P., Vol. 8, No. 2, pp95 to pp124, 1988
Printed in Great Britain.

35. Gluckman R,
Heat Pump Cycles and their Engineering,
Conference on the Application of Heat Pumps for
Cost Effective Heating and Cooling of Buildings,
Chartered Institute of Building Services,
University of Nottingham, April 1983.

36. Raznjevic K,
Handbook of Thermodynamic Tables and Charts,
Publisher - Metran Hill, 1976.

37. Wilson JTR,
Thermophysical Properties of Refrigerant 12,
Department of Industry / National Engineering Laboratory,
Publisher - HMSO, Edinburgh, 1966.

38. Hill JM and Jeter SM,
Techniques for obtaining improved initial estimates of explicit
state variables for computer-based thernodynamic property routines,
ASHRAE CRANS. 1990,Vol.96, Part Two, Paper No. 3417,309-316.

39. Martin JJ,
Equations of State,
Applied Thermodynamics Symposium,
Industrial and Engineering Chemistry,
Volume 59, number12, December 1967.

40. Pepper JB and Smith CH,
Dynamic Characteristics of Room Heaters,
Laboratory Report Number 46,
The Heating and Ventilation Research Association,
Bracknell, 1967.

41. Van Der Ree H,
Heat Pumps Combined With Thermal Storage,
TNO-Division of Technology for Society Laan Van Westenenk,
501, 7334 DT Apeldoorn, The Netherlands. June 1981.

42. Dale HCA and Crawshaw CM,
Some Characteristics of Human Controller of Domestic Heating,
Ergonomics Research Group, University of Hull,
Building Services Engineering Research & Technology,
Volume 4, Number 1, 1983.

43. Fitzgerald D
Room Thermostats - Choice and Performance,
Laboratory Report Number 42,
The Heating and Ventilation Research Association,
Bracknell, 1967.

44. Basnett P, Mould AE and Siviour JB,
Some Effects of Ventilation Rate, Thermal Insulation and Mass on
the Thermal
Performance of Houses in Summer and Winter,
Energy and Housing, Special Supplement to Building Science,
Pergamon Press, !975.

45. Basnett P,
Building Mass, Plant Size and COP.
Batiment International, Building Research & Practice Nov./Dec. 1983.
Vol. 16. No 6. pp362 - 365.

46. Jones WP,
Air Conditioning Applications and Design, pp7,
Edward Arnold, London, 1980.

47. I.H.V.E. Guide Book A, pp AZ 8 and 9,
Published by The Institute of Heating and Ventilating Engineers, 1970.

48. O'Sullivan PE,
Thermal Comfort,
Energy and Housing Special Supplement,
Building Science,
Pergamon Press, 1975.

49. Wyon DP,
The Effects of Ambient Temperature Swings on
Comfort, Performance and Behaviour,
Archives des Sciences Psysiologiques,
Volume 27, Number 4, 1973.

50 Faithful DC and Hewett GA,
Demonstration heat pump operating instructions and performance notes,
P. H. Hilton td., Stockbridge, Hants. 1981

51 European Committee of Manufacturers of Refrigeration Equipment
Year Book
International organisations,
Volume 1, 1990/1991

52 McMullan JT and Morgan R,
Heat pumps,
Energy Study Group, The New University of Ulster,
Adam Hilger Ltd., Bristol, 1981

53 Dossat RJ,
Principles of refrigeration, second edition,
John Wiley and Sons, New York, 1981

54 McMullan JJ, Murphy n and Hughes DW,
The effect of oil on the performance of heat pumps and refrigerators,
Heat Recovery Systems and Combined Heat and Power,
Volume 8, Part 2, pp117
Published in Great Britain.1988.

55 Steven H and Lindley A
The race to heal the ozone hole
New Scientist, pp 48 - 51, 16 June 1990.

56 Editorial, Building Services, C.I.B.S.E. Journal
Volume 15, Number 1, pp 3, January 1993.

57 Editorial, Briefing, Doubts over the future of HCFCs
Heating and Air Conditioning
Pub. Maclean Hunter, Energy Publication Group, pp 2, March 1994.

58 Greencool Refrigerants, Case Studies, 1997
Park Gate Business Centre. Ref. 2.97*UK

59 Sand JR, Vineyard EA and Nowak RJ
Experimental Performance of the Ozone
Safe alternative Refrigerants, Ashrae Transactions
Volume 96, Part 2, 1990.

60 Bouma JWJ
Frosting and Defrosting behaviour of outdoor coils
of air-source heat pumps
Pub. Commission of the European Communities, Energy.
Final Report, EUR 7281 EN 1981.

61 Private Communication
The Electricity Council.